UNIVERSITÀ DI PARMA

UNIVERSITA' DEGLI STUDI DI PARMA

DOTTORATO DI RICERCA IN SCIENZE DELLA TERRA

CICLO XXXVII

Behaviour of lower continental plate associated to a collisional orogen: structures, seismic-stratigraphy, deformations timing and local geophysical characters of foreland area with examples from Sicily channel and Adriatic region (Central Mediterranean).

Coordinatore:

Chiar.mo Prof. Fabrizio Balsamo

Tutore:

Chiar.mo Prof. Andrea Artoni

Dottorando: Dr. Aasiya Qadir

Anni Accademici 2021/2022 – 2023/2024

Contents

Abstract

Subduction zones are crucial for Earth's dynamics and are characterized by the convergence of tectonic plates with one of it diving down the other; the subducting plate, or lower plate, is governed by flexural subsidence and extensional stresses which keep on migrating towards the orogenic wedge where it experiences the thrust sheet loading. When the two continental plates converge and collide (continent-continent collision), the lower plate is characterized by a foreland basin which preserves the evidence of extensional tectonics as well as the deformation signs caused by the loading of the orogenic wedge.

For this PhD research, the aim is to investigate and characterize the geometry of the deformation timing and the geophysical characters in the foreland area of the Sicily Channel which belongs to the northern margin of the subducting African plate under the European plate to constrain the underlying mechanism and their variation through space and time. The intricate relation of the extensional and compressional tectonic settings ahead of the Sicily–Maghrebian orogenic system has been documented. The areas close to this orogenic wedge show complexity in the tectono-stratigraphic framework due to the migration of extensional stresses on the forebulge more towards the orogenic wedge which acts as a load on the bending lower plate. The confluence of the opposing extensional and compressional tectonic regimes occurs giving rise to structural and stratigraphic complexities. The analysis was performed with the aid of subsurface data and the satellite gravity and heat flow measurements which were complemented by high-resolution bathymetric data across the focused region. The anomalous behavior of geophysical and heat flow characters through depth crustal models of the focused region presented in this thesis confirms the presence of volcanic bodies and change in the lithospheric thickness with the migration of extensional stress that affects also the orogenic wedge. The Sicily Channel serves as a natural laboratory, revealing that this foreland region has preserved the record of dynamic processes (extension and compression), controlling lithosphere deformation in the lower plate. Thus, compressive deformations have extended far beyond the major orogenic front and affected a vast region of the subducting lower plate which otherwise has been under extension due to its bending. But, this work revealed that extension can propagate inside the orogenic wedge orthogonal to the trends of its major folds and thrusts which are both extended/dismembered and again compressed (causing positive inversion) in a short period of time (Pleistocene-Holocene – about 2 Ma). This envisages a more complex geodynamic relationship between the lower plate and the associated orogenic wedge in a collisional mountain chain.

Chapter 1

Introduction

1.1. Introduction of subduction zones

Subduction zones play a critical role in continuing the planet dynamics and known for one of the most noteworthy geological features on Earth (Stern, 2020). The mechanism of the subduction zone happens by the moving of two tectonic plates toward each other, in which one plate is overriding to the another and beneath one is forced under the other (Fig. 1.1a) (Hamilton, 1994).

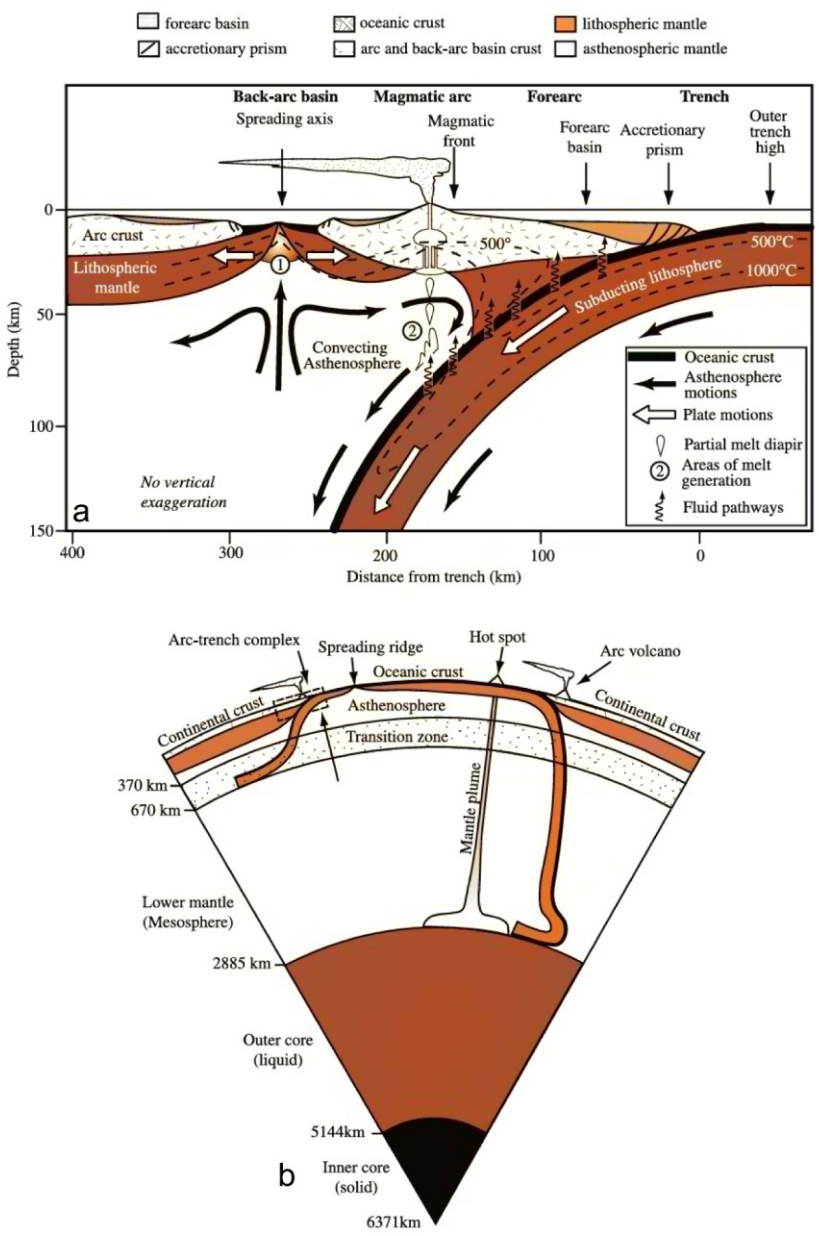

Fig. 1.1. (a) The interaction between the principal crustal and upper mantle portions and the genesis of forearc and backarc basins and magmatic arc. (b) Representation of subduction zones through the center of Earth which shows the rise of a mantle plume from an old, subducted slab (modified from Stern, (2002).

This ongoing phenomena of two plates eventually goes into subduction down into the Earth's mantle which is related to most holistic and influential geological events, including mountain building, deep-sea trenches, and volcanic arcs, aside from powerful earthquakes and tsunamis (Fig. 1.1b) (Kearey et al., 2009).

The onset and behaviour of subduction zones is only controlled by the interplay of these and other factors, given that the density, state of thermal structure, and the large number of weak zones in the lithosphere (Davies and Stevenson, 1992). Since subduction is not a systematic process, the tectonic environments and geological consequences of its zones are also highly variable (Zheng and Zhao, 2017). To comprehend the inception of subduction, two semi-quantitative and generic models have been postulated: spontaneous model and induced model. Spontaneous subduction refers to the negative buoyancy of the lithosphere above the underlying asthenosphere, whereas induced subduction is initiated by external forces, such as the ones resulting from tectonic collisions or mantle plumes (Fig. 1.1) (Stern and Gerya, 2018; Baes et al., 2021).

For this study, the most interesting region to understand the mechanisms and the processes for the subduction zones in the Central Mediterranean region is the Sicily Channel due to its convergent way for the African and Eurasian plates. In turn, this tectonic zone has a very complex geological setting that is controlled with the interaction involving subduction, collision, inheritance and extension. The subduction in the Central Mediterranean started during the Mesozoic, leading to such important geology as the Maghrebides, Hellenic Arc and the Apennine and Alpine Mountain ranges (Cavazza and Wezel, 2003; Harangi et al., 2006).

Subduction of the African Plate under the Eurasian Plate in the Central Mediterranean is characterized by several segmentation of the subduction zone with a specific pattern of deformation and seismic activity (Vidal et al., 2000; Dilek and Sandvol, 2009). Slab rollback from oblique subduction is associated with trench retreat, as the subducting slab moves back and the associated trench retreats (Sdrolias and Müller, 2006; Balázs et al., 2021). Such a situation has important implications for the

tectonic evolution of the region and leads to the formation of back-arc basins, forearc basins and magmatic arc (Sdrolias and Müller, 2006). The process of slab rollback and trench retreat has been increasingly recognized in the evolution of the Central Mediterranean subduction zone (Balázs et al., 2022; Malinverno and Ryan, 1986). With the ongoing subduction of the African plate, the slab undergoes a process called rollback, wherein the subducting slab moves backward, consequently resulting in trench retreat (Gerya, 2022). This process has huge implications for the tectonic evolution of the region since back-arc basins open up and new tectonic features are formed (Sdrolias and Müller, 2006).

1.2. Development of foreland basins:

Foreland basin is known as an elongated trough that developed on the continental crust with the linear compressional orogenic activity for potential sediment accommodation. This zone is mainly governed by geodynamic activity specially with the flexural subsidence with the control of thrust sheet loading (Roure, 2008; Allen and Allen, 2013). Foreland basins have four different depozones, referred to as the wedge-top, foredeep, forebulge and back-bulge (Fig. 1.2) (DeCelles and Giles, 1996). These depozones consist of sediments and the accommodation of these sediments depend on its location at the time of deposition, which is mostly related to their ultimate geometric relationship with the thrust belt (Fig. 1.2) (Chapman and DeCelles, 2015). Foreland basins are generally related to the topography and dimensions of the orogenic wedges and to the response of the subducted lithospheric slabs which are deformed and downward moving by flexural bending; the latter having variations in terms of spatial scale extension over the different portions of the plate. With this, the wideness of the depression as foreland basins are useful to interpret the physical strength of the underlying lithosphere which simply sinks vertically into the mantle on the principle of Airy isostasy (Lamb and Watts, 2010).

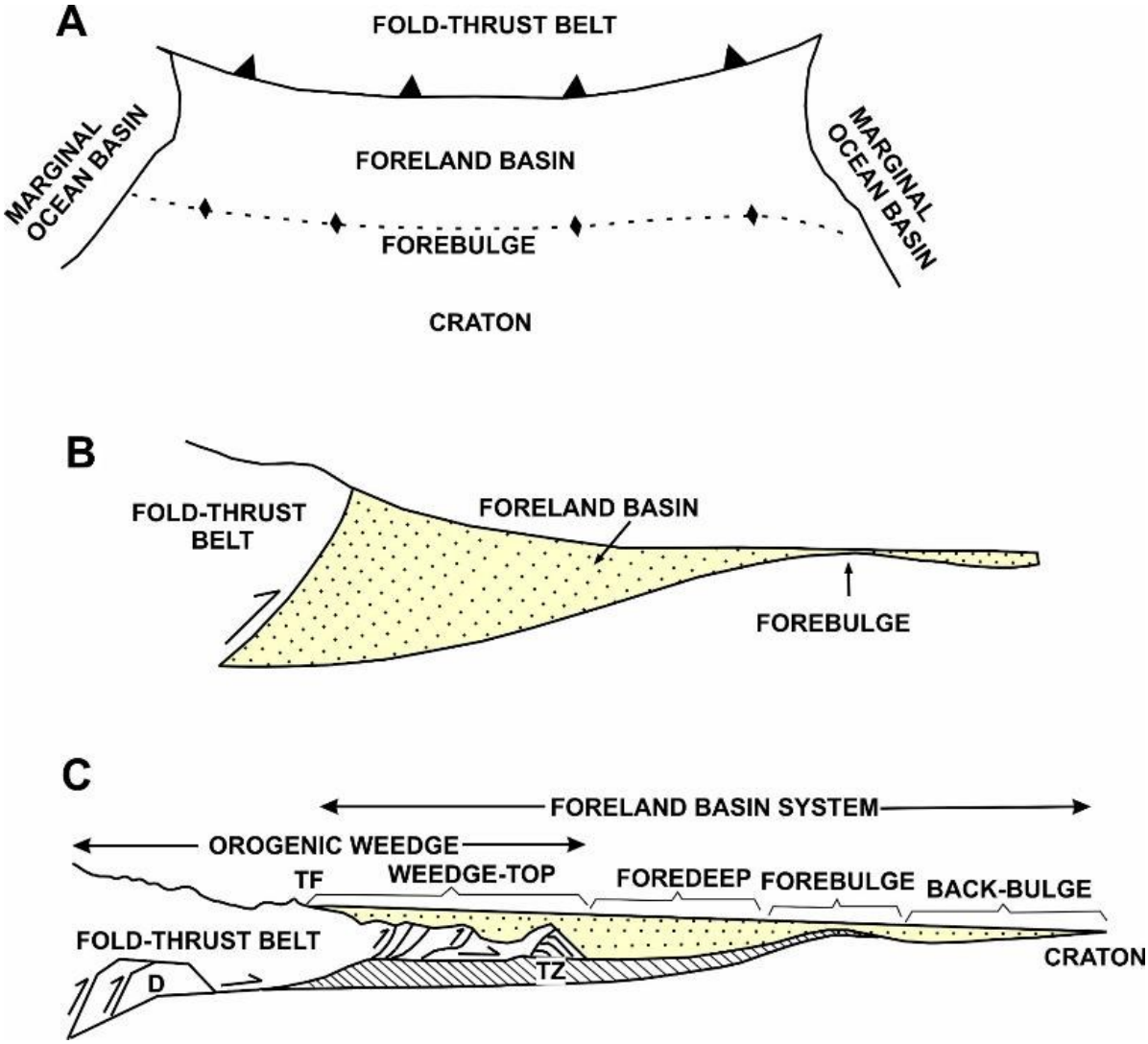

Fig. 1.2. (A) Schematic diagram showing a pair of oceanic basins bounding the foreland basin (B) The cross-section geometry of the foreland basin after the interaction with the fold-thrust belt. (C) the foreland Basin system with the significant components of the wedge-top, foredeep, forebulge and back-bulge depozones. The diagram is modified from DeCelles and Giles, (1996).

Flexural isostasy is also applicable for the and relatively shallow foreland basins as the narrower Alpine foreland basins of Europe (Mascle and Puigdefâbregas, 1998), which is formed by the relatively younger lithosphere that was further developed by Mesozoic rifting activity. Moreover, the topographic loading with the orogenic wedges and with the sedimentary fill of foreland basins, more external forces work on the lithosphere, including slab-pull, slab-detachment and slab roll-back, are important in shaping the geometry of pro wedge and retro wedge foreland basins (Ziegler et al., 2002) (Fig. 1.3). Depending on these activities and forces acting on the foreland basins, the different loading

components and forces are presented by the combined system of vertical loads, shear forces, and bending moments (Fig. 1.3) (Ziegler et al., 2002).

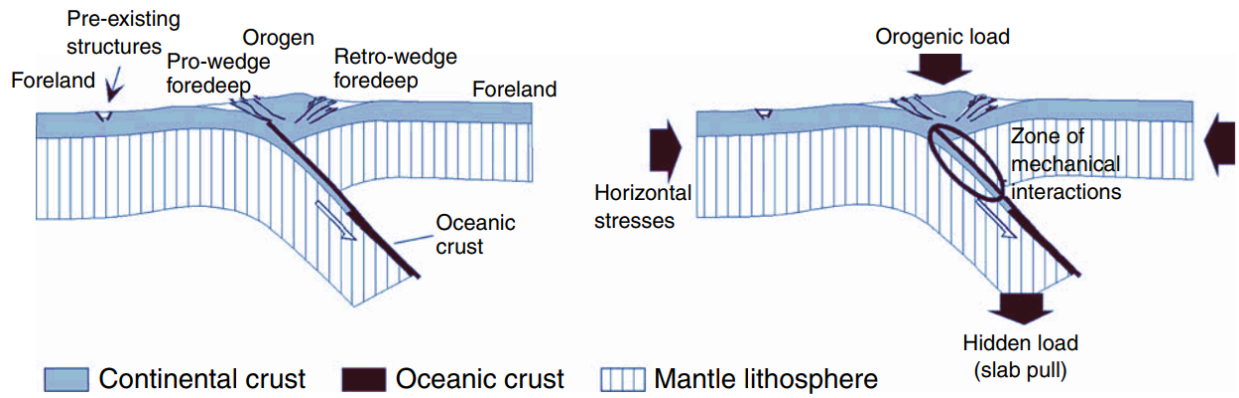

Fig. 1.3. Role of the forces to control the sinking of the retro- and pro-wedge foreland basins when the mechanical coupling between the lower and upper plate occurs (modified from Ziegler et al., 2002).

The present study on Central Mediterranean subduction zones with the crucial case in the Sicily Channel, gave a great understanding of the general processes that govern plate tectonics (Pepe et al., 2010). The Sicily Channel has a complex characterization with a series of relief highs and lows, rift basins, and volcanic structures (Civile et al. 2014; Cavallaro et al., 2017; Fedorik et al., 2018; Lodolo et al., 2019; Civile et al., 2021; Milia et al., 2021; Volpi et al., 2022; Civile et al., 2021; Maiorana et al., 2023; Micallef et al., 2024; Civile et al., 2024). Due to its complex nature of development, it is a useful study to elucidate a key frontier for the geodynamical setting in the Central Mediterranean and it has also submarine prolongation of the Apennines-Maghrebides orogenic belt within the African Plate foreland basin (Fig. 1.4).

The presence of the Pelagian Block which is known as part of the African continental plate is driven with the association of collision with the Eurasian plate and it is also making an interesting factor to further complicate the tectonic events of the Sicily Channel (Carminati et. al., 2010; Camfort et al., 2020). This collision caused in the development of the Apennines-Maghrebides orogenic belt, which crops out in northern Tunisia and Sicily (Carminati and Doglioni, 2005). One of the main challenges

in understanding subduction zones, particularly in complex regions as the Central Mediterranean, is the reconstruction of pre-orogenic paleogeography.

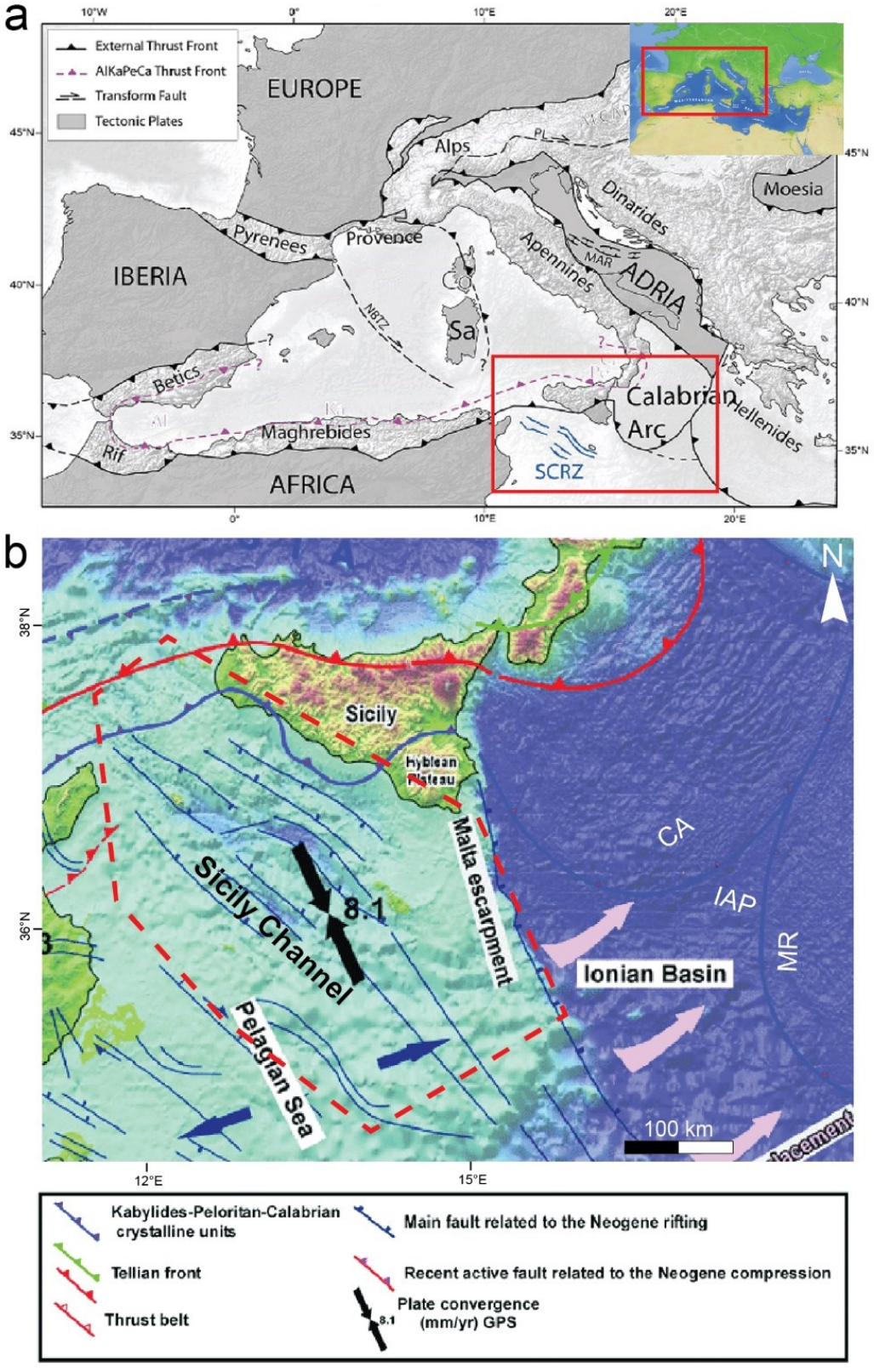

Fig. 1.4. (a) Illustrates the tectonic map of the Western and Central Mediterranean Sea (taken from Le Breton et al. (2021). (b) Structural features and the geodynamic setting of the Sicily Channel with the representation of main thrust fronts (Billi et al., 2011; Faccenna et al., 2011; Catalano et al., 2013; Gharbie et al., 2014). The dotted polygon in (b) displays the main area of focus in this thesis. CA: Calabrian Arc; IAP: Ionian Abyssal Plain; MR: Mediterranean Ridge.

In such cases, tectonic history is mostly masked by long-duration tectonic activity, which caused reshaping and incorporation of the originally existing geological features in the orogenic belts. These make a very difficult situation to reconstruct the original configuration of the plates and other tectonic features at the onset of subduction.

Located in the North African margin, the Sicily Channel is a foreland-foredeep-chain system that includes Sicilian Maghrebian chain, the Gela foredeep, and the Pelagian foreland (Fig. 1.4b) (Argnani, 1990; Butler et al., 1992; Civile et al., 2010; Catalano et al., 2013; Civile et al., 2021). Recent complex tectonic activities including extensional-compressional events in the Sicily Channel have been recognized which are responsible for developing a set of rift basins, such as Malta, Pantelleria, and Linosa basins that are drifted towards the central rift system of the channel and the Sicilian Fold and Thrust Belt (Dart et al., 1993; Argnani, 1990; Catalano et al., 1995; Sulli 2000; Civile et al. 2010; Ferranti et al., 2019; Civile et al., 2021; Milia et al., 2021; Volpi et al., 2022; Maiorana et al., 2023, 2024). Widespread anorogenic volcanism has occurred in the Sicily Channel mainly in Plio-Pleistocene times (Rotolo et al. 2006; Lodolo et al., 2012, 2019; Civile et al., 2008; Maiorana et al., 2023; Micallef et al., 2024). The volcanism and the extensional structures of these basins are connected (Civile et al., 2018; Lodolo et al., 2012; Maiorana et al., 2023; Micallef et al., 2024). All these basins have been the subject of very intensive geological investigations, suitable to offer valuable insights into the tectonic evolution of the region (Reuther & Eisbacher, 1985; Boccaletti et al., 1987; Cello, 1987; Argnani, 1990; Catalano et al., 1995; Civile et al. 2010; 2021; Maiorana et al., 2023).

Moreover, the Ionian Sea to the east is preserving the transition from oceanic to continental as well as the incipient collision stage with (possible) remnant ocean (Stern, 2002; Stern and Gerya, 2018). The region between the African and Eurasian plates is characterized by mixed continental and

transitional oceanic lithosphere; hence, it acts as a perfect natural laboratory to explore the early stages of continent–continent collision. Both the areas (Sicily Channel and Ionian Sea) (location in Fig. 1.14b) have also experienced inversion tectonics which is evidenced by the basins present in these areas (Gamberi and Argnani, 1995; Sulli, 2000; Cavallaro et al., 2017; Civile et al. 2021; Chizzini et al., 2022; 2023; Maiorana et al., 2023). The interplay of the kinematics of the Maghrebian collision zone and the transfer zone in the Ionian Sea is often linked to the inversion tectonics in the Sicily Channel (Gamberi and Argnani, 1995; Civile et al. 2021; Maiorana et al., 2023).

The Adriatic region is another region of the Central Mediterranean Sea which is well defined by the polyphase tectonic repetitive events for the basin formation with the association of normal faults that are reworked or reactivated by compressional deformation (Scisciani, 2009; Pace et al., 2015; Scisciani et al., 2019; Chizzini et al., 2022, 2023) which are related to a tract of the Apenninic-Maghrebian fold-and-thrust belts with trends almost orthogonal the trends of the same belt in Sicily. The researches which are currently carried out not only provide further understanding of the geodetic deformations that arise from the African and Eurasian plate convergence process, but they also provide added insight into the process of change from oceanic to continental subduction. Ongoing research, such as that in the Sicily Channel, helps geologists unravel the deep mysteries of subduction, providing forth new insight on the processes that shape our planet and the hazards accompanying these great geological forces.

Thus, considering the Sicily Channel as the main case study to decipher the complexity of the tectonics in the lower continental plate associated with a collisional orogen, the main aims of this thesis are:

1. to better define the complexity of the tectonics of the subducting plate (African plate) in its northern margin (Sicily Channel) during the phase of collision.
2. to study the evolutionary history, geometry and deformation timing in the foreland areas of Sicily Channel and the adjacent orogenic wedge with a special focus on their interaction.

3. to draw a relationship between the geophysical characters, volcanism and crustal thickness variation from foreland areas to fold-and-thrust belt.
4. to improve the tectono-stratigraphic features of the Sicily Channel as relate to deep crust by defining a velocity model for key seismic reflections and analysis of potential and heat flow fields.
5. starting to approach and attempting to compare the Sicily Channel and Adriatic foreland area to evidence the similarities and differences in their tectono-stratigraphic evolution.

1.3. Thesis summary

1.3.1. Review of the Plio-Quaternary structures of the Sicily Channel (Chapter 3)

The origin and the tectonic evolution of the Sicily Channel is connected to the complex geodynamic history of the Central Mediterranean (Finetti 1984; Jongsma et al. 1985; Reuther and Eisbacher 1985; Ben Avraham et al. 1987; Boccaletti et al. 1987; Cello 1987; Finetti and Del Ben 2005; Argnani 1990; Corti et al., 2006; Civile et al., 2021). An extensive investigation of the Plio-Quaternary structures will be carried to decipher the interplay of extensional, compressional, and transpressional tectonic regimes in the Sicily channel from Late Miocene to the present times (details in chapter 3). The investigation will proceed with the aid of the extensive literature review and map repositories to provide an overview of the tectonic events (in the form of tectonic evolutionary maps) that occurred during the Late Miocene/Pliocene to Holocene in the whole Sicily Channel. This chapter is part of a paper submitted to the special edition of the BSGF-Earth Sciences Bulletin with the title “Recent evolution of the Mediterranean realm: Exploring the links between deep and shallow processes in a plate convergent setting”.

1.3.2. Polyphase deformation chronology in the NW Sicily Channel (Chapter 4)

The interface between the preexisting extensional and compressional structures plays a vital role in the evolution of the orogenic systems. Sicily Channel represents such a complex structural style in its NW part where the preexisting normal faults begot from the older rifting events and migrated from the Sicily Channel Rift Zone (SCRZ) and interacted with the Sicily Maghrebian Thrust Belt (SMTB) (Argnani et al., 1986; Antonelli et al., 1988; Corte et al., 2006; Civile et al., 2014). This interaction gave birth to the the inversion structures in the sedimentary infill of the basins as reported by various authors (Gamberi and Argnani, 1995; Catalano and Milia, 1990; Sulli, 2000; Zitellini et al., 2021). We attempt to define, and refine, the chronology (From early Pliocene-Present) of the polyphase deformation events that have hit the three Neogene sedimentary basins in this unique area where the extensional and compressional regimes interface and intersect (see details in chapter 4). To achieve the results the key seismic reflection profiles (CS89-01C2, G82-63 and G82-45) were interpreted with a special focus on Plio-Quaternary sedimentary strata.

1.3.3. Velocity model building for CS89-01 seismic reflection profile (Chapter 5)

The building of velocity models is an essential way to convert the seismic reflection profile or their interpretation into depth so as to get an exact and clear view of the subsurface stratigraphy and structural features like folds and faults (Beche et al., 2007); a geological model can be defined. The depth-converted horizons are in turn an advantageous component to form the crustal model along a seismic profile. We will attempt to build the velocity models for the CS89-01 seismic reflection profile which is a key profile traversing along SSE-NNW in the Sicily Channel (Fig. 5.1). The models will be utilized to convert horizons of the interpretation of the line into depth by utilizing the stacking velocities associated with the line (Sheriff and Geldart, 1995; Etris et al., 2001) (see details in chapter 5).

1.3.4. Tectono-Stratigraphic, Gravimetric and Heat flow along Pantelleria Graben (Chapter 6)

The NW trending Pantelleria Graben being the hub of volcanism in the Sicily Channel (Civile et al., 2010; Lodolo et al., 2012; Jordan et al., 2018., White et al., 2020; Micallef et al., 2024) will be analyzed in the tectono-stratigraphic domain by interpreting the CS89-01, Pant-3 seismic reflection profiles with the emphasis on the fault activities in the Plio-Quaternary strata. Also, the gravimetric and heat flow anomalies will be investigated along and across the grabens considering the aforementioned seismic profiles to better define the connection between the volcanic bodies, Moho and the trends of the geophysical data (see details in Chapter 6).

1.2.6. Foreland areas and orogenic wedge in the Adriatic Sea (METIQ project) (Chapter 7)

A comprehensive literature review of the Quaternary fault systems will be carried out in the Puglia and Marche-Abruzzo regions of the Southern-Central Apennines (details in chapter 7). This chapter provides insights into the main extensional fault systems and the main Appenine frontal thrust in these regions.

We have contributed to the Modello Evolutivo del Territorio Italiano nel Quaternario (METIQ) project and reviewed the kinematics, geometry, timing and surface evidence of the tectonic features and added important Quaternary fault systems in the GIS database. This is a first step for comparing the lower plate behaviour in two different geodynamic settings of the same convergent system driven by the collision of Africa-Adria and Europe plates.

Chapter 2

Data sets and Methodology

2.1 Data and methods for Seismic reflection profile interpretation

This Chapter highlights the details of stratigraphic and structural interpretation of the selected multi-channel seismic reflection profiles available for the Sicily Channel. The seismic profile were mainly in raster format and their interpretation was accomplished in the graphic software Adobe Illustrator® software with the integration of a grid of seismic lines, well data and the existing literature data. The morphobathmetric data sourced from EMODnet (http://www.emodnet-bathymetry.eu/) DTM (2022) significantly contributed to provide information of seafloor topography and to identify the position of recent structural features. The use of an integrated data set required the creation of a dedicated database in GIS environment which allowed to understand the overall geological scenario of the area of interest and construct a tectonic map.

The seismic reflection profiles in the key area of NW offshore of Sicily and the borehole data were obtained from the publicly available 'Visibility of petroleum Exploration data in Italy' (ViDEPI) database (http://www.videpi.com). Then, the SEG-Y format of the Pant-3 line was kindly made available by the National Institute of Oceanography and Applied Geophysics (OGS), Trieste, Italy while, the parts of the CS89-01 line were kindly provided by the Institute of Marine Sciences of the National Research Council of Italy (CNR-ISMAR). The key acquisition parameters and the processing steps of these profiles are mentioned in Tab. 1. Physical characters of the reflectors including amplitude, frequency and continuity and the reflection terminations were considered to identify the major seismic facies and unconformities and related seismic stratigraphic sequences (Vail et al., 1977; Roksandić, 1978; Plint et al., 2000; Abbas et al., 2018; Al-Masgari et al., 2021).

For constraining the stratigraphy of the SE portion of the study area, Riccio Sud-01, Remo Nord-01 wells were used while Paola-01, Piera-01, Orlando-01, Samantha-01, Tulia-01 and Noemi-01 wells were considered to define the stratigraphic set up of the NW part (Fig. 2.1).

Tab. 1.1: The acquisition parameters and the processing steps.

Line name	G82-45, G82-63	Pant-3	CS89-01
Length (km)	32, 48.7	44	326
Vessel	M/V Artic Seal	R/V OGS-Explora	OGS Explora
Recording date	1982	2009	1989
Sample rate(ms)	2	2	4
Fold (%)	4800	3000	3000
Source type	Airgun array	Sleeve guns	Airgun array
Source depth (m)	6	Not available	6
Streamer depth (m)	16.5	Not available	12
Streamer length(m)	2400	1600	2975
Shot interval (m)	25	25	50
Group interval (m)	25	12.5	25

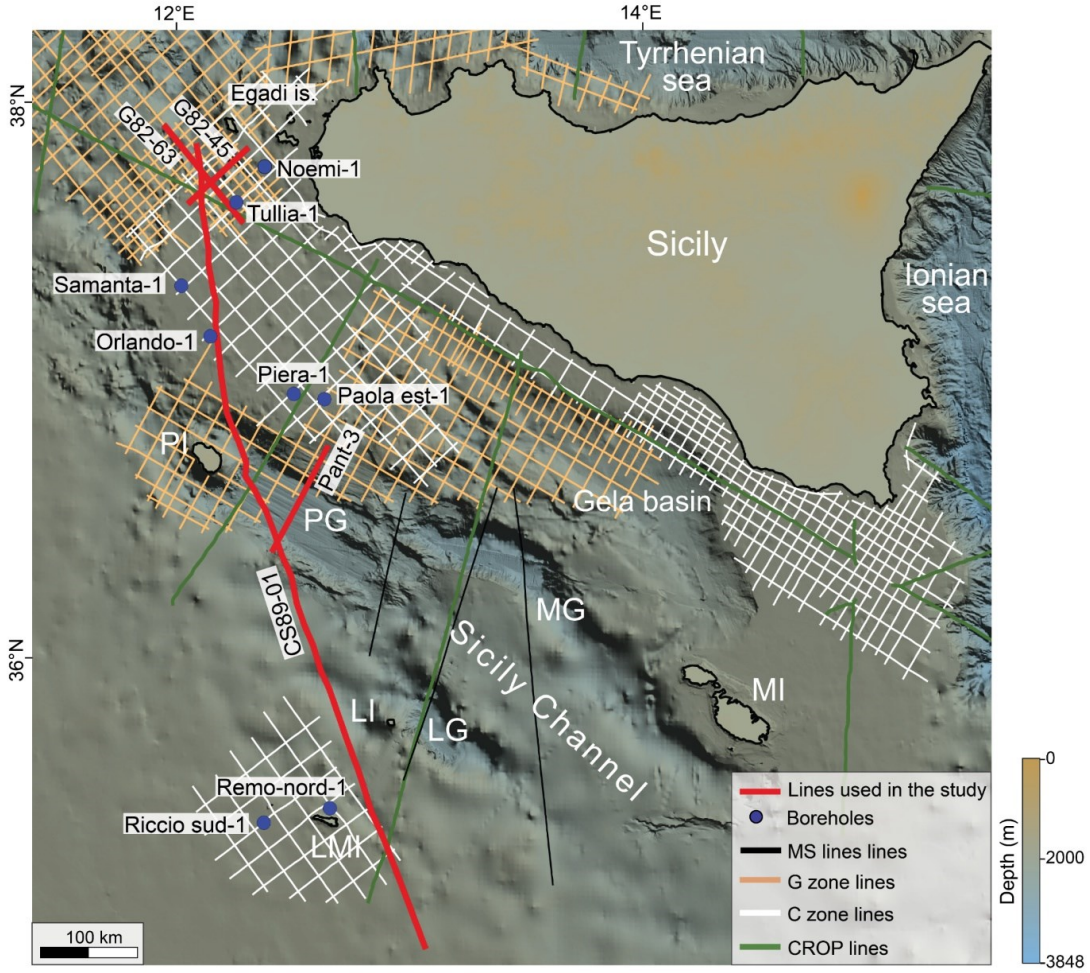

Fig. 2.1. Location of the multichannel seismic reflection profiles and boreholes used in this study. Bathymetry data extracted from EMODnet (http://www.emodnet-bathymetry.eu/) DTM (2022). AB:

Adventure Bank; LG: Linosa Graben; LI: Linosa Island; LMI: Lampedusa Island; MG:Malta Graben; MI: Malta Island; PG: Pantelleria Graben; Pantelleria Island.

Among these wells Orlando-1, Samantha-1 and Tulia-1 were converted to Two Way Travel (TWT) time and projected on the nearest CS89-01C2 and G82-63 seismic reflection profiles. The visualization of the lithology thickness and depth of these well logs in time was possible only by taking into account the velocities (Stripling, 1958; Brie et al., 1998). The Tulia-1 well was converted to time using the sonic log velocities reported in microsec/ft and the standard velocities were assigned to each lithology section for Orlando-1 and Samanta-1 wells to convert them into time (Christensen and Mooney, 1995) as the sonic velocities are not reported for them. The primary stratigraphic contacts in the time domain were confirmed by comparing the reflectors with high acoustic impedance to the significant lithological contacts in well logs. This was done in order to determine the primary horizons in seismic lines and to calibrate seismo-stratigraphic units.

2.1.1 Overview of the Seismic reflection method and its principles

The seismic reflection method is the widely used technique for subsurface imaging and data collection (Sheriff and Geldart, 1995; Ashcroft, 2011; Bertoni et al., 2020). In this method, the sound waves propagate in the sub-surface visualized as wavefronts or raypaths, interact with different rock interfaces depending on the variable rock properties (acoustic impedance, contrast, etc.) (Hill and Rüger, 2019; Al-Masgari et al., 2021) (Fig. 2.2).

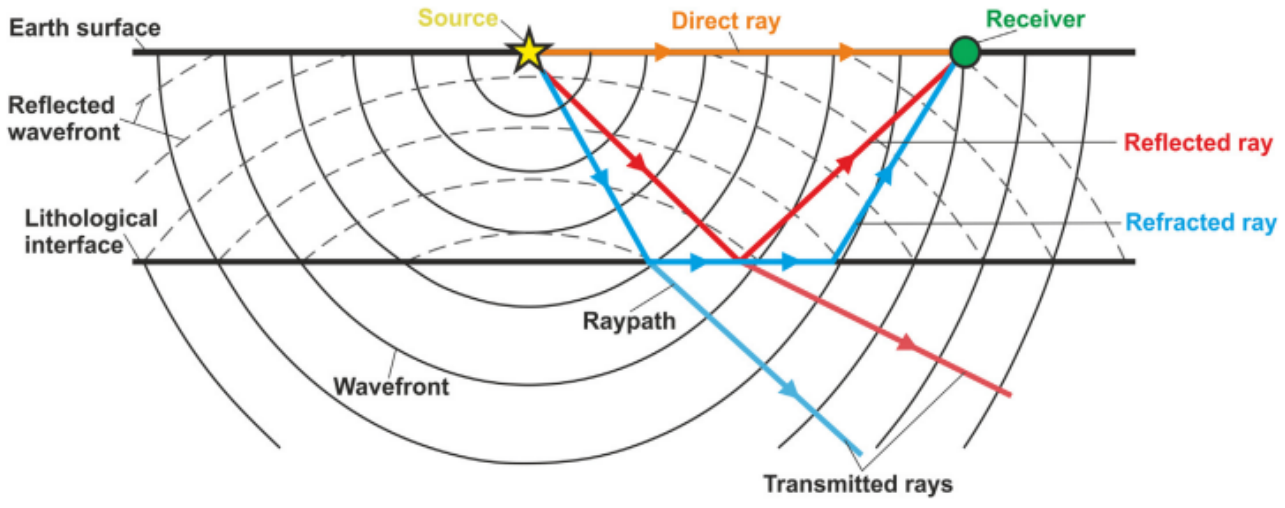

Fig. 2.2. Illustration showing the source of seismic wave and how it is reflected or refracted at rock interface and finally recorded by the receiver at the surface (after Ashcroft, 2011).

Some of the waves get bounced back to the surface and some of them refract and rest of them are transmitted through a rock interface (Ashcroft, 2011) (Fig. 2.2).

The refracted or reflected energy is recorded by geophones in terrestrial surveys and hydrophones (contained in streamer cable) in marine surveys. The latter usually involves the use of air gun to generate source waves (Fig. 2.3) (Soubaras, 1996). The recorded energy at the geo-hydro-/phone is processed to remove the seismic noise produced by diffractions, multiple reflections, direct and refracted surface waves, etc

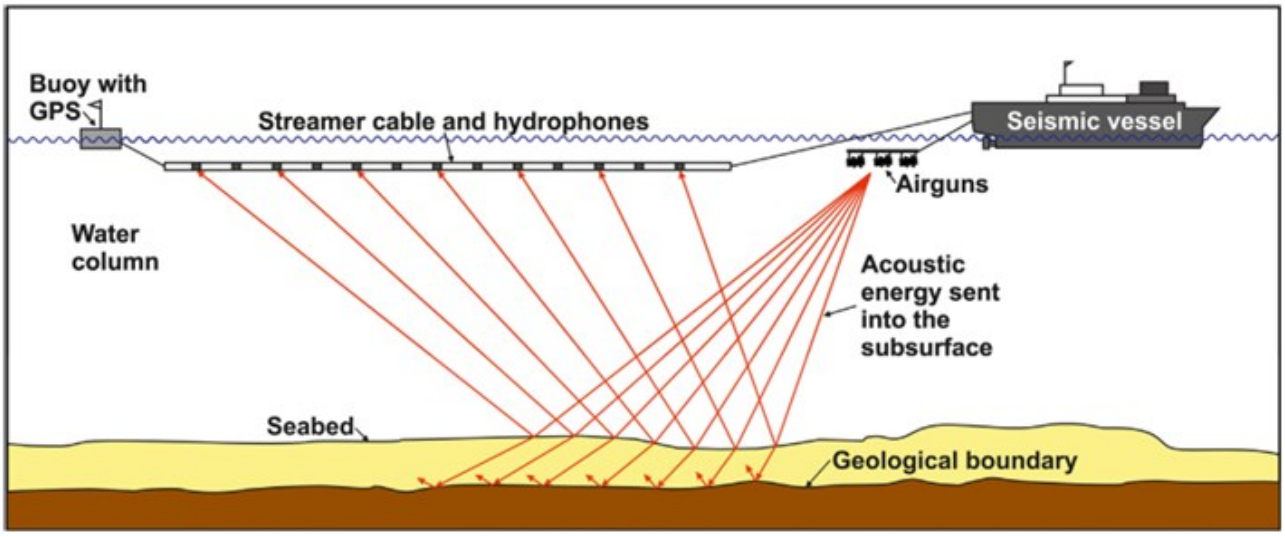

Fig. 2.3. The set up of 2D marine survey involving the use of air guns as seismic source and hydrophones as receivers (after Cox et al., 2020).

The processing involves several steps which are classified into four groups: data preparation, data correction, data reduction and data enhancement (Cox et al., 2020) (details in Fig. 2.4). After performing the processing steps the data becomes finally suitable for analysis and interpretation for unveiling information about the tectonic structures, stratigraphy, fluid migration, volcanism so on and so forth (Biondi et al., 2006; Bond et al., 2012).

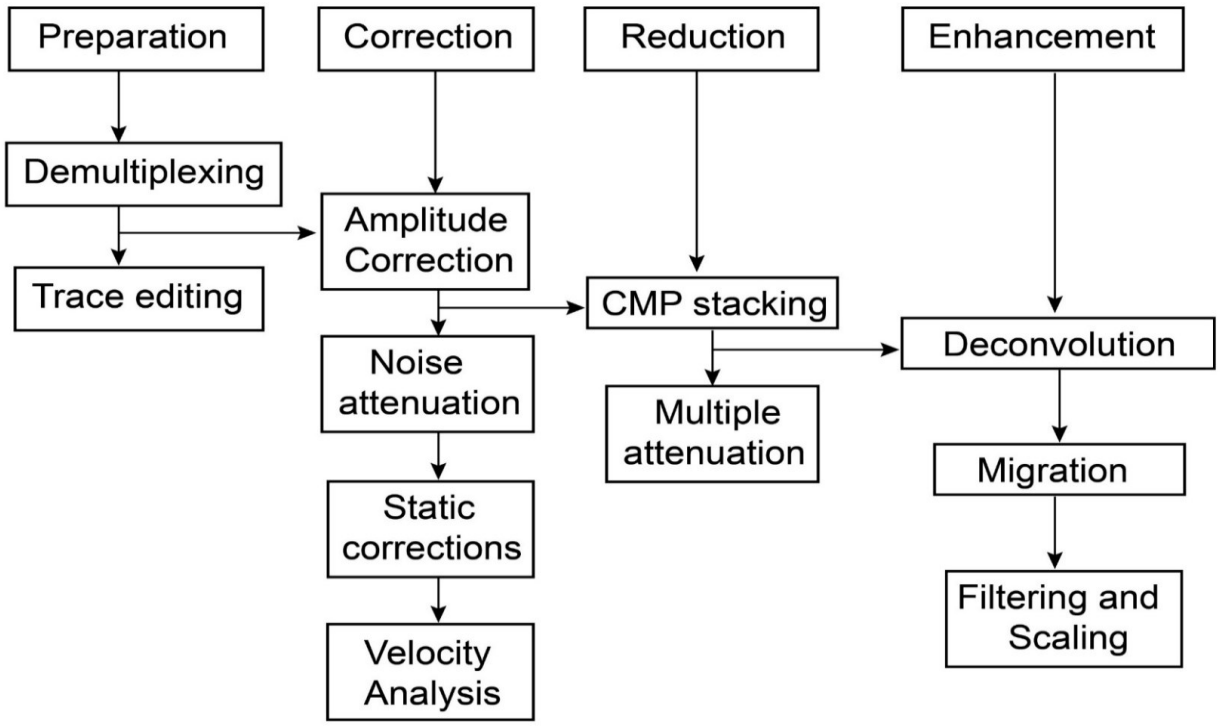

Fig. 2.4. Simplified workflow of the processing steps to remove the seismic noise from the data to create an interpretable image. Depending on the desired data the steps can be re-sequenced or skipped (after Dondurur, 2018; Cox et al., 2020).

The variation of seismic reflections is based on the reflection parameters: configuration, continuity, amplitude, frequency, and shape of the reflections (Van Wagoner et al., 1990) understand the basin infill architecture and with the integration of well data different seismic stratigraphic sequences can be marked (Fig. 2.5a). The reflection terminations (onlap, downlap, toplap, truncation) are pivotal to mark the unconformities inside or between a seismic sequence depending on their termination pattern against the contact (Mitchum and Vail, 1977; Vail, 1987; Al-Masgari et al., 2021; Posamentier et al., 2022) (Fig. 2.5b).

Information from the data is taken as per the needs of the interpreter. For instance, the structural geologist focuses more on the tectonic features and the sedimentologist is more interested in extracting information about sedimentary environments and facies. The foundation of good seismo-stratigraphic interpretation to identify seismic sequence is the proper identification of seismic facies and the reflection terminations (Vail, 1987; Al-Masgari et al., 2021; Posamentier et al., 2022).

a

Seismic facies unit	Seismic examples (vertical scale represents 100 ms)	Line drawing interpretations	Amplitude and frequency characteristics	Spatial distribution/ typical occurrence
Parallel discontinuous	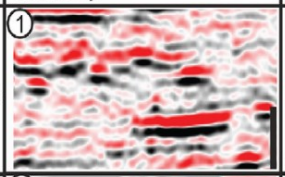		Low to high amplitude, medium frequency	Occurs at shallower depths (alluvial plain sed.)
Sub-parallel fairly continuous	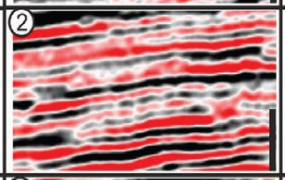		High amplitude, high frequency	Occurs above the prograding clinoforms (delta sed.)
Clinoform - Continuous, discontinuous alternating	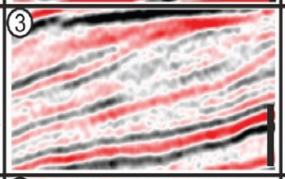		Medium to low amplitude, high frequency	Occurs between deep and shallow depth sediments (prograding shelf-margin slope)
Hummocky discontinuous	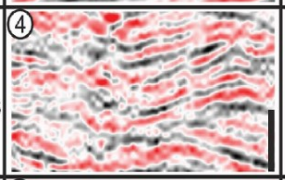		Medium to low amplitude, high frequency	Occurs between deep and shallow depth sediments (prograding shelf-margin slope)
(Sub-)parallel continuous	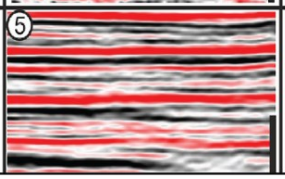		Medium to high amplitude, low to high frequency	Present within and just above of the half-graben infill

b

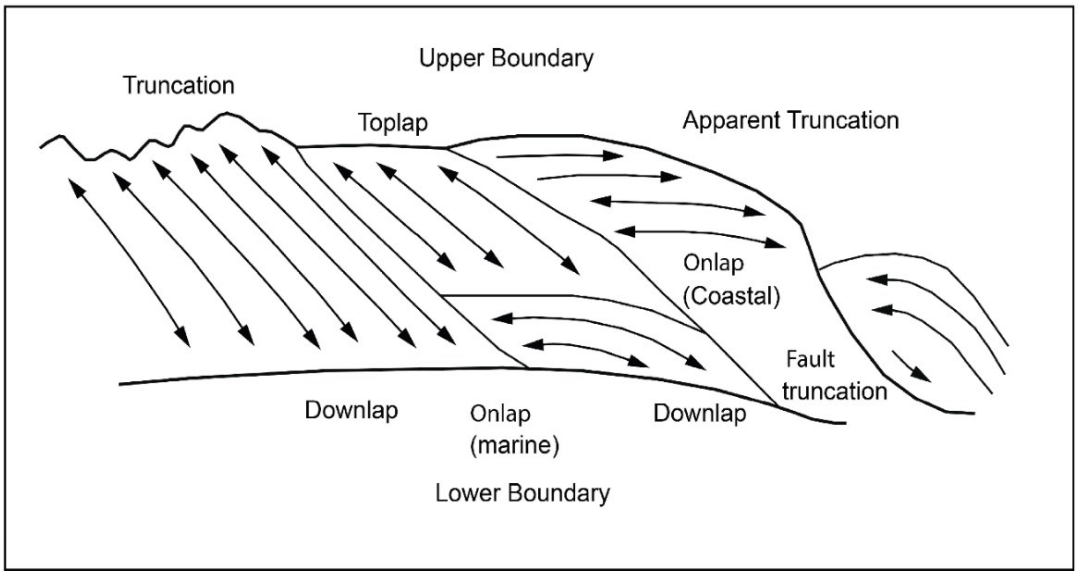

Fig. 2.5. (a) Reflection parameters (taken from Balázs et al. (2016). (b) the reflection terminations at Upper and Lower boundaries (modified from Emery and Mryes, (1996); Al-Masgari et al. (2021).

2.2. Data and methods for gravimetric and heat flow analysis

To assess the lithospheric thickness and the relationship of gravity and heat flow anomalies with the volcanism in the study area, especially in Pantelleria Graben, the Bouguer and Free air gravity anomaly and heat flow maps and crustal models were generated. The data for gravity maps was derived from 'The World Gravity Map (WGM2012)' (https://bgi.obs-mip.fr/gravity-maps/) provided by the Commission for the Geological Map and available in the resolution of 2' × 2'. The WGM2012 includes Bouguer, free-air, and isostatic anomaly maps computed from Earth global gravity models EGM2008 and DTU10 at a worldwide scale in the spherical model along with the 1'x1′ resolution terrain corrections considering the contribution of atmosphere, land, oceans, lakes etc. (Bonvalot et al., 2012). The heat flow data was taken from 'The Global Heat Flow Database (GHFDB)' (https://www.ihfc-iugg.org/) which is the worldwide compilation of world heat flow data managed by the International Heat Flow Commission (IHFC) commenced since 1963.

The 2D gravimetric model was produced along seismic transects CS89-01 and Pant 3, which were first interpreted in the structural and stratigraphic domain in this PhD research. The CS89-01 line passes across the Pantelleria Graben and stretches to Adventure Bank and the Pant-3 crosses the graben orthogonally. The seismic horizons and the faults marked on them were converted to depth in order to insert the depth of Moho and construct a crustal models. In the generated crustal models, the Moho depth was assumed as per the results of Cassinis et al. (2003); Grad et al. (2009). (Fig. 2.6). The 2D gravity and heat flow maps were constructed in GIS environment in the WGS84 geographic reference coordinate system. The trace of the navigation along the acquisition transects of the seismic reflection profiles were also imported in the GIS environment to produce gravimetric and heat flow curves with respect to their shot points.

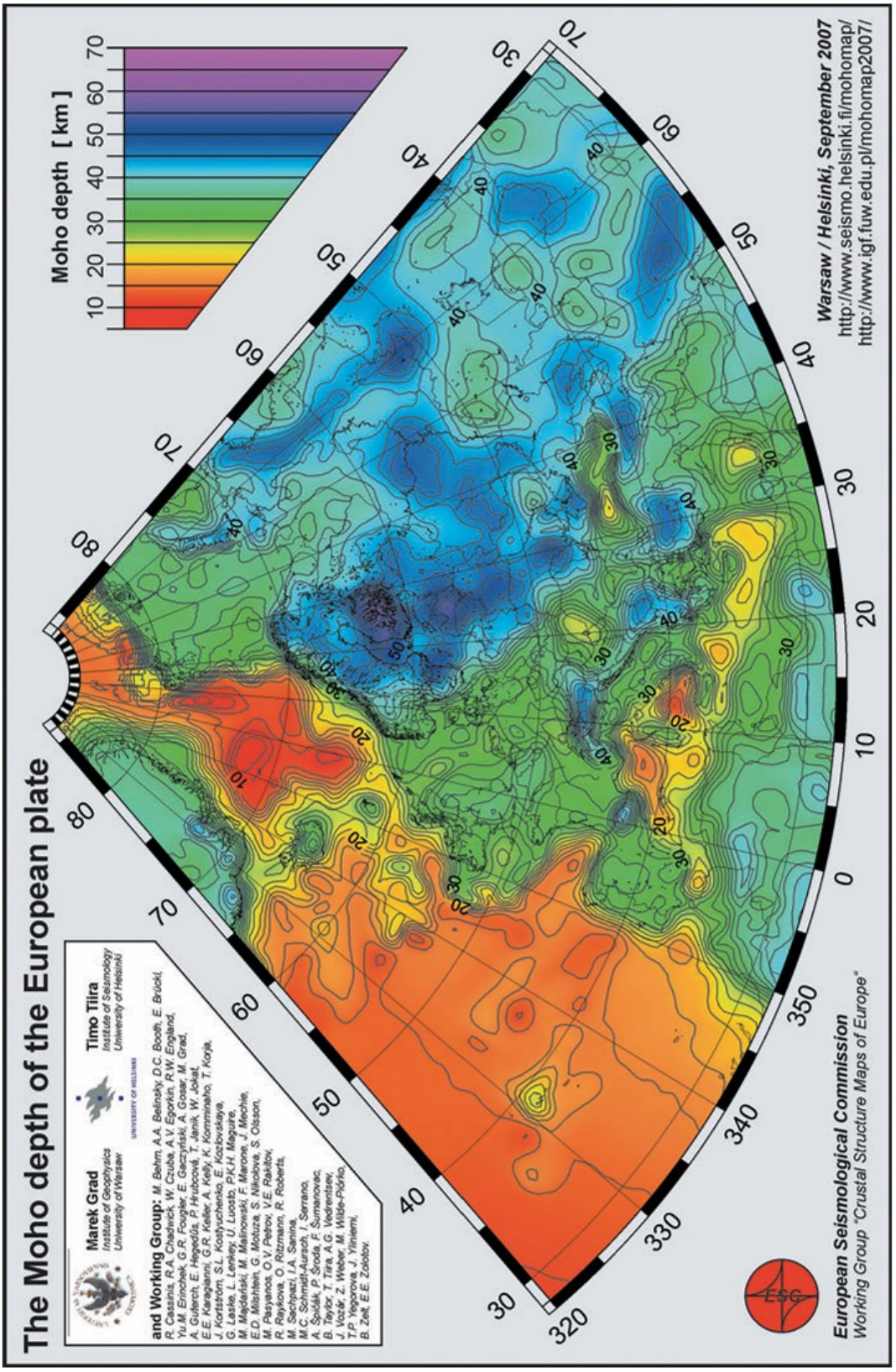

Fig. 2.6. The Moho depth map of the European Plate (after Grad et al., 2009).

Chapter 3

Review and detailed analysis of the Plio-Quaternary tectono-stratigraphic architecture and evolution in the Sicily Channel (Central Mediterranean)

Note: This Chapter is the paper in preparation for submission to the special edition of the BSGF-Earth Sciences Bulletin titled "**Recent evolution of the Mediterranean realm: Exploring the links between deep and shallow processes in a plate convergent setting**". editors Christian Gorini, Anouk Beniest, Andréa Billi, Nicolas Chamot-Rooke, Jacques Déverchère, Agnes Maillard and Juan I. Soto**: Chizzini, N., Maiorana, M., Qadir, A., Le Breton, E., Palano, M., Artoni , A., Polonia, A., Sulli, A., Gasperini, L., Torelli L. Review and detailed analysis of the Plio-Quaternary tectono-stratigraphic architecture and evolution in the Sicily Channel (Central Mediterranean).**

Abstract

Although foreland regions are often perceived as stable zones, the Sicily Channel—situated in the central Mediterranean between Sicily and Tunisia and regarded as the continental foreland of the Sicilian Maghrebian chain—reveals significant tectonic complexity. It comprises three major tectonic troughs (Pantelleria, Malta, and Linosa grabens) formed by the ongoing extension of Africa. This area includes a foreland-foredeep-chain system encompassing the Pelagian foreland, the Gela foredeep Basin, and the offshore section of the Neogene-Quaternary Sicilian-Maghrebian chain. Based on an extensive review of available literature, including previously published multichannel seismic reflection profiles and structural maps, we provide a detailed analysis of the stratigraphic architecture and key tectonic features that have influenced the Sicily Channel during the Plio-Quaternary. Furthermore, we assess the timing of these events to gain a comprehensive understanding of the region's Plio-Quaternary tectonic evolution. Our findings demonstrate that the Sicily Channel is not merely a simple rifted foreland zone but is characterized by recurrent extensional and compressional phases during the late Neogene/Plio-Quaternary. This evidence indicates that distinct tectonic regimes can coexist within a foreland area, reinforcing the idea that foreland zones actively record dynamic processes driving lithospheric deformation and are prone to tectonic reactivation.

3.1. Introduction

Foreland basins, commonly considered as the areas ahead the orogens not already affected by accretionary processes, are key tectonic elements in the periphery of orogenic belts, forming in direct response to continental under thrusting (Allen et al., 1986; Allen and Allen, 1990; Cloetingh et al., 1994; Ziegler et al., 1994, 1995; DeCelles and Giles, 1996; DeCelles, 2012; Cloething et al., 2015; Royden and Faccenna, 2018). In the past few years, a number of marine campaigns and studies have been carried out in the Sicily Channel with the goal of determining the main tectonic structures affecting this region, their timing of activity, and ultimately suggesting a geological evolution for this area (Finetti, 1984; Argnani et al., 1986; Antonelli et al., 1988; Lentini et al. 1990, 1994, 1996; Catalano et al., 1996, 2000; Finetti and Del Ben, 2005; Civile et al., 2008, 2010, 2014, 2016; Cavallaro et al., 2017; Meccariello et al.; 2017; Civile et al., 2018; Fedorik et al., 2018; Ferranti et al., 2019; Civile et al., 2021; Volpi et al., 2022; Maiorana et al., 2023).

All the recent studies recognized the existence of both contractional and extensional structures in the Sicily Channel. The latter were believed to be positive inverted faults that enucleated from inherited Mesozoic extensional discontinuities. These structures were explained as being caused by the compressive stress exerted from the surrounding fold-and-thrust belts (Egadi Thrust Front-ETF and Gela Thust System-GTS) transmitted to the Sicilian foreland and more generally, as related to the ongoing Africa-Europe convergence process (Civile et al., 2021; Cavallaro et al., 2017; Maiorana et al., 2023). Nevertheless, all the works focusing on the Sicily Channel limited their investigation strictly on single sectors of this complex area. Consequently, an overall overview is still lacking. The goal of this research is to fill this gap by offering these important but missing documentations. Based on an extensive review of the available literature, including already-published multichannel seismic reflection profiles and structural maps, we examine the major tectonic structures located in the Sicily Channel discussing also their timing, including the Capo-Granitola Sciacca (CGFSZ) offshore sector and the Adventure Plateau, as well as the frontal part of the GTS (Fig. 3.1), in order to provide a more

comprehensive and updated structural map of the Sicily Channel and the surrounding areas. We also focus on an overall Plio-Quaternary evolution of the Sicily Channel in relation with the Mesozoic paleogeography of this area highlighting the main tectonic processes that shaped this complex area, thus providing some new general insights on foreland tectonics that could be extended for other study of foreland areas worldwide.

3.2. Geological setting and post-Messinian evolution of the Sicily Channel

3.2.1. Geographic location and structural evolution

The Sicily Channel is a wide, shallow-water platform that stretches across an area of approximately 250,000 km^2, located between Tunisia and Sicily in the northern part of the African continental plate, or the so-called Pelagian Block or Northern portion of Africa Plate (Fig. 3.1) (Burrollet et al., 1978; Argnani et al., 1986; Butler et al., 1992; Torelli et al., 1998; Lickorish et al., 1999; Holland et al., 2003; Corti et al., 2006; Civile et al., 2014; Cavallaro et al., 2017; Meccariello et al., 2017; Fedorik et al., 2018; Ferranti et al., 2019; Civile et al., 2021; Milia et al., 2021; Volpi et al., 2022; Maiorana et al., 2023, 2024; Micallef et al., 2024; Civile et al., 2024). Reaching its southernmost point near Linosa Island, the Sicily Channel terminates at the West with Adventure Plateau, and at the East with the Malta Plateau (Fig. 3.1).

During the Messinian, the disconnection of the Mediterranean Sea connection to the Atlantic Ocean led to the Messinian Salinity Crisis (MSC- Butler et al., 1995; Roveri et al., 2014; Manzi et al., 2020, 2021; Pellen et al., 2022), a significant event that impacted the paleogeographic and environmental evolution of the Mediterranean region, including the Sicily Channel (Krijgsman et al., 1999; Butler, 2009; Lofi et al., 2011; Roveri et al., 2014; Aksu et al., 2018; Günes et al., 2018; Camerlenghi et al., 2020; Manzi et al., 2020, 2021). This event led to a prominent sea-level drop probably in the order of hundreds of meters (de Alteriis, 1995) and the consequent emersion and diffusive erosion of a large part of the banks/seamounts of the Sicily Channel (Civile et al., 2015; Cavallaro et al., 2017;

Meccariello et al., 2017), as well as the sedimentation of very thick, locally up to 3 km, evaporites in the Ionian Sea to the East (Lofi et al., 2011; Roveri et al., 2014; Haq et al., 2020; Manzi et al., 2020, 2021).

Fig. 3.1. Bathymetric map showing the main structural elements of the Sicily Channel region - AP: Adventure Plateau; ATF: Adventure Thrust Front; CGSFZ: Capo-Granitola Sciacca Fault Zone; SRFS: Scicli-Ragusa Fault System; ETF: Egadi Thrust Front; GTF: Gela Thrust Front; GTS: Gela Thrust System; MG: Malta Graben; LG: Linosa Graben; PG: Pantelleria Graben (after Maiorana et al., 2024, in: Gasparo Morticelli et al., 2015; Civile et al., 2018; Sulli et al., 2021). The localization

of the study area is marked by a yellow dotted box. Bathymetry data from EMODnet (https://emodnet.ec.europa.eu/en); Inset structural map from Le Breton et al. (2021).

In the Late Miocene a strike-slip regime affected this sector of the African plate, as well documented at Lampedusa Island (Grasso and Pedley, 1985; Meccariello et al., 2017). A continental rift-related process, started since the Lower Pliocene and controlled by sub-vertical normal faults, led to the formation of the Malta, Linosa, and Pantelleria WNW-ESE-oriented elongate grabens (Finetti, 1984; Boccaletti et al., 1987; Cello, 1987; Grasso and Torelli, 1999; Carminati and Doglioni, 2005; Civile et al., 2010; Ghielmi et al., 2012; Cavallaro et al., 2017; Meccariello et al., 2017; Civile et al., 2021; Maiorana et al., 2023), potentially with a dextral strike-slip component, especially in Malta and Linosa grabens (Catalano et al., 2009). Changes in asthenospheric flows, along with this Lower Pliocene extensional tectonic phase, prompted the Moho to rise under the major grabens of Malta, Pantelleria, and Linosa; this resulted in volcanic manifestations near the grabens' margins (Maiorana et al., 2023). The scattered anorogenic volcanism is mainly concentrated on the islands of Pantelleria and Linosa (Rotolo et al., 2006; Civile et al., 2013; Micallef et al., 2024), in the Adventure Plateau, and in the Sciacca offshore (Peccerillo, 2005; Rotolo et al., 2006; Civile et al., 2013; Lodolo et al., 2019; Civile et al., 2024; Micallef et al., 2024) (Fig. 3.2).

In the Lower-Upper Pliocene, the ongoing advancing of the GTS triggered a first compressional tectonic stage evidenced by the positive inversion of pre-existing extensional faults, especially in the Madrepore Graben (Civile et al., 2021; Maiorana et al., 2023). A strike-slip transfer zone developed at this time, named Capo Granitola-Sciacca Fault Zone (CGSFZ), which is interpreted by different authors as a wide active lithospheric structure that exhibits left-lateral kinematic movement, crossing the central part of the Sicily Channel (Argnani et al., 1986; Antonelli et al., 1988; Fedorik et al., 2018; Civile et al., 2018; Ferranti et al., 2019; Palano et al., 2020; Civile et al., 2021) (Fig. 3.1).

Throughout the Upper Pliocene to Lower Pleistocene, the region was affected by both extensional regimes relating to the Sicily Channel rifting and compressional regime marked by positive inverted

faults (Civile et al., 2021; Maiorana et al., 2023). Extensional tectonics is still active today, associated with a compressive regime, whose origin has been recently ascribed to a possible plate re-organization and change of subduction polarity (Zitellini et al., 2020; Sulli et al., 2021). An ongoing stretching of the African plate continued to occur, in particular south of the Gela Basin, marked by the development of WNW-ESE to NW-SE-oriented extensional faults (Cogan et al., 1989; Cavallaro et al., 2017).All these events could be related to the fast slab retreat of the Calabrian Arc (Faccenna et al., 2001a, 2001b), potential slab tearing (Arab et al., 2020), and the independent motion and rotation of the Adria Plate relative to Africa and Europe (Le Breton et al., 2017).

3.2.2. Seismicity and geodetic data

Historical seismicity in the Sicily Channel is poorly documented and limited to few small magnitude earthquakes (M<4.7) located close to Pantelleria Island (Fig. 3.2a). Inland Sicily was the locus of destructive earthquakes as the 1963 M_w7.3 Noto valley and the 1968 M_w6.4 Belice events (Guidoboni et al. 2007). Occurrence of moderate historical earthquakes have been documented also along the Sicilian southern coast (1652, 1724, 1727, 1817, 1831), and likely located offshore. Some of these events could be related to volcanic activity of the offshore area, even if there is evidence solely for the 1831, 1891 and 1816-17 seismic sequences (Spampinato et al., 2017 and references therein). Seismic monitoring of the Sicily Channel started in early 80s when a one-component station was installed on Pantelleria islands (Spampinato et al., 2017). Since then, other stations have been installed on Linosa and Lampedusa islands, resulting however in a not optimal network geometry which have also showed discontinuous functioning due to the lack of regular maintenance. Despite these limitations, a set of low-to-moderate earthquakes have been recorded, evidencing a vivid tectonic activity of the channel (Fig. 3.2a) and highlighting two significant fault zones that extend offshore into the Sicily Channel, located to the east and west of the GTS, respectively. The first is to the west and runs from Sciacca to Linosa Island in an NNE-SSW direction, corresponding to the CGSFZ (Figure 1) (Calò and Parisi, 2014; Civile et al., 2018; Fedorick et al., 2018; Ferranti et al.,

2019; Civile et al., 2021). The second is the Scicli Ragusa Fault System (SRFS) (Fig. 3.1) extending from southeast Sicily, through Ragusa, to the offshore Sicily Channel.

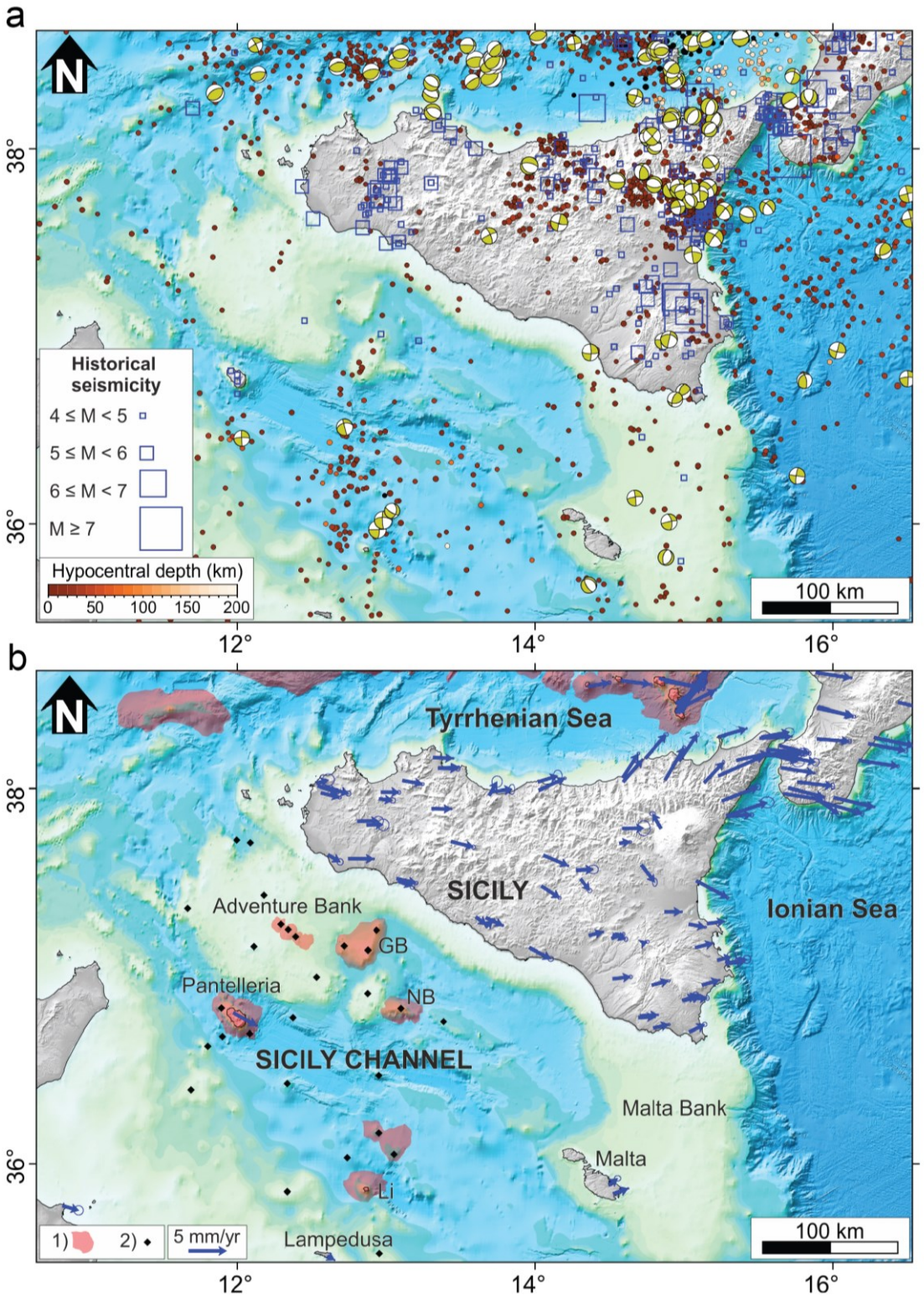

Fig. 3.2. (a) Historical (blue squares) and instrumental seismicity (circles, colored as function of the hypocentral depth) over the study area. Historical seismicity has been collected from the SHARE European Earthquake Catalogue (https://www.emidius.eu/SHEEC/) and Spampinato et al. (2017) and

cover the 1000-1985 time interval. Instrumental seismicity is from ISIDE INGV database (https://terremoti.ingv.it/iside; ISIDe Working Group, 2007) and cover the Jan. 1985 - Aug. 2024 time interval. Focal mechanisms are from the GCMT (https://www.globalcmt.org; Ekström et al., 2012) and the TDMT (https://terremoti.ingv.it/en/tdmt; Scognamiglio et al., 2006) catalogs. b) Geodetic velocity field (blue arrows) referred to a fixed African plate frame. Other symbols are: 1) volcanic fields (from the EMODnet database; https://emodnet.ec.europa.eu); 2) volcanic centers (Wurtz et al., 2015; Lodolo et al., 2019). Abbreviations are as following: Be, Belice Valley; HP, Hyblean Plateau; GB, Graham Bank; NB, Nameless Bank; Li, Linosa; La, Lampedusa. Bathymetry data from EMODnet.

The entire fault zone has shown evidence of left-lateral strike-slip activity (Catalano et al., 2008), which is associated with the formation of bend geometries that are both restraining and releasing between the various en-echelon segments (Grasso and Reuther, 1988). Available focal mechanisms for the Sicily Channel (for events with M_w>4) show prevailing strike-slip features; few events with normal mechanism have been located immediately southward of Malta islands, while events with reverse mechanism are located in south-eastern Sicily (Fig. 3.2a).

The geodetic monitoring of the Sicily Channel is currently limited to a few GNSS stations continuously operating from since 2001. Estimated GNSS velocities, referred to an Africa-fixed reference frame (Fig. 3.2b) highlight that LAMP station shows a residual velocity of ~1 mm/yr towards SSE, evidencing a small deviation with respect to Africa plate. Stations located on the Hyblean-Malta block are moving toward ENE with rates of ~2.3 mm/yr, while stations in Pantelleria (PZIN) and on western Sicily move toward E and SE, with rates ranging between ~3.8 and 2.1 mm/year, respectively. More in detail, the diverging pattern of MALT and LAMP stations show a significant stretching across the Linosa and Malta Grabens, while the motion of PZIN with respect to MALT and LAMP stations suggest a general contraction of the central sector of the regions.

3.2.3. Volcanic activity

The widest magmatic manifestations in the Sicily Channel are exposed on Pantelleria Island (Fig. 3.2b), where rocks show an age of 0.324-0.003 Ma (Mahood and Hidreth, 1983; Civetta et al., 1998; Micallef et al., 2024). Linosa island (Fig. 3.1), instead, formed between 1.06 and 0.53 Ma (Lanzafame et al., 1994), consists of a volcanic building that develops partly above the sea level (Calanchi et al.,

1989; Corti et al., 2006; Lodolo et al., 2012). Recent bathymetric data show that only roughly 3.6% of the total volcanic complex (about 165 km^2) is comprised of the emergent part of Linosa, indicating how much uncertainty there still is regarding the area's volcanic product's submarine extension (Tonielli et al., 2019).

The Sicily Channel is also characterized by historical volcanic activity. The oldest magmatic activity has been discovered in a submerged volcanic seamount east of Nameless Bank, occurred in the late Miocene (Beccaluva et al., 1981). Later, in the pre-Last Glacial Maximum (ca. 20 ka B.P.) a tectonic event near the CGSFZ produced several volcanic structures (Lodolo et al., 2019). A few other noteworthy and recent eruptions occurred in 1831 in Ferdinandea Island's Graham Bank at a depth of about 200 m which gave rise to the temporary island known as Foerstner volcano, which was about 65 m above sea level (Corti et al., 2006).

The region's youngest eruptions occurred in 1891 approximately 5 km northwest of Pantelleria, where a submerged volcanic eruption was documented (Washington, 1909), in 1941 at the Pinne Marine Bank, located at the southeast wedge of Graham Bank (Imbò, 1965; Carapezza et al., 1979), as well as in 1981 near Pantelleria Island, approximately 5 km northwest of the island (Washington, 1909). Near the Graham Bank region, several geomorphic features associated with fluids emissions were recognized by Spatola et al. (2018). The diffused pockmarks, mounds, volcanic seamounts show a fault-controlled geometry in agreement with the Plio-Pleistocene extensional faults affecting the NW Sicily Channel as observed for volcanic seamounts around the Pantelleria Graben (e.g. the Angelina seamount) which also show a volcano-tectonic origin (Civile et al., 2010; Lodolo et al., 2012).

3.3. Stratigraphic framework of the Sicily Channel

The Sicily Channel consists of stratigraphic successions pertaining to the African continental margin, that after convergence and collision with the European plate, shortened and went on to form the tectonic units and domains of the Sicilian Maghrebian chain (Antonelli et al., 1988; Catalano et al.,

1996). Since the Late Triassic, three main carbonate platform successions, represented by the Trapanese (in the Adventure Plateau), Saccense (in the Sciacca zone), and Iblean (in the Gela and Hyblean offshore) are found in the Sicily Channel (Fig. 3.3, 3.4a-f).

In detail, the Trapanese-Saccense expand from the Adventure Plateau to the GTS (Fig. 3.1); the Saccense succession is similar to the Trapanese succession, except for Lower Oligocene-Miocene when the uplift of the Western sector of the Sicily Channel reorganized the distribution of emerged lands, wide regional highs (e.g. Mazara-Sciacca high) and shallow-water to outer shelf carbonate deposits in the Iblean sector to the East (Antonelli et al., 1988). The Late Triassic-Middle Lìassic shallow platform dolomites and limestones (Sciacca and Inici Fms.) pass upward to Toarcian-Eocene pelagic seamount and deep marine limestones and marls (Buccheri, Chiaramonte, Hybla and Amerillo Fms.) (Figs. 3.3, 3.4a, b, c) (Antonelli et al., 1988; Catalano et al. 1996). In comparison, the clastic sequences are sedimentary rocks of the coastal and external platform (Fortuna, Ain Grab, Corleone, Terravecchia, and Ribera Fms.) mixed with open platforms and shallow water marl and limestone (San Cipirello, Mahmoud, and Nilde Fms.) and evaporitic deposits (Gessoso Solfifera Fm.) (Fig. 3.3). The Sicily Channel as the whole African margin shows in the Lower Cretaceous a typical deep-water sedimentation (Hybla and Amerillo Formation) (Fig. 3.3).

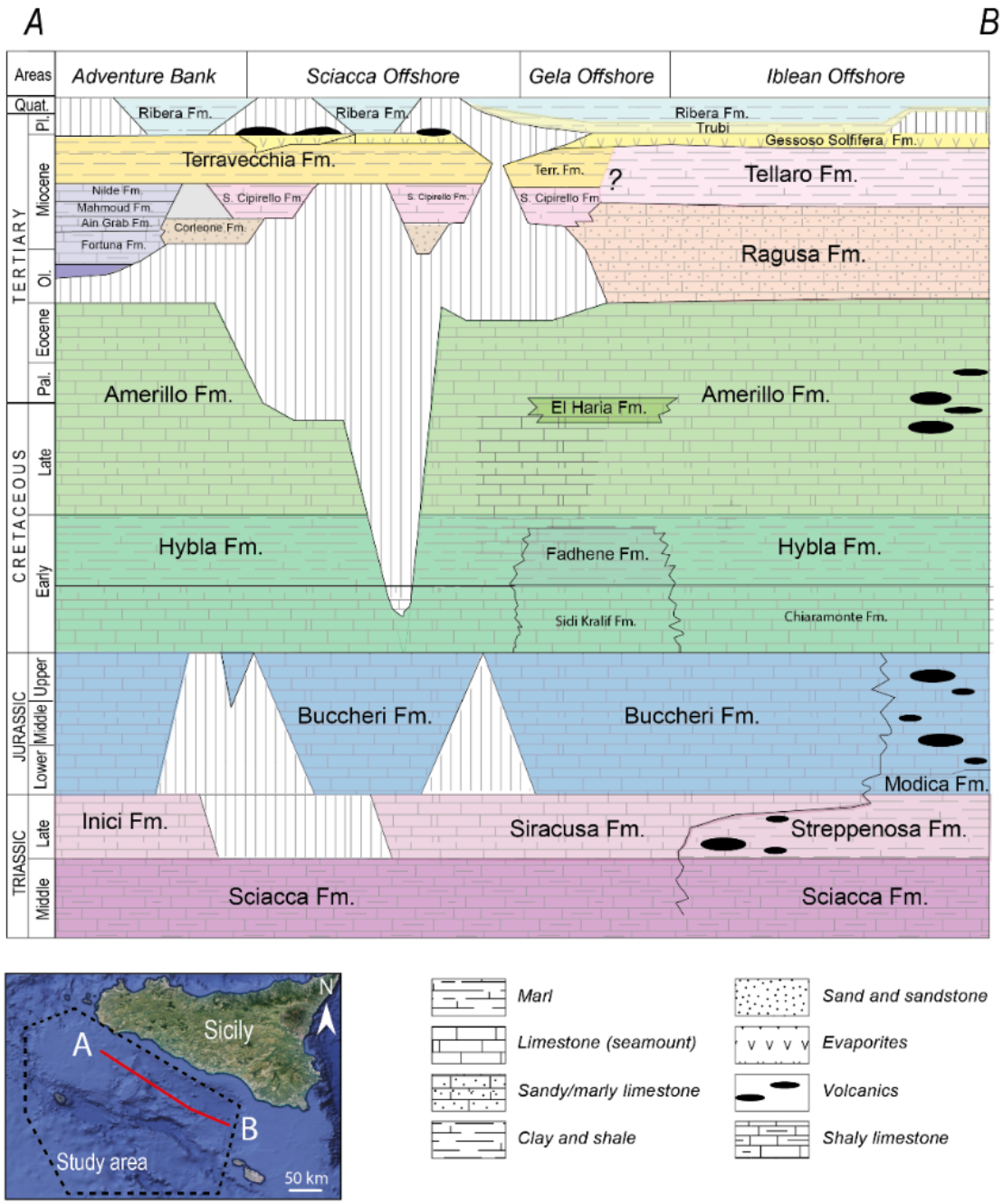

Fig. 3.3. Lithostratigraphic correlation chart along section profile A-B, located on lower left corner map; for details see section 3.3 in the manuscript (after Antonelli et al., 1988).

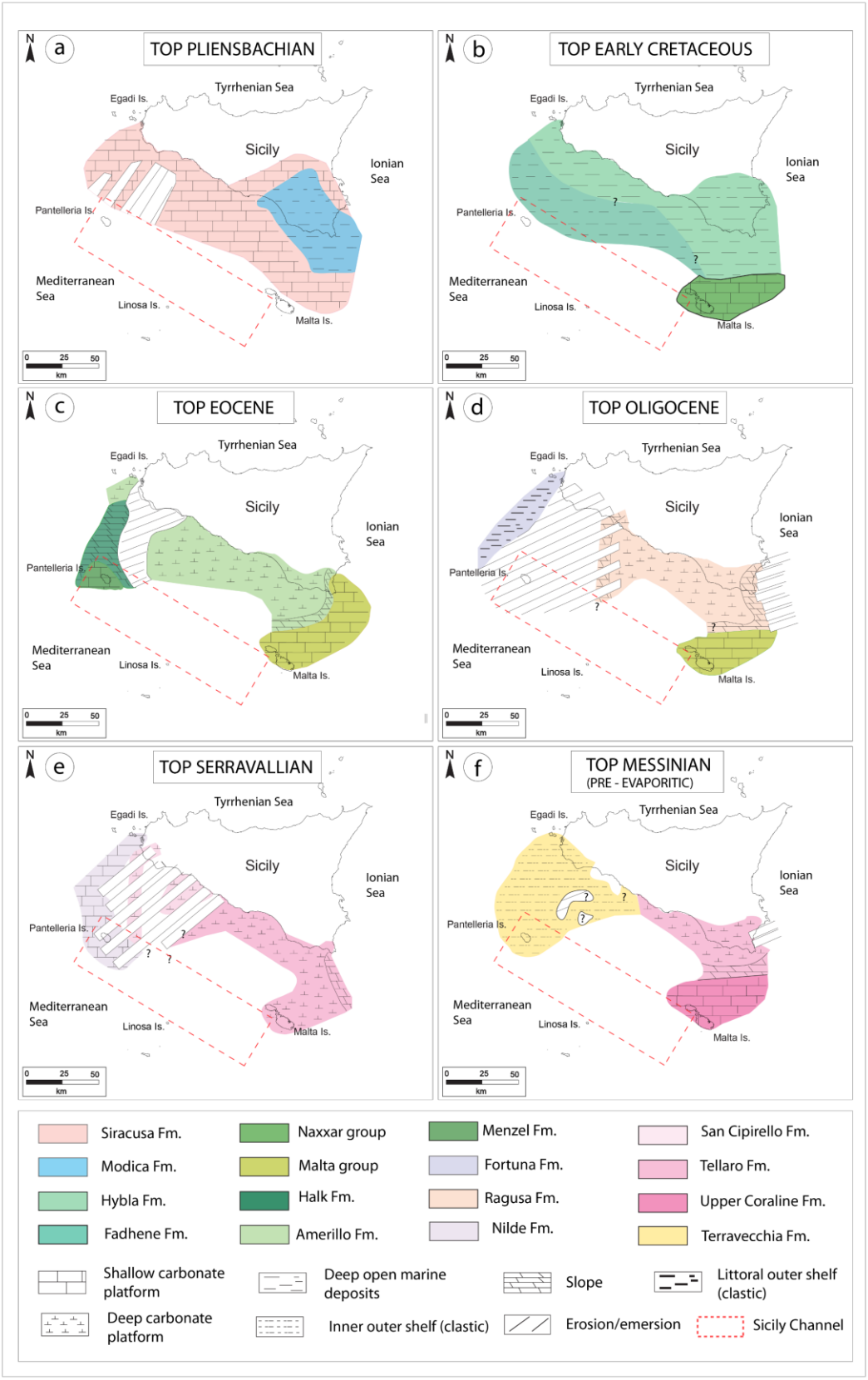

Fig. 3.4. Meso-Cenozoic paleogeographic evolution of the central and eastern sectors of the northern side of the Sicily Channel; a) top Pliensbachian (Lower Jurassic), b) top Early Cretaceous, c) top Eocene, d) top Oligocene, e) top Serravallian, f) top Messinian; refer to the text for details (after Antonelli et al., 1988).

The Sicily Channel as the whole African margin shows in the Lower Cretaceous, typical deep-water sedimentation (Hybla and Amerillo Fms.) (Figs. 3.3, 3.4b). These latter sedimentation conditions persist until the Oligocene, a period in which a variation occurs between sedimentation in the Iblean zone and the Madrepore Bank, where shallow-sea carbonate sedimentation (Ragusa Fm.) (Figs. 3.3, 3.4c, d) persists, and the Adventure Plateau zone, where clastic sedimentation occurs (Antonelli et al., 1988).

The Hyblean domains, extending between the Ragusa-Malta Plateau and offshore of the Agrigento coast, presents a sequence manly consisting of Late Triassic-Middle Liassic shallow platform and deep marine carbonates and shales (Gela, Noto, Streppenosa, Siracusa and Modica Fms.) followed by Toarcian-Eocene pelagic seamount and deep marine limestones and marls (Buccheri, Chiaramonte, Hybla and Amerillo Fms.) which are covered by external platform carbonates, marl, and evaporitic deposits (Ragusa, Tellaro and Gessoso-Solfifera Fms.) of the Oligocene-Miocene age (Figs. 3.3, 3.4d, e, f).

The sedimentation and evolution of the Sicilian Channel area records also the event that occurred in the Upper Miocene (5.96 and 5.33 Ma) following the isolation of the Mediterranean basin from the Atlantic basin: the Messinian salinity crisis (MSC) (Andretto et al., 2021; Haq et al., 2020; Roveri et al., 2014; Manzi et al., 2020, 2021). This event, which occurred as a consequence of the closure of the Strait of Gibraltar, resulted in the sedimentation of considerable amounts of evaporitic deposits (referred to as the Gessoso Solfifera Fm.) (Figs. 3.3, 3.4f).

After the Messinian event, clastic deposits of the Plio-Quaternary age (Trubi and Ribera Fms.) are prevailing (Fig. 3.3). They record a quick return to marine conditions, with megafloods (Micallef et al., 2017) and sea-bottom currents able to accumulate contouritic deposits (Van Dijk et al., 2023), followed by alternating clay and marls and sand deposited from shelfal area to deeper pelagic basins formed inside the grabens and foredeep that still shape the seafloor bathymetry (Fig. 3.1) associated to a complex tectonic and volcanic activity all over the Sicily Channel.

3.4. Data and methods

An extensive review of the Sicily Channel literature was conducted to extract the post-Messinian major tectonic and structural features, also highlighting the main regional unconformities in order to better constrain the stratigraphic architecture of this area and the timing of activity of the main tectonic structures.

We report the line drawing of 9 seismic lines (Fig. 3.5), named Line 1 to Line 9 (Figs. 3.6-3.11), drawn with the Adobe Illustrator software from the interpretation of seismic profiles already published in the literature (see Tabs. 3.1,3.2), for seismic lines reference and details) covering the most representative Sicily Channel sectors (respectively Adventure Plateau, Sciacca offshore, Gela Basin, Malta, Linosa and Pantelleria Grabens) (Fig. 3.1).

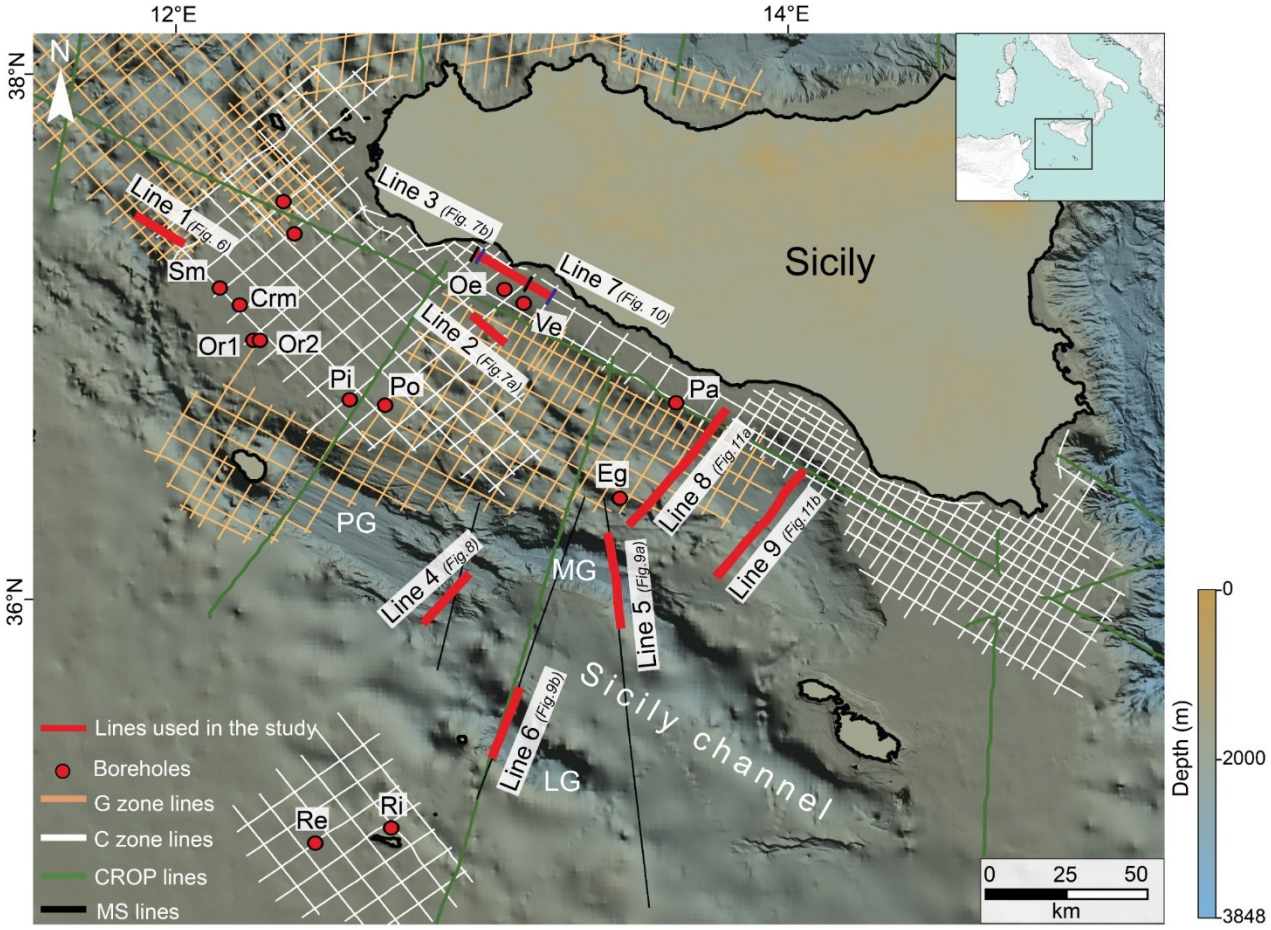

Fig. 3.5. Available seismic dataset and boreholes in the study area, derived from the literature and open access database (ViDEPI). Red lines correspond to the seismic profiles reported in this work. Bathymetry data derived from EMODnet (https://emodnet.ec.europa.eu/en). Crm: Corvina Mare 1;

Eg: Egeria 1; LG; Linosa Graben; MG: Malta Graben; Oe: Orione est-1; Or1: Orlando-1; Or2: Orlando-2; Pa: Palma-1; PG: Pantelleria Graben; Piera-01, Paola est-01; Re: Remo Nord-1; Ri: Riccio Sud-01; Samanta-1; Ve: Venere-1.

The most representative horizons, significant for the current study, were categorized for the different sectors of the Sicily Channel based on their attributed age and their significance with respect to the different tectonic phases occurred in these areas (Tab. 3.3).

A compilation of the structural data (line extension, kinematic, age) were extracted from the available literature (see Fig. 3.12 for the literature considered) and public database, such as INQUA, (http://portalesgi.isprambiente.it/it/node/627) and ITACHA (https://sgi.isprambiente.it/ithaca/viewer/index.html), in order to create a summary structural map of the Sicily Channel (Fig. 3.12). The map was georeferenced with World Geodetic System (WGS) 84 coordinate reference system on a bathymetric data derived from EMODnet (http://www.emodnet-bathymetry.eu/), and different colours were assigned to the structural features coming from different authors/databases to highlight the information source (Fig. 3.12).

Tab. 3.1. Reference, location, orientation of the seismic lines and well data used in this review.

Line name	**MS119, MS120**	**Pant-1**	**C90-117**	**CS71-SC17, CS71-SC15**	**C-1007 , C259**
Available in	ViDEPI	OGS	Agip	CNR-ISMAR	ViDEPI
Recording date	1980	2009	1996	1970	1968
Sample rate (ms)	4	2			2
Fold (%)	1200	3000			1200
Recording filters	8-126 Hz	Anti-alias			10-80 Hz
Energy source	Flexotir	Sleeve guns			AquaPulse
Streamer length (m)	2400	1600			1600
Channel	48	120			24
Group interval (m)	50	12.5			67
Shot interval (m)	100	25			137

Tab. 3.2. Source and acquisition parameters of the seismic lines.

Line name	Literature	Area covered	Orientation	Wells used for stratigraphic correlation (ViDEPI database)
Line 1 (C90-117)	Civile et al. (2014)	Adventure Plateau	SE-NW	Samanta-01, Corvina Mare-01, Orlando-01 and Orlando-02
Line 2 (C-1007)	Federik et al. (2018)	Sciacca zone	SE-NW	Orione est-01 and Venere-01
Line 3 (C-529)	Federik et al. (2018)	Sciacca zone	SE-NW	Orione est-01 and Venere-01
Line 4 (Pant-1)	Civile et al. (2021)	Pantelleria graben	NE-SW	Piera-01, Paola est-01 and Egeria-01Samanta-01, Corvina Mare-01 and Orlando-01
Line 5 (MS120)	Maiorana et al. (2023)	Malta graben	SSE-NNW	Riccio Sud-01, Remo Nord-01, Palma-01 and Egeria-01
Line 6 (MS119)	Maiorana et al. (2023)	Linosa graben	SSW-NNE	Riccio Sud-01, Remo Nord-01, Palma-01 and Egeria-01
Line 7 (C-529)	Catalano et al. (1996)	Gela foredeep	NE-SW	Noemi-01 and Orione-est-01
Line 8 (CS71-SC15)	Cavallaro et al. (2017)	Gela foredeep	NE-SW	Palma-01 and Egeria-01
Line 9 (CS71-SC17)	Cavallaro et al. (2017)	Gela foredeep	NE-SW	Palma-01 and Egeria-01

Tab.3.3: Main horizons in the different Sicily Channel sector investigated in this study.

Area	Name	Colour	Age Ma	Description	Reference
Adventure Plateau *(Fig. 3.6)*	Top of Carbonate succession (TCS)		23	The boundary between predominantly Triassic to Paleogene carbonate succession and the Miocene siliciclastic and carbonate clastic deposits.	Civile et al. (2014)
	Base of Terravechia (TT)		11.6	The base of Tortonian to Messinian succession composed mostly of silty clay and quartz sands.	
	Top of Miocene (TMS)		5.3	The unconformity is probably associated with a Messinian erosional surface that distinguishes the thin layer of the Plio-Quaternary unit and the Miocene section.	
Capo Granitola Sciacca Fault Zone *(Fig. 3.7a)*	Top of Carbonate succession (TCS)		66-34	TCS separates the upper Miocene unit and the lower Mesozoic carbonates.	Fedorik et al. (2018)
	Top of Miocene (TMS)		5.3	TMS separates the Plio-Quaternary unit consisting of clays and the Miocene section including Clays with some Marls.	
(Fig. 3.7b)	Top of Carbonate succession (TCS)		66-34	TCS separates the upper Miocene unit and the lower Mesozoic carbonates.	Fedorik et al. (2018)

	Top of Miocene (TMS)		5.3	TMS separates the Plio-Quaternary unit (PQ3) consisting of clays and the Miocene section including Clays with some Marls.	
	Top of Trubi (PQ3)		3.6	PQ3 is an unconformity, marks a division between the Early Pliocene unit comprising mostly of Marls and the Late Plio-Quaternary unit consisting of Clays.	
Pantelleria Graben *(Fig. 3.8)*	Top of Carbonate succession (TCS)		66-34	Separating the Carbonate platform deposits and the pelagic carbonate succession.	Civile et al. (2021)
	Top of Miocene (TMS)		5.3	The boundary between siliciclastic Oligocene- Miocene succession and the Plio-Quaternary syn-rift deposits.	
	Top of Trubi (PQ3)		3.6	PQ3 is found in the extreme NE and it divides the Plio-Quaternary syn-rift deposits and the undifferentiated Plio-Quaternary unit.	
	Top of Calabrian (PQ1)		0.8	The sequence is visible on the whole profile and distinguishes the undifferentiated Plio-Quaternary unit seismically.	
Malta Graben *(Fig. 3.9a)*	Top of Carbonate succession (TCS)		66	The boundary between upper cretaceous carbonates and the Miocene unit.	Maiorana et al. (2023)
	Top of Miocene (TMS)		5.3	The sequence marks the top of Messinian, separates the bottom evaporites and the lower Plio-Pleistocene succession.	
	U1		3.3	The Plio-Pleistocene unit features unconformities (U1 and U2), with a younger extensional event occurring between them. The figure highlights relief affecting the sea floor indicating a contractional phase was or is still active in the graben.	
	U2		1.33		
Linosa Graben *(Fig. 3.9b)*	Top of Miocene (TMS)		5.3	The boundary between the Messinian evaporites and the lower Plio-Pleistocene succession.	Maiorana et al. (2023)
	U1		4.1	An extensional phase dated from Zanclean to Calabria with a 0.36 mm/yr sedimentation rate was observed by Syn deposits between U1 and U2.	
	U2		1.4		
	U3		0.8	This Upper Calabrian unconformity has sealed the rollover anticline formed by positive inversion.	

Gela Foredeep *(Fig. 3.10)*	Top of Miocene (TMS)		5.3	The Messinian reflector divides the Mesozoic carbonates and the evaporites.	Catalano et al. (1996)
	Top of Trubi (PQ3)		3.6	The unconformity divides the pelagic marly limestones (Trubi Fm.) from the bottom Messinian evaporites.	
	Top of Calabrian (PQ1)		0.8	The unconformity suggests the beginning (Middle Pliocene) and the end (Middle Pleistocene) of the Gela thrust system accretion.	
Gela Foredeep *(Fig.3.11a)*	Top of Carbonate succession (TCS) *(only in Fig. 3.11a)*		66-34	The sequence is found in the Maderpore bank and marks a boundary between the Jurassic to Lower Miocene carbonate succession and Oligocene to Early Miocene Carbonates and Marls.	Cavallaro et al. (2017)
	Top of Ragusa fm. (TR) *(only in Fig. 3.11a)*		40-23	The sequence represents the top of Ragusa formation in the Maderpore bank and separates the Carbonates and Marls of Oligocene age and middle-upper Miocene silty marls. It appears to correspond to the diffraction hyperbola band.	
(Fig. 3.11b)	Top of Miocene (TMS)		5.3	The sequence divides the Messinian evaporite unit and the carbonate and Marl succession of Oligocene.	
	Top of Trubi (PQ3)		3.6	The base of the Plio-Quaternary unit (PQ3) interpreted as syn tectonic, distinguishes rhythmically bedded pelagic marly limestones of Trubi formation and the Messinian evaporites.	
	Base of Gelasian (PQ2)		2.6	The erosional unconformity related to a relative sea-level drop marks a boundary between Zanclean–Piacenzian deposits and the Gelasian to the Calabrian unit.	
	Top of Calabrian (PQ1)		0.8	The depositional sequence boundary refers to the peak of regression in the area.	

3.5. Review of Plio-Quaternary structural features in the Sicily Channel

3.5.1. Adventure Plateau

Situated in the northwest of the Sicily Channel, the 80,000 km^2 Adventure Plateau is the shallowest portion of the Sicily Channel, with average water depths of little more than 150 m (Figs. 3.1, 3.2, 3.6) (Corti et al., 2006; Civile et al., 2014).

In the Tortonian, a contractional deformation, coeval with the opening of the Tyrrhenian Sea and southward propagation of the Sicilian Maghrebian front, produced tectonic slices partially detached from the carbonate substratum, separated by ESE-verging thrusts and back thrusts (Catalano et al. 2000; Civile et al., 2015).

During the Messinian, the northern part of the Adventure Plateau was affected by widespread compressional tectonics. ESE-verging thrusts and back-thrusts were generated, all belonging to the orogenic domain known as External Thrust System or Pelagian-Sicilian Thrust Belt, which represents the lowermost structural level of the Sicilian–Maghrebian Chain (Lentini et al. 1990, 1994, 1996; Antonelli et al., 1988; Argnani et al., 1986; Civile et al., 2014). This compressional tectonic is evidenced by the ETF, to the NW, and by the ATF to the SE (Catalano et al., 1985, 1995; Lentini et al. 1990, 1994; Civile et al., 2014; Milia et al., 2021) (Figs. 3.6, 3.12). Associated to the NE-trending Thrust System, the so-called Adventure Foredeep developed (Argnani et al. 1986, 1987; Argnani 1993a, b; Civile et al., 2015): a wide basin filled by clastic sedimentation, affected by contraction and partially detaching from its substratum during the Late Messinian (Argnani 1993a, b; Grasso 2001).

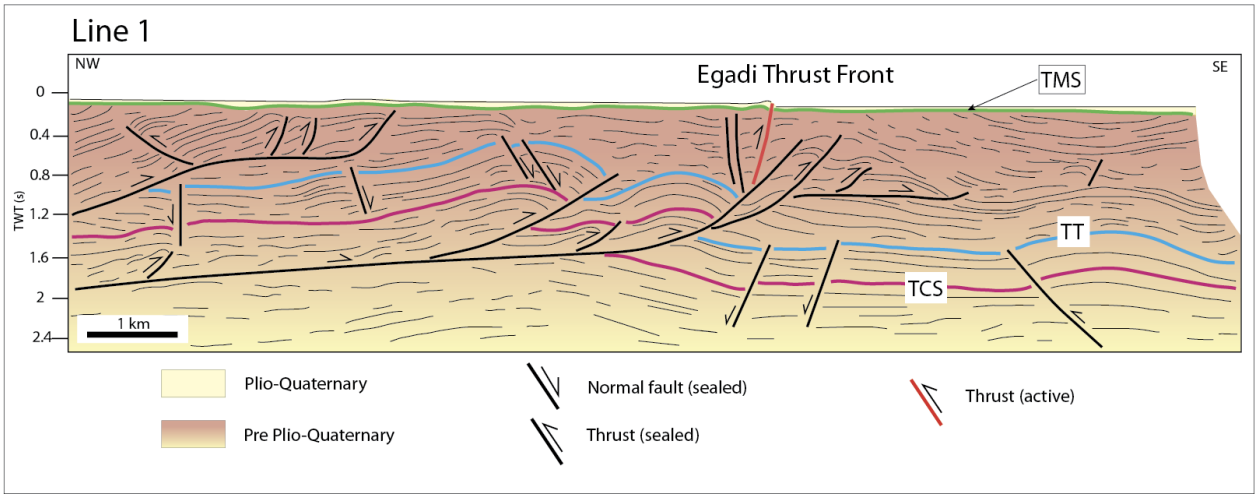

Fig. 3.6. Seismic Line 1 through the Adventure Plateau, modified after Civile et al. (2014); see Fig .3.5 for location and Tab. 3 for description of the main horizons (TCS: Top of Carbonate succession; TT: Base of Terravechia; TMS: Top of Miocene). Recent reactivation of the SE-verging Egadi Thrust Front (ETF) is visible, as it clearly affects the seafloor.

Lentini et al. (1990) suggested that the Plio-Quaternary deposits sealed this compressional system. Instead, Torelli et al. (1993) proposed a recent reactivation of the ETF. Civile et al. (2014) interpreted the ETF as marked by several SE-verging thrusts affecting the Top of Carbonate succession (TCS, c. 23 Ma) and the base of Terravecchia (TT, c. 11.6 Ma) horizons (Figs. 3.6, 3.12; Tab. 3.3). The TT horizon is clearly folded and disrupted, however the (Top of Miocene) (TMS, c. 5.3Ma) and the shallowest Post-Messinian, Plio-Quaternary sequence has a thickness of around 0.1 s/TWT and is generally undeformed in the seismic line (Fig. 3.6), except for a SE-verging thrust that clearly affects both the Pre and-Post-Messinian successions as well as the seabed, thus testifying to recent to present day tectonic reactivation of the ETF (Figs. 3.6, 3.12).

3.5.2. The Capo Granitola and Sciacca Fault Zone

The north-western part of the Sicily Channel and the front of the Sicilian-Maghrebian Chain host a wide NS-trending, lithospheric-scale transfer zone (Argnani et al., 1988; Argnani, 1990; Civile et al., 2008, 2010, 2014; Di Stefano et al., 2015; Palano et al., 2020). This is associated to a wide left lateral active fault zone (Fig. 3.2), that is believed to affect the entire continental crust and the upper mantle

to a depth of at least 70 km, as suggested by relocated seismicity and geochemical evidence (Caracausi et al., 2005; Calò and Parisi, 2014).

Monaco et al. (1996) interpreted the faults recognized offshore of Sciacca, as thrusts with late Quaternary activity and as the offshore extension of the causative fault of the 1968 Belice earthquake's (Fig. 3.2). Moreover, Catalano et al. (2000) recognized in the Sciacca area a carbonate imbricate fan (extending from the Tyrrhenian coast to the latitude of the Sciacca area) involving deposits composed of shallow to deep water carbonates and Tertiary terrigenous and clastic carbonate deposits belonging to the Trapanese and Saccense domains. Their interpretation suggest that the recent deformation is sealed by post-Messinian basinal strata.

Di Stefano et al. (2008, 2015) and Lentini et al. (2014) suggested instead that undeformed sequences of the Pelagian block are present in the Sciacca area, in continuity with those outcropping in the Hyblean plateau of southeastern Sicily. Di Stefano et al. (2015) recognized a shelf to deep water transition in the Sciacca area interpreted as a segment of the rifted southern passive margin of the Permo-Triassic Ionian Tethys that, at present, runs roughly N-S from San Vito Lo Capo to Sciacca (see location in Fig. 3.1). They suggest that this weakness zone may have been reactivated as a major right-lateral strike-slip fault on the basis of the variable direction of the horizontal stress field acting in the Central Mediterranean area since Late Miocene (Mantovani et al., 2014).

Recently, the Sciacca fault zone has been deeply investigated through the acquisition of seismic reflection profiles of variable depth and detailed morphobathymetric data. Fedorik et al. (2018) describes the N-S trending transfer zone as bounded by the Capo Granitola (CG) Fault to the west and by the Sciacca Fault (SF) to the east, those delimiting a 30-km-wide, mostly undeformed basin. The Sciacca Fault was formerly identified by several authors (Argnani, 1990; Casero and Roure, 1994; Antonelli et al., 1988; Nigro and Renda, 2002; Finetti, 2003; Lentini et al., 2006; Ghisetti et al., 2009).

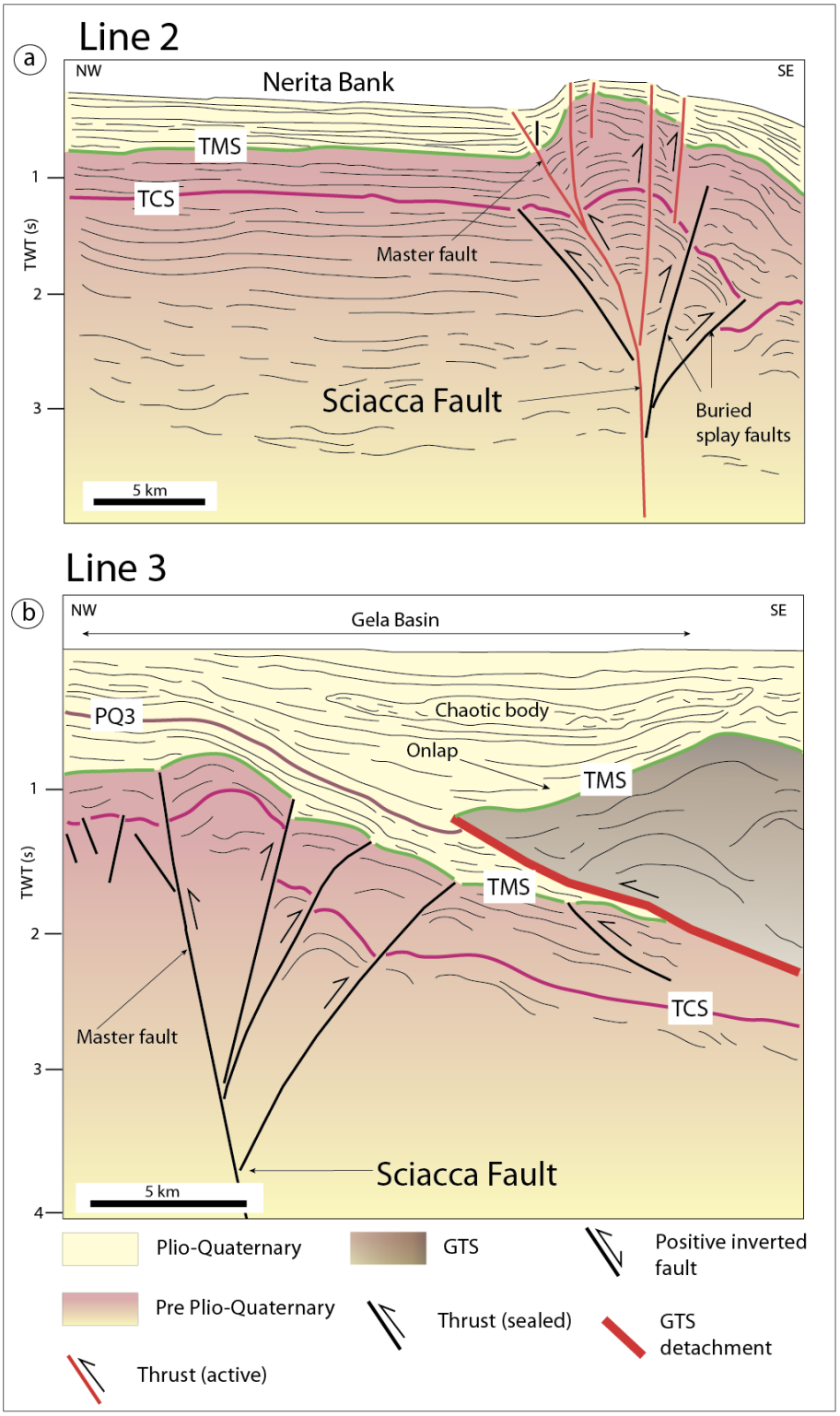

Fig.3.7. (a) Seismic Line 2 and (b) Seismic Line 3 through Sciacca Fault zone, modified after Fedorick et al. (2018); see Fig. 3.5 for location and Tab. 3 for description of the main horizons (TCS: Top of Carbonate succession; TMS: Top of Miocene). The profiles show a positive flower structure associated with the Sciacca Fault, deforming the Plio-Quaternary and Pre Plio-Quaternary strata.

The western fault (Capo Granitola) does not show clear evidence of present-day tectonic activity, and, toward the south, it is connected with the volcanic area of the Graham Bank (Fedorik et al.,

2018). Fedorik et al. (2018) interpreted the SF as compatible with a right-lateral kinematics, that was reactivated in left-lateral during the Pliocene, as testified by the TMS unconformity disruption (Fig. 3.7a,b) and present day focal mechanisms (Fig. 2.a). They divided the SF into northern and southern part. Along the northern segment between the Sicilian coast and the northern margin of the Nerita Bank, the SF seems sealed by Late Pliocene-Quaternary deposits (Fig. 3.7b). Conversely, the southern segment, between the Nerita and Terrible banks, shows clear evidence of active tectonics, particularly evident along the Nerita Bank (Fig. 3.7a).

Ghisetti et al. (2009) interpreted the SF as a positive flower structure related to a N-S transpressive left lateral system that bounds the 'Sciacca High'- an emergent salient of the Pelagian-African platform. Civile et al. (2018) furthermore, interpreted it as a part of the the N-S transfer zone naming it the CGSFZ, a fault system with evidence of Quaternary tectonics which developed along a late Miocene foreland structural high (Miocene peripheral bulge of the Sicilian-Maghrebian Chain). Part of the foredeep basin was later inverted along the CGFZ and, since late Pliocene, a change from right- to left-lateral strike-slip tectonic regime with a compressional component of movement has been proposed (Fedorik et al., 2018).

On the other hand, Ferranti et al. (2019) suggest that the CGSFZ was active in left lateral transpression since Late Miocene-Early Pliocene (earlier than in the other abovementioned interpretation), when preexisting Late Tortonian-Early Messinian (Late Miocene) extensional or transpressional basins were inverted.

3.5.3. Pantelleria Graben

Widely rectangular in shape, the Pantelleria Graben is a large depression of around 90 km in length and 30 km in width, broadening to about 40 km around the Pantelleria Island (Figs. 3.1, 3.12) (Reuther and Eisbacher, 1985; Civile et al., 2008, 2010). It is characterized by a linear NW-trending flank controlled by NE-SW-dipping steep extensional faults with the same orientation (Figs. 3.1, 3.8, 3.12).

The southeastern border of the Pantelleria Graben is crossed by the NE-oriented seismic line reported in Fig. 3.8, which shows in the SW part of the line, a structural high capped by a 0.78 s/TWT thick Post Messinian (Plio-Quaternary) succession. Here, the Top of Calabrian horizon (PQ1, c. 0.8 Ma; Tab. 3.3) divides the less deformed upper section of the Post-Messinian deposits, which is approximately 0.25 s/TWT thick, from the lower, 0.32 s/TWT thick, deformed part (Fig. 3.8). The substantial thickness of the Post Messinian (Plio-Quaternary) deposits visible in the Pantelleria Graben's southern edge (Fig.3.8), according to Civile et al. (2021), suggests that the basin's original extent was wider than it is now, and that the succession that makes up the southern edge was later uplifted.

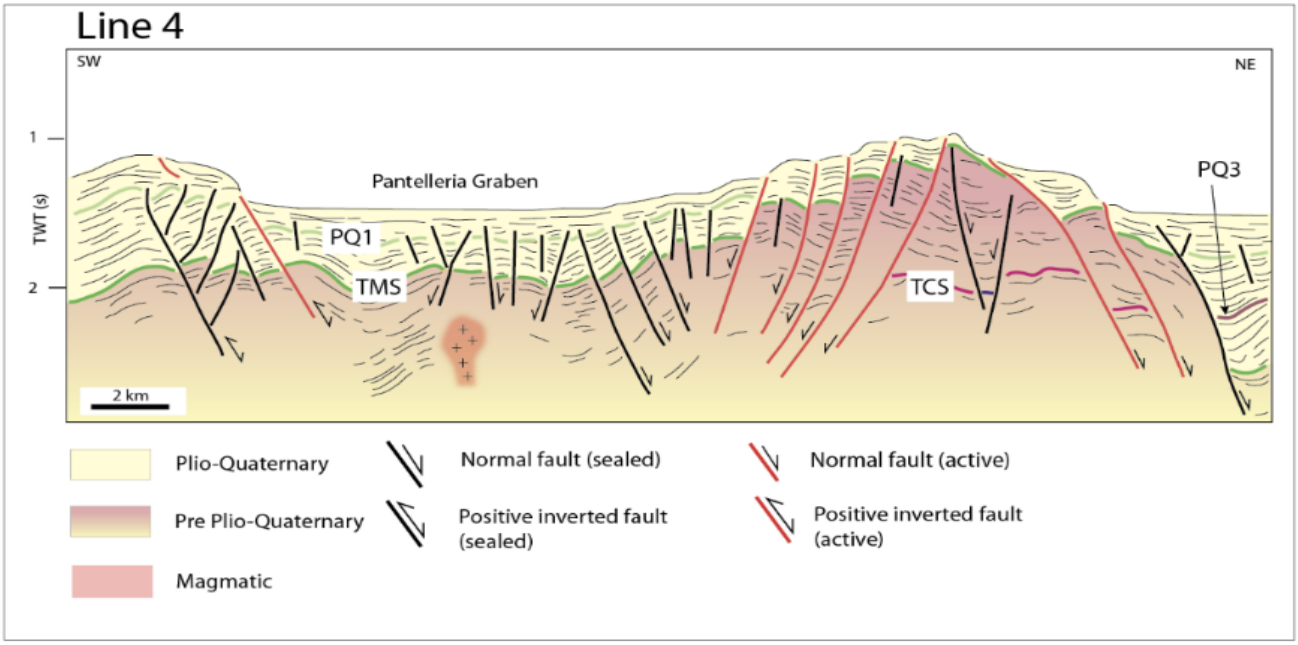

Fig. 3.8. Seismic Line 4 through the Pantelleria Graben, modified after Civile et al. (2021); see Fig. 3.5 for location and Tab. 3 for description of the main horizons (TCS: Top of Carbonate succession; TMS: Top of Miocene; PQ3: Top of Trubi; PQ1: Top of Calabrian). The southern termination of the Pantelleria Graben is shown with highlighted a possible positive tectonic inversion; the folding in the sedimentary Plio-Quaternary infill of the graben is linked to the existence of a supposed buried magmatic intrusion by Civile et al. (2021).

As previously mentioned, the main factor developing the Pantelleria Graben is an ongoing extensional faulting. However, according to a new interpretation proposed by Civile et al. (2021), the moderate folding that is evident in the graben's infill may be related to the existence of a supposed buried magmatic intrusion (Fig. 3.8). Here, several high-angle NE-SW-dipping and NW-SE-oriented normal

faults disrupt the TMS and the PQ1 horizons but are sealed by the shallower Plio-Quaternary sediments (Fig. 3.8, 3.12).

As suggested by Civile et al. (2021), the location of TMSs between the Graben infill and its southern edge indicates that a possible positive tectonic inversion, probably with a transpressive feature, likely occurred along the WNW-oriented, NNE-dipping fault that borders the Pantelleria Graben to the southwest, uplifting the basin (Figs. 3.8, 3.12). The juxtaposition of two zones with distinct tectonic deformations in this area (the transpressive and extensional regimes) raises the possibility of a potential NE-trending strike-slip structure between them (Civile et al., 2021). On the other hand, the northern margin of the Pantelleria Graben is marked by a NW-trending structural high affected by an array of high-angle NW and SW-dipping extensional faults (Fig. 3.12).

3.5.4. Malta and Linosa grabens

The Malta Graben is a NE-oriented tectonic depression that develops over 160 km in a sigmoidal form (Figs.3.1, 3.12) (Civile et al., 2021; Maiorana et al., 2023). A maximum width of about 22 km is observed in the northwestern of the graben, while in the southern one, it widens up to 30 km (Civile et al., 2021). The maximum water depth of roughly 1700 m is reached in the northwestern part of the graben (Figs. 3.1, 3.12), which is bounded by two prominent seafloor scarps associated with two prominent high-angle NW-trending and NE-SW-dipping extensional faults, as already evidenced by previous works (Figs. 3.8a, 3.11) (Dart et al., 1993; Putz-Perrier and Sanderson, 2010; Civile et al., 2021; Maiorana et al., 2023).

According to Civile et al. (2021) and Maiorana et al. (2023), the graben's margins show evidence of wide magmatic intrusions (Fig. 3.9a). The Post-Messinian (Plio-Quaternary) infill is around 1.52 s/TWT (Fig. 3.9a), and within it there exist two major unconformities, i.e., U1 and U2, which record distinct deformational episodes (Fig. 3.9a). The Malta Graben records a younger extensional event, highlighted by the syn-rift geometry of the unit between U1 (c. 3.3 Ma) and U2 (c. 1.33 Ma; Tab. 3.3), followed by a second event related to the positive inversion of pre-existing extensional structures

affecting U2. It follows a renewed extension, highlighted by the presence of normal faults affecting the seabed (Maiorana et al., 2023).

Overall, the internal geometry of the Malta Graben is characterized by a roll-over anticline structure formed during an extensional phase, later inverted causing the folding of the deposits overlying the TMS and of the seafloor of the central Malta Graben (Fig. 3.9a) (Maiorana et al., 2023). In fact, the seafloor is positively relieved, at least 500 meters above the sea level, affected by a positive inverted fault NW-SE trending penetrating both the Pre- and Post-Messinian sediments, and cutting the unconformities U2, U1 and TMS (Figs. 3.9a, 3.12); this indicates contractional tectonics recently occurred inside the Malta Graben (Maiorana et al., 2023).

Proceeding to the south, the Linosa Graben consists of a narrow depression with a width of about 20 km and a maximum water depth of over 1550 m (Figs. 3.1, 3.12) (Civile et al., 2021; Maiorana et al., 2023). The Post-Messinian (Plio-Quaternary) graben sedimentary fill has a maximum thickness of around 2 s/TWT (Fig.3.9b) and contains three unconformities, i.e., U1 (c. 4.1 Ma, U2 (c. 1.4 Ma), and U3 (c. 0.8 Ma; see Tab. 3.3). Two high-angle extensional faults that dip SW-NE and NW-SE, penetrate the Pre- and Post-Messinian sediment establishing a staircase pattern, and are associated to seabed scarps on both sides of the graben (Figs. 3.9b, 3.12) (Civile et al., 2021; Maiorana et al., 2023). The Plio-Quaternary infill between U1 and U2 exhibits a syn-rift geometry that indicates an extensional phase (Fig. 3.9b). The internal geometry of the Linosa Graben shows the existence of a rollover anticline involving the TMS (Fig. 3.9b), extending for about 6-7 km with a NW direction (Civile et al., 2021; Maiorana et al., 2023). However, a NW-SE striking and SW dipping fault that affects the TMS and the U1 is well imaged inside the graben, but it is sealed by the shallowest Plio-Quaternary sediments (Fig. 3.9b).

Civile et al. (2021) and Maiorana et al. (2023) recently interpreted this peculiar structure as a possible positive inverted fault that shortens the rollover anticline, which appears to be sealed by the U3 unconformity. According to Maiorana et al. (2023) and Civile et al. (2021), the post-Messinian

sediment lying above the U2 are interpreted as a post-rift succession that is up to 0.82 s/TWT thick. They are separated into an upper undeformed part (0.3 s/TWT) and a lower part that is up to 0.48 s/TWT thick. The upper part is marked by sub-parallel reflectors with onlap terminations against the U3, with the latter serving as the boundary between them. Finally, according to recent findings by Civile et al. (2021) and Maiorana et al. (2023), the Linosa Graben exhibits shallow magmatic intrusions concentrated along the margins of the graben (Fig.3.9b), whose Maiorana et al. (2023) attributes to Linosa II volcanic activity (Fig. 3.2).

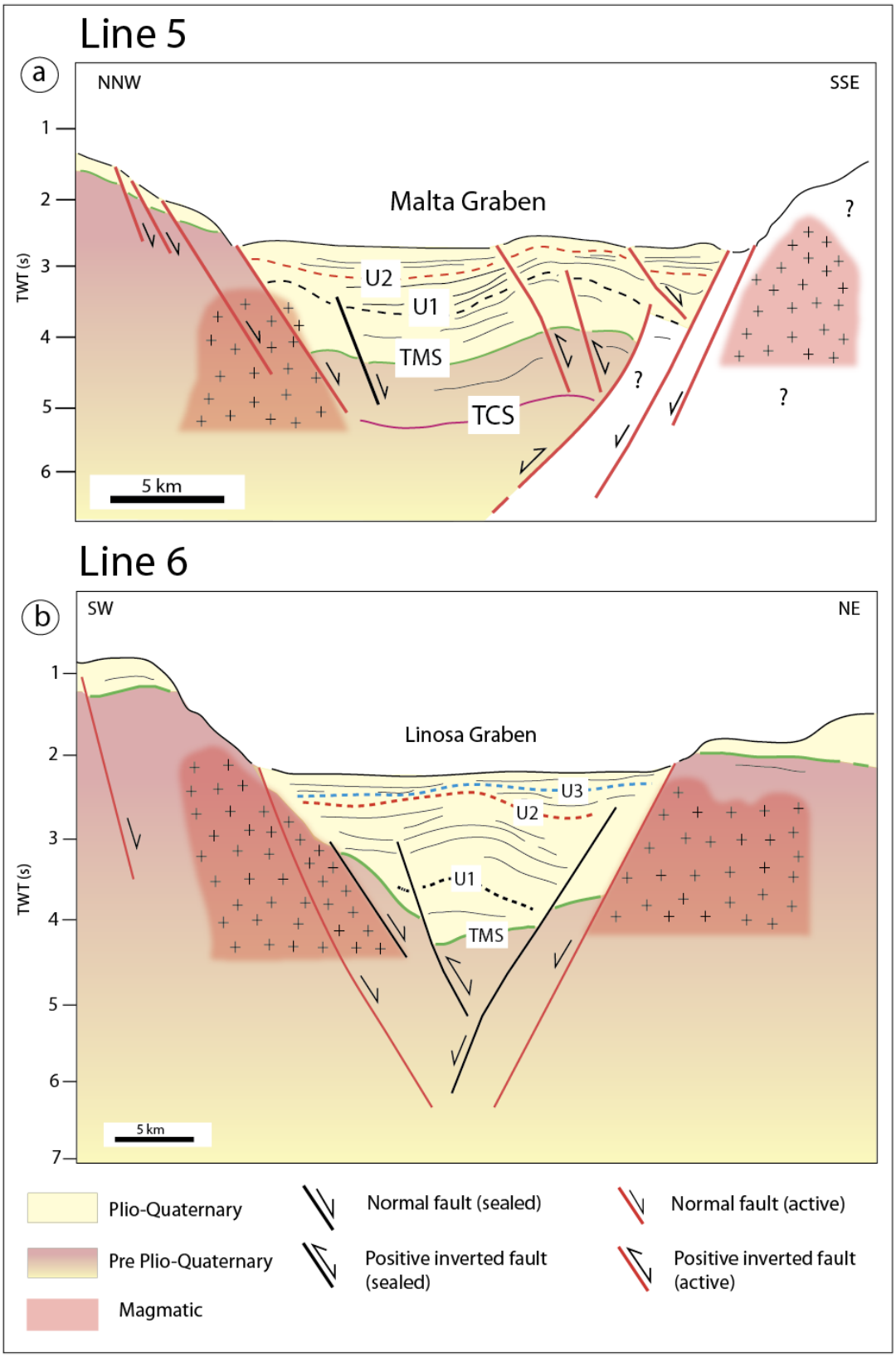

Fig. 3.9. (a) Seismic Line 5 through Malta Graben and (b) Seismic Line 6 through Linosa Graben, modified after Maiorana et al. (2023); see Fig. 3.5 for location and Tab. 3.3 for description of the main horizons (TCS: Top of Carbonate succession; TMS: Top of Miocene).

3.5.5. The Gela Thrust System (GTS)

As the leading edge of the Sicilian–Maghrebian fold-and-thrust belt, the GTF forms an accretionary wedge representing the youngest and outermost thrust sheet of the GTS (Figs. 3.1, 3.7b, 3.10, 3.11a, 3.12) (Ogniben 1969; Lentini, 1982; Catalano et al., 1996; Ghisetti et al., 2009; Cavallaro et al., 2017). The GTF extends 20-25 km offshore the coast between Sciacca and Gela, facing the Sicily Channel, where it forms a large south-facing arc (Figs.3.1,3.12) (Ogniben, 1969; Catalano, 1987; Argnani, 1989; Grasso et al., 1991; Butler et al., 1992; Lickorish et al., 1999; Catalano et al., 1996; Corti et al., 2006; Ghisetti et al., 2009; Cavallaro et al., 2017; Maiorana et al., 2023). A foredeep basin, the so called ‘’Gela Basin’’, stretches ahead of the GTF as a WNW-ESE-trending, narrow, and weakly deformed elongated depocenter (Figs. 3.1, 3.7b, 3.10, 3.11a, 3.12), mainly composed of 1-1.2 s/TWT thick post-Messinian sediments (Plio-Quaternary) (Figs. 3.7b, 3.10, 3.11a).

Structures of GTS resulted from the wedge's internal deformation as well as the accretion of foredeep deposits into the thrust sheets (Lickorish et al., 1999). Bianchi et al. (1989) show the GTS to be a composite structure with a higher unit consisting of Oligocene-Serravallian sandstones, Tortonian clays (Terravecchia Fm.) and younger Messinian-Pliocene units thrust onto a further sequence of Tortonian clays. The allochthonous nature of the GTS was reported by Butler et al. (1992) and Lickorish et al. (1999) who called it “Gela Nappe’’. They proposed that the latter is composed of a stratigraphic package that is repeated tectonically and internally shortened by a number of minor thrusts, the basal detachment of which is situated on top of the Lower Pliocene Trubi Fm. (PQ3 c. 3.6 Ma; Figs. 3.7b, 3.10), on the basis of seismic reflection data and petroleum exploration wells.

Based on wells correlations, Catalano et al. (1996) and Cavallaro et al. (2017) indicated that the wedge is composed of imbricated clastic, evaporitic, and carbonate units from the Oligocene to Pleistocene in age, laying on the Pleistocene sediments of the Ribera Fm. of the Gela Basin. However, all prior study pointing that the GTS is a thin-skinned accretionary wedge characterized predominantly by compressive tectonics and a chaotic internal geometry marked by discontinuous, folded and faulted reflections, as a results of tectonic accretion processes (Figs. 37b, 3.10, 3.11a).

The GTS stacked units' total thickness is ~1.5 s/TWT (Figs. 3.7b, 3.8, 3.11a). Close to the major deformation front, SW vergent thrust sheets form a leading imbricate fan system, which overtrhusts the NE dipping lower-Upper Pliocene foreland deposits and are sealed by the Plio-Quaternary sediments of the Gela Basin (Figs. 3.7b, 3.10, 3.11a). Its basal detachment thrust, which develops between 1.6 and 2.4 s/TWT, dips inland, exhibits an overall displacement of more than 5 km at an angle of ~8° (Figs. 3.7b, 3.10, 3.11a) and truncates the PQ3 and the sediments below (Figs. 3.7b, 3.10). Moreover, the undulation of the basal detachment shown in Figs. 3.7b, 3.11a, suggest that some normal faults were reactivated with reverse features (Cavallaro et al., 2017; Fedorick et al., 2018), while Catalano et al. (1996) do not show evidence of such positive reactivation of previous extensional features (Fig. 3.10).

The TMS unconformity marks the top of the GTS, which is capped and draped by a thin (0.3-0.4 s/TWT) sedimentary cover (Figs. 3.7b, 3.10, 3.11a), ascribed to Pliocene age by Lickorish et al. (1999); the latter is folded on the top of the nappe indicating that during the Pliocene the accretionary wedge was still moving and also subject to internal shortening. The GTF is clearly onlapped by Post-Messinian (Plio-Quaternary) sediments of the Gela Basin (Figs. 3.7b, 3.10, 3.11a). Internal thrusts involved the top of the GTS (TMS, c. 5.3 Ma), the PQ3 (c. 3.6 Ma) and the PQ1 (c. 0.8 Ma) interpreted in the Gela Basin, as reported by Catalano et al. (1993, 1996) (Figs. 3.7b, 3.10, 3.11a).

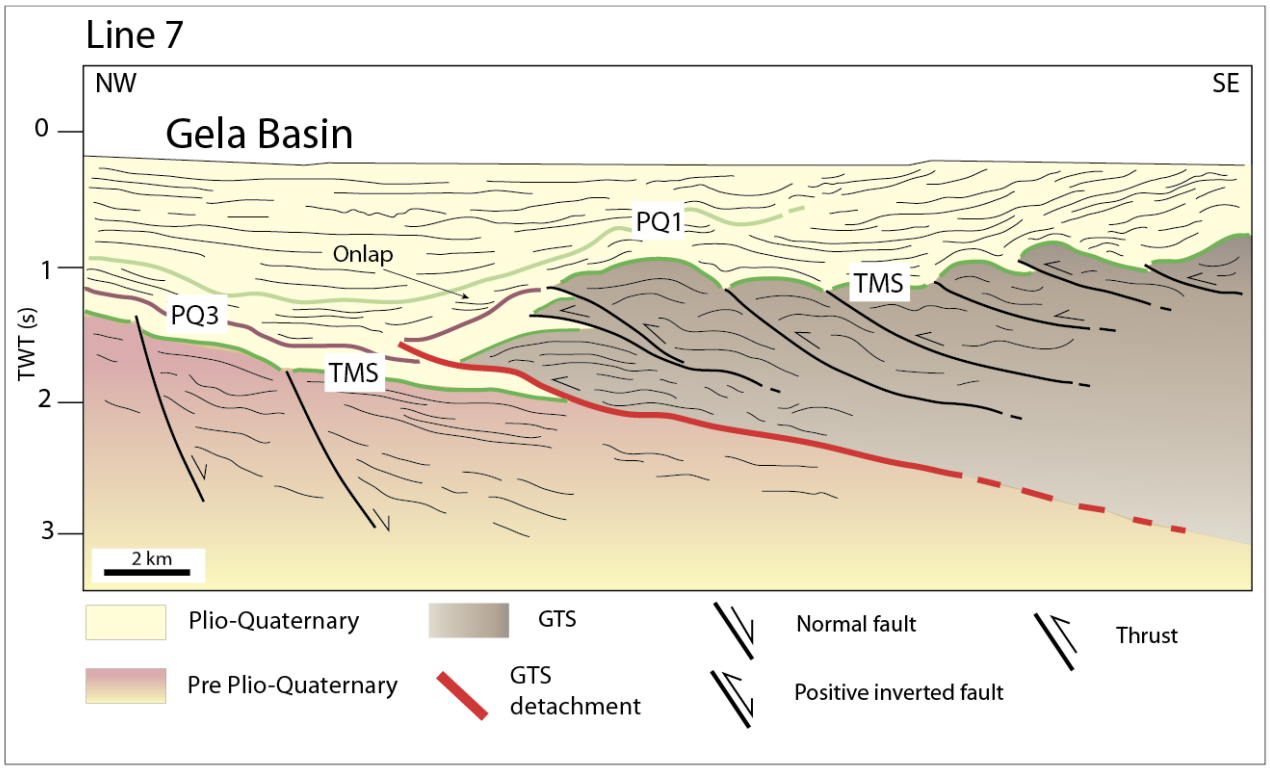

Fig. 3.10. Seismic Line 10 through the Gela Foredeep Basin, modified after Catalano et al. (1996); see Fig. 3.5 for location and Tab. 3.3 for the description of the main horizons (TMS: Top of Miocene; PQ3: Top of Trubi; PQ1: Top of Calabrian). The Gela Basin extends south of the Gela Thrust System (GTS characterized by onlap termination against the GTS. The latter, marked by several SW-verging thrusts, clearly deforms the TMS and PQ3 horizons.

On the top of the GTS, the Zanclean (c. 5.3 Ma) to Gelasian (c. 2.6 Ma) strata seem to be gradually folded, indicating that the accretionary wedge was still advancing southward and undergoing deformation due to internal shortening during this period. Furthermore, as noted by prior authors (Trincardi and Argnani 1990; Lickorish et al. 1999; Cavallaro et al., 2017), the GTS's surface slope plunges toward the Gela Basin, showing the gravitational instability of the sediments resting above the nappe, expressed by shallow and buried landslide bodies in the Gela Basin (Figs. 3.2, 3.7b, 3.11a).

3.5.6. The Madrepore Bank

The southern sector of the GTS is defined by the presence of the Madrepore Bank (Figs. 3.1, 3.11a, 3.12), a fault-bounded, 50 km long by 18 km wide, NW–SE trending monocline whose top has a depth range from 175 to 750 m bsl (Fig. 3.1) (Cavallaro et al., 2017; Maiorana et al., 2023). It is

mainly composed of a Pre-Messinian succession, lacking the Post-Messinian (Plio-Quaternary) cover (Fig. 3.11a) (Cavallaro et al., 2017).

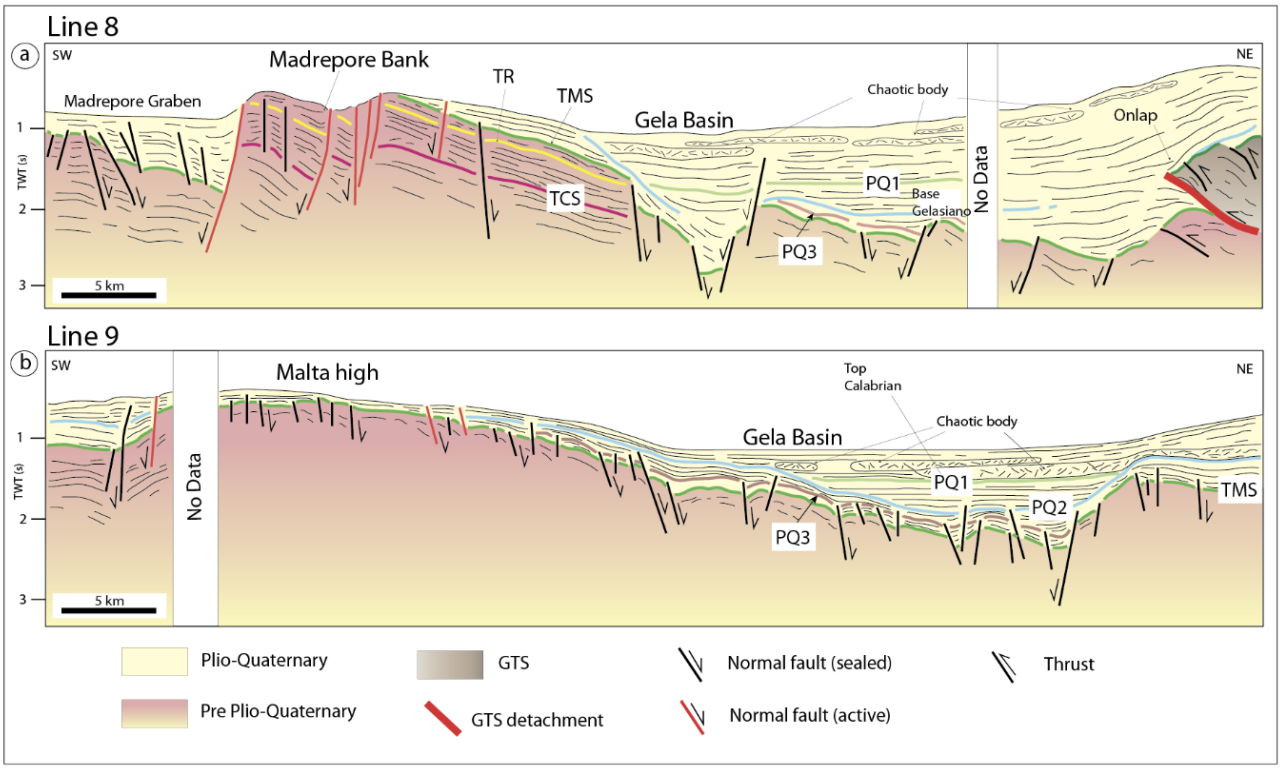

Fig. 3.11. (a) Seismic Line 8 and (b) Seismic Line (b) through the Gela Foredeep Basin, modified after Cavallaro et al. (2017); see Fig. 3.5 for location and Tab. 3 for description of the main horizons (TCS: Top of Carbonate succession; TR: Top of Ragusa; TMS: Top of Miocene; PQ3: Top of Trubi; PQ2: Base of Gelasian; PQ1: Top of Calabrian). In (a) the Gela Basin, marked by onlap termination against the Gela Thrust System (GTS) and the Madrepore Bank; the latter is characterized by the absence of Plio-Quaternary sediments on its top and displays active extensional faults as they reach the seafloor; in (b) the Gela Basin and the Malta High, which is covered by a thin layer of Plio-Quaternary deposits and marked by widespread extensional tectonics.

To the south, the Pre-Messinian succession is covered by the middle-upper Miocene silty marls of the Tellaro Fm., in turn, overlain by the Messinian evaporites and by a thin cover of Zanclean–Piacenzian (c. 5.3-3.6 Ma) sediments. The Pre-Messinian succession is mainly composed of carbonates and marls (Ragusa Fm. - Oligocene–Early Miocene), limestones (Amerillo Fm. - Late Cretaceous–Eocene), marls (Hybla Fm. - Early Cretaceous), mudstones (Fadhene and Sidi Kralif Fms. - Early Cretaceous) and marls (Buccheri Fm. - Middle Jurassic) (Fig.3.3), according to correlations with the Egeria 1 well log proposed by Cavallaro et al. (2017).

According to findings in this area (Antonelli et al., 1988; Corti et al., 2006; Cavallaro et al., 2017), there have been localized reactivations of earlier normal faults that trend NW-SE (Figs. 3.11a, 3.12). A sharply SW-dipping and NW-SE-striking normal fault system over the Madrepore Bank is shown in Fig. 3.10a, affecting the whole post-Messinian succession, disrupting the TCS, TR (Top of Ragusa, Oligo-Miocene) and the TMS horizons, as well as, clearly reaching the seabed. Among them, one W-dipping and NW-SE-striking normal fault separate the Madrepore Bank from a depression, i.e, the Madrepore Graben (Maiorana et al., 2023), filled of about 0.8 s/TWT of Post-Messinian (Plio-Quaternary) sediments; the latter seal a NW-SE-oriented normal fault system that also penetrates in the Pre-Messinian succession (Fig. 3.11a).

3.6. Discussion

3.6.1 Tectonic evolution of the Sicily Channel from late Miocene to Quaternary time

Overall, the Mediterranean region underwent contractional deformation during the Late Miocene due to the convergence between Africa and Eurasia (Dercourt et al., 1986; Dewey et al., 1989). This resulted in the development of the Calabrian arc and of the Sicilian-Maghrebian thrusts front, in the northwest of Sicily (Fig. 3.12) (Antonelli et al., 1988; Civile et al., 2021; Sulli et al., 2021). Within the regional context, the Sicily Channel started to correspond as the foreland area of such a chain. The selected seismic lines reported in this study (Figs. 3.5-3.10), integrated with a detailed review of the already published literature, allow us to reconstruct the main tectonic evolutionary steps of this area from the Late-Miocene up to Plio-Quaternary (Figs. 3.13, 3.14, 15) of this foreland area.

In the Late Miocene-Lower Pliocene Southern Apennines and Ionian Slabs retreated rapidly (Civile et al., 2021). Suddenly, a reorientation of the stress field and a change in the boundary conditions for the Central Mediterranean occurred, establishing a transitional area between the slow relative NW movement of the African plate and its eastward opening (Civile et al., 2021).

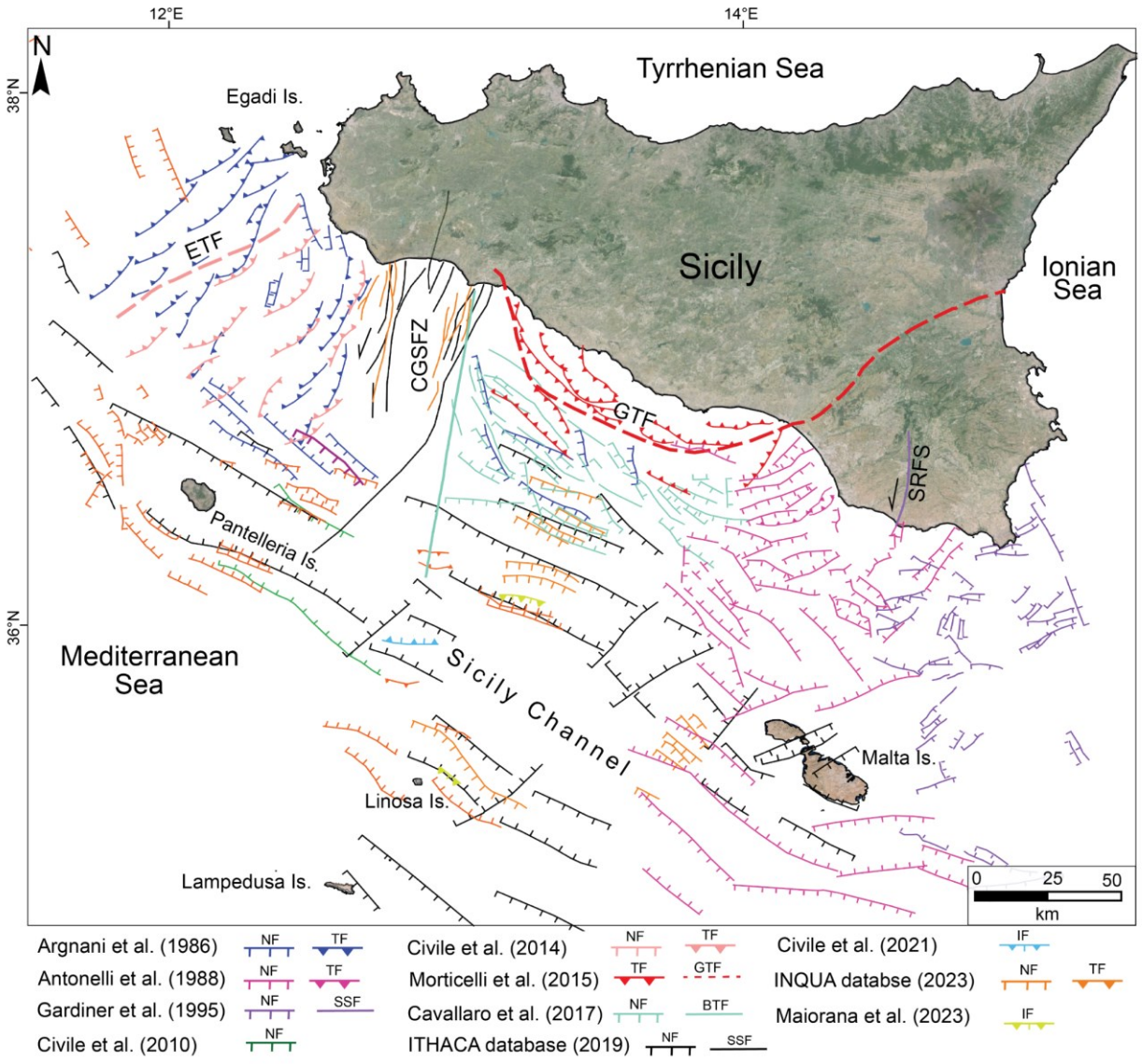

Fig. 3.12. Map compilation of all tectonic structures of Sicily Channel that have been active since Late Miocene time (for Late Miocene-Early Pliocene, see Fig. 3.13; for Pleistocene see Fig. 3.14; for Active see Fig. 3.15). CGSFZ: Capo-Granitola Sciacca Fault Zone; ETF: Egadi Thrust Front; GTF: Gela Thrust Front; IF; Inverted Fault; SRFS: Scicly Ragusa Fault System; NF; Normal fault; TF; Thrust fault; SSF; Strike-Slip Fault.

This differential motion was accommodated along the Sicily Channel by the onset of i) the opening of the Pantelleria, Linosa, and Malta Graben, resulted from a NW-SE-oriented extension of the African plate's foreland area (Corti et al., 2006; Catalano et al., 2009; Civile et al., 2010; 2021; Maiorana et al., 2023), possibly with a dextral strike-slip component (Catalano et al., 2009; Civile et al., 2021); and ii) the two roughly NS-trending regional-scale shear zones developing: the CGSFZ to NW, activated since the Late Miocene (Ferranti et al., 2019) or the Lower Pliocene (Fedorik et al.,

2018; Civile et al., 2021), and the SRFS to NE, developed mainly onland and extending also offshore toward Malta Island for a minimum length of 40 km (Gardiner et al., 1995; Pellegrino et al., 2016) (Fig. 3.13). Both of them are the result of the reactivation in a strike-slip stress regime of previous Mesozoic discontinuities (see maps in Fig. 3.4) (Antonelli et al., 1988; Pellegrino et al., 2016).

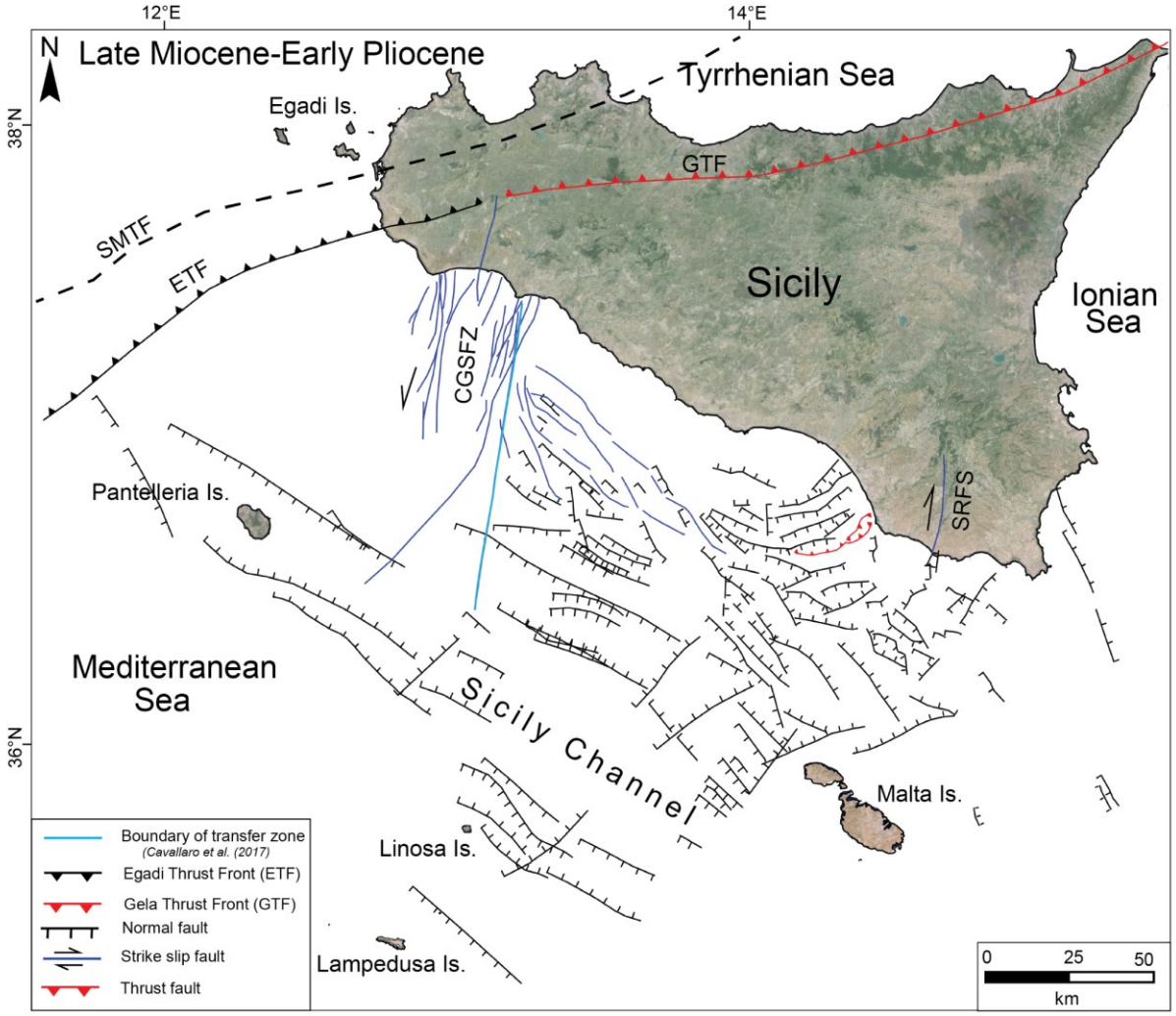

Fig. 3.13. Map of the active Late Miocene-Early Pliocene structural features in the Sicily Channel derived from Fig. 3.12 (see section 3.6.1 for detail). CGSFZ: Capo Granitola Sciacca Fault Zone; SRFS: Scicly Ragusa Fault System; SMTF: Sicily-Maghrebian Thrust Front; ETF: Egadi Thrust Front; GTS: Gela Thrust Front.

In addition, NW-SE and NE-SW- oriented extensional faults developed near Malta Island and the SRFS (Antonelli et al., 1988; Gardiner et al., 1995) (Fig. 3.13).

During the Lower Pliocene, the Siclilian-Maghrebian thrust front was segmented by the CGSFZ, resulting in two opposing and verging fold-and-thrust belts: the SE-verging ETF and the SW-verging

GTS (Argnani et al., 1986; Civile et al., 2014; Morticelli et al., 2015) (Fig. 3.13). These belts were both marked by vigorous compressional tectonics that were exemplified by thrusts and backthrusts (Civile et al., 2021) (Fig. 3.13). Moreover, the GTS advance induced positive reactivation in the Madrepore Graben, in agreement with the first stage of advancement of the GTS dated to the Piacenzian (3.13 Ma) as reported by Cavallaro et al. (2017), Civile et al. (2021), and Maiorana et al. (2023).

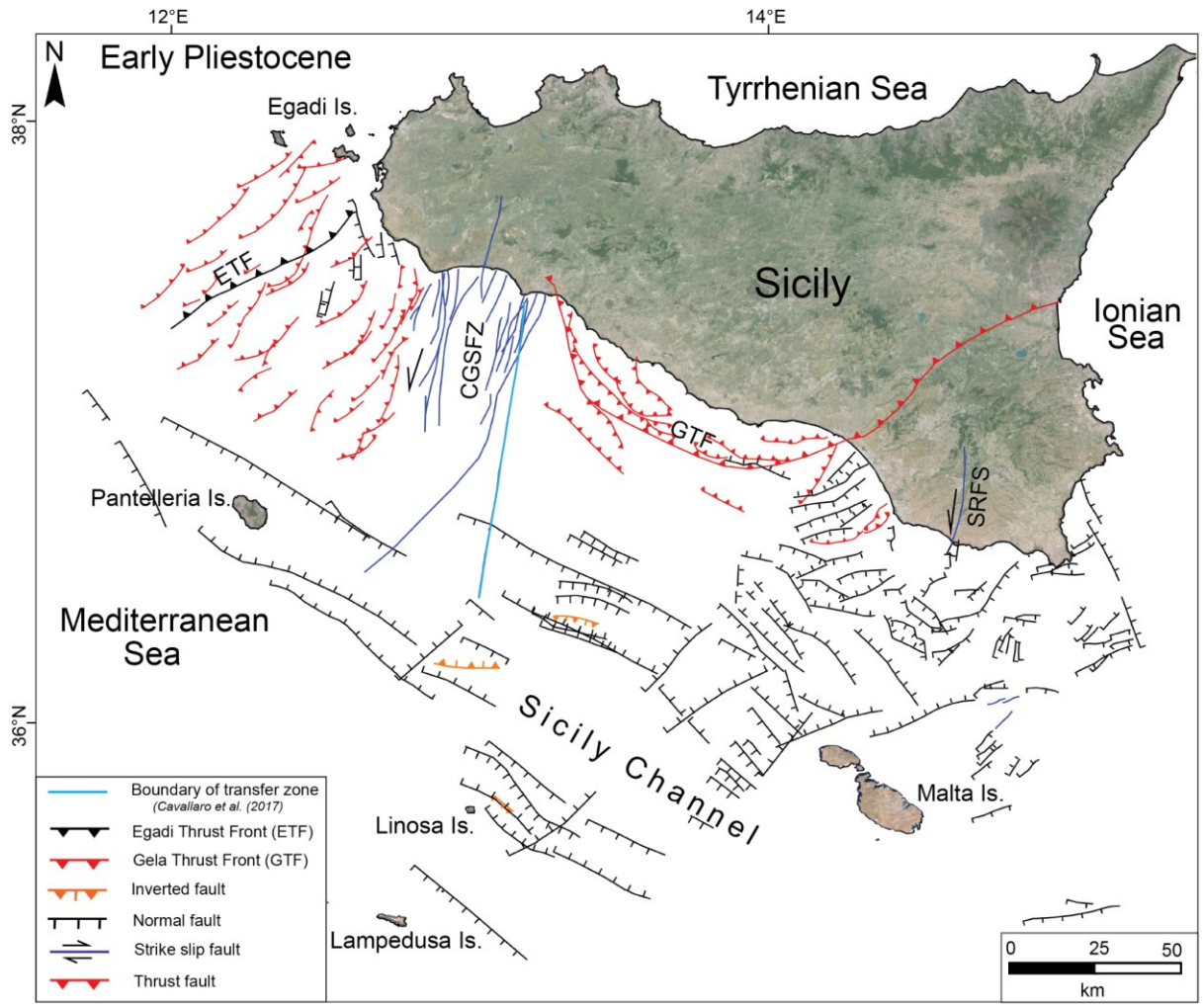

Fig. 3.14. Map of the active Early Pleistocene structural features in the Sicily Channel extracted from Fig. 3.12 (detail in section 3.6.1). CGSFZ: Capo Granitola Sciacca Fault Zone; SRFS: Scicly Ragusa Fault System; ETF: Egadi Thrust Front; GTS: Gela Thrust Front.

In Early Pleistocene, the subduction in the Southern Apennines was inhibited by the entrance of the continental Apulian lithosphere at the trench, and the subduction process was active only in the Ionian domain with the retreat of the oceanic slab that induced the rapid SE migration of the Calabrian Arc

(Civile et al., 2021). The ongoing GTS advancing to SSW transmitted compressive stress to the Sicilian foreland, inducing positive reactivation of previous SE-dipping and NW-SE-oriented extensional faults in the Linosa and Malta grabens (Cavallaro et al., 2017; Civile et al., 2021; Maiorana et al., 2023) (Fig.3.14), thus recording the last stage of the GTS advancement, in 0.8 Ma (upper Calabrian) (Di Stefano et al., 1993; Cavallaro et al., 2017; Maiorana et al., 2023).

Simultaneously, compression persisted in the NW sector of the Sicily Channel as well: the ETF kept moving to the SW and was characterized by a few minor NW-verging back thrusts as well as many SW-verging thursts (Argnani et al.,1986; Catalano et al., 2000; Civile et al., 2014) (Fig. 3.14).

Extensional tectonics related to the Malta, Linosa, and Pantelleria Grabens remained active (Antonelli et al., 1988; Civile et al., 2010; Cavallaro et al., 2017; Civile et al., 2021; Maiorana et al., 2023), as well as the system of NW-SE and NE-SW oriented extensional faults located in the easternmost part of the Sicily Channel, between Malta Island and the SRFS (Antonelli et al., 1988; Gardiner et al; 1995) (Fig. 3.14).

In the meantime, strike-slip faulting activity continued in the lithospheric discontinuities CGSFZ and SRFS, which combined with the GTS compressive stress were probably partly responsible for the positive inversion observed in Malta, Linosa, and Pantelleria Grabens (Fig. 3.14).

Throughout the entire CGSFZ, transpressional tectonic was active, and the SRFS may have shifted from a right-lateral to a left-lateral strike-slip motion sense which produced by a change in the direction of the African plate motion with respect to the fixed Eurasia, from NW to NE (Mantovani et al., 2014). (Fedorik et al., 2017; Ferranti et al., 2019; Civile et al., 2021). However, shortening in the GTS ceased around the end of the Early Pleistocene when the GTS reached its present-day position (Catalano et al., 1996, 2013; Civile et al., 2021; Maiorana et al., 2023); in contrast, shortening related to ETF persisted (Civile et al., 2014) (Fig. 3.15).

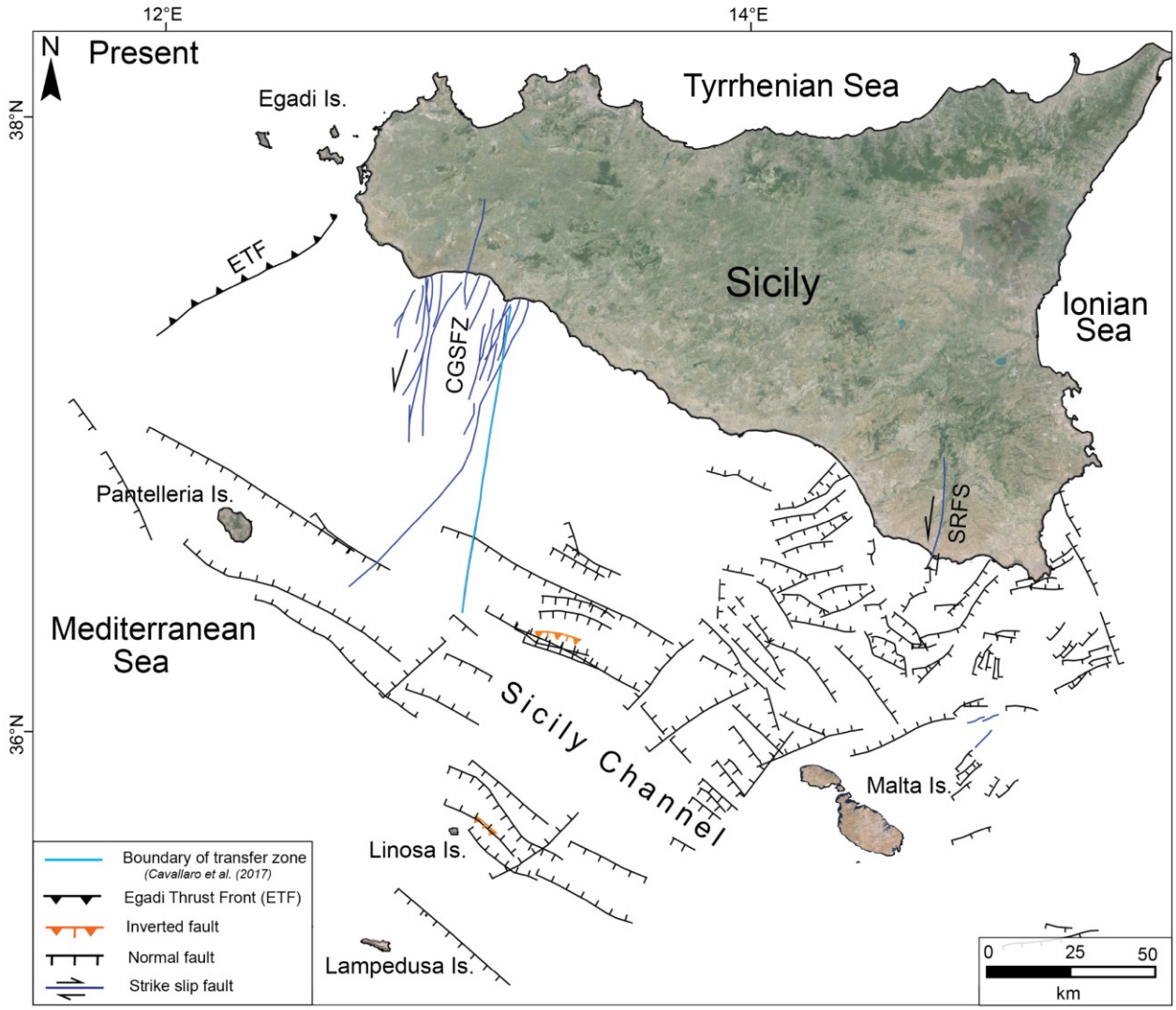

Fig. 3.15. Map of the present day active structural features in the Sicily Channel, derived from Fig. 3.12 (refer to section 3.6.1 for detail). CGSFZ: Capo Granitola Sciacca Fault Zone; SRFS: Scicly Ragusa Fault System; ETF: Egadi Thrust Front.

At present day, Malta and Linosa Grabens show signs of positive inversion of former extensional faults (Fig. 3.15). These are primarily two NW-SW oriented and SW-dipping positive inverted faults that are thought to be a reaction to a potential plate reorganization and shift in subduction polarity (Sulli et al., 2021; Maiorana et al., 2023), as a results of the associated stress field (Sulli, 2000) that causes localized reactivations of such pre-existing extensional faults, which are prone to reactivation since they reflect zones of weakness (Maiorana et al., 2023). This last stage is also accommodated by the ongoing activity of CGSFZ (Fig. 3.15) which today is tectonically active, as testified by the

occurrence of seismic events depicting a roughly N-S arrangement with focal mechanisms characterized by strike-slip kinematics (Fig. 3.2a).

However, the available GNSS data, collected in the last two decades (Fig. 3.2b), show a diverging pattern between MALT and LAMP stations, suggesting a significant stretching across the Linosa and Malta Grabens, which could indicate a very early incipient reactivation of the above-mentioned faults with extensional kinematics, not yet recorded in the sedimentary cover of the Sicily Channel shown in seismic profiles (Fig. 3.15). Such a recent feature is supported by the few available focal mechanisms, showing normal faulting features (Fig. 3.2a).

Also, ETF is active till date (Fig. 3.6) as suggested by the seafloor deformation described by Torelli et al., (1993, 1995); Civile et al. (2014) (Fig. 15). Towards the eastern part including the Malta plateau the normal faults seem to be more recently active as they have recently formed a series of seafloor horst blocks (Antonelli et al., 1988; Gardiner et al., 1995) (Fig. 3.15).

3.6.2. Plio-Quaternary structures in the Sicily Channel and implications on foreland (unstable) tectonics

The detailed review and analysis of the seismic reflection profiles reported in this study, along with the building of a general structural map, indicates widespread evidence of Plio-Quaternary tectonic activity affecting the Sicily Channel, despite the region's foreland nature suggests it should be part of a relatively stable continental area. According to the structural map in Fig. 3.12, the Sicily Channel is home of three major coexisting tectonic regimes.

The southernmost portion of the area features a pure and continuous extensional regime, exemplified by a NW-SE-striking normal fault system, at approximately 170 km from the surrounding orogens fronts (ETS and GTS). This extensional regime continues the predominant mode of deformation as it moves toward the northeast, here responsible for the development of both surface and deep Plio-Quaternary tectonic structures. The evidence of this process are the extensional faults forging the

grabens of Pantelleria, Linosa, and Malta (Fig. 3.1, 3.2), as well as for the establishment of the roughly N-S trending volcanic belt that stretches from Lampedusa to Malta (Civile et al., 2008) (Fig. 3.2). Nonetheless, a new tectonic regime -a compressional regime- appears, localized and concentrated inside the grabens. But extensional focal mechanisms and the current increasing distance between LAMP and MALT stations (Fig. 3.2 a, b) suggest a recent stretching along the NE-SW direction in the grabens (Fig. 15) (at 129 km from the ETS-GTS).The greatest evidence is found in NW-SE-oriented high-angle reverse faults, whose origin can be inferred as the positive inversion of previous Mesozoic normal faults (Cavallaro et al., 2017; Civile et al., 2021; Maiorana et al., 2023). By contrast, a strike-slip/transpressional regime, typified by the CGSFZ, arises proceeding to NNW. It is noteworthy that the CGSFZ disrupts the NW-SE extensional faults connected to Malta, Linosa, and Pantelleria grabens in the NNW portion of the region, resulting in the overlap of two distinct tectonic regimes: strike slip/transpressive and extensional (Fig. 3.12).

All of the tectonic structures related to the previously described regimes generally penetrate the deeper Pre-Pliocene layers, including the faults that are positively inverted, thus suggesting thick-skinned tectonics in the Sicily Channel (basement involved) (Cavallaro et al., 2017; Civile et al., 2021; Maiorana et al., 2023). Given that the inverted faults enucleated from basement-affecting faults, which are linked to the rifting tectonic stage that preceded the compressive regime's development, this indicates a strong relationship between the two. In this sense, it is well known that positive inverted faults are generally largely influenced by the geometry and orientation of the structures developed during the previous phase of extension (Nalpas et al., 1995; Ziegler et al., 1995; Amilibia et al., 2005; Del Ben et al., 2010; Rodríguez-Salgado et al., 2022). In particular, reactivation of extensional faults often occurs as reversal when the pre-existing extensional fabric is almost orthogonal to the direction of shortening (Ziegler et al., 1995; Cooper and Warren, 2015; Rodríguez-Salgado et al., 2022).

The GTS stress field, that induced the Sicily Channel's inversions since the Middle Pleistocene (Cavallaro et al., 2017; Civile et al., 2021; Maiorana et al., 2023), was almost orthogonal to the NW-SE-striking extensional faults, according to the recently published evolutionary model of Maiorana et al. (2023). As a result, these faults were reactivated in a compressive regime. There are several cases in the Mediterranean area where compressional stresses were transmitted several kilometers from the main deformation fronts, inducing the inversion of rifted and/or flexed foreland basins, thus sharing similar features with the Sicily Channel. Among them, the northern Tunisia, marked by a widespread compressional Eocene phase that led to reactivation as reverse of several extensional faults (Masrouhi et al., 2008; Khomsi et al., 2009; Rigane et al., 2011); the Adriatic Sea, characterized by reverse reactivation of Mesozoic normal faults associated with the main phase of emplacement of the outer Apennine chain (Calamita et al., 1991; Scisciani, 2009; Satolli and Calamita, 2012; Pace et al., 2015); and the Ionian Sea, marked by several positive inverted faults generated due to the stress transmitted by the Calabrian Arc-Hellenic fold-and-thrust belt to the southern Adria Plate (Del Ben, 2009; Del Ben et al., 2010; Basso et al., 2021; Chizzini et al., 2022, 2023).

It is important to point out that the presence of fluid-related features, well documented in the Sicily Channel in the form of pipes, bright spots, buried mud volcanoes, zones of acoustic blanking, and seafloor fluid seeps (Spatola et al., 2018; Civile et al., 2023; Maiorana et al., 2024) may, in the presence of such compressive stress, facilitate the reactivation of extensional faults as reverse because they could reduce the friction along the fault plane (Sibson, 1995).

The intrusion of magmas and the consequently high heat flow are two further factors that can favor a significant intra-plate deformation in this area. It is generally known that, from a rheological point of view, the lithosphere of a rift that is destabilized by increased heat flow and/or magma intrusion is not as strong as that of thermally stable rift zones (Ziegler et al., 1995; Rooney, 2017; Shillington, 2020; Pérez-Gussinyé et al., 2023). The existence of several extensive volcanic zones (Fig. 3.2) and magmatic intrusion (Figs. 3.8, 3.9) most of them linked to a Moho rising at relatively shallow depths up to 17–18 km in the Malta and Linosa grabens (Maiorana et al., 2023), may have contributed to

weakening the Sicily Channel and making it prone to tectonic deformation with a high variability of tectonic regimes.

However, it is necessary to emphasize that regional plate tectonics is primarily responsible for controlling foreland tectonics and its architecture (Richardson, 1992; Zoback, 1992; Ziegler et al., 1995; Doglioni et al., 1999; Carminati et al., 2010; Wang et al., 2023; Zheng et al., 2023). In the Sicily Channel, the interplay between slab-pull and roll-back, as plate driving forces, are considered as the main processes triggering the extensional tectonics affected this area during Plio-Quaternary and currently shaping it (Argnani, 1990; Govers and Wortel, 2005; Rosenbaum et al., 2008; Argnani, 2009; Arab et al., 2020; Maiorana et al., 2023). In this scenario the slow and oblique convergence and collision between Africa and Eurasia started since the Late Cretaceous (Bellon and Letouzey, 1977; Dercourt et al., 1986; Dewey et al., 1989; Stampfli and Borel, 2004; Mascle and Chaumillon, 1997; Polonia et al., 2011; Jolivet et al., 2021) associated with periods of plate-boundary reorganization, whose occurrence was already evidenced in this area by Sulli et al. (2021) in recent (Lower Pleistocene to present) times, are held responsible for the nearly contemporaneous inception of compressive tectonic in this area.

3.7. Conclusions

Based on a detailed review of the already-published structural and stratigraphic data of the Sicily Channel, we have provided, for the first time, a general overview of the main tectonic features affecting this complex area, as well as a tectonic evolution since the Late Miocene to Present day. Overall, all the previous considerations allowed us to establish the following broad findings:

1) Having its origin in a simple stage of passive rifting, the Sicily Channel developed from the interaction of multiple tectonic processes operating in a regional scale (slab pull and slab roll-back in particular) and linked to the complex geodynamic system of the Central Mediterranean, implying that regional plate tectonics represents the primarily responsible for controlling foreland architecture.

2) Structural discontinuities and preexisting weakness zones, such as previous extensional faults, are generally prone to reactivation in a compressional way, because they correspond to zones of preferential strain concentration that may favor the establishment of an intra-plate compressive regime, even if these zones are located far from the orogens. Moreover, the interplay between the early structural grain of a plate and the compressive stress orientation plays an important role in the localization of present-day tectonic structures as well as on the future basin architecture.

   Considering the Sicily Channel as a natural laboratory, we can state that foreland regions can assume the role of sensitive recorders of the dynamic processes that control lithosphere deformation and are naturally susceptible to tectonic inversion. This is particularly true if they include a strongly faulted crust, as other regions in the Mediterranean area feature (Adriatic and Ionian Seas).

   This new compilations / structural maps of the Sicily Channel is of interest for anyone working on geohazards of this complex region and relate seismic event to active structures, as well as for interpreting and better constraining the kinematics of this area and other foreland locations worldwide.

Chapter 4

A special case of inversion newly found in the Egadi thrust front interacting with the Sicily channel (foreland) rifting

4.1. Introduction

The positive inversion occurs when there is a reversal in the slip of normal faults subsequently due to compressional or transpressional forces which results in the development of the contractional features (Bally, 1984). The normal faults make the space for the sediments (syn-rift) in their hanging walls (Gawthorpe & Leeder 2000). The presence of the syn-rift deposits is a prerequisite for interpreting the inversion and its consequences on the rest of the sedimentary infill (Bally, 1984; Cooper et al. 1989). After the occurrence of inversion, the post-rift sequence highlights the shortening, and the pre-rift sequence remains in extension (Fig. 4.1).

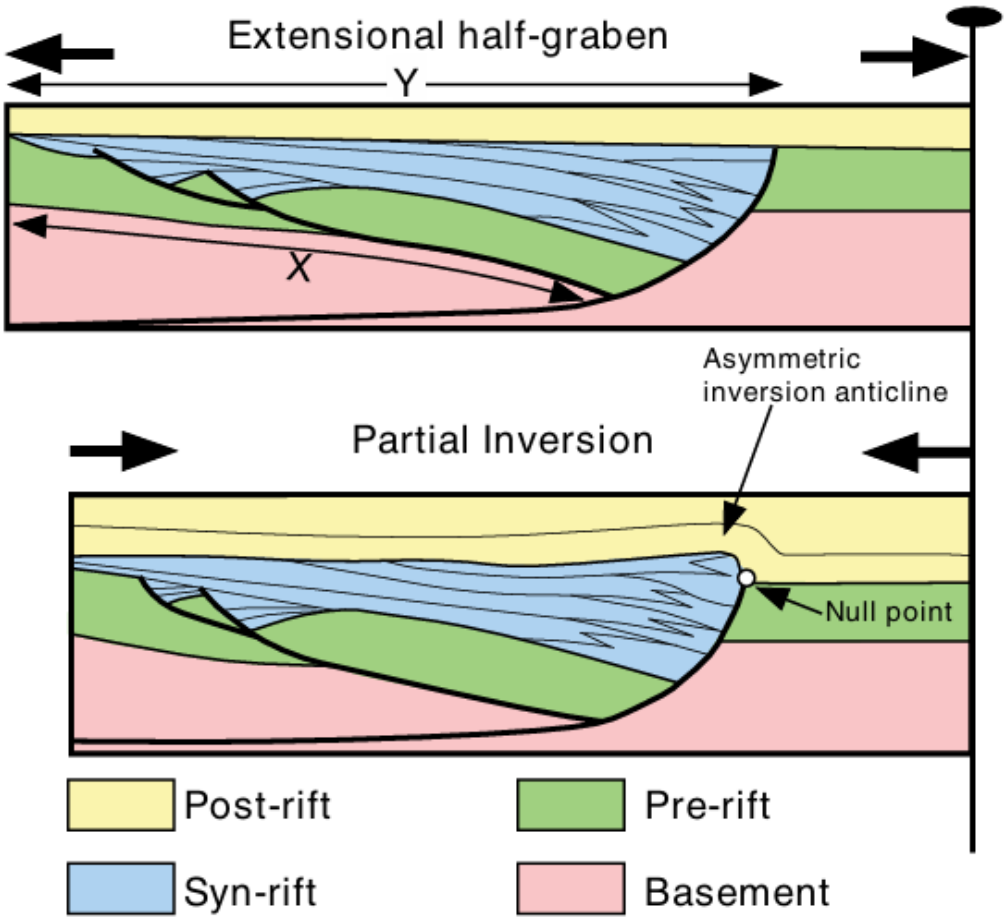

Fig. 4.1. Sketch of the basin inversion concept (taken from Bally, 1984).

In most of the orogenic belts of the globe, the inversion structures have been detected that suffered the extensional event first and later experienced the shortening (Fosdick et al., 2011; Jammes et al.,

2014; Raimondo et al., 2014; Dielforder et al., 2019; Jourdon et al., 2019; Fossen et al., 2020; Wolf et al., 2021). The evolution of orogens is characterized by the interaction between preexisting extensional structures and compressive deformation. This interaction is significant in depicting the structural setting of orogenic systems and in deciphering their tectonic evolution (Scisciani et al., 2002). This complex structural style is evident in fold-and-thrust belts, where compressive forces interfere with preexisting faults inherited from older rifting events (Tavarnelli et al. 2004; Pace and Calamita 2014). The Sicily Channel embodies all the tectonic elements described above. It is an archetype that represents the coexistence of extensional and contractional structures. For instance, the NW-oriented grabens (Pantelleria, Linosa, and Malta) formed during the Early Pliocene rifting event, exist together with the Sicilian Fold and Thrust Belt (exists in the NW portion). Positive inversion tectonics has hit this region due to different causes at different times (Gamberi and Argnani, 1995; Sulli, 2000 Cavallaro et al., 2017; Civile et al., 2021; Maiorana et al., 2023). In the Western and Northwestern offshore, the inversion structures are often present in the sedimentary fill of extensional basins which formed due to the compressional pulses owing to the kinematics of the Maghrebian collision zone (Catalano and Milia, 1990; Gamberi and Argnani, 1993). The inversion in the basins present in the Egadi shelf is possibly linked to the change in the stress field from E-W to N-S (Gamberi and Argnani, 1995; Sulli, 2000). The contractional structures in north-central Sicily Channel have been developed due to the Neogene–Quaternary southward advancing of the Gela Thrust System Catalano et al. 1993; Cavallaro et al., 2017).

The chapter is focused on the complexity of the offshore of NW Sicily Channel, which reveals the coexistence of two independent tectonic settings of extension and compression. These tectonic events and the timing of the polyphase deformation events were not clearly demonstrated in past studies which showed prevailing compressional structures related to the Maghrebian Orogen (Gamberi and Argnani, 1995; Gamberi and Argnani, 1993; Tavarnelli et al., 2003). But the analyses carried out onthree key multichannel seismic reflection profiles (CS89-01C2, G82-63 and G82-45) (Fig. 4.2, 4.6-4.11) sheds light on the chronology of the polyphase deformation events that have hit the study area

in the past and that affected the sedimentation rate analysis of the Plio-Quaternary succession in the basins (B1, B2 and B5) (Fig. 4.2a, b).

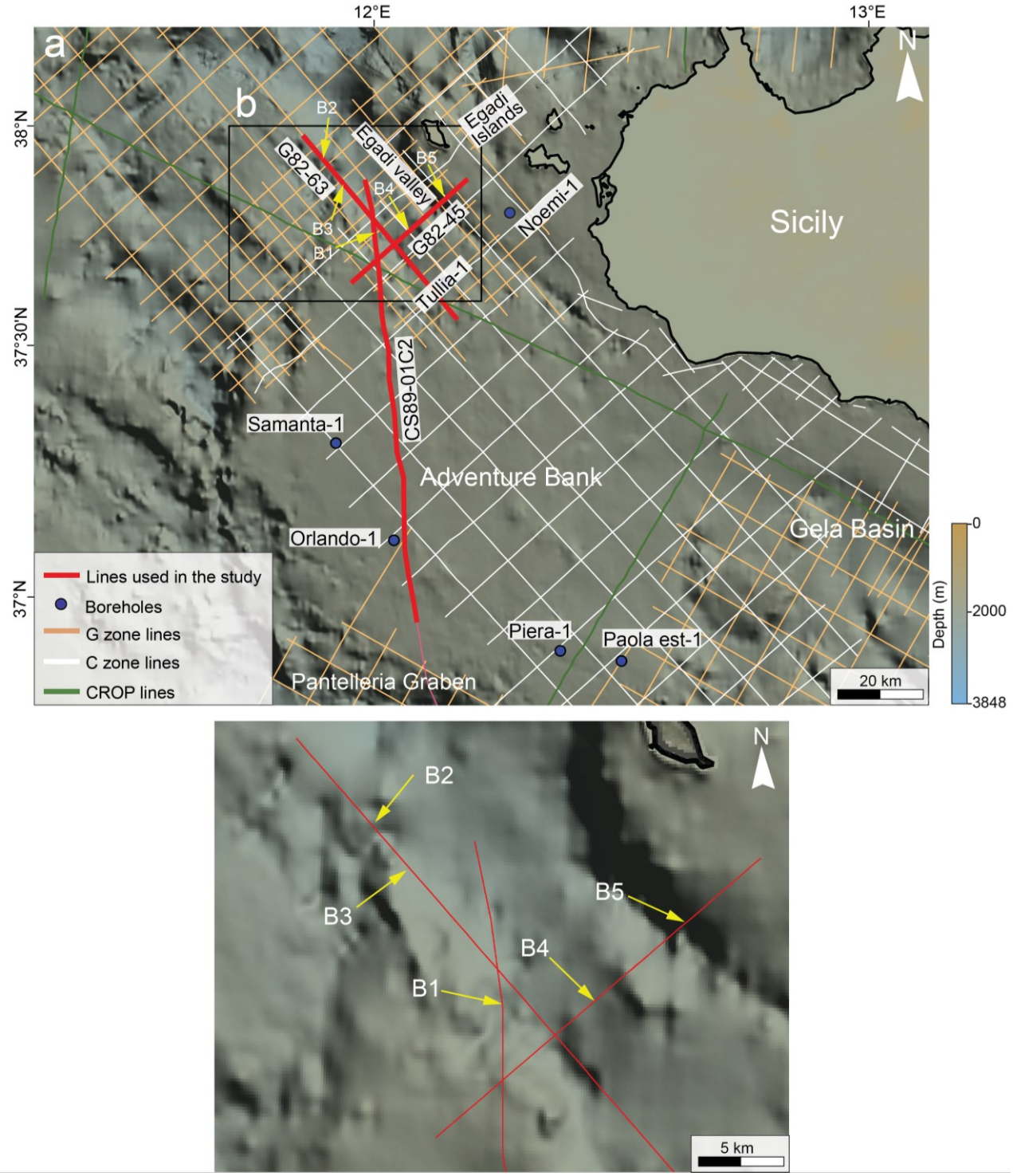

Fig. 4.2. (a) Location of the multichannel seismic reflection profiles and wells used in this study. (b) B1, B2, B3, B4 and B4 represent the position of different basins analyzed to achieve the results. Bathymetry data extracted from EMODnet (http://www.emodnet-bathymetry.eu/) DTM (2022).

4.2. Geological setting and study area

The post-collisional convergence between the European and African plates and the coeval sinking and rollback of the Ionian Ocean crust beneath the Tyrrhenian Sea developed the Sicily Maghrebian Thrust Belt (SMTB) which stretches across North Africa, Northern Sicily and can be prosecuted in Calabrian Arc of Peninsular Italy (Roure et al. 1990; Pepe et al. 2000, 2005; Faccenna et al., 2004; Rosenbaum and Lister 2006; Chiarabba et al., 2008; Corradino et al., 2022) (Fig. 4.1).

Sicily Channel is part of the northern African margin which is the location of three main NW SE trending tectonic grabens (Pantelleria, Linosa and Malta), developed from the Early Pliocene rifting event (Winnock, 1981; Jongsma, Reuther & Eisbacher, 1985; Boccaletti, Cello & Tortorici, 1987; Cello, 1987; Dart, Bosence & McClay, 1993; Argnani, 1990; Catalano et al., 1995; Civile et al. 2010; 2021) (Fig. 4.3). A N-S trending transfer zone (TZ) marks the division between the Pantelleria graben and the Linosa and Malta grabens. Most of the area of the Channel features shallow water depth (< 400 m) except the three main grabens. The Pantelleria Graben is 1.3 km deep, the depth of Malta and Linosa grabens range between 1.6-1.7 km. All three grabens are filled with thick pile of Plio-Quaternary sediments and have preserved the evidence of tectonic evolutionary history. Since the Early Pliocene, the NE-SW and ESE-WNW extensional structures associated with rifting crosscut the foredeep basin and the thrust structures associated with the Sicily Maghrebian orogenic wedge (Cello, 1987; Catalano & Milia, 1990; Roure et al. 1990; Casero & Roure, 1994; Catalano et al. 2011; Pepe et al. 2000, 2005).

During the late Miocene tectonic phase, the external thrust system of NW offshore Sicily was overthrusted by rootless nappes of Sicily Magrebian orogen (Catalano et al., 1995; Bello et al., 2000; Elter et al., 2003). The contractional structures associated with this process generated ESE and NNE-SSW verging thrusts (Argnani, 1986, 1993b; Civile et al., 2015., Grasso, 2001; Civile et al., 2015). The southern segment or front of this domain is the ESE-oriented Egadi Thrust Front (ETF) which connects Sicilian and African Maghrebides (Civile et al., 2014; Torelli et al., 1993) (Fig. 4.3). The

detached stack of thrust sheets is associated with ETF that formed the NE-striking imbricate structures (Argnani et al., 1987; Catalano Sulli 2000). These stacked units in the internal position consist of Mesozoic-Cenozoic carbonates and shales and the upper Paleogene Numidian flysch forms their external part (Antonelli et al., 1988; Lentini et al., 2006). According to Torelli et al. (1993, 1995) and Civile et al. (2014) the deformation of seafloor by ETF suggest that it is still active. However, Lentini et al. (1990) consider this frontal thrust inactive as it is buried under Plio-Quaternary deposits.

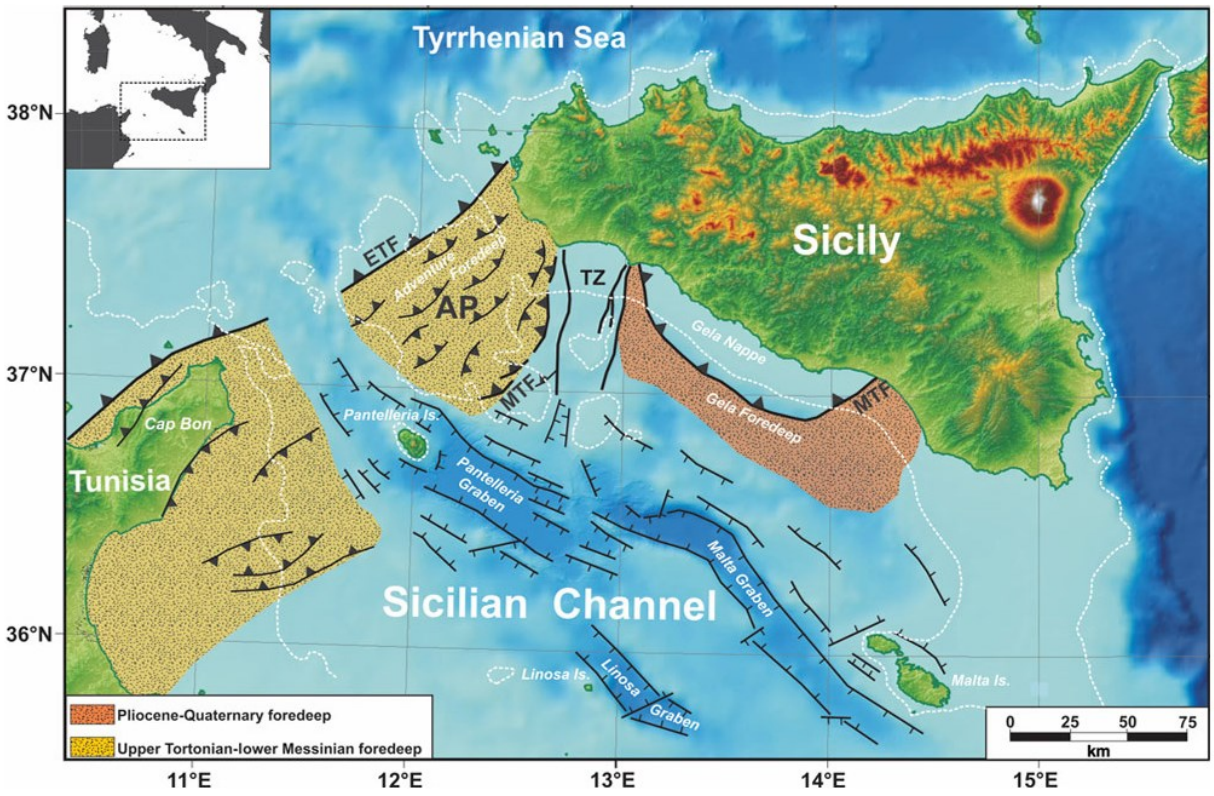

Fig. 4.3. Simplified structural map of the Sicily Channel and the adjacent areas (after Civile et al., 2015). AP– Adventure Plateau; TZ: NS-trending transfer zone; ETF: Egadi Thrust Front; MTF: external front of the Sicilian–Maghrebian thrust belt.

The offshore of Sicily including the Adventure Plateau is the unique area where the evidence of both extensional and compressional tectonics is found. The coexistence of extension and compression (occurring at the external side of ETF) in the NW of Sicily Channel highlights the tectonic complexity of the region (Argnani et al, 1986; Patacca et al., 1990; Corte et al., 2006; Civile et al., 2014). Since the late Pliocene, a widespread tectonic inversion of the previously formed normal faults has been reported in the Plio-Quaternary sediments of the extensional basins existing in the NW offshore Sicily

(Catalano et al., 1985; Compagnoni et al., 1989; Trincardi and Zitellini, 1987; Argnani and Trincardi, 1991; Bartole et al., 1991; Boccaletti et al., 1992; McClay and Buchanan, 1992; Torelli et al., 1991; Gamberi and Argnani 1995., Sulli 2000). It was evidenced by syn-rift growth reflections assuming antiform shape, tilted onlaps and anomalous thickness of these sedimentary units and the folded seafloor topography highlights the recent reactivation of some of them (Catalano and Milia, 1990; Gamberi and Argnani, 1993; Sulli, 2000; Tavarnelli et al., 2003; Cuffaro et al., 2012). The positive inversion has been commonly recognized in the grabens due to compressive forces transmitted by the ETF to the foreland (Giunta et al., 2000; Nigro and Renda, 2001; Cuffaro et al., 2012).

4.3. Results and interpretation

4.3.1. Seismo-Stratigraphic succession

For constraining the stratigraphy of the study area, Paola-01, Piera-01, Orlando-01, Samantha-01, Tulia-01 and Noemi-01 wells were considered to define the stratigraphic succession. The correlation of wells in Fig. 4.4 is illustrated to demonstrate the main stratigraphic units and its lateral variation in the area. Among these wells Orlando-01, Samantha-01 and Tulia-01 were converted to Two Way Travel (TWT) time and projected on the nearest CS89-01C2 and G82-63 seismic reflection profiles (Fig. 4.1). The visualization of the lithology thickness and depth of these well logs in time was possible only by taking into account the velocities (Stripling, 1958; Brie et al., 1998; Wong et al., 2009). The primary stratigraphic contacts in the time domain were confirmed by comparing the reflectors with high acoustic impedance to the significant lithological contacts in well logs (Fig. 4.5a, b). This was done in order to determine the primary horizons in seismic lines and to calibrate seismo-stratigraphic units. Different seismic reflections from different lithologies allowed us to distinguish the different seismic facies. The integration of significant reflections, well-log and the already available seismic facies data in the literature paved the way to mark the various seismo-stratigraphic sequences. The reflection terminations (onlap, top lap and truncations) helped us to identify

unconformities in the basins. In the focused area, we have identified eight major seismic facies (A-J) which have been grouped into six main seismo-stratigraphic units (Figs. 4.5a, b, 4.6).

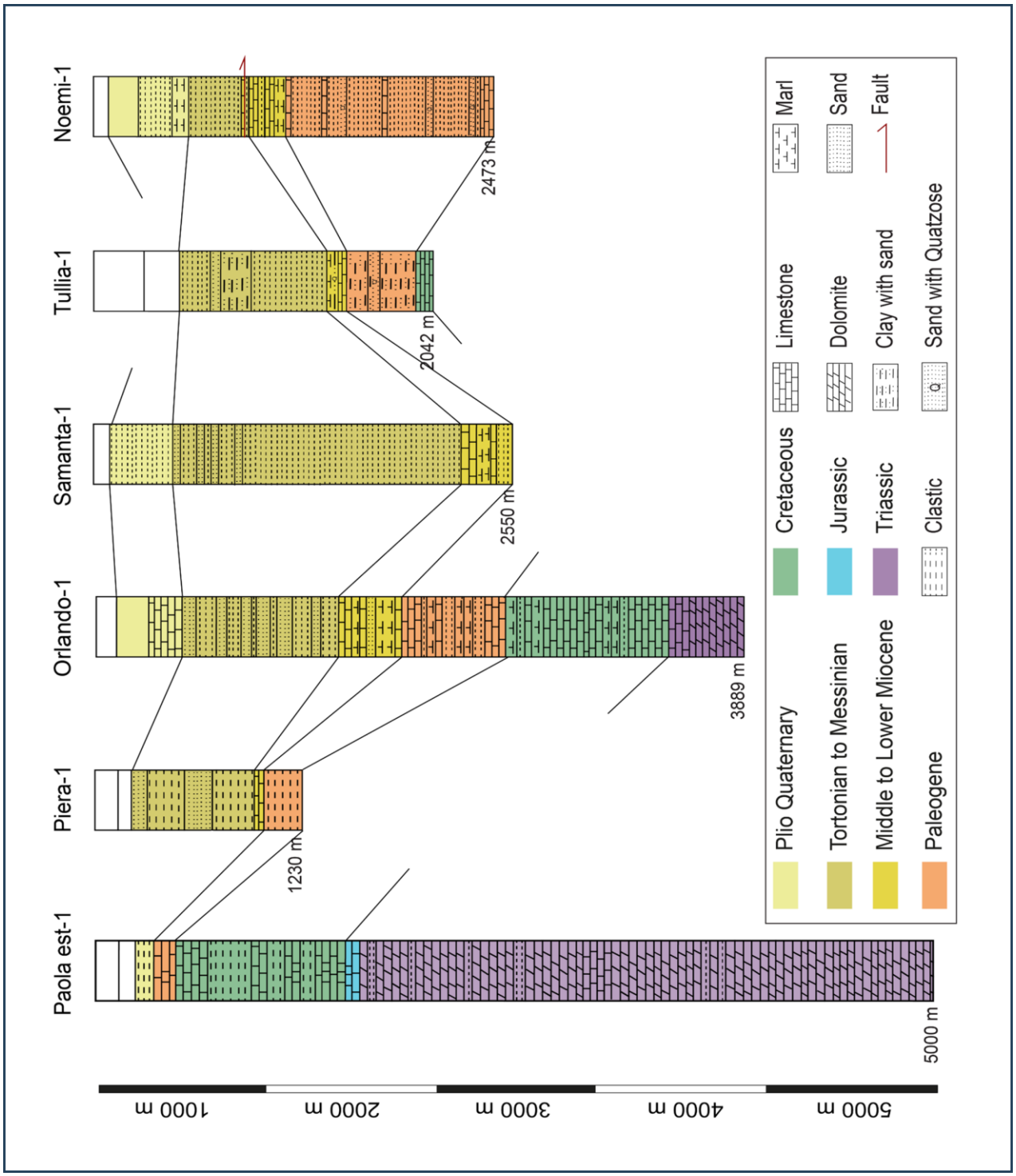

Fig. 4 4. Stratigraphic correlation among the wells used in this study. The well data is taken from (ViDEPI) database (http://www.videpi.com). Refer to Fig. 4.2 for the location of these wells.

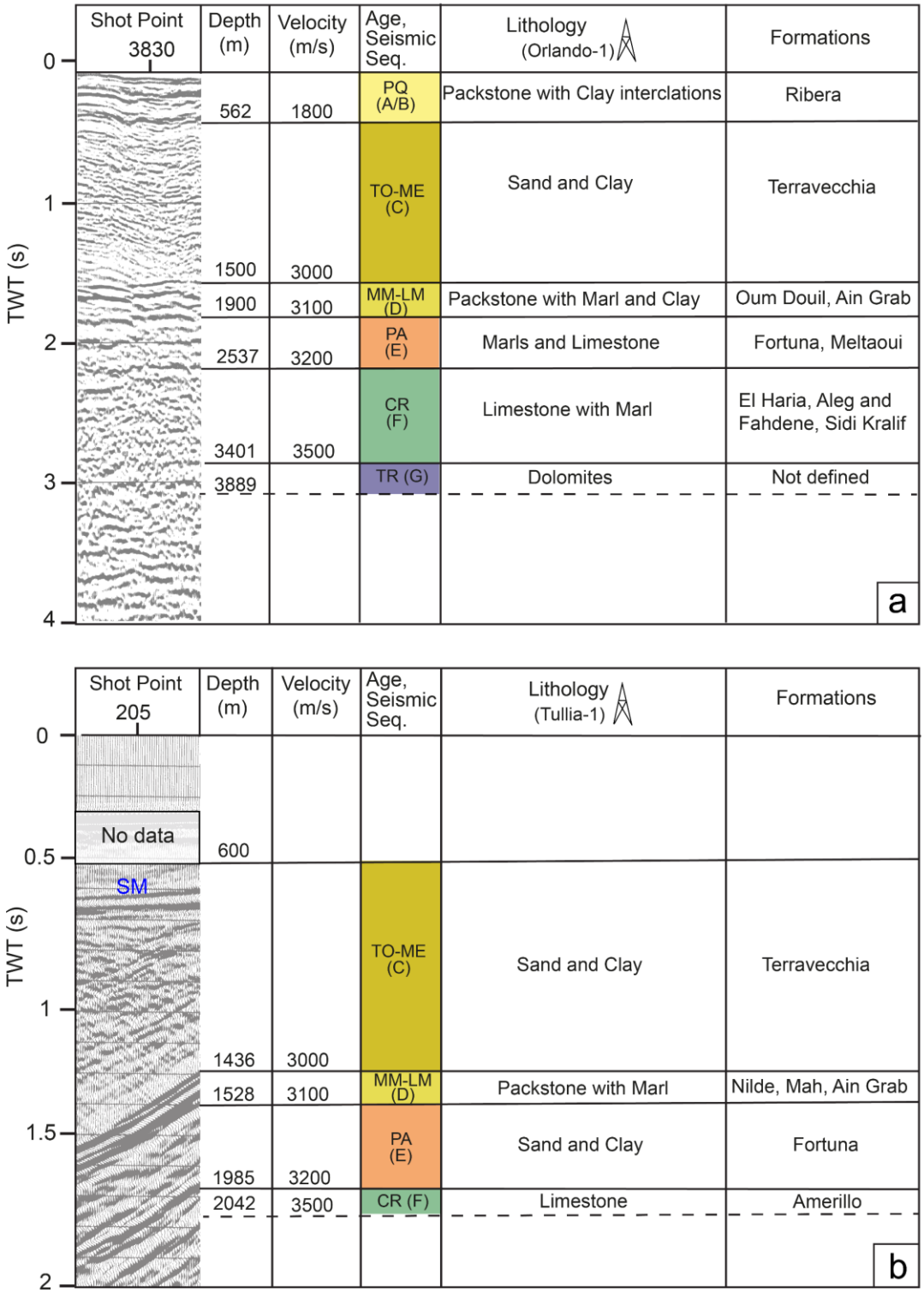

Fig. 4 5. Stratigraphic sequences of the Orlando-1 and Tullia-1 well logs used to calibrate the seismic units in CS89-01C2 (at shot point 3830) and G82-63 (at shot point 205) profiles respectively. The depth is evaluated for each unit which is linked to the respective lithology type and the formations. The dashed line represents the uncertainty of the boundary on the profiles owing to the low resolution of the data. PQ-Plio-Quaternary; TO-ME: Tortonian to Messinian; MM-LM: Middle Miocene-Lower Miocene; PA: Paleogene; CR: Cretaceous; TR: Triassic; SM: seafloor multiple.

Seismic sequence	Seismic example	Prevailing seismic facies
A Plio-Quaternary *(PQ)*	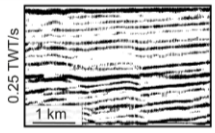	High to medium amplitude, low frequency and parallel to sub parallel reflections.
B Plio-Quaternary *(PQ)*	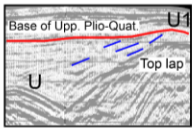	Semi transparent, medium amplitude, low to medium frequency and poorly layered reflections higlihghting the top lap against the top unconfirmity.
C Tortonian to Messinian *(TO-ME)*	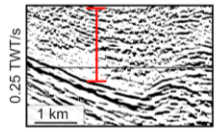	Poorly layered, Medium to high amplitude, medium frequency choatic reflections with transparent bottom.
	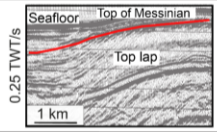	Medium to high amplitude, low frequency and semi contineous reflections showing top lap terminations.
D Middle to Lower Miocene *(MM-LM)*	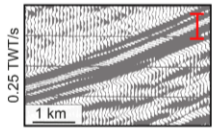	High amplitude, low frquency, contineous reflections present discretly.
E Paleogene *(PA)*	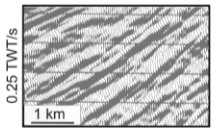	Medium to high amplitude, low frequency and semi contineous reflections.
	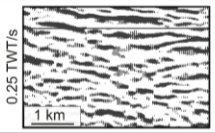	High amplitude, low frequency and semi contineous reflections .
F Cretaceous *(CR)*	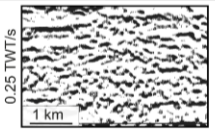	High amplitude, low frequency reflectors with poor lateral continuity.
G Basement	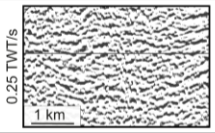	High to medium amplitude, variable frequency and discontineous reflectors.
H Volcanic body	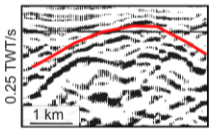	High amplitude, low frequency and choitic reflections below the red solid line.
I Volcanic body	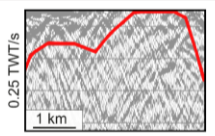	High amplitude, medium requency and choitic reflections below the red line.

Fig. 4.6. The different seismic facies and seismic features identified from investigated seismic profiles. PQ: Plio-Quaternary; TO-ME: Tortonian to Messinian; MM-LM: Middle Miocene-Lower Miocene; PA: Paleogene; CR: Cretaceous: TR-Triassic.

The Plio-Quaternary facies (A and B) exhibit high to medium amplitude, continuous, parallel to sub-parallel reflectors. The upper layered facies are of the Ribera formation mark its presence in the NW

part of the Sicily Channel including the Adventure Bank. This veneer of deposits is dissected by an unconformity from the Lower-Plio-Quaternary sediments. The unconformity was identified based on the top lap terminations against the base of Upper-Plio-Quaternary deposits and the divergent geometry of the reflections (Fig. 4.6, 4.9, 4.10). The semi-transparent packages of reflectors at the base of the parallel and layered Upper Plio-Quaternary sequence are linked to the extensional tectonic phase that hit the Sicily Channel in Early Pliocene (Civile et al., 2014; Cavallaro et al, 2017; Civile et al., 2021; Maiorana et al., 2023) and is usually present in the deeper basins (Figs. 4.5-4.13).

Downwards a thick pile of Tortonian to Messinian deposits (Terravecchia fm.) is found in the area of investigation which is also known in the literature (Civile et al., 2015, Millia et al., 2021., Miaorana et al., 2024) and well-analysis (Orlando-1, Samanta-1 and Tulia-1) carried out in this study. The facies C facies is seismically expressed by semi-transparent, high to mid-amplitude and poorly layered reflectors (Figs. 4.5-4.13) and consists mostly of silty clay and quartz sands. The sequence is topped by a prominent, and high acoustic impedance contrast reflector corresponding to Messinian unconformity (top of Messinian evaporites/erosional surface) that limits the sequence from Plio-Quaternary succession (Figs. 4.5-4.13). The continuous reflector is also termed as 'M reflector' and is considered as the representative of the Miocene erosional surface and represented as U in this chapter (Fig. 4.7-4.13) (Torelli et al., 1995; Lofi et al., 2011; Günes et al., 2018). During the Messinian compressional tectonic phase, these deposits detached from the substratum and incorporated into the chain (Argnani 1993a, b; Grasso 2001).

The seismic packages of facies D are high-amplitude, continuous with a low frequency. These deposits comprise of packstones with marls of Lower to Middle Miocene formations (Oum Douil, Nilde, Mahmoud, Ain Grab) (Figs. 4.4-4.13). This thin sequence is encountered discretely in the Adventure Bank and in the Egadi shelf.

The high amplitude, low frequency, and semi-continuous reflections referring to seismic facies E is bordered on the top by the base of the Miocene unit (Fig. 4.4-4.13). The seismic unit encompasses a mixture of Marls, Limestones, and argillaceous succession corresponding to the Metlaoui and Fortuna

formations of Eocene to Upper Oligocene age respectively (Fig. 4.4-4.13). Following downward, seismic facies F is characterized by high amplitude and low-frequency reflections with poor lateral continuity which are associated with the thick Cretaceous Carbonate deposits with the presence of some Marls (Anselmetti and Eberli, 1993; Catalano et al., 1996; Sulli, 2000) (Figs. 4.4-4.8). It was difficult to recognize this unit on G82-63-45 profiles due to the low resolution of the data.

Seismic facies G, seismically consists of high to medium amplitude and variable frequency reflectors that lack continuity and are often covered by diffraction effects (Fig. 4.4-4.13). These reflections are attributed to the crystalline basement by Catalano et al. (1996); Sulli (2000) and Pepe et al (2020).

The seismic expression of magmatic bodies (seismic facies H) was identified based on their reflectivity pattern, boundary and shape. These are characterized by high amplitude, low frequency and chaotic to granular reflections. Based on the reflection characteristics two possible magmatic bodies have been identified in the study area: one in the SSE portion of the Adventure Bank (Fig. 4.7) which has mostly influenced the Cretaceous and Paleogene units and another one in the Egadi shelf (Figs. 4.9, 4.11) which has intensely deformed all the stratigraphic units except Upper Plio-Quaternary.

4.3.2. Structural analysis of CS89-01-C2 seismic line

The seismic profile stretches from the northern termination of Pantelleria Graben to Egadi shelf in the SSE to NNW orientation (Fig. 4.2). The line passes through Adventure Bank which is an area characterized by shallow water depths. The SSE part is dominated by extensional tectonics that may be linked to the Early Pliocene rifting event that developed the Sicily Channel Rifting Zone (SCRZ) (Fig. 4.2) and the NNW part highlights the occurrence of both extensional and compressional tectonics.

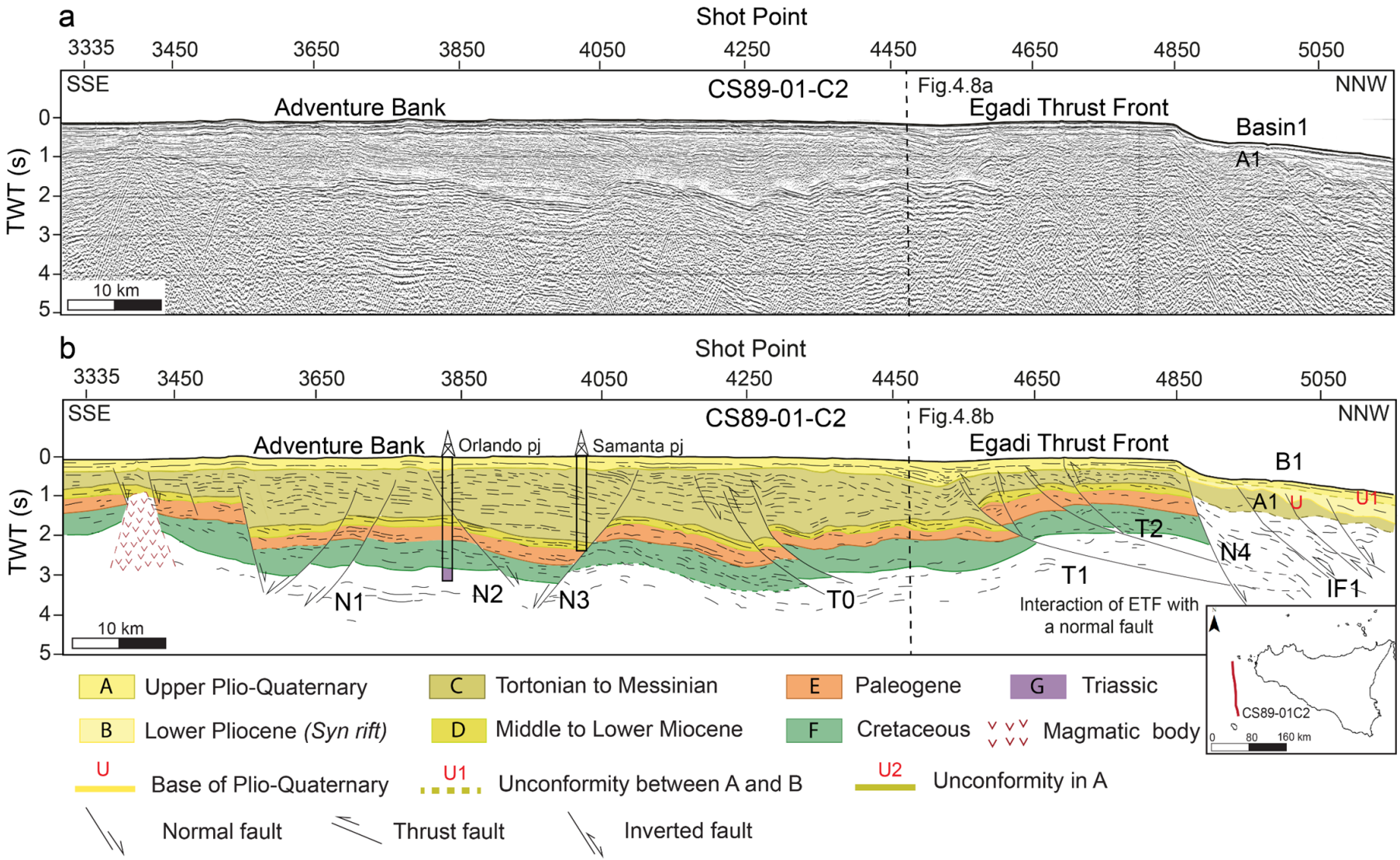

Fig.4.7. (a) uninterpreted and (b) interpreted seismic line illustrating the coexistence of the extensional and compressional structures and the interaction of structures of Egadi Thrust Front (ETF) (T1 and T2) with a NW dipping normal fault that is flanking the Basin 1. The basin features inverted faults, and the Plio-Quaternary unit has been divided with U1 and U2 unconformities. Refer to Fig.4.2 for the location and to Fig.4.14 to see the structural features.

The Adventure Bank on the SSE side is dominated by normal faults (reach to a depth of 3.5 TWT/s) which roughly have NW trend. Some of these are buried under Tortonian to Messinian sediments and some by Plio-Quaternary deposits (Fig. 4.7a, b).

The SSE dipping N1 and N3 normal faults show variable throws; N1 highlights a modest throw and N3 shows a considerable offset and has intensely deformed the Cretaceous to Miocene stratigraphic units associated with it (Fig. 4.7b). Also, to the extreme of SSE, a magmatic body (bounded by two sub-vertical normal faults) has intruded the sedimentary strata which is related to the extensive volcanic activity that occurred mainly on the Pantelleria and Linosa Islands coupled with the early Pliocene rifting event (Rotolo et al., 2006; Civile et al., 2008) (Fig. 4.7b).

4.3.2. Egadi thrust front interaction with a normal fault and the inversion tectonics

The ETF has been recognized on the profile towards the NNW side where its structures are interacting with a normal fault (Figs. 4.7b, 4.8b). The main structures of ETF are named T1 and T2 and the basin (B1) in the NNW side is characterized by the Plio-Quaternary sediments which have a maximum thickness of ~ 410 m (Figs. 4.7b, 4.8b, 4.14).

The T2 seems to affect the whole stratigraphic strata along with the seafloor indicating the ETF is active also during the C seismic sequence (Tortonian-Messinian) which is consistent with the previous studies of (Torelli et al., 1993, 1995; Civile et al., 2014). The semitransparent reflectors of the Plio-Quaternary sequence reflect the presence of Lower Pliocene deposits (Fig. 4.5), and their syn-rift geometry testifies their origin with the Pliocene rifting phase. The unconformity U forms the base of the Lower Pliocene sediments, the latter separated from the Upper Plio-Quaternary unit by unconformity U1. Between U and U1 unconformities, the extensional tectonic phase was recognized. The gentle folding is observed in the whole Upper Plio-Quaternary unit (post-rift strata), and it continues to the sea floor. It means that B1 has possibly suffered a polyphase tectonic deformation;

the rifting event developed it since the Lower Pliocene and later an inversion tectonic phase hit it. Moreover, the planar NW-SE trending normal fault (N4) (Figs. 4.7a, b, 4.8a, b) has crosscut the ETF and developed a basin B1 that reveals the almost orthogonal interaction with these thrust structures.

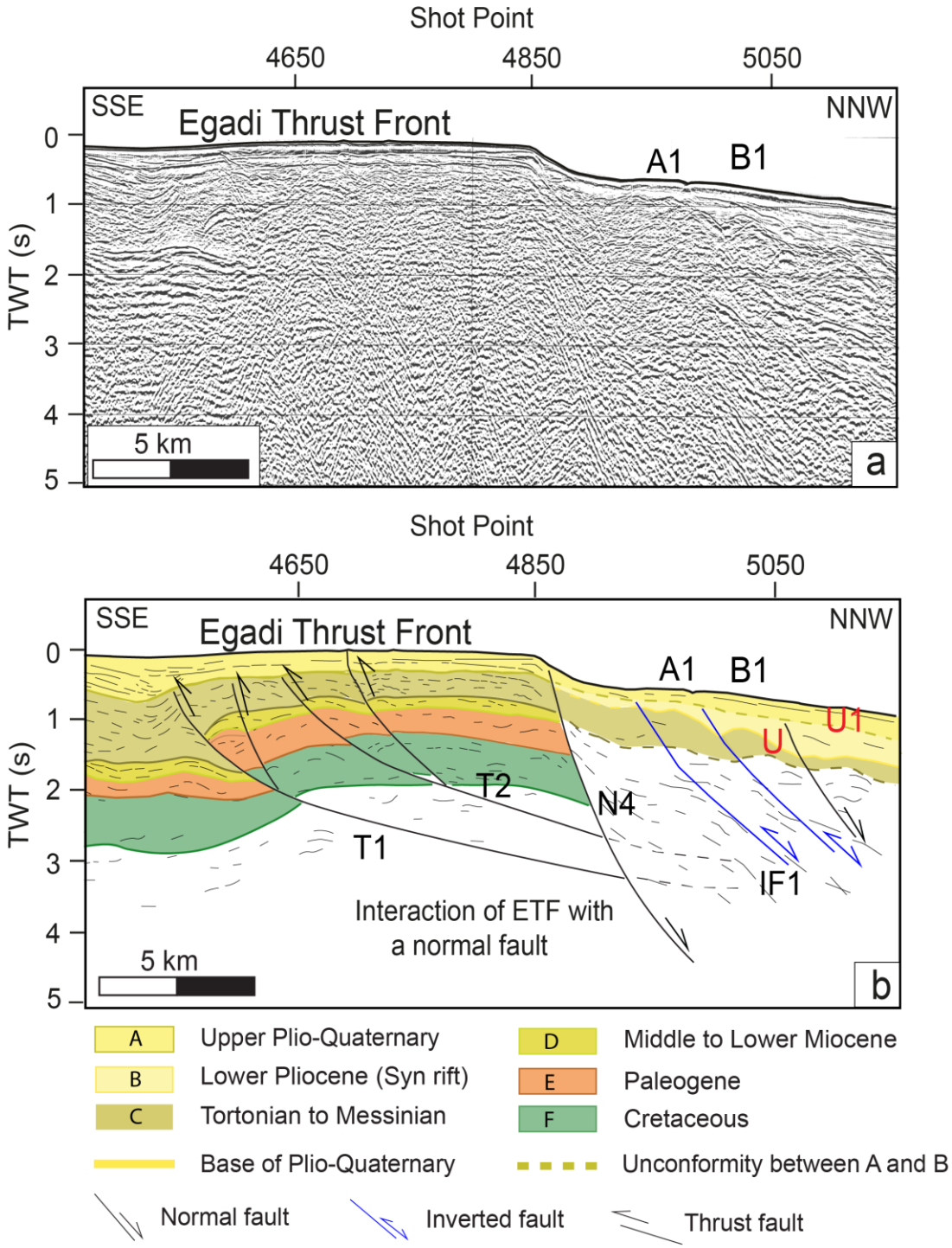

Fig. 4.8. (a) Uninterpreted and (b) shows the overlap of the two independent tectonic processes of extension and compression which is clear from the interaction of ETF with the normal fault N4. The

deformation of the seafloor hints that the ETF is active till date. The Basin 1 (B1) in (b) was inverted due to the compressional pulses which is evident from the folding of the Plio-Quaternary deposits.

4.3.3. Structural analysis of G82-63 seismic line

In order to constrain better this possible inversion, other seismic profiles were analyzed. The seismic line G82-63 passes across the Egadi valley in the SE-NW direction (Fig. 4.2). The interpretation of the line reveals that in the SE portion of the Egadi shelf, is characterized by thick C (Tortonian to Messinian) deposits and towards the NW portion these deposits show a decrease in thickness. The major thrust structures (T1 and T2) of ETF which are NE trending are also visible on this profile and they affect the thickness changes of the C sequence (Figs. 4.8, 4.14).

Between shot points 750 to 1300, the low-angle normal faults show modest offsets, the NW-dipping faults are sealed by C sequence and the SE dipping ones cut the same sequence. Basin 2 (B2) and Basin 3 (B3) have developed from the extensional tectonic event of the Early Pliocene. The structural high (H1) interpreted in the NW portion of the line is flanked by NW and SE dipping normal faults (Figs. 4.9b, 4.14) on both sides and its top is capped by a thin layer of Upper Plio-Quaternary deposits.

Positive Inversion in Basin 2

Basin 2 (B2) extends to a length of 6 km on the NW side of the study area. The Plio-Quaternary unit of 382 m thickness covers the sedimentary sequence in the basin which is determined by taking the average velocity of 1550 m/s. The unconformity U marks its base and U1 unconformity divides the A (upper Plio-Quaternary unit) and B (lower Plio-Quaternary unit (Figs. 4.9a, b, 4.10a, b). The U2 Unconformity further separates the upper unit and this unconformity was recognized by the onlap of reflections on U1 (Figs. 4.9 a,b, 4.10 a, b).

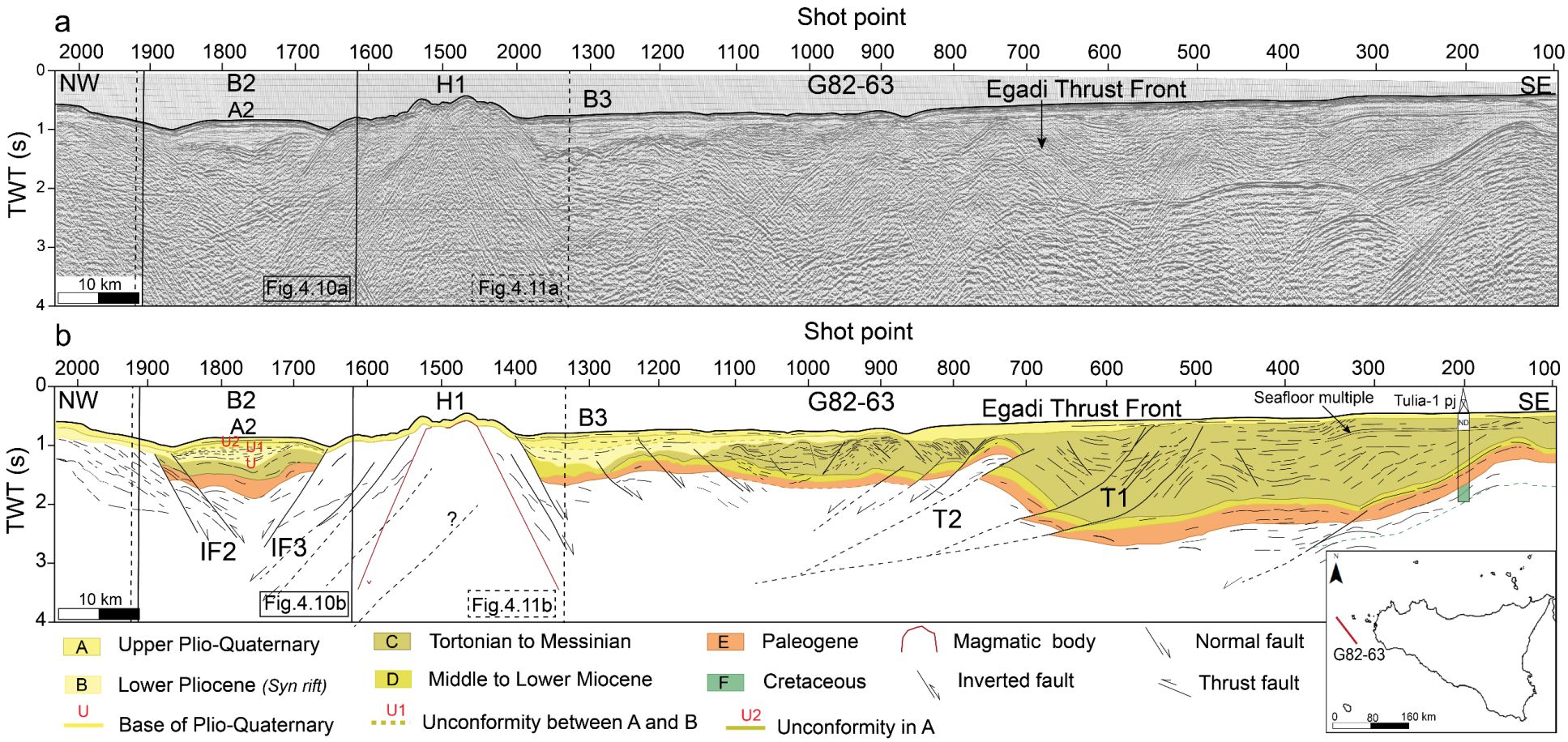

Fig.4.9. (a) Uninterpreted and (b) Interpreted seismic line showing the Egadi Thrust Front (ETF) (T1 and T2); in the SE side, a possible magmatic body intruding the structural high (H1) at shot point 1500 is shown, as well or the two NW dipping thrust faults are present there. The solid black square represents Fig.4.10 a,b and the dashed black square represents Fig.4.11. Refer to Fig.4.2 for the location and Fig.4.14 for the structural features.

The lower sequence of Plio-Quaternary (deposits between U and U1) denotes the syn-rift geometry and semi-transparent seismic packages (Fig.4.8b, 4.9b); thus, these deposits may relate to the Sicily Channel rifting and coeval to the opening of the Tyrrhenian Sea (Fabbri et al., 1981; Kastens et al., 1988; Faccenna et al., 2001a, 2001b; Corti et al., 2006). These deposits feature two anticlines inside the basin: one in the NW side and the other one in the SE side with higher amplitude fold (Figs.4.9b). The folding involves the A unit along with the sea floor and they likely are the result of the polyphased inversion of the basin caused by the reactivation of the NE-SW trending normal faults bordering B2 (Fig. 4.10, 4.11).

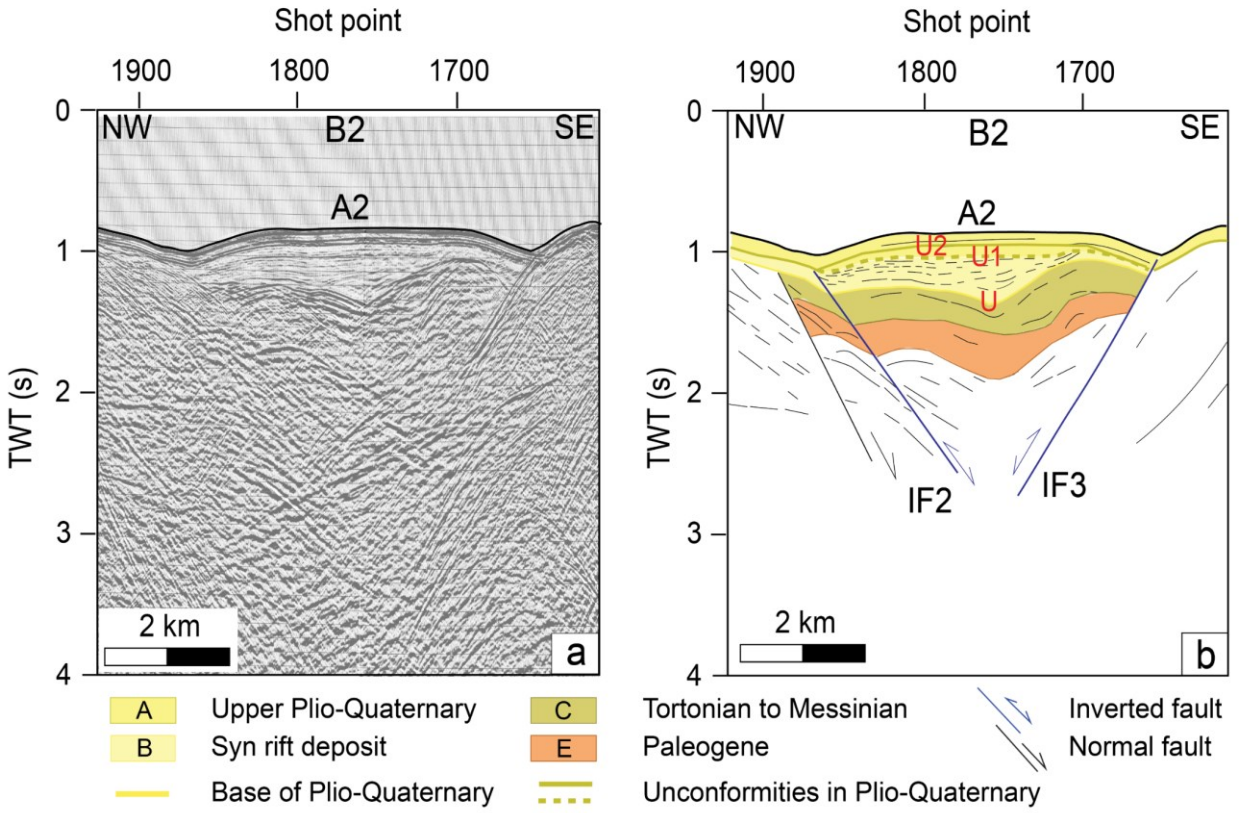

Fig. 4.10. (a) uninterpreted and (b) interpreted part of line G82-63, which features the deformation of the sedimentary infill by the reactivated normal faults (IF3 and IF4). Based on reflection terminations it was possible to divide the Plio-Quaternary unit into A and B units by unconformity U1 and further divide A unit by unconformity U2. Each unconformity is linked to a compressional tectonic event that has shaped the basin.

Impact of magmatism on the positive inversion

The presence of the magmatic body in the adjacent structural high (H1) may suggest that the anticlines in B2 are also linked to the magmatism. The inversion in B2 by the reactivation of the pre-existing normal faults might be also controlled by the magmatic intrusions. There may be magmatic intrusions that do not extend to the shallow levels (Fig. 4.11). However, the low resolution of the seismic data did not allow us to directly correlate the folding in the sedimentary units with the magmatic intrusions. The magma emplacement process and the basin's proximity are linked; the magma takes advantage of the faults and migrates along them. We suppose that the proximity of B2 and the faults bordering it with the magma injection point have played a role in controlling the inversion process. We noticed the variable folding in B2; the SE part seems more folded (tighter and higher amplitude fold) than the NW part. We assume that the intrusion had more influence on the SE side (Fig. 4.11). Because of the above reasons, the inversion in this portion of the basin seems more or also controlled by the magmatism than the NW portion.

There is also the possibility of the presence of two NW dipping thrust faults could in the H1 as indicated by some reflections.

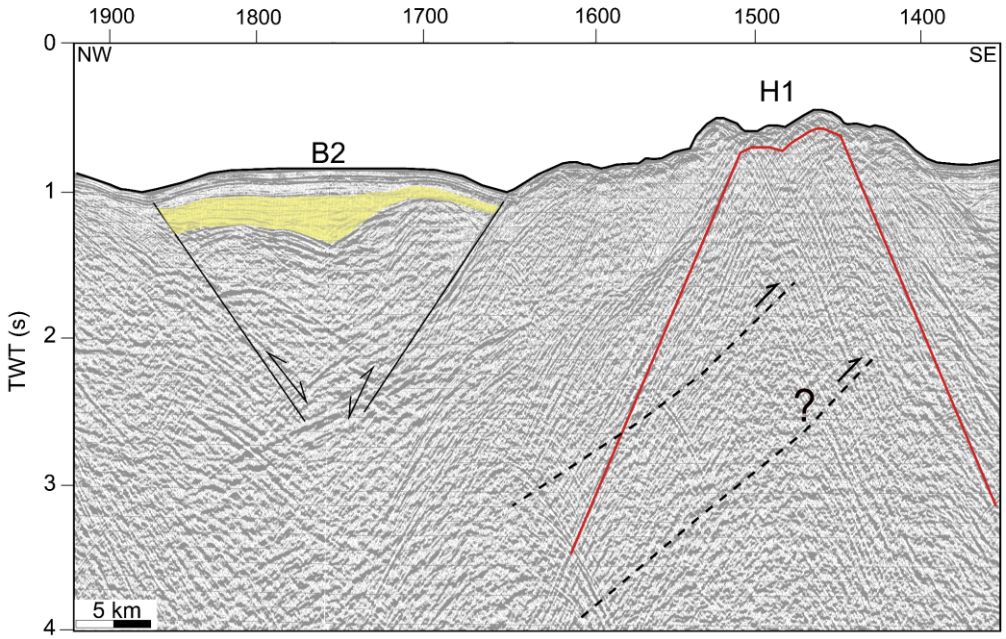

Fig. 4.11. The inversion in B2 may have been controlled by the magmatic intrusions as well whose existence is still uncertain (Fig. 4.14). The magma emplacement process and the basin's proximity are linked; the magma takes advantage of the faults and migrates along them.

4.3.4. Structural analysis of G82-45 seismic line

The line stretches in NE-SW orientation (Fig. 4.2). It features the two basins (B4 and B5) which are separated by a structural high (H2) (Fig. 4.12a, b). There is a flat surface to the SW direction of B4 which is affected by low-angle normal faults showing modest throws. A high-angle normal fault (N6) towards the extreme of NE with NW-SE trend has impacted the Plio-Quaternary unit along with the sea floor (Figs. 4.12, 4.14). At shot point 1000, a planar and a listric normal fault (N4) (ESE trending) mark their presence in B4 with a decreasing angle of dip with increasing depth (Figs. 4.12, 4.14). These faults are no longer active as they are buried under the Upper-Plio-Quaternary deposits. The extensional displacement along these faults has developed an asymmetrical anticline rollover. The Lower-Plio-Quaternary deposits show growth strata along these faults, thus indicating their syn-rift nature (Fig. 4.12 a, b). A SW dipping reverse fault (R1) has displaced the sedimentary units of the structural high (H2) (Fig. 4.11b). However, the top thin layer of A unit draping the H2 does not show appreciable displacement along the fault. From B5 towards the NE side displays variable seismic characteristics between 100 to 250 shot points. The top lap termination was noted at 200 shot point which is indicative of the unconformity (U1) that dissects A and B (Fig. 4.11).

Mild inversion in Basin 5

Basin 5 (B5) lies in the NE part of the seismic line and extends in the SW-NE direction (Fig. 4.2). The B5 exhibits a WNW trend like Pantelleria, Linosa and Malta grabens. This implies that the same extensional event has shaped the B5. Towards the SW the basin is bounded by two NE dipping normal faults and two low-angle normal faults between shot points 350 and 400 which dip towards SW (Figs. 4.12a, b, 4.13a, b). The basin has suffered different deformation phases highlighted by the main unconformities in the Plio-Quaternary unit. The unconformity U forms the base of the Plio-Quaternary unit that limits the sequence C. The U1 dissects the A and B units. The lower Plio-Quaternary deposits show syn-rift or divergent geometry, it hints at their formation from the rifting event of the Early Pliocene (Fig. 4.13).

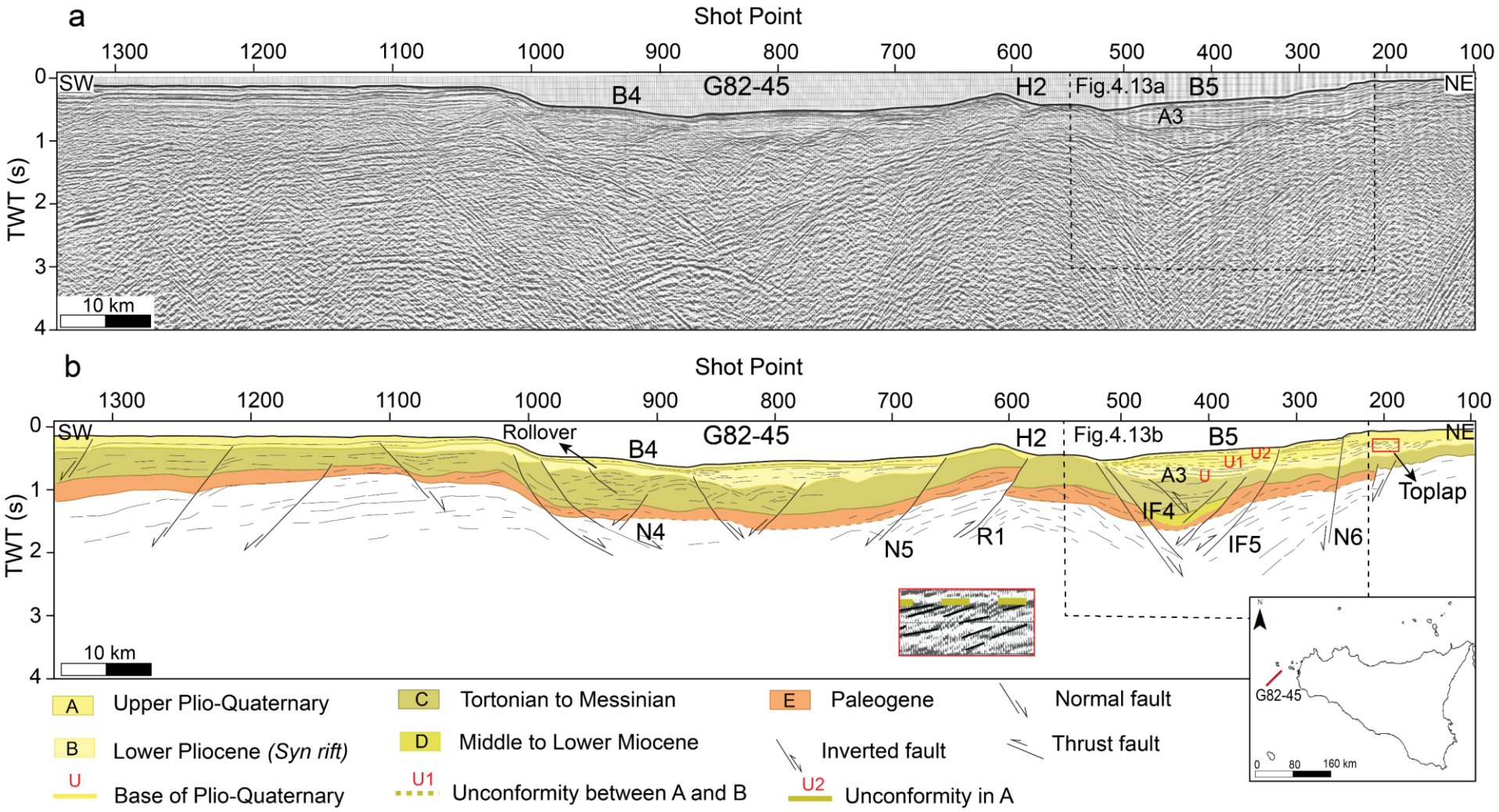

Fig. 4.12. (a) uninterpreted and (b) interpreted seismic line highlighting a listric fault (N4) with a rollover in Basin 4 (B4). The sedimentary units of structural high (H2) are intensely deformed by a reverse fault (R1). The two reactivated normal faults (IF4 and IF5) are present in Basin 5 (B5) which has undergone polyphase deformation phases. The red square inside (b) shows the top lap terminations. For structural features

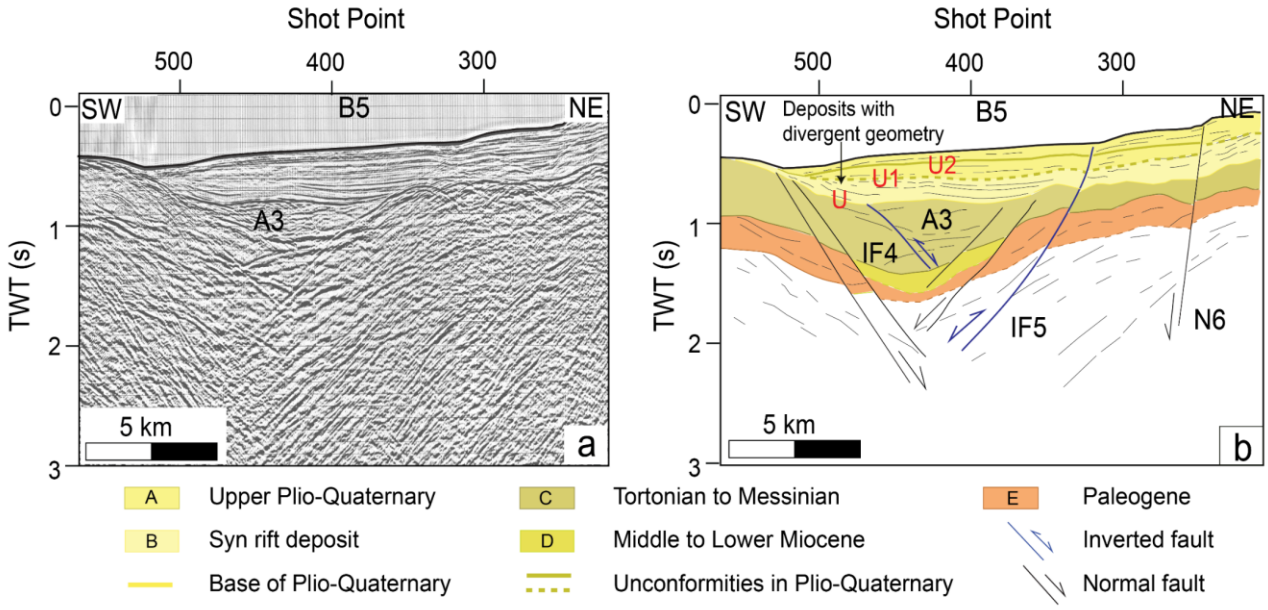

Fig. 4.13. (a) uninterpreted and (b) interpreted portion of the G82-45 line showing the mild inversion of Basin 5. The pre-existing normal faults were reactivated due to a compressive force and thus inverted the basin. To define the polyphase deformation events the Plio-Quaternary unit was separated by unconformities (U1 and U2). The normal fault (N6) has impacted the seafloor which gives a clue of its active nature.

This extensional event was observed between U and U1 unconformities. It was followed by a second event of deformation that caused the reactivation of the pre-existing normal faults (IF5 and IF6) which in turn folded the deposits overlying the U unconformity. Due to the reactivation of IF5, the central part of the basin has undergone mild inversion. Later a renewed extensional event was identified in B4 as indicated by the normal fault (N6) affecting the whole strata of Plio-Quaternary and the sea floor (Figs. 4.12, 4.13, 4.14).

4.4. Structural map: the interaction of extensional and compressional structures

The NW of Sicily Channel is characterized by NW trending normal faults and a thrust and fold system (Fig. 4.14). The occurrence of these structural features suggests that the area is shaped by two tectonic forces; compression that gave birth to the Sicily Magrebian chain and the extension that developed rifting in the Sicily Channel (Argnani 1988; Giunta et al., 2000; Corte et al., 2006; Civile et al., 2014). Our analysis of the seismic lines also reveals the coexistence of thrust and normal fault structures of

the extensional and compressional regimes and their interaction in the NW of Sicily Channel. The source of the extension transfer toward the fold and thrust belt should be Pantelleria Graben (Fig. 4.2, 4.13). The studies of and Torelli (1993, 1995) and as per Corte et al. (2006) reveal that many extensional and compressional structures have impacted the seafloor, the thrust structures almost orthogonally crosscut by these normal faults. The prominent thrust front (ETF) has also suffered recent reactivation (Torelli et al, 1993, 1995; Civile et al., 2014). The integration of these previous studies and our analysis resulted in a new structural map (Fig. 4.14).

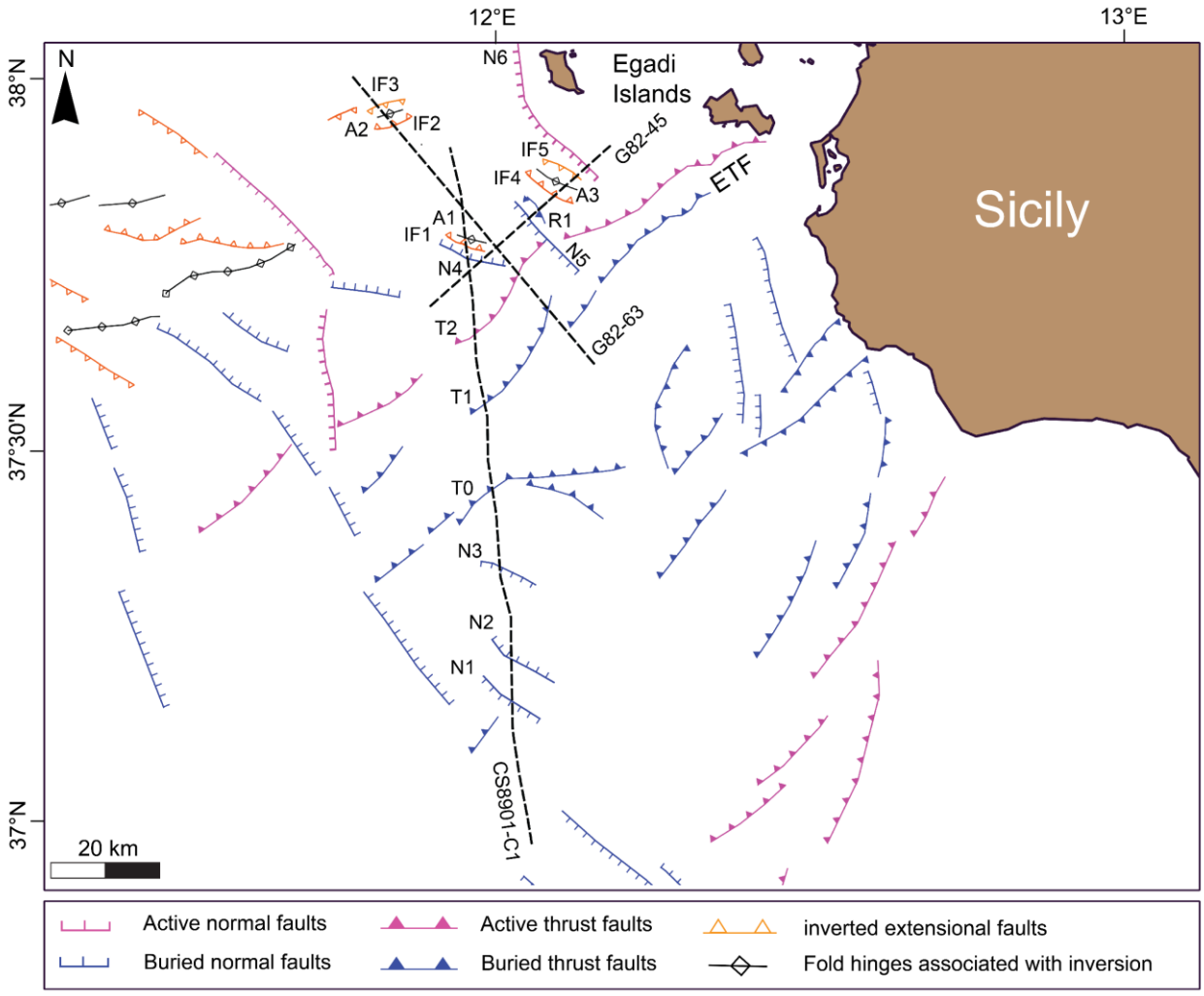

Fig. 4.14. Structural map generated from the analysis of selected seismic lines with the integration of a dense grid of other seismic lines falling in the NW of Sicily Channel and the which is shown in Fig. 4.2. N1-N6 refers to the identified normal faults in the area, IF1-IF6 are the inverted normal faults and the A1, A2, and A3 represent the fold hinges associated with the inverted faults. T0 is a thrust fault dipping NW and T1 and T2 are the thrust structures of Egadi Thrust Front (ETF).

The Sicily Maghrebian Thrust Belt (SMTB) is characterized by ESE verging thrust faults (Argnani et al., 1987; Lentini et al. (1990); Torelli et al., 1995; Civile et al., 2014) formed during Late Miocene compressional event. Such thrust faults including ETF that is a front of the Apennine Maghrebian orogen which has also been documented in this study (Fig. 4.14). The ETF (structure T2) has locally deformed the sea floor which also points out they are still active or the morphology they created is still preserved at present day sea-floor (Figs. 4.7a, b, 4.8a, b, 4.14). The structures of ETF intersect with the normal fault (N4) almost orthogonally which is again in line with the study conducted by Corti et al. (2006). The observations reveal the occurrence of deformation trends and regimes: the NE-SW oriented extension (Sicily Channel rifting phase) that developed the basins (B1-B5) discussed in this chapter.

The normal faults show mostly modest throws and in some positions, they reach the seafloor (N6 in Figs. 4.12, 4.13, 4.14). N6 is a NW-trending normal fault (also reported in Antonelli et al., 1988) that penetrates through the Plio-Quaternary unit and shows the deformation of the seafloor. The preexisting normal faults have possibly been inverted (IF1-IF5) in the Pleistocene which may be attributed to the compressional stress transmitted by the ETF with a renewed compressional phase. According to Gamberi and Millia (1990) only the normal faults approximately E-W trending and flanking basins in the NW of the Sicily Channel have suffered inversion. The inverted faults IF2, and IF3 marked in B2 have the same trend (roughly E-W). However, the other inverted faults here recognized (IF1, IF4, IF5) possess the same NW-SE trend as that of boundary faults of SCRZ.

4.5. Discussion

4.5.1. Chronology of deformation phases and the possible driving factors

The ages of the polyphase deformation events were evaluated for the three different basins (B1, B2 and B5) located in the NW Sicily Channel. The Plio-Quaternary deposits drape and is syn-tectonic to these basins and it was evidenced that the thickness of these deposits is higher in the basins than in the flat areas (Figs. 4.7- 4.12). The sedimentation rate in these basins was calculated for the Late

Miocene-Pliocene boundary that ages Zanclean (5.33 Ma) by taking into account the maximum thickness of the Plio-Quaternary unit. For B1, B2, and B5 the thickness of these deposits was estimated 410 m, 390 m, and 390 m respectively and for each basin, a different sedimentation rate was obtained (Tab. 4.1). Depending on this thickness the sedimentation rate for each basin was evaluated to determine the chronology of polyphase deformation events represented by unconformities U, U1 and U2 (Figs.c4.8a, b,4.10a, b, 4.13a, b). The unconformity U forms the base Plio-Quaternary unit and this unit was divided by an unconformity U1 into Upper Plio-Quaternar (post-rift deposits; A) and Lower Pliocene (syn-rift deposits; B) based on the divergent geometry of the reflectors in the lower unit (Figs. 4.8a, b, 4.9a, b, 4.12a, b). The B1 was hit by an extensional phase (rifting event) whose evidences are found in the deposits between U and U1. It was revealed from the obtained sedimentation rate (77 m/ma) that this event began in Zanclean (3.8 Ma) and ended in Calabrian (1.4 Ma) in B1 (Tab. 1). The same extensional event is dated approximately Piacenzian-Calabrian in B2 (3-1.2 Ma) and (2.9 -1.6 Ma) in B5 using the obtained sedimentation rate (73 m/ma) for both the basins. After the dormancy of the young extensional tectonic regime, the compressional pulses gave birth to contractional features in the basins (Catalano and Milia., 1990; Gamberi and Argnani, 1993, 1995; Sulli, 2000; Sulli et al., 2021; Loreto et al., 2021). All three basins were deformed by this local inversion deformation phase that reactivated the pre-existing normal faults. The age of the inversion phase was determined from the maximum thickness of the post-rift deposits overlying the unconformity U1 in B1, B2 and B5 and the sedimentation rate determined previously. The syn inversion unit was deposited after 1.4 Ma in B1, 1.2 Ma in B2, and in B5 inversion phase was dated (1.6-0.8 Ma) (Tab. 4.1). The folding of the post-rift deposits has even affected the sea floor in B1 and B2 (Fig. 4.6-4.9). A more intense inversion event has occurred in B2 which is indicated by the formation of a wide anticline on the seafloor that is ENE-directed (Fig.4.14). These evidences suggest that this localized inversion phase was or is still active in basins B1 and B2. However, in B5, a renewed extension event (post-Calabrian; 0.8 Ma) was recognized by the extensional displacement of the seafloor caused by the impact of normal faults reaching the seafloor (Figs. 4.12-14). The cause

of the renewed extensional tectonics may be the isostatic adjustment of the Earth's crust to the emplacement of the tectonic features that resulted during inversion (Sulli, 2000).

Tab. 4.1. Chronology of the deformation related to different tectonic events based on sedimentation rate analysis based on the age of the lower boundary of the Plio-Quaternary succession (U unconformity – base of the Pliocene or base of the Zanclean of 5.33 Ma.

B1 (CS89-01C2)				
	Processes involved	**Thickness (m)**	**Age (Ma)**	**Sedimentation rate (m/ma)**
U-U1	Extension	300	3.8	77
U1-U2-seafloor	Inversion	110	1.4	77
B2 (G82-63)				
	Processes involved	**Thickness (m)**	**Age (Ma)**	**Sedimentation rate (m/ma)**
U-U1	Extension	220	3.0	73
U1-U2	Inversion	86	1.2	73
U2-Seafloor	Inversion	84	1.2	73
B5 (G82-45)				
	Processes involved	**Thickness (m)**	**Age (Ma)**	**Sedimentation rate (m/ma)**
U-U1	Extension	215	2.9	73
U1-U2	Inversion	120	1.6	73
U2-Seafloor	Renewed extension	55	0.8	73

4.5.2. Geodynamic evolution of the Sicily Channel at the intersection with the Egadi Thrust Fronts

By integrating the outcomes of this study, sedimentary and structural analysis and chronology of polyphase deformation events and the literature studies it is possible to outline the geodynamic evolution of the Sicily Channel including the NW side.

During the Late Miocene, a major tectonic shift occurred in the Mediterranean subduction regime; the Eurasian plate collided with the North African plate that led to the stretching of the Tyrrhenian basin in the Northern part and the origin of the SMTB and foredeep in the Sicily Channel (Uyeda, 1982; Catalano et al., 1996; Guegen et al., 1998; Sartori, 2003; Guarnieri, 2006; Roure et al., 2012; Sulli et al., 2021) (Fig. 4.15a).

In the Early Pliocene, the extensional event occurred in the Sicily Channel which emerged the major morphological structures Pantelleria, Linosa, and Malta grabens (SCRZ) (Argnani, 1990; Catalano et al., 1995; Gamberi and Argnani 1995; Civile et al., 2010, 2021; Maiorana et al., 2023) (Fig. 4.15b).

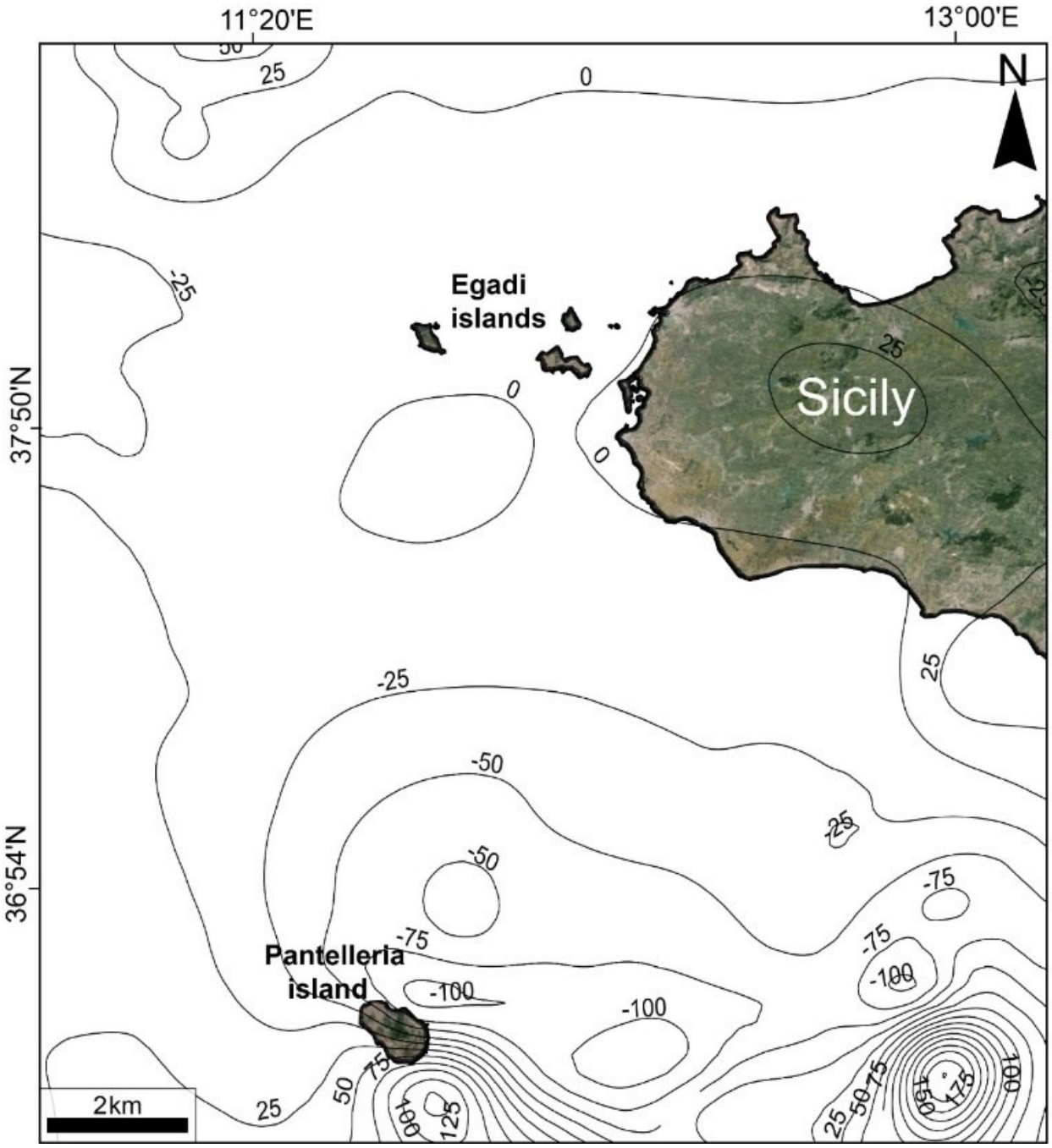

Fig. 4.15. Magnetic anomaly map with contour interval 20 nT showing the smooth trend of the magnetic anomaly in the study area. The magnetic anomaly data is derived from (https://geomag.org/models/emag2.html).

The three prominent grabens are controlled by NW-striking right-lateral strike-slip faults (TZ) (Catalano et al., 2009). From the Pantelleria Graben, the rift and the associated normal faults extended

further NW within the accretionary prism that points out the extensional structures have overlapped or cut the compressional ones and thus generated unique and complex fault arrangement as also identified in this study (Figs. 4.7a, b, 4.8a, b, 4.14) (Gamberi and Argnani 1995; Antonelli 1998; Corte et al., 2006; Civile et al., 2014; Milia et al., 2021).

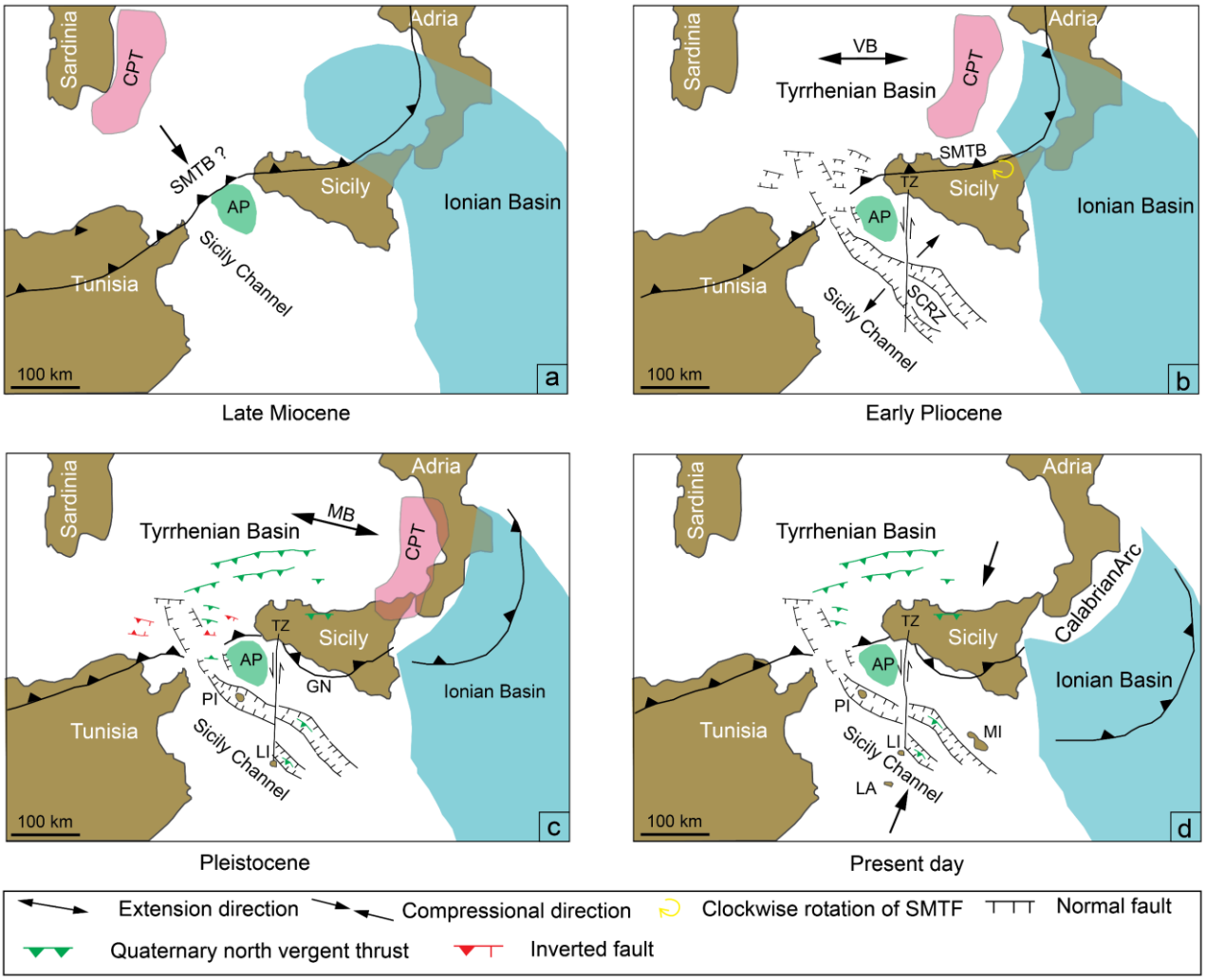

Fig. 4.16. Kinematic sketch of the geodynamic evolution of the Sicily Channel including the NW portion since the Late Miocene (modified from Civile et al., 2021). The crosscut relation of the extensional faults (rifting) with the SMTF is derived from Antonelli et al. (1998). The inversion faults have been extracted from Catalano and Millia 1990, and Quaternary north vergent thrust structures of North Sicily and Linosa and Malta grabens are extracted from Sulli et al. (2021) and Maiorana et al. (2023) respectively. (a) In Late Miocene the SMTB emplacement took place. (b) In the Early Pliocene, the clockwise rotation of SMTB (which includes ETF) initiated and the extensional event occurred in the Sicily Channel which emerged SCRZ. From the Pantelleria graben, the rift and the associated normal faults extended further NW within the accretionary prism that points out the extensional structures have overlapped SMTB. (c) During the Early Pleistocene, the extensional basins positioned on the top of SMTB developed inversion in their sedimentary fill (dated Calabrian) that was probably due to the variation in stress field direction. (d) The recent inversion has occurred in the Linosa and Malta grabens and the North of Sicily. The same structures are found in the NW

offshore of Sicily whose evidence are preserved in the folded geometry of the seafloor. AP- Adventure plateau; GN-Gela nappe; LA-Lampedusa Island; LI-Linosa island MB-Marsili basin; MI; Malta island; PI- Pantelleria island; SCRZ-Sicily Channel Rift Zone; SMTB-Sicily Maghrebian Thrust Belt; TZ-Transfer zone; VB -Vavilov basin.

At the same time the extensional basins positioned on the top of SMTB developed inversion in their sedimentary fill (dated Calabrian) (Fig. 4.16c) that was probably due to the variation in stress field direction (with N-S to NNW-SSE stress axis) which may be the consequence of the cessation of the SE-directed migration of the Calabrian arc (Trincardi and Zitellini, 1987; Gamberi and Argnani 1995; Catalano and Milia., 1990; Sulli 2000; Zitellini et al., 2021). On the same side, the modestly inverted basins with NW-SE trend as that of the main grabens of the Sicily Channel were subjected to a renewed extensional phase (Milia et al., 2021; Maiorana et al., 2023).

Currently, the Ionian slab seems at the last development stage. The Linosa and Malta grabens have locally suffered inversion recently in the Sicily Channel (Maiorana et al., 2023) which is linked to the compressive force (generated by the change in subduction polarity) responsible for the recent inversion in the North of Sicily (Sulli et al., 2021) (Figs. 4.14, 4.16d). The same structures are found in the NW offshore of Sicily whose evidences are preserved in the folded geometry of the seafloor. The active contractional structures present in the basins from the Tyrrhenian margin to the Sicily Channel may hint towards the variable deformation intensity and orientation of the basins (Sulli et al., 2021; Zitellini et al., 2021; Maiorana et al., 2023). These structures may be the product of the change in subduction polarity which gives rise to significant variation of stress in the plate interiors (Gamberi and Argnani 1995; Catalano and Milia., 1990; Sulli, 2000; 2021; Zitellini et al., 2021) or local compression linked to a trascurrent shear zone developing inside the Sicily Channel.

4.6. Conclusion

The investigation of the multichannel seismic reflection profiles carried out with the integration of bathymetry, well data, a dense grid of lines, and literature allowed to speculate the complex tectonic evolution of the basins of NW offshore of Sicily by considering the framework of the Plio-Quaternary

unit which has preserved the evidences of geodynamic history of the Central Mediterranean. The evolutionary history is summarised as follows and the their dating is based on interregional unconformities here dated based on the estimated sedimentation rates averaged over 5 .33 Ma (age attributed to the unconformity U at the base of the Plio-Quaternary succession);

1. After the development of SMTB in Late Miocene, the Pelagian block and the thrust belt suffered an extensional event which is evidenced by the divergent geometry in the Lower Plio-Quaternary deposits. This extensional phase ended in Calabrian and gave birth to the Pantelleria Graben (PG), Linosa Graben (LG), Malta Graben (MG) in the Sicily Channel. The extensional features stretched from Pantelleria Graben (PG), further NW and interacted with the thrust structures of the accretionary prism almost orthogonally. This deformation phase ceased in the Upper Calabrian.
2. The extensional phase was followed by the contractional phase in Lower Pleistocene which Inverted the basins in the NW offshore Sicily since 1.1 Ma which was related to the switch in the stress direction field. The volcanic activity may also have played a role in controlling this inversion process in some basins. In the NW-SE trending basin the inversion phase ended around 0.8 Ma and afterward a renewed extensional event hit it.
3. The B1 and B2 highlight a different evolutionary history than the B5 basin. The inversion event maintained its consistency in the B1 and B2 basins as evidenced by the seafloor folding and the B5 has experienced a renewed extensional event locally after the inversion phase.

Chapter 5

Velocity model construction and time-to-depth conversion from a vintage seismic reflection profile for improving constraints on subsurface geological model: a case study from Sicily Channel, Central Mediterranean

General introduction to chapter

Velocity models are crucial for converting seismic reflection profiles or the stratigraphic horizons into depth, providing a clear view of subsurface stratigraphy and structural architecture like folds and faults (Beche et al., 2007). It was important to understand the kinematics of faults in real depth in the foreland area of SCRZ which later interact with orogenic wedge in the NW portion. The vintage seismic reflection profile (CS89-01) resulted to be very useful for this aim because, as many vintage profiles, provide the stacking velocities and interval velocities derived from Dix's formula (Dix, 1971). So, the velocity models for CS89-01 profile were constructed, Furthermore, the CS89-01 profile stretches from Lampedusa shelf (SSE) to Adventure Bank (NNW) (location in Fig. 5.1), a key location as it crosses almost the entire area investigate in this thesis. The velocity models were utilized to convert seismic horizons and faults to depth from time. The depth profile provides important information about the geological setting down to 6 km depth in this sector of the Sicily Channel, which was intensively investigated in the past and recently (Zarudzki, 1972; Winnock, 1981; Finetti, 1984; Calanchi et al., 1989; Dart et al., 1993; Civile et al., 2010; Sulli et al., 2012, 2013; Civile et al., 2021; Maiorana et al., 2023). The depth-converted horizons were in turn, used to develop its crustal model which clearly shows the relationship between increasing crustal thickness while moving from foreland area to orogenic wedge (details in chapter 6).

The construction of the velocity models was initiated from the stacking velocities associated with the seismic profile. The initial velocity models were built with the Spline interpolation method and later improved by the application of Gaussian convolution operator and data exclusion filter to obtain good results. The results have also been validated and compared with the depth profile built with MOVE suite.

Abstract

Seismic reflection profiles are crucial for studying subsurface geology at various depths, providing essential information for water, hydrocarbons, raw materials exploration, geohazard analysis, and geothermal field planning. However, the assessment, extraction, usage of and risks associated with these natural resources require a solidly constrained subsurface geological model based on the definition of the velocities field along the seismic reflection profile. The well-known uncertainties in subsurface velocity field definition call for the integration of all the available data, including vintage seismic profiles which, despite typically in raster or paper format, contain the stacking velocities and associated interval velocities. This study aims to build a velocity model for time-to-depth conversion of seismic horizons and faults marked using the interval velocity reported on a vintage seismic profile and contribute to improve the subsurface geological model in the Sicily Channel, Central Mediterranean. Spline interpolation is used for initial velocity model building of the shallower part (3.5 sec TWT) of the seismic profile CS89-01, derived from stacking velocities of 31 Common Depth Point (CDP) gathers. That was followed by the Gaussian convolution operator and data exclusion filter to improve the accuracy of the initial velocity model. The time-to-depth converted seismic reflection profile is a regional cross-section that covers almost the entire Sicily Channel, crossing part of the northern margin of the African Plate, from Tunisia to eastern Sicily. This study provides a new subsurface velocity field which can be applied, or taken into account, for most part of the Sicily Channel when structural and stratigraphic interpretations will be carried out in specific sites and where uncertainties in subsurface geological model exist (e.g., in the present study, the volcanic bodies in the Pantelleria Graben).

5.1. Introduction

The increasing number of public web-database (e.g., ViDEPI, https://www.videpi.com; SNAP, https://snap.ogs.trieste.it) and archives of research institutions that contain images of seismic reflection profiles printed on paper and/or scanned in raster format provide valuable information of the subsurface geology for different areas (Diviacco et al., 2015; Sopher, 2018; Cicala et al., 2022, 2024). This increase in the public accessibility of the vintage seismic profiles is consequential to both the decline in the demand for the acquisition of new seismic reflection surveys and the advancements in the acquisition and processing techniques that generate higher-quality images; the latter are often not available to public. Among the principal causes of this decline are i) attempts to develop a carbon-free society (decarbonization), ii) prioritizing the cessation of hydrocarbon extraction, iii) ending the exploration and production activities in mature/abandoned fields iv) fostering the circular economy through raw material recycling and reuse v) avoidance of the loud noise caused by seismic sources in the marine environment that can pose a significant threat to aquatic life. Nonetheless, these data are crucial for studying subsurface geology at various depths, providing essential information for water, hydrocarbons, raw materials exploration, geohazard analysis, and geothermal field planning.

Seismic profiles characterized by a broad geographical extension (Diviacco et al., 2015, 2018), acquired and processed between the 1960s-1990s, are now widely available and potentially represent the only public repository of subsurface data in some areas (e.g. ViDEPI database). These vintage profiles are crucial for geoscience research, as modern high-resolution subsurface data sets are expensive and not accessible to the public. They help researchers to understand a region's tectonic and geological history and can be used for earthquake and geohazards studies (Berra et al., 2019; Maffucci et al., 2020; Buttinelli et al., 2022). These profiles may continue to be the sole publicly available information for the exploration of renewable energy sources, such as geothermal, green H_2, and essential raw materials (e.g.,

lithium, graphite, nickel, cobalt, etc.) and to identify and characterize the potential sites for Carbon Capture Storage (CCS) projects (Civile et al., 2013; Volpi et al., 2015; Proietti et al., 2022; Bashir et al., 2024). The cost of the exploration of these energy sources is greatly reduced as the researchers can easily access the vintage seismic profiles without carrying out new surveys for prospecting. In addition, they can be used to construct models to find and characterize new exploitable resources in the subsurface (Giustiniani et al., 2015; Buttinelli et al., 2022). Thus, the use of these profiles can play a pivotal role in transitioning society to an environmentally sustainable state. Many vintage seismic reflection profiles are often in paper format, with most public databases (e.g., ViDEPI website) providing scanned pdf-format profiles. However, seismic profiles in time do not provide a comprehensive understanding of subsurface features as they represent an altered image of the geometries of the subsurface geological bodies (Etris et al., 2001; Thore et al., 2002; Pon and Lines, 2005; Usman et al., 2021a).

Time-to-depth conversion of seismic horizons and faults through detailed velocity models is an essential way to improve the accuracy of the subsurface stratigraphy and structural features like folds and faults (Beche et al., 2007) that is executed by using interval velocities (Sheriff and Geldart, 1995; Etris et al., 2001). Seismic profiles or their interpretation (most recent non-vintage profiles) in digital format are easy to convert into depth and can be analyzed using dedicated software (e.g. IHS Kingdom of S&P, Decision Space suite of Landmark, Petrel™ of Schlumberger, Oasis Montaj of Geosoft, MOVE suite of Petex) but the maintenance, licensing, and specialized functionality costs make them expensive to use for the public and small companies. Because of these reasons the vintage seismic reflection profiles recently received particular attention (Miles et al., 2007; Usman et al., 2021a; Conti et al., 2022; Buttinelli et al., 2022).

Therefore, the main objective of this work is to develop velocity models derived from stacking velocities that are reported in vintage seismic profiles to convert seismic horizons and faults into depth for a specific case study: the Sicily Channel. The velocity models involve the use of interpolation tests (i.e., Kriging, IDW, and Spline) and refinement techniques (i.e., Gaussian convolution operator and data exclusion filter) to achieve good results. The velocity field was calculated for vintage seismic profile CS89-01 that was converted from time-to-depth for the first time and it contributes to better constrain the subsurface geological model of the Sicily Channel which has been recently attentioned for CCS (Maiorana et al., 2024) and is favorable for geothermal energy source zones due to recent and active volcanism (Minissale et al., 2019; Civile et al., 2023).

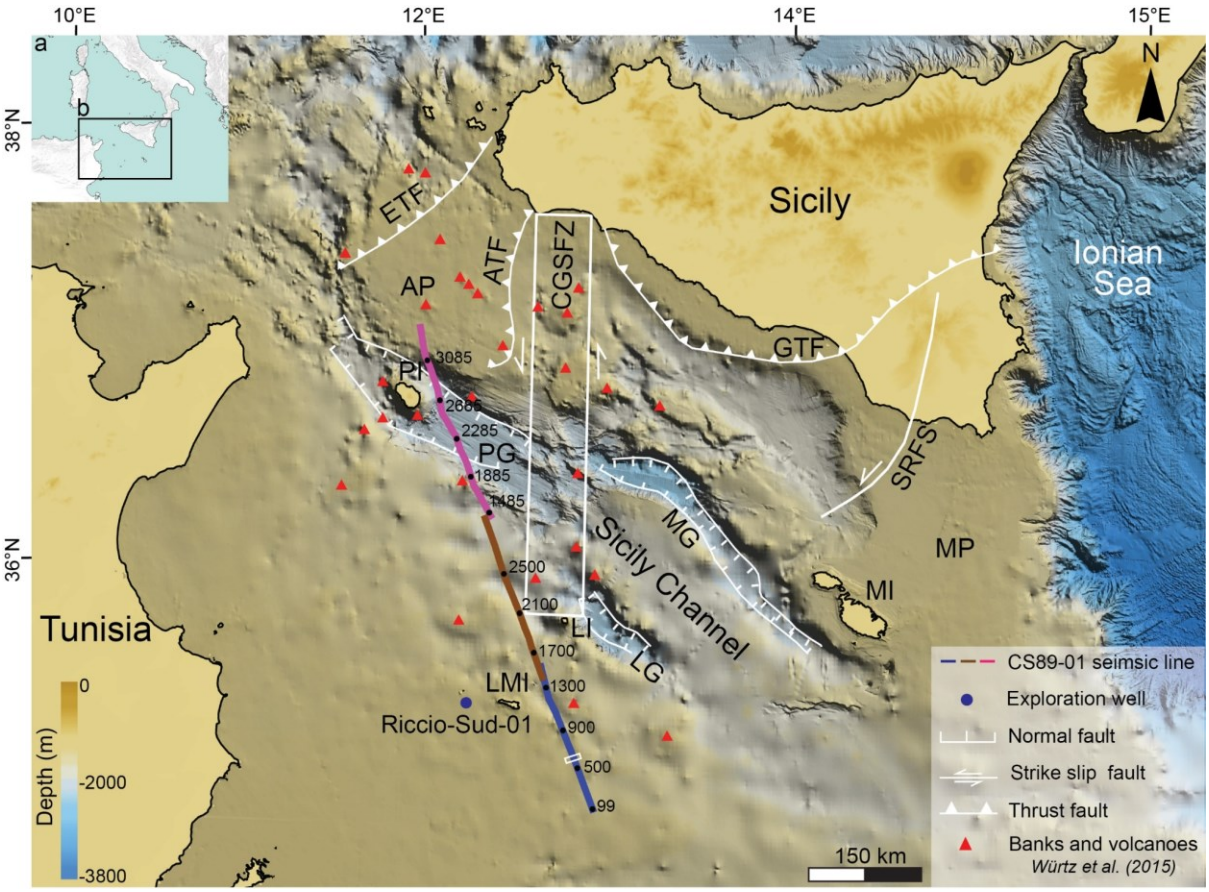

Fig. 5.1 (a) Study area location (b) Structural map of Sicily Channel and the position of Riccio Sud-01exploration well and multichannel seismic reflection profile CS89-01 (after Torelli et al., 1991, 1995; Argnani and Torelli., 2001). Bathymetry data extracted from EMODnet (http://www.emodnet-bathymetry.eu/) DTM (2022). The white rectangle on the line between

shot points 500 and 900 displays the position where the well is calibrated with the depth-converted stratigraphic units. The main structural features are from Civile et al. (2021). AP: Adventure Plateau, ATF: Adventure Thrust fault, CGSFZ: Capo Granitola-Sciacca Fault Zone, ETF: Egadi Thrust fault, LG: Linosa Graben, LMI: Lampedusa Island, LI: Linosa Island, MG: Malta graben, MI: Malta Island, PG: Pantelleria Graben, PI: Pantelleria Island, STF: Sicilian Thrust Fault, SRFS: Scicli Ragusa Fault System.

The results have also been validated and compared with the depth profile built with MOVE suite. In addition, the velocity models of the Sicily Channel, which exist in the literature (Scarascia et al., 1994; Cassinis et al., 2003) focus more on the deeper part including crust and mantle, while the velocity models obtained in this study focus on the shallower portions (down to 6 sec TWT ≈ 6 km).

The CS89-01 profile crosses the Sicily Channel (Central Mediterranean Sea) from SSE to NNW, highlighting the stratigraphic and structural setting of the area at a regional scale and across various basins and sub-basins (Fig. 5.1). As many vintage seismic profiles, this is a scanned paper copy not available in digital format in any database, but it contains the stacking velocity information (Fig. 5.2a, b, c; Supp. Mat. 5.1). Furthermore, this portion of the seismic profile is well known in the literature (Torelli et al., 1991, 1995; Argnani and Torelli, 2001) (Fig. 5.2a', b', c'). For the first time, its seismic horizons and faults are converted to depth from time, providing new insights into the geological setting down to 6 km depth in this sector of the Sicily Channel, which was intensively investigated in the past and recently (Zarudzki, 1972; Winnock, 1981; Finetti, 1984; Jongsma et al., 1985; Reuther and Eisbacher, 1985; Calanchi et al., 1989; Dart et al., 1993; Civile et al., 2010; Sulli et al., 2012, 2013; Civile et al., 2021; Maiorana et al., 2023).

5.2. Brief geological framework of the study area

The SE-NW oriented Sicily Channel (Fig. 5.1) is strictly related to the convergence of African and Eurasian plates in the Neogene which played a significant role in the tectonic evolution of the Central Mediterranean region (Uyeda, 1982; Guegen et al., 1998; Faccenna et al., 2001a,

2001b; Carminati et al., 2021; van Hinsbergen et al., 2020). The Sicily Channel is developed and shaped by two geodynamic processes: the Neogene formation of the Sicilian-Maghrebian Chain and the Early Pliocene rifting (Finetti, 1984; Reuther and Eisbacher, 1985; Argnani, 1990; Torelli et al., 1995; Grasso et al., 1999; Finetti, 2005; Carminati et al., 2012, 2021). This Pliocene rifting phase paved the way for the formation of the most prominent NW-trending Pantelleria, Linosa, and Malta grabens (Fig. 5.1) (Zarudzki, 1972; Winnock, 1981; Jongsma et al., 1985; Reuther and Eisbacher, 1985; Civile et al., 2010; Civile et al., 2021). The largest Pantelleria Graben (Civile et al., 2010; Civile et al., 2021) is separated from the Linosa and Malta Grabens by the Capo Granitola-Sciacca Fault Zone (CGSFZ), a wide N-S-oriented transfer zone originated in the Lower Pliocene and characterized by a left-kinematic movement, featuring shallow banks that exhibit the presence of volcanic bodies (Fig. 5.1) (Colantoni et al., 1975; Winnock, 1981; Argnani et al., 1988, Argnani, 1990; Rotolo et al., 2006; Ghisetti et al., 2009; Civile et al., 2014; Calo and Parisi, 2014). Plio-Pleistocene, rift-related volcanism evidence is preserved in the Pantelleria and Linosa islands (Zarudzki, 1972; Finetti, 1984; Calanchi et al., 1989; Dart et al., 1993; Rotolo et al., 2006; Lodolo et al., 2012; Micallef et al., 2024).

Sicily Channel succession consists of the thick crystalline basement (Cassinis et al., 2003; Tesauro et al., 2008; Milia et al., 2018; Civile et al., 2021) overlain by the Triassic to Jurassic platform carbonate unit followed up by Lower Cretaceous and Upper Cretaceous to Eocene successions, consisting of limestones with intercalations of marls and clay (Reuther and Eisbacher, 1985; Jongsma et al., 1985; Torelli et al., 1995; Civile et al., 2010; Civile et al., 2014; Civile et al., 2021). The Upper Miocene (Tortonian to Messinian) siliciclastic deposits can be found in the deeper parts of the Neogene basins of the Lampedusa shelf (Grasso et al., 1991a, 1991b; Torelli et al., 1995). Finally, the sequence culminates with Plio-Quaternary

clayey sediments (Bihu-Duval et al., 1985; Torelli et al., 1995; Argnani and Torelli, 2001; Civile et al., 2010, 2014, 2021).

5.3. Data and Materials

The deep, 235 km long, multi-channel seismic reflection line CS89-01 was acquired by the Institute of Marine Sciences of the National Research Council of Italy (CNR-ISMAR) in 1989 and is available only in paper copy. The acquired data were recorded on magnetic tape and in a format that cannot be read anymore. It extends across the Sicily Channel in the SSE - NNW direction (Figs. 5.1, 5.2). The seismic horizons and faults marked on the CS89-01-time profile by Torelli et al. (1991, 1995) and Argnani and Torelli (2001) were converted to the depth from the given interval velocities. The ages of the stratigraphic units are based on the data from Riccio-Sud-01 well located 60 km away from the line and the literature, mainly Torelli et al. (1991, 1995). The acquisition parameters and processing steps for obtaining the seismic reflection profiles in TWT are listed in Table 1. The interval velocities data for time-to-depth conversion were extracted from 31 Common Depth-Point (CDP) gathers out of the total 32 CDP gathers reported on the header of the profile (Fig. 5.2a, b, c); the interval velocities of the 32 CDP are available in Supplementary Material 5.1, 5.2. The stacking velocities are more accurate for the shallower part of a seismic line (Sheriff and Geldart, 1995; Yilmaz, 2001) down to ~ 3.5 sec in the case study.

Line drawings of the seismic reflection profiles were generated with the graphics software Adobe Illustrator®, while ArcGIS was used for velocity data modeling and interpolation method testing. Golden Surfer software was used for refinement filters (Gaussian convolution and data exclusion filters) (complete workflow in Fig. 5.3).

Tab. 5.1. Acquisition parameters, geometry and processing sequence of CS89-01 multichannel seismic reflection profile

Acquisition parameters	Acquisition geometry	Processing

Shot by	OGS	Energy source	Air gun	Bination	50/62 Hz
Vessel	OGS Explora	Source depth	6 m	Trace sum	Trace sum of two adjacent traces
Recorder	SERCEL SN-358	Streamer	2975 m	Velocity analysis	Stacking velocity
Sample rate	4 ms	Streamer depth	12 m	NMO correction	Application of NMO correction and mute
Field filters	Low 8 Hz High 77 Hz	Shot interval	50 m	Stack	3000%
Coverage	3000%	Groups interval	25 m	Filter	200ms zero-phase bandpass filter

5.4. Methodology

In this study, the interval velocities were taken from the boxes represented on the top of (CDP gathers with interval velocities obtained from Dix's formula (Dix, 1971) in Fig. 5.2a, b, c and Suppl. Mat. 5.1) to construct the velocity models and depth profiles. As a representation of the methodology steps, we have considered two seismic horizons (yellow-base of Upper Cretaceous and blue-base of Paleogene) and the interval velocities associated with a part of the line highlighted in Fig. 5.2b, b'. We have used the interval velocities between the yellow and blue horizons (Fig. 5.3a) to convert them to depth. After the application of filters to the initial velocity models, there was some change in the velocity field which again was used to calculate the depth for these horizons (Fig. 5.3).

The horizons and faults were also converted from time-to-depth using '2D depth conversion tool' in MOVE suite (academic license provided by Petex). The fixed interval velocities were attached to the top surface of each unit in the velocity column as per the lithology. In detail, the 'Database method' was applied; this uses a spreadsheet that contains interval velocity values for each horizon to convert them into depth.

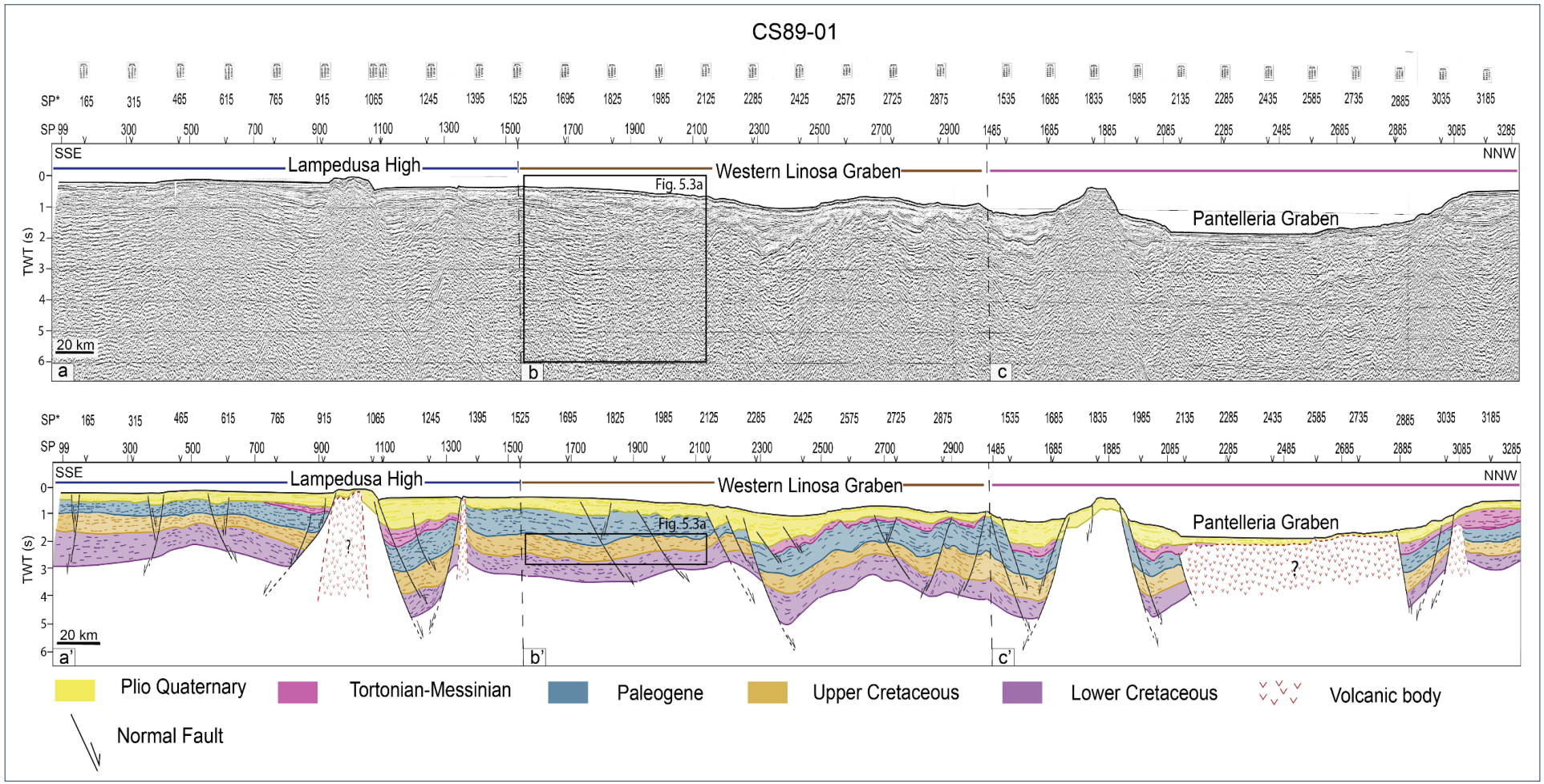

Fig. 5.2 (a) (b) (c) Uninterpreted and (a') (b') (c') interpreted parts of multichannel seismic reflection profile CS89-01 (after Torelli et al., 1991, 1995; Argnani and Torelli., 2001). The Lampedusa high is flanked by a listric fault (approximately between shot points 700 and 900), the Western Linosa graben located along SSE-NNW direction is flanked by an NNW trending major planar normal fault approximately between shot points 2100 and 2300 and the Pantelleria Graben is intruded by the volcanic body; SP: shot points; SP*: shot points corresponding to the position of the Common Depth Point (CDP) gathers on which the stacking was performed in 1989. The highlighted portions of (b), (b') were considered for the representation of methodology.

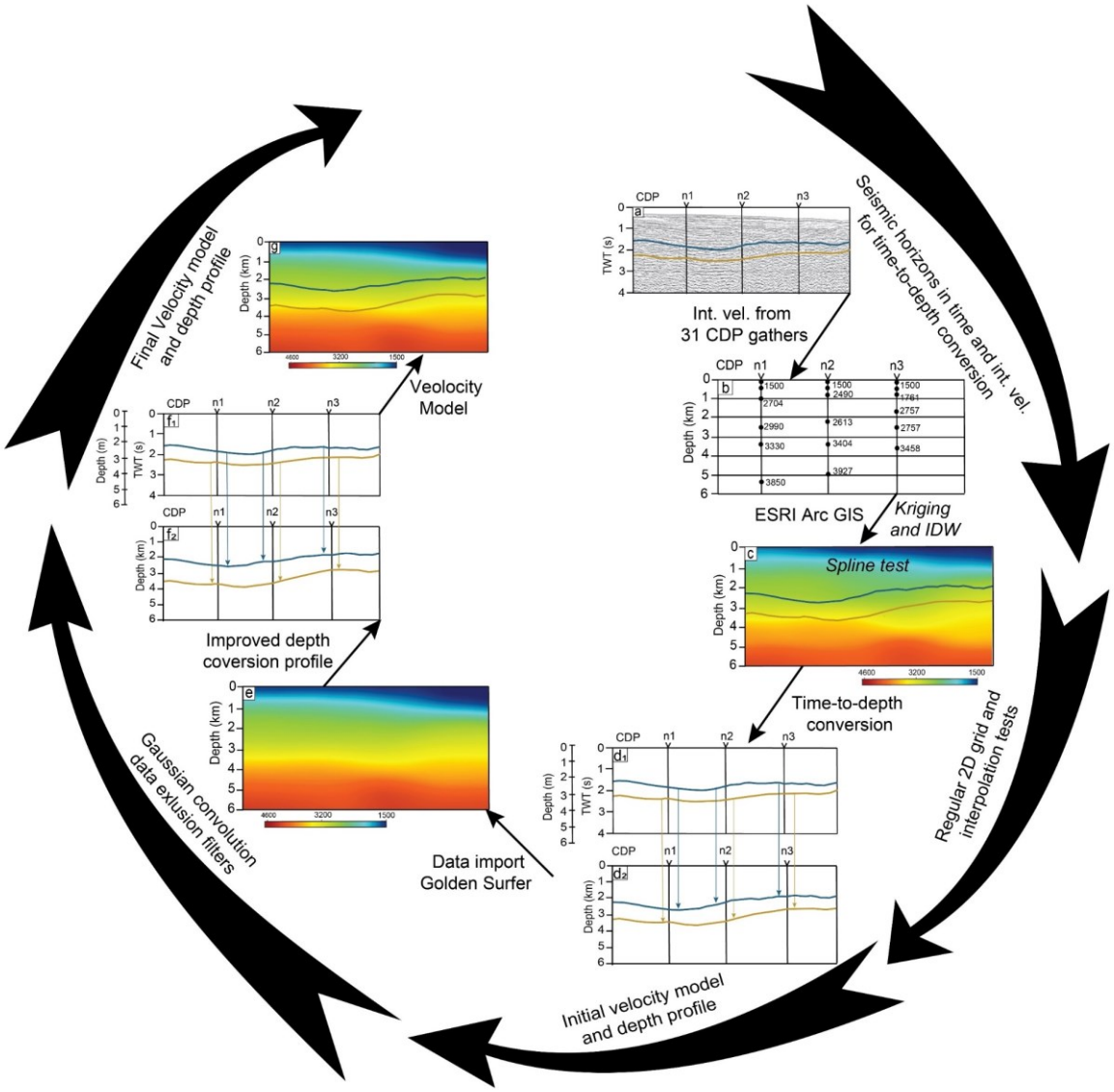

Fig. 5.3. Workflow for the construction of velocity models and depth conversion of seismic horizons and faults from the interval velocities. (a) part of the seismic profile representing the exact position of stratigraphic horizons (yellow and blue) in time, highlighted in Fig. 5.2 (b) interval velocity grid of (a) based on the data in Supplementary material 5.2 (for the velocities associated to CDP n1, n2, n3 refer to SP* 1695, 1825, 1985 respectively) (c) initial velocity model obtained by adopting Spline interpolation on the interval velocity grid (b); (d_1, d_2) illustration showing how the horizon was moved as per calculated depth from interval velocity (first depth profile) (e) final velocity model achieved by the application of Gaussian Convolution and data exclusion filter (f_1, f_2) show how the horizons are moved according to calculated depth from the final velocity model. (g) the depth converted horizons (f) are overlaid on the velocity model (e).

5.4.1. Initial velocity model and first depth profile

The interval velocities were spatially arranged in a grid (Fig. 5.3b) with respect to depth (for the interval velocity values of CDP n1 (SP* 1695), n2 (SP* 1825) and n3 (SP* 1985), details in Supplementary material 5.2). The gap of the velocity field of two adjacent vertical lines was filled with interpolated interval velocities. The spline interpolated model (initial velocity model; Fig. 5.3c) was considered in this study over the Kriging and IDW models. The velocity model was utilized to make the first attempt of depth conversion of horizons and faults (Fig. 5.3c and d).

Spline interpolation

Spline interpolation is a powerful interpolation tool that uses a mathematical function for the estimation of values and results in a model that connects the input data points in a pattern (Franke, 1982). It effectively approximates a smooth curve through a set of data points (Unser, 1999; Costa and Schleicher, 2011; Santos et al., 2013; Azubuike and Akpan, 2017; Cuevas et al., 2023). The mathematical expression for a spline of n^{th} order is given as follows:

$$\beta^n(x) = \frac{1}{n!}\sum_{k=0}^{n+1}\left(C\,{}_{k}^{n+1}\right)(-1)^k\,(x+\frac{n+1}{2}-k)^n \qquad (2) \qquad \text{(Cohen et al., 1980)}$$

Where, $\beta^n(x)$ and $\left(C\,{}_{k}^{n+1}\right)$ are the n^{th} order Spline and the binomial coefficient, respectively. In this study despite employing a discrete velocity data set (Cuevas et al., 2023), the initial velocity models developed by the Spline interpolation method are smoother and more continuous than the models built by the IDW and Kriging methods (for details see Appendix A in Supp. Mat.).

5.4.2 Refinement techniques

The application of refinement techniques enhances the quality of the initial velocity models by suppressing the unwanted noise; the proper adjustment of the control parameters of the refinement techniques can make their performance more efficient. The Gaussian Convolution operator (Shekar and Sethi, 2018; Jiang and Scott, 2020) and data exclusion filter (Rointan et al., 2021) were used to improve the accuracy of the initial model (Fig. 5.3e-g).

Gaussian convolution operator

Gaussian convolution filter is a low-pass filter that suppressed the noise and emphasized the large-scale features in the initial model (Fig. 5.3c) (Cabello et al., 2015; Agustina et al., 2017). The Gaussian operator works optimally and convolves the velocity model with a Gaussian function (Jiang and Scott, 2020), which is expressed in 2D as follows:

$$f(x) = \frac{1}{2\pi\sigma^2} exp\_(\frac{x^2+y^2}{2\sigma^2}) \qquad (3) \qquad \text{(Rosie, 1966)}$$

Where, x and y refer to the two vertices and σ is the standard deviation of the distribution.

The below-mentioned Gaussian convolution mask coefficients were implemented in a 3x3 neighborhood on the model, which did not impact its overall intensity and quality.

$$\frac{1}{16} = \begin{bmatrix} 1 & 2 & 1 \\ 2 & 4 & 2 \\ 1 & 2 & 1 \end{bmatrix}$$

Removal of inconsistent velocity components

The application of the Gaussian convolution mask improved the velocity model to a greater extent, but there still remained some incorrect velocities in the model. To remove the inconsistent velocities from the velocity model, the geology of the area (structural highs and grabens) along which the line passes was taken into consideration. Thus, the velocity model

was updated by eliminating error components by opting for the Data Exclusion Filter (Fig. 5.3e). The filter works with Boolean expressions (Gries and Schneider, 1993) to specify the criteria to remove the inconsistent velocity components. The filter works on an already saved grid that contains depth and velocity values as nodes, the inaccurate velocity data points were specified in the Data Exclusion filter text box for each model.

5.4.3. Final velocity model and depth profile

The final velocity model achieved after the application of filters (Fig. 5.3e) helped us to build a final depth model (Fig. 5.3f and g) which made the subsurface picture even more clear. The final depth profile was superimposed on the final velocity model (Fig. 5.3g) which was useful to analyse the model in detail. For details of interval velocity and depth in Fig. 5.3f refer to SP* 1685, 1825 and 1985 in Supplementary material 5.3.

5.5. Results

5.5.1. Time-to-depth conversion of the vintage CS89-01 profile in the Sicily Channel

The seismic horizons and the faults from the CS89-01 line (in time) which correspond to different geological contexts in the Sicily Channel were converted to the depth from the initial velocity models (Fig. 5.4, 5.5Ba', b', c'). To assess the goodness of the refinement techniques a second depth profile (Fig. 5.7, 5.8b) was built from the improved velocity models (Fig. 5.6) and described in the following sections as the resulting subsurface geological model valid for the length of the profile.

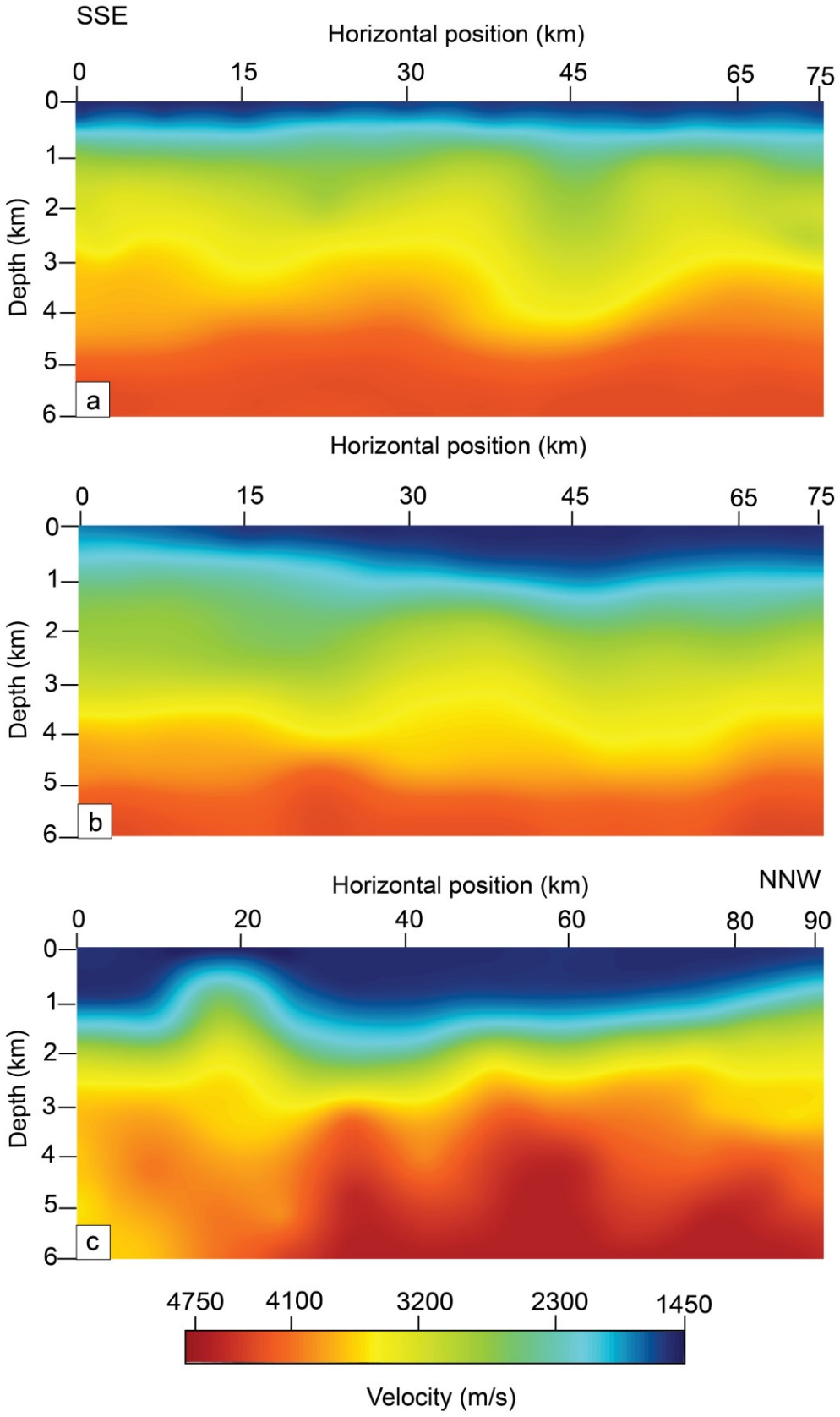

Fig. 5.4. (a'), (b'), (c') Final velocity models after the application of the Gaussian convolution operator and data exclusion filter.

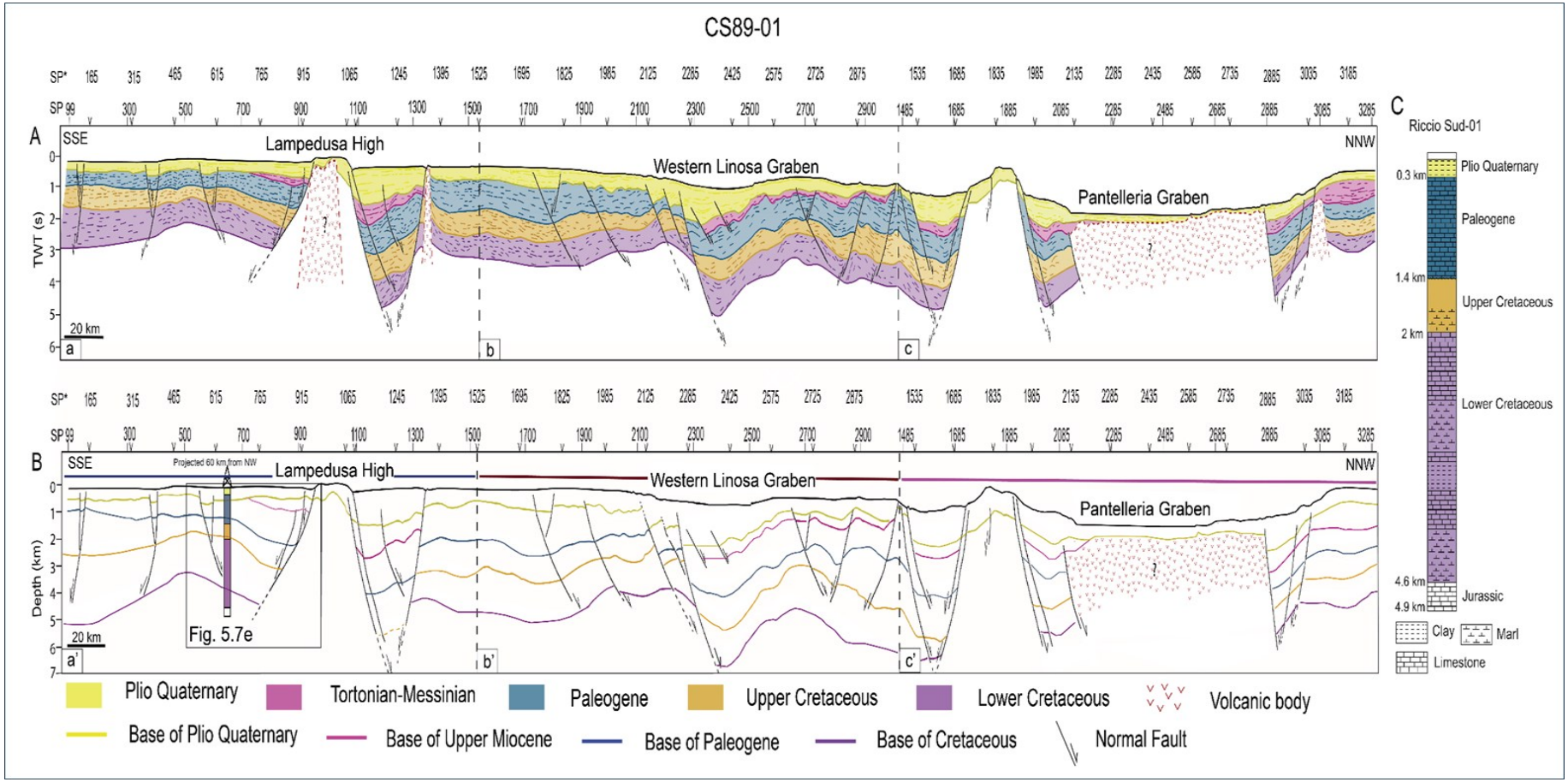

Fig. 5.5. Seismic horizons and faults in time (Aa, b, c), (after Torelli et al., 1991, 1995; Argnani and Torelli., 2001) and depth converted horizons and faults (B) of the CS89-01 using interval velocities. (C) Stratigraphy of Riccio Sud-01 well (projected 60 km from NW) calibrated in (a) does not show good correspondence with depth converted horizons (see section 5 for more detail). Depth converted profile shows (a, b, c) that the area is affected by major extensional faults. Lampedusa high (a) is flanked by a listric fault and Western Linosa graben (b) is deformed by master planar fault. (c) Pantelleria Graben in the NNW side showing complete stratigraphic succession from Cretaceous to Plio-Quaternary. SP* : Shot point number corresponding to the Common Depth Point (CDP) gathers.

5.5.2. Stratigraphic and structural analysis from both the depth profiles

In the area of the Lampedusa shelf (SSE) the average thickness of the Lower Cretaceous stratigraphic unit is 1.9 km in Fig. 5.5Ba' and the same stratigraphic unit shows an average thickness of 2.3 km in Fig. 5.7a, Fig. 5.8b.

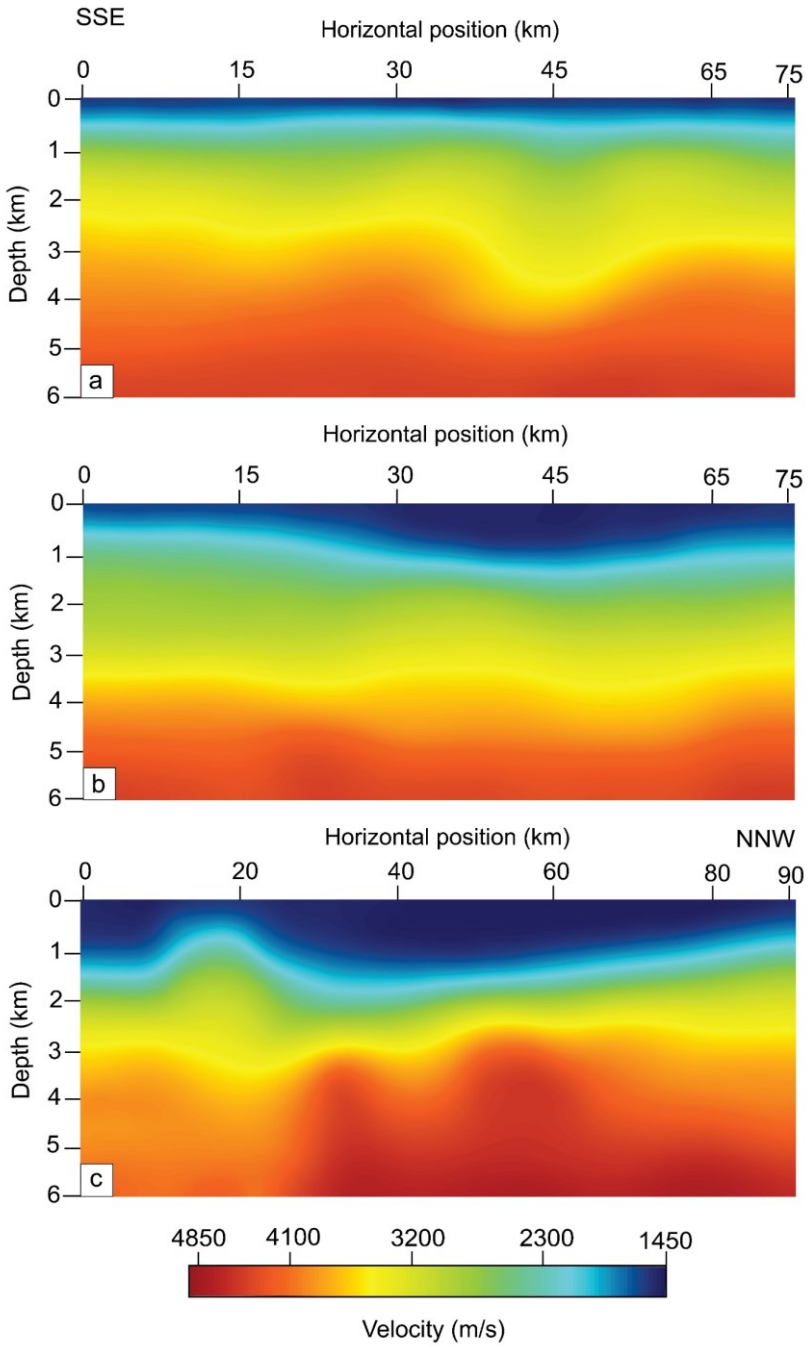

Fig. 5.6. (a') (b') (c') Final velocity models after the application of the Gaussian convolution operator and data exclusion filter.

The Paleogene unit overlies the Cretaceous sediments, with an average thickness of 0.8 km in the first depth profile and ~ 1km in the second depth profile. The overlying Tortonian to Messinian unit has a thickness of ~ 0.6 km and ~ 0.7 km in Fig. 5Ba' and Fig. 5.7a and Fig. 8b respectively. The Plio-Quaternary unit caps the complete stratigraphic sequence, with a thickness difference of 0.2 km between two depth profiles.

The ~ 1.2 km thick Lower Cretaceous sequence in the Western Linosa graben is overlain by ~ 0.8 km Upper Cretaceous sediments (Fig. 5.5Bb'). These units have an average thickness of 1km in Figs. 5.7b, 5.8b. The Paleogene and Tortonian to Messinian units follow upward the sequence. In Fig. 5.5Bb' the Paleogene unit is ~ 1.3 km thick and in Fig. 5.7b the same unit is ~ 1.3 km thick and the Messinian unit in (Fig. 5Bb' and Fig. 5.7b) shows ~ 1 km thickness.

The top of the sedimentary fill, Plio-Quaternary has a maximum thickness of ~ 1.1 km in Fig. 5.5Bb' and ~ 1 km in Figs. 5.7b, 5.8b. The stratigraphic succession from Cretaceous to Plio-Quaternary appears interrupted by the volcanic bodies towards the Pantelleria Graben (Figs. 5.5Bc', 5.7c, 5.8b).

Both the profiles feature Lampedusa high which is flanked by a listric fault (between shot points 700 and 900). In Fig. 5.5Ba' this fault reaches a depth of ~ 5 km while the extension of the fault in Figs. 5.7a, 5.8b is ~ 5.2 km. Western Linosa graben is deformed by a master planar normal fault (approximately between shot points 2100 and 2300) (Torelli et. al., 1995). The fault extends to ~ 6.3 km and ~ 6 km depth in the first and second depth profiles (Figs. 5.5Bb', 5.7b, 5.8b) respectively.

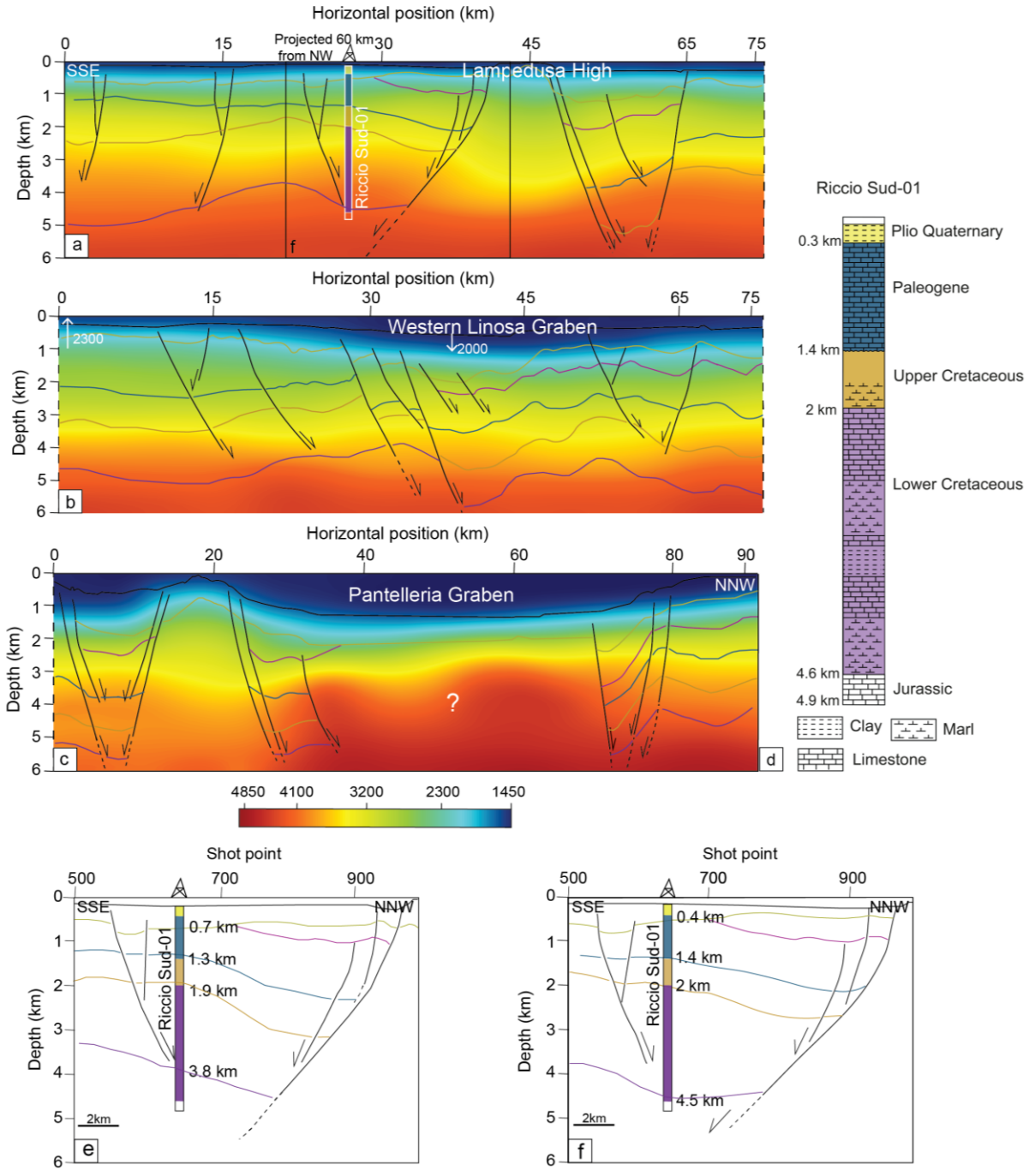

Fig. 5.7. Depth-converted stratigraphic horizons and faults from improved velocity models overlaid over them. (a) No indication of the presence of a volcanic body in the Lampedusa high and the calibration of Riccio Sud-01 well. (b) Velocity contrast at a distance of ~ 2 km and Western Linosa graben at a depth of ~0.8 km. (c) Antiform shape of velocity contours between 20 km and 70 km may be the evidence of the presence of a volcanic body in Pantelleria Graben. (d) Stratigraphy of Riccio Sud-01 well (e) Magnified image from the first depth profile (Fig. 5.5Ba') in which the stratigraphic units do not coincide with well data. (f) Magnified image from the second depth profile, showing the stratigraphic units in good correspondence with the well data. The depth values mentioned on the right side of the well in (e), (f) indicate the depth

of each horizon at that point achieved after depth conversion. See the location of the line in Fig. 5.1 and refer to Fig. 5.5, for the meaning of stratigraphic horizons.

5.5.3. Velocity analysis from final velocity models for uncertain portion

In the Lampedusa high, there is uncertainty regarding the presence of volcanic bodies intruding the high or a carbonatic horst. There were similar uncertainities for Malta (Lentini et al., 2006) and Pantelleria Graben where the evidence of buried magmatic bodies were finally defined (Figs. 5.2a, c) (Orsi et al., 1991; Civile et al., 2008, 2010).

The geological models defined along the CS89-01 profile reveals a broader range of velocity values from 1450 m/s to 4900 m/s around the Lampedusa High (Fig. 5.6). Depth-converted stratigraphic horizons using the refined horizontal variation of the interval velocities (Supp. Mat. 5.3) were overlaid on the final improved velocity models (Fig. 5.7a, b, c). The final velocity model (Fig. 5.7a) does not feature high velocities at shallow depths which are congruent with the absence of volcanic bodies in the Lampedusa High.

5.6. Discussion

In this study, the velocity modeling and time-to-depth conversion of the horizons and faults of a vintage seismic reflection profile CS89-01 (Figs. 5.1, 5.2a, b, c) that crosses the Sicily Channel from the Lampedusa shelf to the Adventure Plateau has been performed. Final velocity models (Fig. 5.6, 5.7a, b, c) are congruent with the velocities presented in Cassinis et al. (2003) for the lines from different parts of Sicily Channel including Pantelleria Graben. Fig. 5.7a does not indicate high velocities at shallow depth may be due to the small scale of the volcanic body, which corresponds to the lack of intruding volcanic bodies in the Lampedusa High. The antiform shape of high-velocity contours at depth in the Pantelleria Graben (Fig. 5.7c), confirm the occurrence of a volcanic body in the graben, as reported in previous work (Zarudzki, 1972; Civetta et al., 1984; Civile et al., 2010; Lodolo et al., 2012; Civile et al., 2021). The seismic facies analysis also supports the presence of volcanic bodies in the graben.

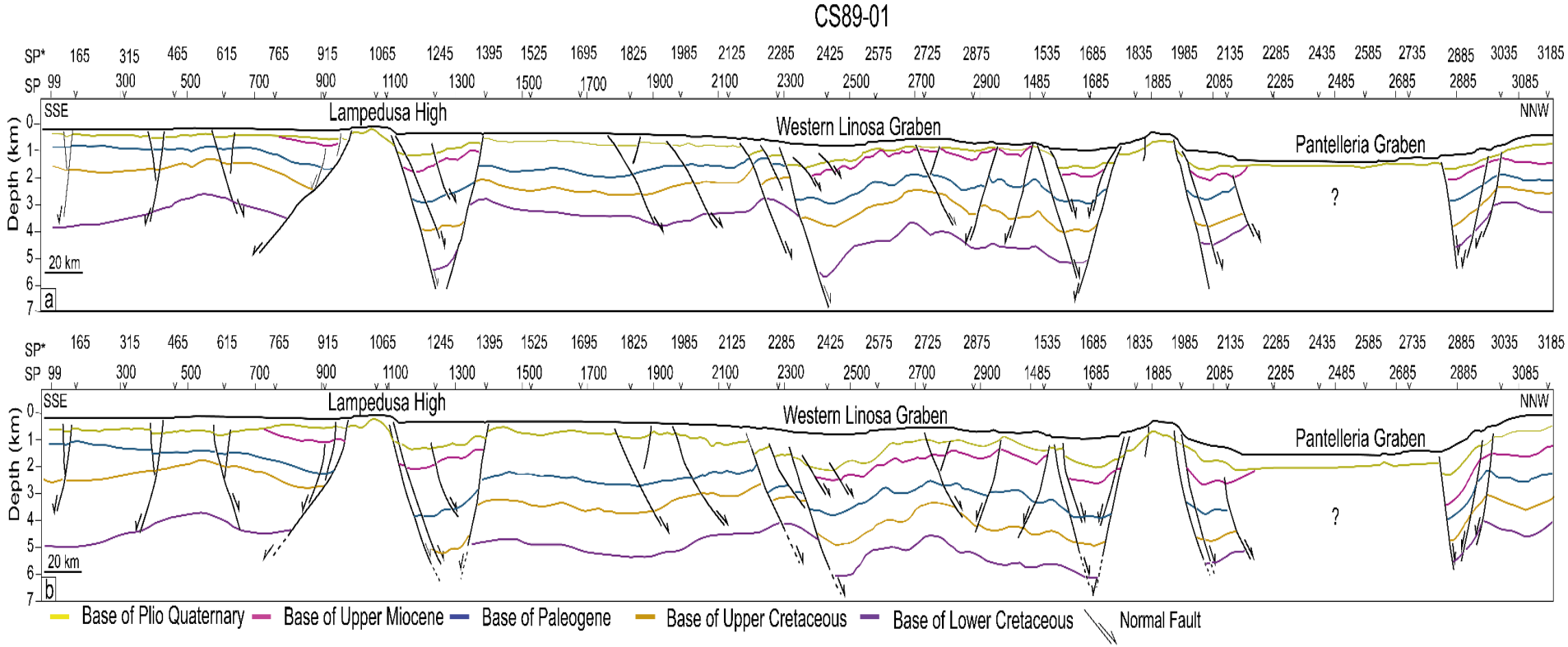

Fig. 5.8. (a) Depth converted horizons and faults of CS89-01 line in MOVE software which is obtained by using the fixed velocities (b) Depth converted horizons and faults of the same line by following the workflow (Fig. 5.3). (a), (b) highlight the differences in the thickness of stratigraphic units and the fault geometry.

The velocity difference at various positions (i.e., ~ 2 km and ~ 39 km) at the same ~ 1 km depth in the velocity model (Fig. 5.7b) may suggest the contrasting sediment compaction levels or the abundance of clayey sediments of the Plio-Quaternary unit in the Western Linosa graben (Rossi et al., 1996; Civile et al., 2021).

The stratigraphic unit thicknesses in (Fig. 5.7a, b, c) are consistent with the interpretation described by Civile et al. (2008, 2021). The average thickness of Plio-Quaternary stratigraphic succession in the main Linosa graben is found to be 1.5 km by the authors of these studies. In our study, we determined the thickness of another part of the graben extending from SSE to NNW on the CS89-01 line, which is around 1.1 km (Fig. 5.7b). Moreover, we used stratigraphy of Riccio well for comparison of the thickness values. Assuming that the stratigraphy of the well is representative of the stratigraphy of the whole Lampedusa shelf, we projected the well on the line (60 km from NW) where it crosses the Lampedusa shelf. The depth-converted stratigraphic units (Fig. 5.7a, f) and the stratigraphy reported in the well log show a good correspondence. A less precise calibration is observed in the first depth profile which was obtained from the initial velocity models (Figs. 5.4 a, b, c; 5.5Ba', 5.7e).

We also performed a time-to-depth conversion of the seismic horizons and faults of the same profile with the dedicated tool of Move Suite (see Supp. Mat. Fig. 5.8a) to validate the results of the geological model we obtained (Fig. 5.7). The depth profile achieved with MOVE Suite does not feature volcanic bodies, as they are localized bodies compared to the length of the profiles and because of the lateral constant interval velocities associated to the stratigraphic unit. Local depth models were constructed, and they show distortion of the faults' geometry in their vicinity (details in Supp. Mat. Appendix B). The depth conversion in MOVE would have been more complicated if the 'checkshot method' was opted (compared to the depth conversion represented in Fig. 5.3) but it would provide results more comparable to ours.

Nonetheless, the depth profile (Fig. 5.8a) built in MOVE and the final depth profile (Fig. 5.8b) generated by following the workflow represented in Fig. 5.3 still highlights differences in the thickness of the stratigraphic units and the fault geometry.

The thickness of stratigraphic units (Fig. 5.8) is more in Fig. 5.8a, with the Lower Cretaceous base being ~1 to 2 km lower in Fig. 5.8b than in Fig. 5.8a and the listric fault bordering the Lampedusa high has a more gentle dip in Fig. 5.8a. The difference in unit thicknesses emerge because the fixed velocities were used for each unit in MOVE suite and interval velocities from numerous CDP's were utilized for depth conversion (Fig. 5.3). The fault geometry difference may owe to the use of graphic software as the faults are marked manually concerning the depth achieved for stratigraphic units. Therefore, although the multiple-step velocity modeling applied in this study and MOVE Suite provide an overall similar geometry of the stratigraphic layers and faults, in the details they provide some differences that could be solved only with additional subsurface data for site-specific investigation.

This work was done to improve the applications of the input analogue dataset for velocity modeling and consequent time-to-depth conversion of seismic horizons and faults of a raster/vintage seismic reflection profile. The velocity modeling dataset was used to reduce the uncertainties in the time-to-depth conversion but still, the input dataset could be suitable if required seismic profiles are just available in scanned paper form for which the velocity modeling and time-to-depth conversion is performed (Fig. 5.3). There are other ways to convert raster files into Seg-Y format which could in turn be helpful for depth conversion which are reported in other works (Buttinelli et al., 2022; Cicala et al., 2024).

5.7. Conclusion

The study suggests that for an old, large sized and noisy vintage seismic reflection profile in raster format, the velocity model building and depth conversion of horizons and faults from stacking velocities are a promising approach.

The depth profile provides a detailed image of the stratigraphic units and structural features found across the Sicily Channel from NNW to SSE that involves multiple steps, from velocity modeling to the construction of the final depth model. For this purpose, Spline interpolation is used to build initial velocity models of the CS89-01 line. The velocity models and depth-converted seismic profiles provide overall insights into the geological and structural information like the thickness of different stratigraphic successions and the occurrence of volcanic bodies in the Pantelleria Graben.

The availability of vintage seismic profiles helps researchers explore renewable energy sources at a lower cost than investing in modern subsurface data or conducting new surveys. Time-to-depth conversion of horizons and faults of these vintage profiles through a multiple refinement of velocity model, as proposed in this study, is a requisite to gain cost-effective information for finding these energy and material resources during this transition time based on well/better constrained subsurface geological models.

Chapter 6

Gravimetric and Heat flow analysis along two significant seismic reflection profiles (CS89-01 and Pant-3) with known tectono-Stratigraphy, passing through the Pantelleria Graben

6.1. Introduction

Sicily Channel is a unique area that reveals significant differences in the crustal structure owing to the variable rock densities and the occurrence of different tectonic events at different times. In the previous studies, either gravity anomaly or heat flow analysis has been carried out in the Sicily Channel to investigate its crustal structure (Morelli et al. 1975; Boccaletti et al., 1984; Della Vedova et al., 1987; Civile et al. 2008). The involvement of heat flow anomaly data with the gravity anomaly data is lacking in the literature. Also, there are some spots in the Sicily Channel Rift Zone (SCRZ) (Figs. 6.1-6.4) that have preserved the signs of the inversion tectonics that came into play after the rifting event and they might be evidenced by gravimetric and heat flow anomalies. We attempted to perform a combined analysis of gravity and heat flow along with the tectono-stratigraphic interpretation of two important seismic reflection profiles (CS89-01 and Pant-3) passing through Pantelleria Graben (Figs. 6.5-6.14). The crustal models along these profiles were constructed with the Moho data from Cassinis et al. (2003); Grad et al. (2009).

The Earth is not evenly dense so, its gravity is not the same everywhere. The variations of the gravity field (gravity anomalies) are caused by the heterogeneous mass distribution of Earth's interior (McKenzie, 1967). Knowledge of the distribution of the gravity field is significant for constraining the shallow and deep structure of Earth's crust and upper mantle and for understanding the dynamics of tectonic processes that have shaped them (McKenzie, 1967; Bassett et al., 2015; Hackney, 2020). A gravity anomaly is a difference between the measured gravity at a place and the theoretical gravity value which depends on its latitude (Gibson and Millegan, 1998). Several corrections are applied to obtain anomalies that are comparable over large areas. Depending on the corrections applied, the anomalies are divided into Bouguer and Free-Air gravity anomalies which are commonly used as gravity anomalies (Vine and

Matthews 1963; Chapin, 1996; Cai et al., 2005; Colli et al., 2016). If the correction for latitude and topography are applied on the measured gravity field, the Free Air anomaly is obtained (Jones, 1998; Lee et al., 2009); usually, these anomalies are applicable for offshore areas. The correction for gravitational attraction of topography to the free air anomaly results in the Bouguer anomaly (Featherstone and Dentith 1997; Flis et al., 1998; Nowell, 1999). Heat flow anomaly is another important geophysical parameter that helps to define the thermal structure of the Earth's interior. Radiogenic heat production inside the Earth mainly generates heat which flows outward through the lithosphere. The quantity of heat flux across unit area time is the heat flow which can provide valuable insights into the evolutionary history of the basins (Armstrong and Chapman, 1998). Large gravity and heat flow anomalies may be produced by the density differences caused by the infusive rocks and are often considered to be surface expressions of high temperatures and flow within the mantle (McKenzie, 1967; Tanimoto et al., 2003; Colli et al., 2016).

In this chapter, we are going to incorporate the results of the tectono-stratigraphy, gravity anomalies and heat flow for the Pantelleria Graben, which will be used to study further relationships between volcanism with crustal structure/Moho depth.

6.2. Geological setting and evolutionary history

The Sicily Channel is a shallow marine platform characterized by very irregular bathymetry and the three prominent NW elongated tectonic grabens (Pantelleria, Linosa and Malta) reaching water depths (>1km) (Morelli et al., 1975; Argnani, 1990; Catalano et al., 1995; Torelli et al., 1995; Grasso et al., 1999; Finetti, 2005; Civile et al., 2010., Carminati et al., 2012., Arab et al., 2020., Civile et al., 2021). The N-S-oriented strike-slip fault zone also referred to as the Capo Granitola-Sciacca Fault Zone (CGFZ) extends ~ 200 km between Sicily and Linosa (Fig. 6.1) marks the boundary between Pantelleria graben to the west and Linosa

and Malta grabens to the east (Cello 1987; Argnani 1990; Reuther et al. 1993; Rotolo et al. 2006; Civile et al. 2010; Ghisetti et al. 2009., 2018; Fedorik et al., 2018; Civile et al., 2018, 2021).

The origin of these grabens is complex enough that it has given rise to discussions with multiple ideas on their tectonic frameworks and interpretations (Roure et al., 1990; Béranger et al., 2004; Maiorana et al., 2023).

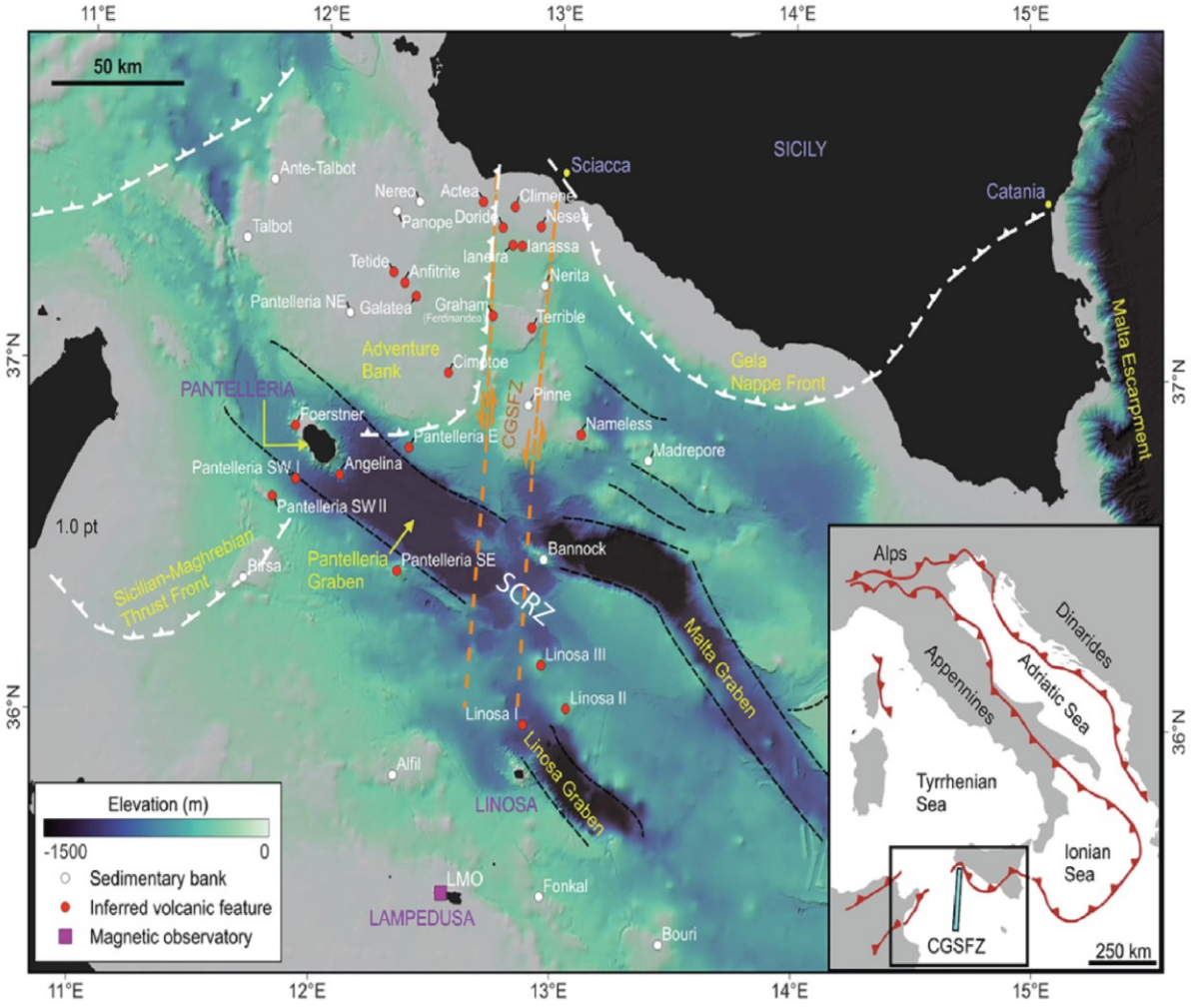

Fig. 6.1. The main structural, and geomorphic features and the Volcanoes, ridges and sedimentary basins in the Sicily Channel taken from Micallef et al. (2024).

They are described as tectonic depressions akin to pull-apart basins that emerged along a dextral shear zone that is positioned in front of the Africa–Eurasia collisional belt (Finetti 1984; Jongsma et al., 1985; Reuther and Eisbacher, 1985; Ben Avraham et al., 1987; Finetti and Del Ben, 2005). According to Argnani, (1990) and Arab et al. (2020), the structures were developed

due to slab rollback of the African plate under the Tyrrhenian basin due to the interplay of mantle convection currents. The grabens have been interpreted as intraplate rift-related features whose origin is linked to the NE-SW oriented movement of Sicilian landform away from the African slab (Illies, 1981; Beccaluva et al., 1983; Finetti, 1984). The analogue modeling described by Corti et al. (2006) suggests the coexistence and overlapping of the two independent tectonic processes the Sicilian–Maghrebian accretion and the passive rifting. More recently Civile et al. (2021) depicted their origin by NW-striking dextral trantensional shear zone and the slow-paced NW-directed movement of the African plate in the Sicily Channel.

The Pantelleria Graben stretches to a length of 90 km and reaches to a depth of −1317 m and towards westward the graben shrinks into a roughly N-S trending depression (Morelli et al., 1975; Argnani 1990; Civile et al., 2010). The crustal thickness in the graben touches the lowest depth at ~17 km and the upper sedimentary fill (Plio-Quaternary deposits) exhibits a thickness of ~ 1km (Argnani, 1990; Scarascia et al., 2000; Civile et al., 2008; 2018; 2021).

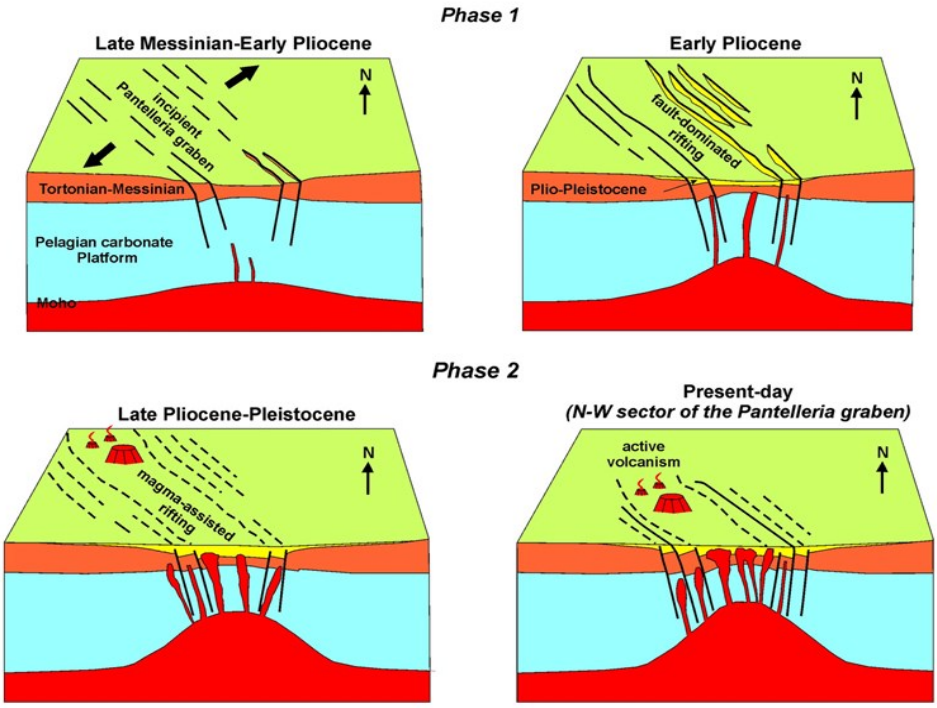

Fig.6.2. Schematic diagram illustrating the evolution of Pantelleria Graben from the first phase (Early Messinian- Early Pliocene) to the second phase (Late Pliocene–Present) (taken from Civile et al., 2010).

Pantelleria Graben represents a good example of a volcanic site, that features large-sized magmatic manifestations emplaced through much of the Quaternary period (Civetta et al., 1998; Jordan et al., 2018; Rotolo et al., 2006). The clearest signature is the presence of NW-SE trending edifice that spreads in the graben over 40 km including its seamount extension.

In the first phase from Late Messinian to Early Pliocene, the extensional phase generated the NW-SE trending normal faults which stretched the Pantelleria Graben to a maximum breadth of ~ 30 km. The configuration of a few of these faults also shows the strike-slip motion (Civile et al., 2010, 2014, 2021) (Fig. 6.2). These long extensional faults extended further from short fault segments (McClay et al., 2002; Morley, 2002; Childs et al., 2017). During this phase, the normal faulting predominantly controlled the rifting of the graben which gave birth to domino-style geometry in its northern portion (Civile et al., 2010). At the end of this phase, the fault-controlled rifting came to an end which was followed by the process of magmatism. In the second phase (Late Pliocene–Quaternary) the localized magmatic intrusions played a vital part in the stretching of graben. The depth of the Moho shallowed to ~17 km along the Pantelleria rift axis due to the continuous stretching and subsidence of crust in the graben that in turn led to the rapid ascending of magma within the graben floor (Argnani, 1990; Scarascia et al., 2000; Civile et al., 2008). The NW portion of the graben experienced maximum stretching which probably led to the maximum magma flux towards it from the SE sector. Thus, the volcanic bodies are concentrated in the NW limit of the graben (Civile et al., 2010; Jordan et al., 2018).

6.2.1. Volcanism in Sicily Channel

The rifting event in the Sicily Channel was coupled with extensive volcanic activity during the Plio-Pleistocene period mainly on the Pantelleria and Linosa Islands (Carapezza et al., 1979; Beccaluva et al., 1981; Calanchi et al. 1989; Peccerillo, 2005; Rotolo et al. 2006; Lodolo et al.,

2012, 2019; Civile et al., 2008; Maiorana et al., 2023; Micallef et al., 2024) (Fig. 6.1). The volcanism dispersion and spatial arrangement of the extensional tectonic structures flanking the prominent grabens are closely linked (Civile et al., 2018; Lodolo et al., 2012) (Fig. 6.3). The oldest volcanic products from the Sicily Channel are about 10 Ma in age (Beccaluva et al. 1981). The recent submarine volcanic eruptions reported on Graham Bank in A.D. 1831 led to the formation of the Ferdinandia cone that has suffered a change in shape due to wave and current erosion (Cavallaro and Coltelli, 2019) and ~5km NW of Pantelleria Island (named as Foerstner 'volcano') in A.D. 1891 (Washington 1909., Colantoni et al. 1975., Conte et al., 2014). The most recent magmatic manifestations are described by Lodolo et al. (2019), who have identified six volcanic edifices near the CGSFZ (Fig. 6.1).

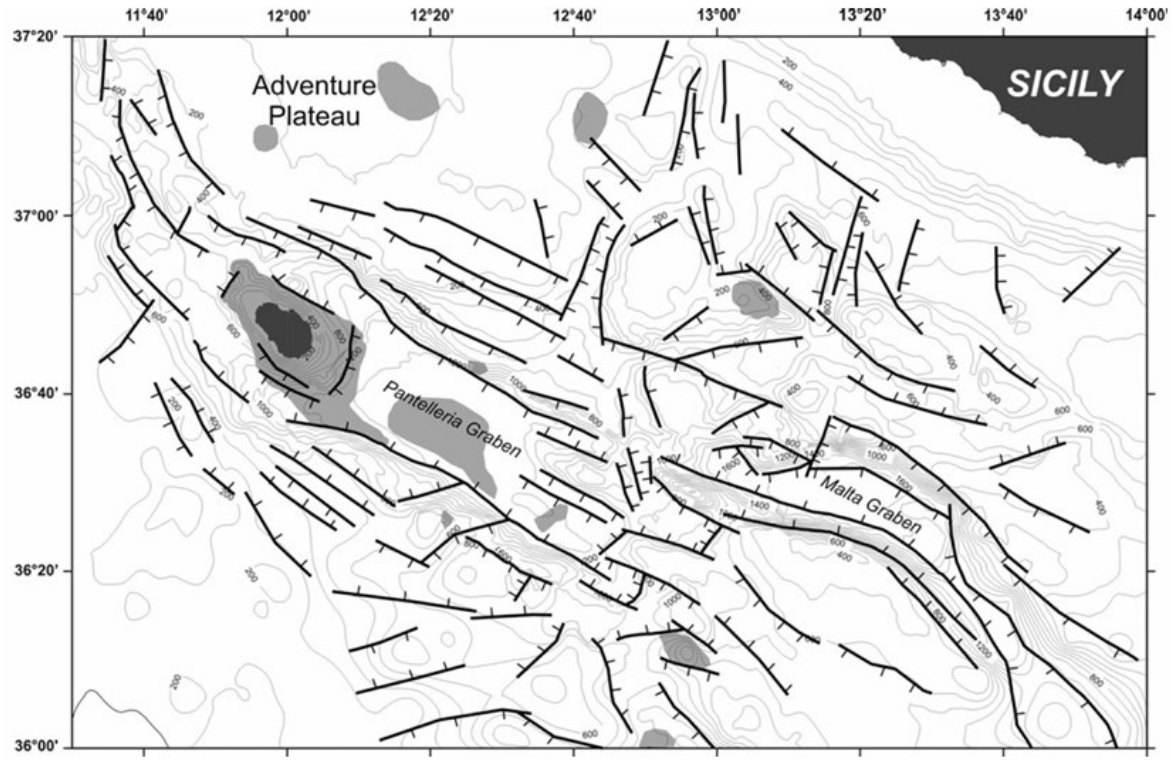

Fig. 6.3. The localization of volcanic occurrences (grey area) and the extensional faults in the Sicily Channel taken from Lodolo et al. (2012).

Among them the five volcanoes were formed before the Last Glacial Maximum (LGM, ca. 20 ka B.P.) and the Actea volcano is considered to be the product of post-Last Glacial Maximum

volcanism (Fig. 6.1). The three grabens have witnessed the volcanism at focused sites that gave birth to huge volcanic morphologies. The volcanism is dated Pleistocene to Holocene in the Linosa and Pantelleria grabens which is concentrated at sites (NW limits) that are intensely impacted by extension and their size reflects the greatest magmatic flux at Pantelleria (Civile et al., 2010., Jordan et al., 2018., White et al., 2020) (Fig. 6.1).

Pantelleria Graben hosts two underwater seamounts; one about 15 km SSE named as Angelina Seamount features significant magnetic anomalies (Lodolo et al., 2012), and the other one about 60 km SE of it shows the presence of alkaline basalts which were sampled from its southern footwall, providing clues of the link with the tectonic activity of the graben (Rotolo et al., 2006) (Fig. 6.1). The surface of the Adventure plateau is dotted by several submerged volcanic edifices (Tetide, Anfitrite, Galatea and Cimotoe) and other shallow bank seamounts (Talbot, Ante-Talbot and Pantelleria Vecchia banks) consisting of Carbonates and Sandstones (Calanchi et al., 1989; Civile et al., 2015; Civile et al., 2016; Micallef et al., 2024) (Fig. 6.1). The CS89-01 and Pant-3 profiles were re-interpreted considering the literature and well-log data from SE to NW of the Sicily Channel (Fig. 3a, b). The CS89-01 is a key seismic profile that stretches across the Channel and covers the main structural features including the Pantelleria Graben and Adventure Bank. The Pant-3 orthogonally transects through the Pantelleria Graben and intersects CS89-01C1 (part of CS89-01) at structural relief (SR) (Fig. 6.4).

6.3. Seismic interpretation

The interpretation of CS89-01 and Pant-3 profiles reveal the presence of pre-rift deposits comprising of Triassic to Miocene Carbonates and a suite of Plio-Quaternary deposits, the lower part of which is the Early Pliocene sequence (syn-rift deposits). These deposits were

recognized by the semi-transparent seismic packages possessing the divergent geometry (Figs. 6.5-6.7, 6.11) followed up by the layered sequence of upper Plio-Quaternary sediments constituted by sands and clays.

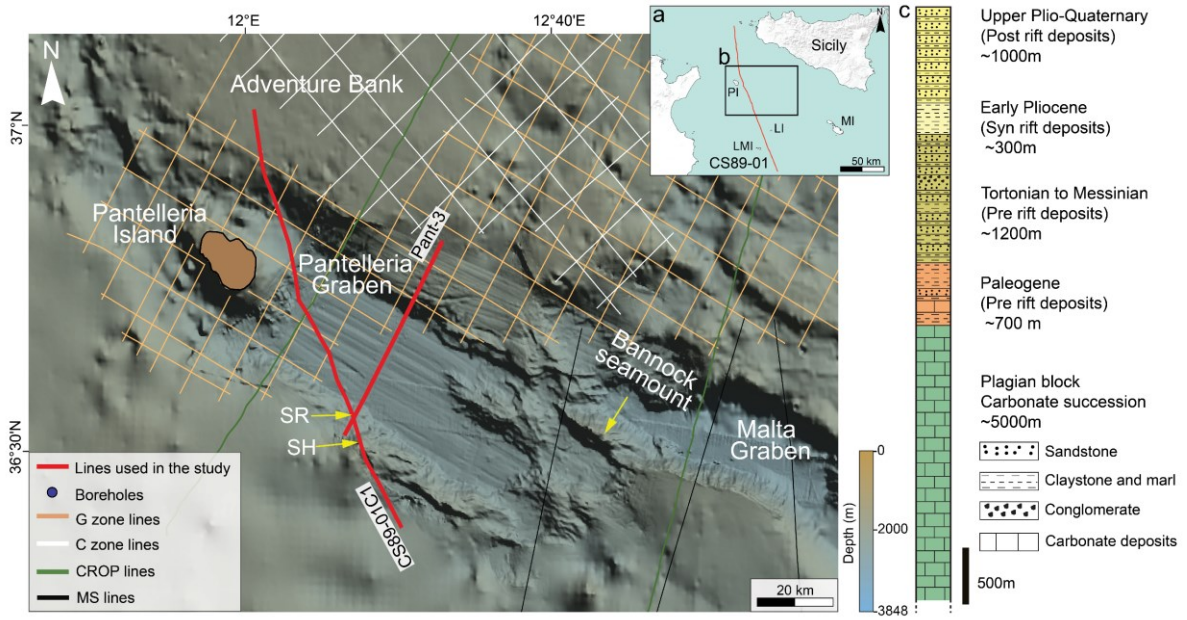

Fig. 6.4. (a) Inset map of Sicily Channel along with the localization of the CS89-01 line. (b) represents the location of CS89-01C1 and Pant-3 and the site of their intersection. (c) shows the simplified lithology from SE to NW in the Sicily Channel (modified from Civile et al. (2010). LI: Linosa Island; LMI; Lampedusa Island; MI: Malta Island; PI: Pantelleria Island; SH: structural high; SR: structural relief.

In the structural domain, the Lampedusa shelf is mainly characterized by the extensional faults as suggested by CS89-01 profile (location in Fig. 6.4a). A SE dipping listric normal fault flanks the Lampedusa high whose rollover is visible between the shot points 400 and 700 (refer to Supp. Mat. Fig. 6.5). A series of NW dipping normal faults with variable throws are found in the SSE of the Western Linosa Graben which is bounded by a SE dipping planar normal fault (Supp. Mat. (Fig. 6.5). In CS89-0C1 profile thin layer of Upper Plio-Quaternary deposits (~ 0.34 s/TWT thick from seafloor) drapes the Pantelleria Graben, the rest of the reflctions below the graben seem affected by magmatic body. The structural high (SH) between Basin A and SR

seem also intruded by a magmatic body which is recognized based on facies and their boundary pattern.

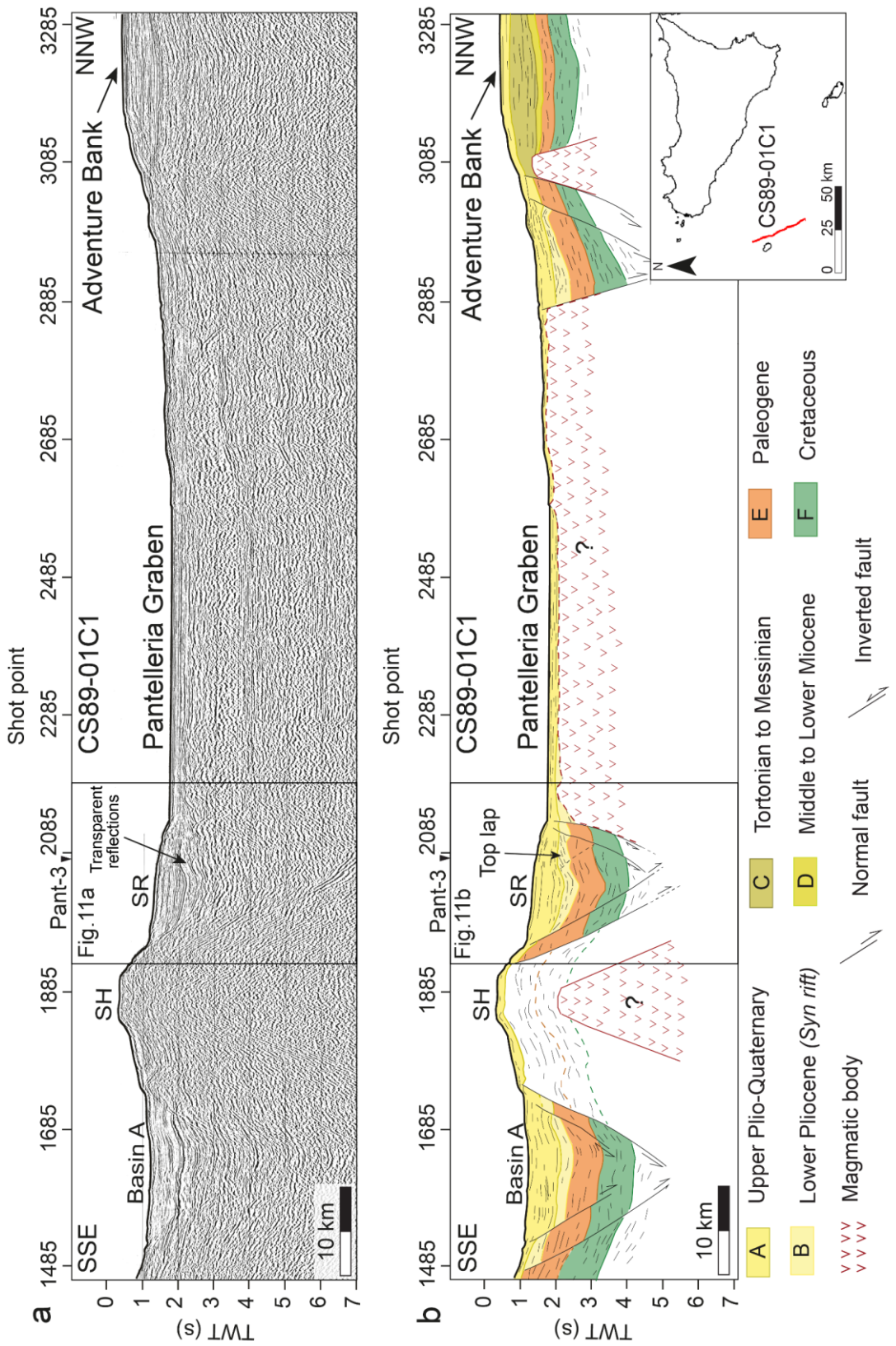

Fig. 6.6. (a), (b) Uninterpreted and interpreted multichannel seismic reflection profile CS89-01C1 which transects along the Pantelleria Graben. The sedimentary infill of Structural relief (SR) that shallows in the graben shows signs of positive inversion. SH: Structural high.

The SH is bounded by an SE dipping master normal fault between the shot points 1685 and 1885 which has displaced the whole sedimentary suite around it and an NW dipping normal fault near shot point 1885 which has affected the sea floor.

The SH is bounded by an SE dipping master normal fault between the shot points 1685 and 1885 which has displaced the whole sedimentary suite around it and an NW dipping normal fault near shot point 1885 which has affected the sea floor. To the NNW sector, a sedimentary basin, another magmatic intrusion is recognized at the starting edge of the Adventure bank. The intrusion has emplaced along a SE dipping normal fault which points out the relationship of magmatism with rifting (Civetta et al., 1984; Rotolo et al., 2006; Civile et al., 2008, 2010).

The Pant-3 profile passes across the Pantelleria Graben orthogonally in the SW-NE direction (Fig. 6.4). A thick heap of Plio-Quaternary sediments is found in the Pantelleria Graben which is interrupted by magmatic intrusions in the central and southern parts (Fig. 6.7). In the graben, the doming of the strata is considered to be caused by these magmatic intrusions by Civile et al. (2010, 2021). According to Civile et al. (2010), the SR has received a good supply of the Plio-Quaternary sediments through the erosion from the adjacent SH (shown in Fig. 6.6).

The product of this erosive action (mass flow deposit) has been delineated by our investigation in the SW limit of the Pantelleria Graben which is indicated by the irregular sloping surface facing towards the graben (Fig. 6.7a). The NE dipping fault (N1) flanking this sloping surface have been active till recent times (Figs. 6.7, 6.12). Towards the NE margin domino-style geometry is found (details in Civile et al. (2010)). In the NE sector of the graben, the lower portion of the Plio-Quaternary sequence highlights growing wedge-shaped (divergent) geometry (Fig. 6.7b). These deposits with syn-rift geometry suggest that they were deposited during the Early Pliocene rifting phase. The antithetic faults associated with a SW dipping

listric fault (N2) which is sealed by the Upper Plio-Quaternary deposits have produced a tilted geometry of syn-rift deposits (Figs. 6.7, 6.12).

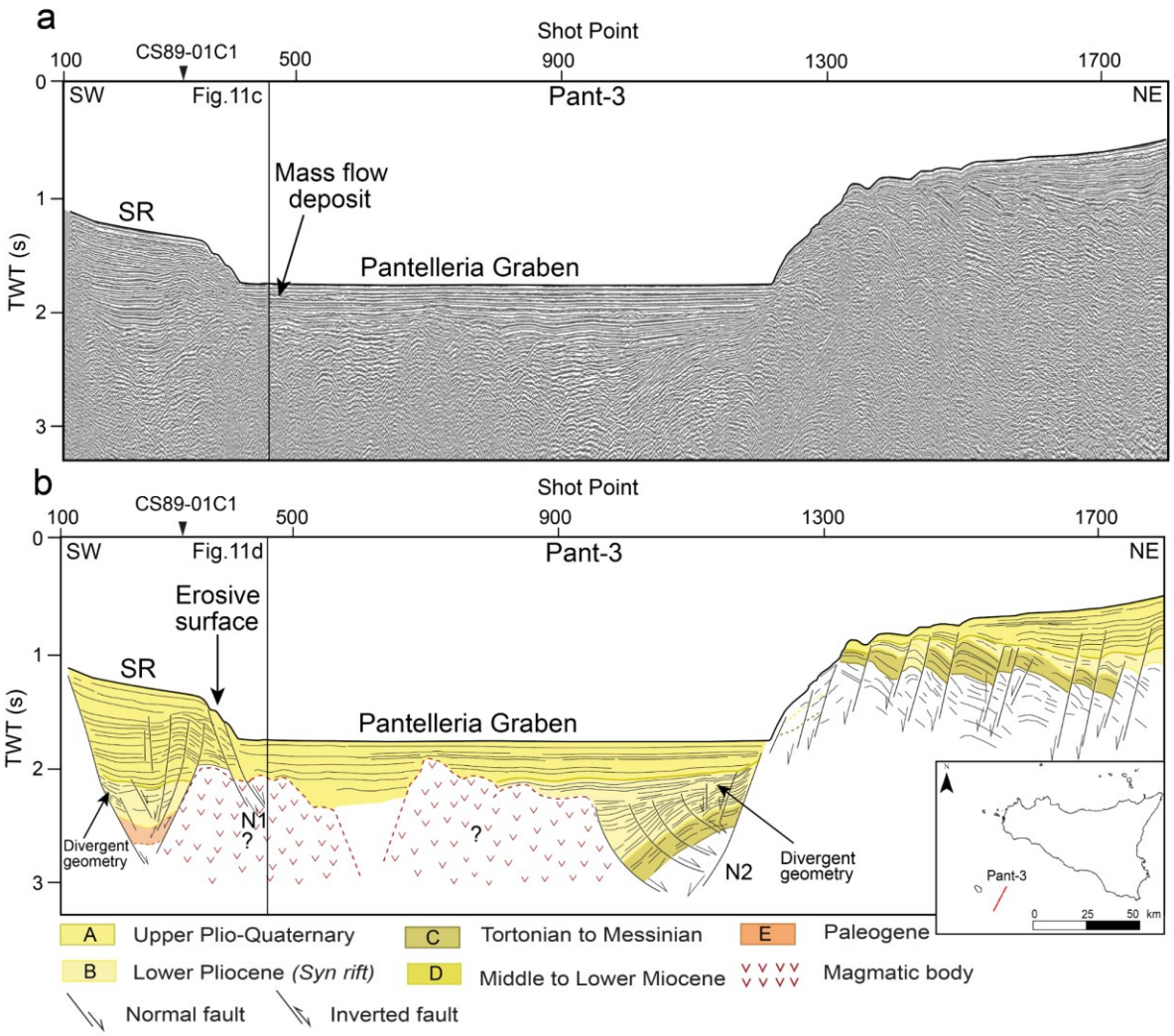

Fig. 6.7. (a) (b) uninterpreted and interpreted multichannel seismic reflection profile Pant-3 which features the domino-style geometry in the NE and positive inversion in Structural relief (SR) in the extreme SW. The southwestern and central portion of the Pantelleria Graben is interrupted by possible magmatic intrusions.

6.4. Geophysical data interpretation

6.4.1. Gravity anomaly maps

The seismic interpretations of CS89-01 and Pant-3 lines (Fig. 6.4) pass through Pantelleria Graben which is the hub of volcanism and thus the gravity analysis allowed us to better define

the connection of volcanism and crustal structure and further constrain the occurrence of volcanic denser bodies in the subsurface. This section presents the results of the analysis of satellite gravity data complemented by 2D seismic interpretation of these lines along with the integration of Moho depth data extracted from the map of Cassinis et al. (2003).

The complete Bouguer anomaly map of the Sicily Channel reveals that data may range from +20 mGal to +89 mGal (Fig. 6.8). The highest gravity anomalies have been observed in the center of the Channel and the Southeastern portion highlights the lowest values (Fig. 6.8). Across CS89-01 line in the Lampedusa shelf, the Bouguer anomaly data trend fluctuates from 21 mGal to +41mGal. Towards the Pantelleria Graben, the anomaly peaks to the highest value (+ 89 mGal) and the value dwindles to the lowest value of +25 mGal in the Adventure Bank.

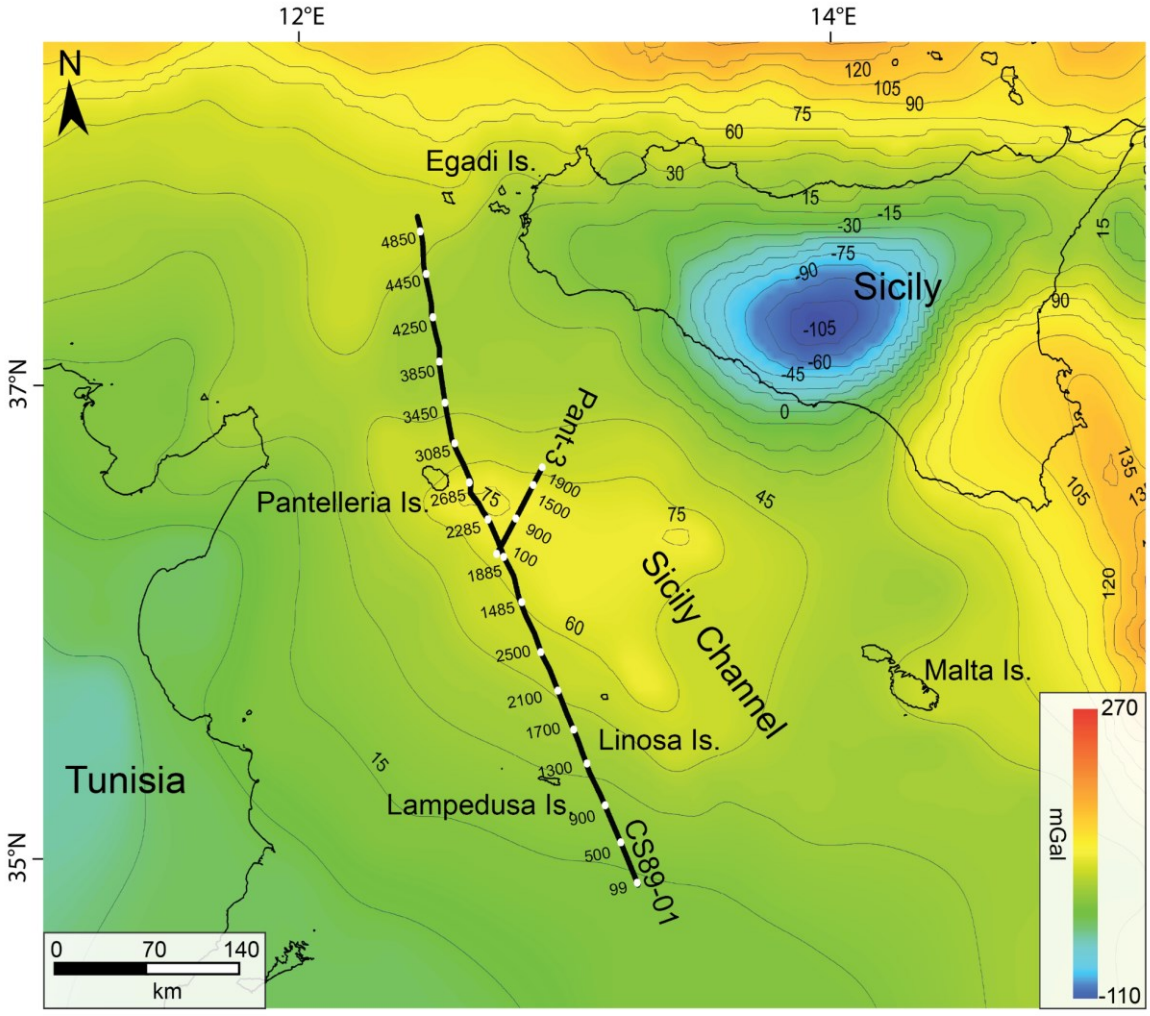

Fig. 6.8. Bouguer gravity anomaly map of Sicily Channel and the location of the seismic

CS89-01 and Pant 3 reflection profiles along which the anomaly curve was generated. The data is was derived from 'The World Gravity Map (WGM2012)' (https://bgi.obs-mip.fr/gravity-maps/).

In orthogonal direction along the Pantelleria Graben, the Bouguer anomaly analysis considering the Pant-3 line, it is clear that at 1300 shot point the anomaly touches its highest value of 86 mGal and after that trend shows a dramatic decrease.

However, the central part reveals a different pattern; the anomaly values fall off to negative. The graben is characterized by negative anomalies (-7 to -12 mGal) across the CS89-01 profile. The anomalies rise dramatically in the Adventure Bank up to +42mGal (at shot point 3450 and towards the extreme NW shows a gradual decrease.

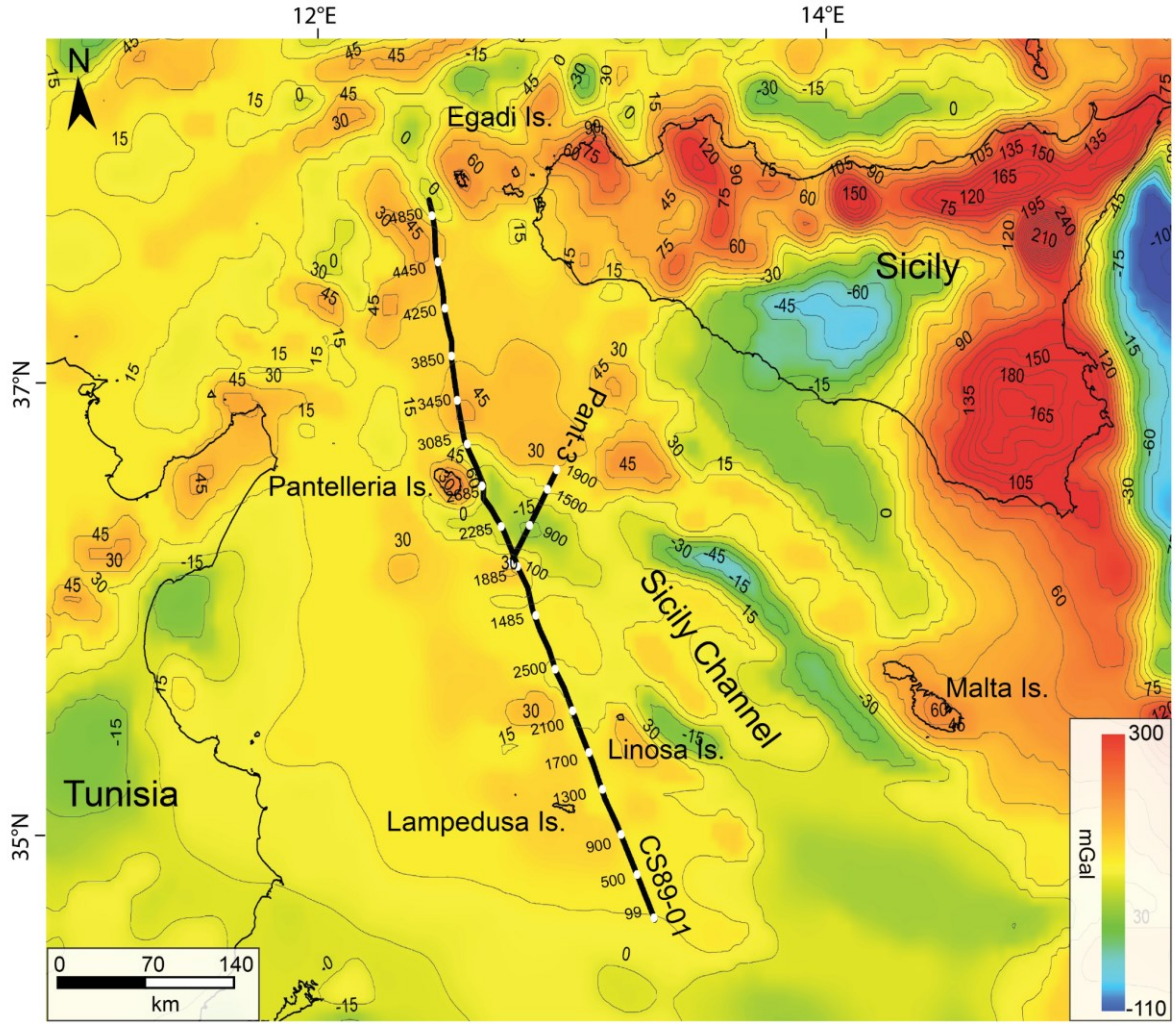

Fig. 6.9. Free Air gravity anomaly map of Sicily Channel derived from 'The World Gravity Map (WGM2012)' (https://bgi.obs-mip.fr/gravity-maps/). The analysis and crustal models of the CS89-01 and Pant-3 seismic reflection profiles were generated.

Orthogonally along the Pantelleria Graben the anomaly decreases to –7mGal which goes on decreasing till -15 mGal at 700 and 900 shot points along the Pant-3 profile. The anomaly touches the positive value at 1500 shot point which continuously goes up to 28 mGal at the 1900 shot point (Fig. 6.9).

6.4.2. Heat flow map

Heat flow values derived from the global heat flow database (https://www.ihfc-iugg.org/) were utilized to achieve the surface heat flow for the Sicily Channel. High surface heat flow has been detected in the central of the Channel, with the highest values up to 105 mWm^{-2} in the northwestern extension of Malta graben and lowest value of 0 mWm^{-2} in the northeastern part of Sicily Channel (Fig. 6.10).

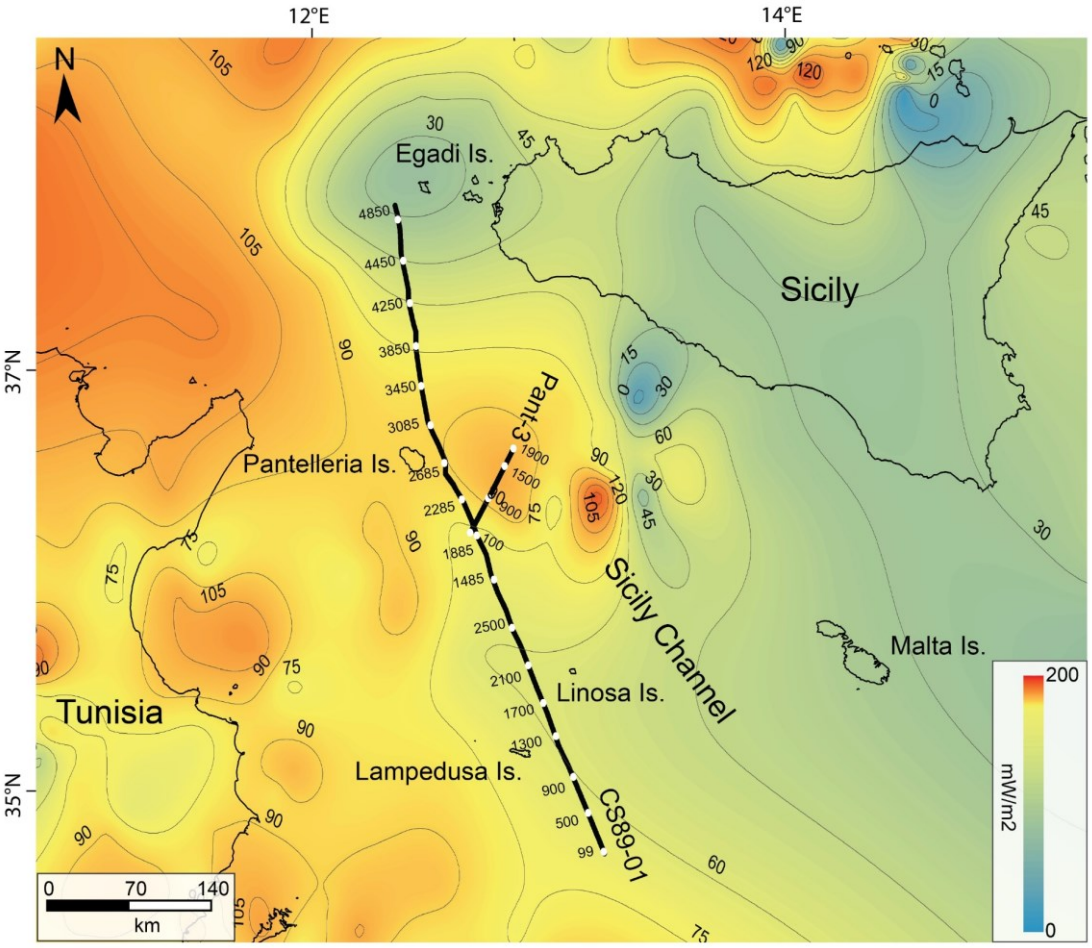

Fig. 6.10. Heat flow map of the Sicily Channel extracted from 'The Global Heat Flow Database (GHFDB)' (https://www.ihfc-iugg.org/). The in-depth analysis of the anomalies was performed along the CS89-01 and Pant-3 multichannel seismic reflection profiles which transect through Pantelleria Graben.

Along the seismic line CS89-01 the SE portion including the Lampedusa shelf highlights the highest heatflow value of 68 $mWm^{-2.}$ Overall, the Pantelleria Graben is characterized by 100 mWm-2 surface heat flow and along the CS89-01 at shot point 3085 the heat flow of 90 mWm^{-2} has been detected in the graben. The heat flow decreases quickly down to 35 mWm^{-2} in the Adventure Bank along the same profile (Fig. 6.10). Considering the Pantelleria Graben from SW to NE the heat flow along the Pant-3 profile rise is consistent up to shot point 1100 which is found to be 103 mWm^{-2} and then towards more NE the heat flow shows a gentle trend up to 1900 shot point.

6.5. Discussion

6.5.1. Inversion tectonics in the southern limit of Pantelleria Graben

The Structural Relief (SR) in the SW sector of the Pant-3 profile shows a thick heap of Plio-Quaternary sequence influenced by magmatic intrusions in the NE portion as suggested by the spherical reflection pattern. The deposits at a depth of ~2.5 TWT/s show a divergent geometry which is indicative of the rifting event (Figs. 6a, 6.11a). The top lap reflection terminations against the upper boundary confirms the presence of an unconformity between two seismic sequences attributed to the upper and lower Plio-Quaternary deposits (Figs. 6.6, 6.11a, b). The syn-rift deposits along with a considerable portion of the Upper Plio-Quaternary deposits highlight the folded reflection geometry which is described as local reactivation of the pre-existing normal faults as reverse faults by Civile et al. (2010). In addition to this observation of the inversion in the SR in the southern limit of Pantelleria Graben, we have provided evidence of inversion at the same site from CS89-01 seismic line (Fig. 6.11a, b). We have

examined the portion of the CS89-01-line that cross-cuts the Pant-3 exactly at the position of SR (Figs. 6.4b, 6.11). The same SR is visible on CS89-01which is bounded by an NW dipping normal fault on the SSE side and draped on the top by the Plio-Quaternary deposits.

We also observed the folded pattern of reflections in the same structure at the 2085 shot point on CS89-01 (Fig. 6.11b), which may be the result of the local reactivation of the previously preexisting normal faults (Fig. 6.11).

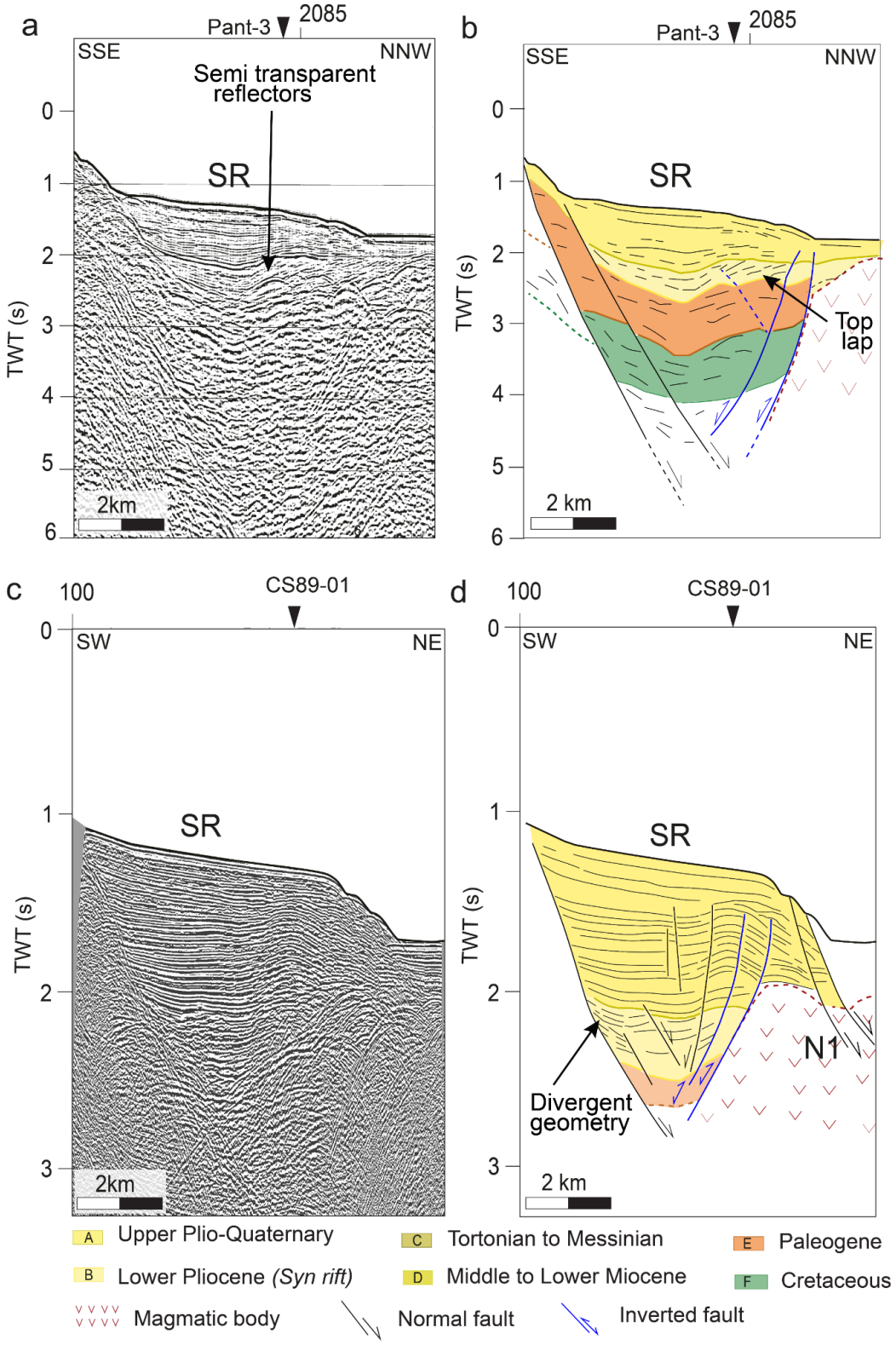

Fig. 6.11. (a) (b), (c) (d) Uninterpreted and interpreted parts of the CS89-01C1 and Pant-3 profiles respectively which highlight the inversion in the structural relief (SR) at the intersection of these two profiles.

The inverted faults are sealed under a portion of Upper Plio-Quaternary deposits which represent the inversion phase that was active locally after the rifting event (documented by the Lower Pliocene deposits), alternatively proceeded by another extensional event. This is evidenced by the deformation of the sea floor by the NW trending normal fault (N1) on the sloping surface of SR (Figs. 6.7, 6.11, 6.12). It suggests that SR has witnessed polyphase tectonic deformation starting from the Early Pliocene. The recent findings of Civile et al. (2021) and Maiorana et al. (2023) shed light on the basin inversion in the SCRZ as a result of the transpressional process driven by CGSFZ and Scicli Ragusa Fault System (SRFS) discontinuities (Fig. 6.12a, b).

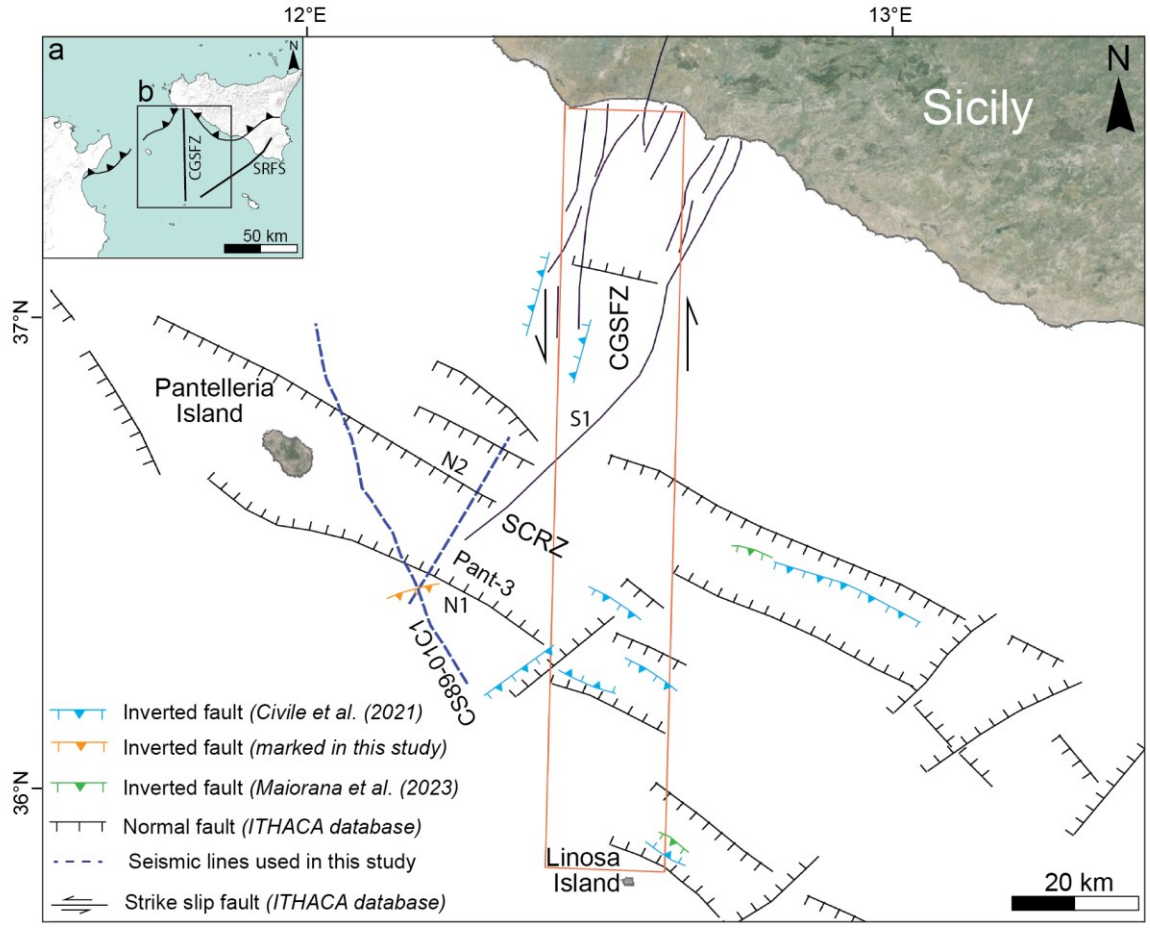

Fig. 6.12. (a) Inset map illustrates the transpressional discontinuities; Capo Granitola-Sciacca Fault Zone (CGFZ), Scicli Ragusa Fault System (SRFS) (extracted from Civile et al. (2021) responsible for the inversion in Malta and Linosa Grbaens. (b) shows the cross-cut relation of CS89-01C1 and Pant-3 seismic lines with the inverted fault and the structural features in the

Sicily Channel rift Zone (SCRZ). N1 and N2 are the boundary normal faults imaged on the Pant-3 profile (Fig. 6.7b).

The inversion phase is dormant in the Malta and Linosa grabens (Civile et al., 2021) and the recent observation suggests that the inversion phase is still active in these grabens which is linked to the change in the subduction polarity of the African Plate (Maiorana et al., 2023). After the Early Pliocene, the CGSFZ was impacted by major transpressional tectonics which has produced the modest inversion in the zone including its southern part where Pantelleria Graben is separated from the Linosa and Malta grabens (Fig. 6.12).

The strike-slip fault (S1) from the ITHACA database highlighted in Fig. (6.12) shows an appreciable extension towards the Pantelleria Graben. From the observations of the literature and the integrated data, we may assume that the impact of the same inversion event linked to transpressional tectonics may have caused the reactivation of the preexisting normal faults in the SR on the SW flank of the Pantelleria Graben.

6.5.2. Building of Crustal models of CS89-01 and Pant-3 profiles

The seismic horizons of the CS89-01 profile were converted to depth using the interval velocity models as the stacking data was available for them (for detail see Chapter 5) with the addition of the depth portion extending to the Egadi Islands. For the Pant-3 profile standard velocities associated with each lithology type were used to convert the horizons to depth (Christensen and Mooney, 1995). Simple depth crustal models were created with only the insertion of some important features (Fig. 6.13, 6.14). For instance, in both models the simplified depth-converted stratigraphic sequences, boundary normal faults and the magmatic bodies marked in the Pantelleria Graben are shown (Fig. 6.13, 6.14). Three main stratigraphic horizons have been delineated on the profiles which consist of variable lithostratigraphic units. The profiles were supplemented with the Moho depth interface taken from Cassinis et al. (2003); Grad et al.

(2009) along these seismic lines to define the relation of crustal structure and volcanism with the analyzed geophysical data.

6.6.3. Gravity Anomaly and Heat Flow Analysis along Pantelleria Graben

The largest positive Bouguer and negative Free Air anomalies are found along and across the Pantelleria Graben as highlighted by the curves over the depth crustal model of CS89-01 and Pant-3 (Figs. 6.13, 6.14). Along the Pantelleria Graben axis, the highest positive Bouguer anomaly detected by Civile et al. (2008) reaches the value of + 80 mGals according to gravity data from Morelli et al. (1975) and other sparse data acquired by Italian commercial exploration surveys. We have found the highest value of up to +89 mGal across the graben along the CS89-01 profile data extracted from satellite gravity data. The Free Air anomaly along the CS89-01 and Pant-3 profiles drop to -12 mGal and -15 mGal respectively. Below the Pantelleria Graben, the heat flow of 100-104 mWm^{-2} has been observed (Figs. 6.13, 6.14) which is in agreement with the heat flow analysis presented in previous works (Boccaletti et al., 1984; Della Vedova and Pellis, 1985; Argnani and Torelli, 2003).

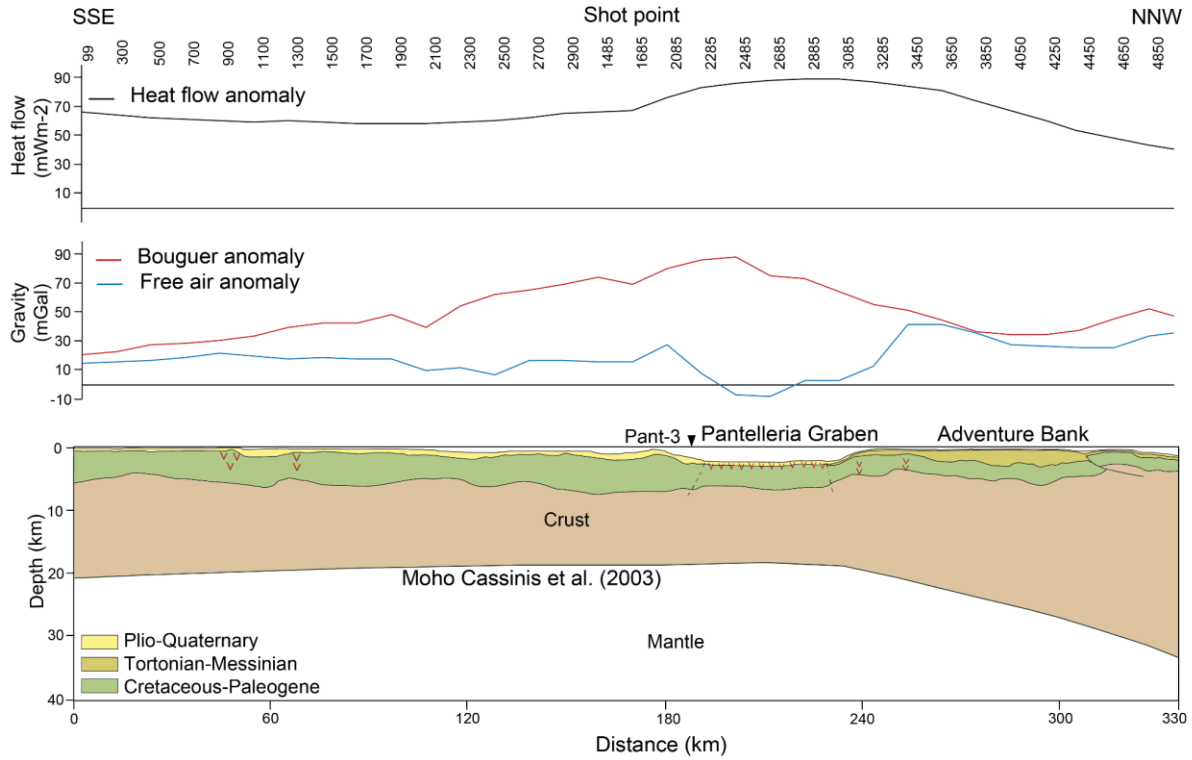

Fig. 6.13. The crustal model along CS89-01 seismic profiles and the curves of gravity and heat flow anomalies along it. The largest positive Bouguer anomaly (+89 mGal), the main negative free air anomaly (-12 mGal), and the high surface heat flow (90 mWm^{-2}) have been observed in the Pantelleria Graben.

Towards NW of the graben, in Adventure Bank the anomalies change. Here Bouguer anomalies values fall off while the Free Air anomalies reach positive values again, and the terrestrial heat flow curve also follows the decreasing path, which shows a relation with the crustal thickness or the Moho depth (Colombi et aI., 1973; Boccaletti et aI., 1984; Della Vedova et al., 1987; Scarascia et al., 2000; Cassinis et al., 2003; Tesauro et al., 2008; Milia et al., 2018).

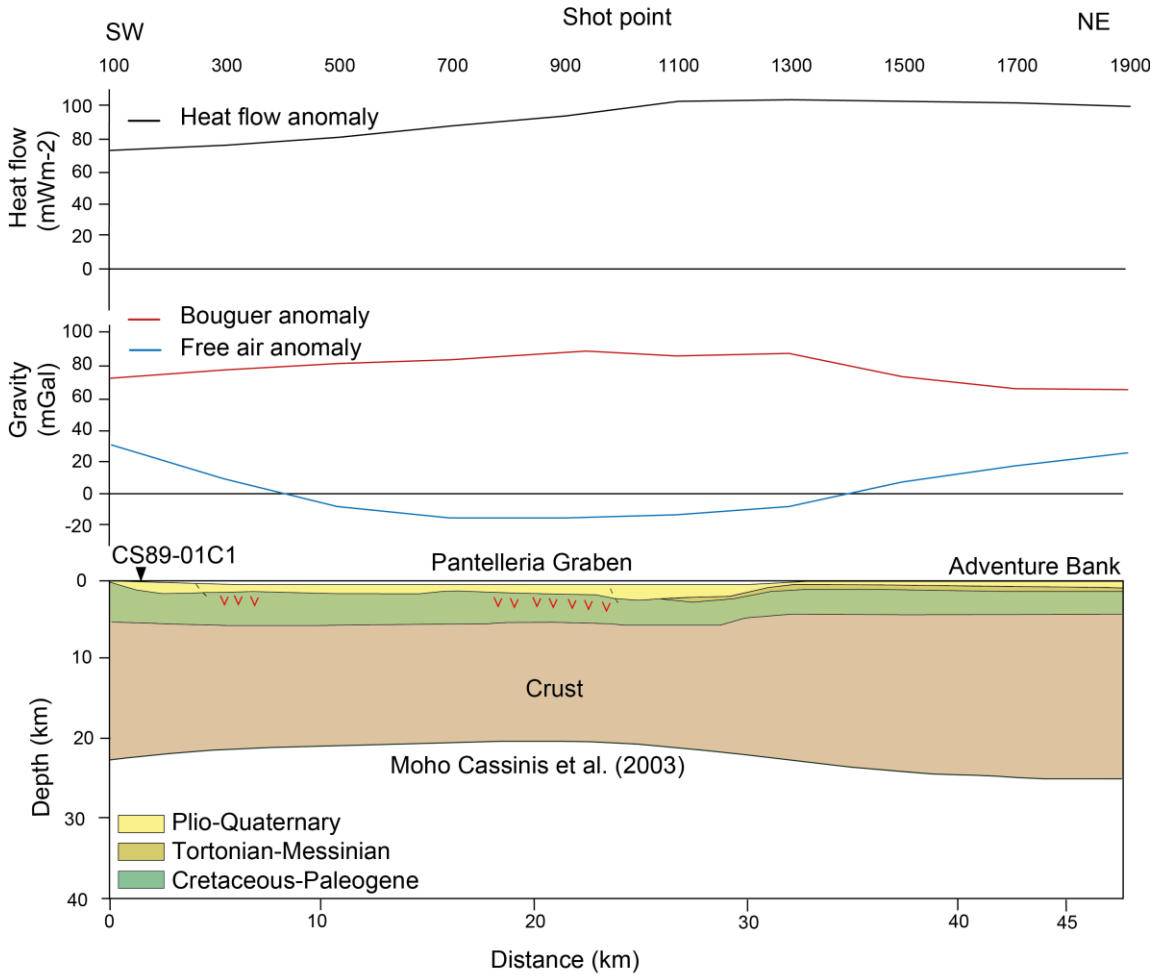

Fig. 6.14. Crustal model along Pant-3 seismic profiles and the curves of gravity and heat flow anomalies along it. In the Pantelleria Graben the Bouguer and Free Air anomalies reach +86 mGal and -15 mGal respectively and the highest terrestrial heat flow touches the highest (103 mWm^{-2}) values.

The gravity and heat flow anomalies are evidence of the thin crust beneath the graben and the thick crust in the Adventure Bank which is in line with the depth of Moho from Cassinis et al. (2003) and the other studies (Scarascia et al., 2000; Finetti and Del Ben, 2005; Tesauro et al., 2008; Milia et al., 2018).

The crustal thickness is ~17 km (Morelli et al. 1975; Civile et al. 2008) beneath the graben and the gravity and surface heat flow anomalies above this thin crustal domain have been produced by the volcanic bodies, reported by (Reuther and Eisbacher, (1985); Civile et al., 2008, 2010; Lodolo et al., 2012).

The volcanic activity on Pantelleria Island could be attributed to a substantial uplift (up to 20 km) of the Moho beneath Pantelleria Graben (Figs. 6.13, 6.14). This uplift might have resulted in the formation of a relatively shallow magma chamber, where rock differentiation processes occurred (Civetta et al., 1988; Chierici et al., 1995). Seismic data have revealed shallow magmatic manifestations in the Pantelleria Graben. The CS89-01 and Pant-3 models, show that they are located ~ 0.2 km and ~ 0.6 km respectively below the sea floor in the graben which agree with the findings of Civile et al. (2010). These magmatic bodies are connected in part to the gravity and surface heat flow anomaly peaks (Della Vedova and Pellis, 1985; Argnani and Torelli, 2003; Behncke et al., 2006; Civile et al., 2010). The main anomalies associated with the substantial magmatic bodies are located near a boundary fault of the southwestern Pantelleria Graben (Lodolo et al., 2012). In Figs. 6. 13 and 6.14, it also seems that boundary faults have played a significant role in determining the distribution of volcanic activity, likely by providing passways for magma along the major fault planes. The volcanic activity observed in the Sicily Channel including the Pantelleria Graben exhibits petrological characteristics consistent with orogenic magmatism, resembling the type of magmatism found in continental rift zones (Corti et al., 2006).

6.6. Conclusion

Through the seismo-stratigraphic interpretation of seismic lines (CS89-01 and Pant-3) intersecting each other at the southwestern limit of the Pantelleria graben, a detailed tectono-stratigraphic framework of the area has been performed. The results are summarised below;

- Mass flow deposits were recognized at the SW margin of the Pantelleria graben linked to the erosion process that possibly deposited the Plio-Quaternary sediments in the structural relief (SR) adjacent to the Pantelleria Graben.

- The observation of the reflection geometry and their termination pattern gave clues to the presence of syn-rift deposits in the area deposited during the main rifting event that led to the formation of Pantelleria Graben coeval to the Linosa and Malta grabens formation.
- An additional insight into the inversion tectonics has been provided in the SR present in the southern limit of the Pantelleria Graben by observing the folded structures in the Upper Plio-Quaternary deposits.
- The interpretation of the considered seismic profiles combined with the gravity and surface heat flow anomaly data reveals the variable trends in the Sicily Channel including the Pantelleria Graben.
- The main positive Bouguer anomaly (+89 mGal), and the main negative Free Air anomaly (-15 mGal) together with high values (103 mWm^{-2}) of heat flow have been detected in the Pantelleria Graben.
- The crustal thinning is evidenced by the shallow Moho depth of 20 km beneath the graben. These anomalies have been produced by the volcanic bodies that have emplaced in the graben during rifting in the Sicily Channel.

Chapter 7

Preliminary investigation of other foreland area and orogenic wedge in the Adriatic Sea: the Quaternary faults in Puglia and Marche- Abruzzo regions (METIQ project for INQUA map)

7.1. Brief Introduction to METIQ project and Contribution

The Modello Evolutivo del Territorio Italiano nel Quaternario (METIQ) project aims to construct a robust Quaternary evolutionary model of Italian territory in terms of a GIS database which includes earthquake catalogues, capable faults and landslides inventories, active volcanoes, landslides etc. The model is developed using a cartographic database derived from available scientific and cartographic data, accessible to everyone via WebGIS. More than 150 people from academic and research institutions have been involved in this project. The preliminary map was named as 'Quaternary Map of Italy' at scale of 1:500.000 was printed for the XXI INQUA Congress, Roma 2023. Figs. 7.1 and 7.2 respectively represent sheets 1 and 3 the preliminary version of the map which includes the Quaternary information about Puglia and Marche-Abruzzo regions.

We have contributed to the sector of tectonics in the area of Adriatic sector and Apulo-Garganic foreland and Bradanic trough. We have reviewed the faults present in the above section (sheet 3) in the frame of kinematics, geometry, timing and surface evidence. The presence of these faults was also re-checked considering the previous maps and literature. We have added the significant Quaternary fault systems in the METIQ database which fall in the Puglia-Marche-Abruzzo regions (e.g., a portion of the Apennine frontal thrust portion, Casoli faults, Jesi-Nereto-Zaccheo front (JNZ) and Conero-Campomare-Tortoreto Front (CT) which will be included in the new version of METIQ Quaternary map. (for detail of the faults see section 7.3).

7.2. Geology and study area

The Central Mediterranean was influenced by the collision between Africa and Eurasia (Faccenna et al., 2001; Carminati et al., 2004; Parotto and Praturlon, 2004; Carminati and Doglioni, 2005; Polonia et al., 2012; Mila et al., 2017; Jolivet et al., 2021). Since Neogene, the

Apennine chain resulted in this geodynamic context (Patacca and Scandone, 1989; Cosentino et al., 2010; Guerrera et al., 2014; Mantovani et al., 2019; Turco et al., 2021). The chain stretches to mainland Italy in the NW-SE direction along the Apennine fold-thrust belt which is convex towards the Adriatic foreland. The shortening along the Apennines varies owing to the inherited Mesozoic paleogeography and contrasting rheology of the Adria plate. The occurrence of several tectonic phases led this belt to reach its current position following the foreland ward advancement of the thrust sheets (Molli et al., 2018; Turco et al., 2021). The structure of the chain is influenced by transverse discontinuities and thrust faults, which facilitate thin-skinned rotations and lead to variations in structural trends. The major transverse discontinuities are located across the Central Apennines (Cassano et al., 2001; Bernardelli et al., 2005; Cosentino et al., 2010; Satolli et al., 2014; Bonini et al., 2015; Lanari et al., 2023). During the Miocene-Pleistocene, the intense shortening of the paleogeographic domains of the Africa-Adria continental margin took place due to the eastward progression of deformation. After the flexural retreat of the subducting Adria lithosphere, the foreland basins showed an eastward movement. The orogenic system followed the NE migration, and the inner domains were affected by the extensional tectonics linked to Late Pliocene–Pleistocene differential regional uplift (Faccenna et al., 2001; Patacca and Scandone, 2004; Della Seta et al., 2004). Simultaneously, NE-verging thrusting in the southern Apennines extensional collapse behind the advancing thrust fronts led to the formation of the Tyrrhenian Basin (Boccaletti et al., 1990; Patacca et al., 1990; Roure et al., 1991; Nicolosi et al., 2006). Both these processes are linked to the rollback of the west-dipping Apulian-Ionian slab (Royden, 1993; Faccenna et al., 2001). The uplifted blocks were developed by the normal dip-slip faults by the displacement of the previous geological structures (Dramis, 1993; Della Seta et al., 2004). The same faulting and regional differential uplift led to the emergence of central Adriatic Piedmont. The evidence of

these processes is found in the Puglia-Marche-Abruzzo sector, off the outermost ridges of the Apennines (Centamore et al., 1996; Miccadei et al., 2013; Delchiaro et al., 2024).

The Puglia-Marche-Abruzzo sector belongs to the Adriatic foothills, which is limited to the east by the Adriatic Sea and to the west by the Apennine chain. The evidence of Quaternary tectonic deformation is preserved in the surface-exposed geomorphological features in this tectonically active portion of the region (Figs. 7.1-7.4) (Currado and Fredi, 2000; Della Seta et al., 2008). These regions are characterized by a complex geological–structural setting as testified by deep-seated buried thrust structures from the geophysical data (Calamita et al.,1994; Bigi et al., 1999; Artoni et al., 2013; Molli et al., 2018).

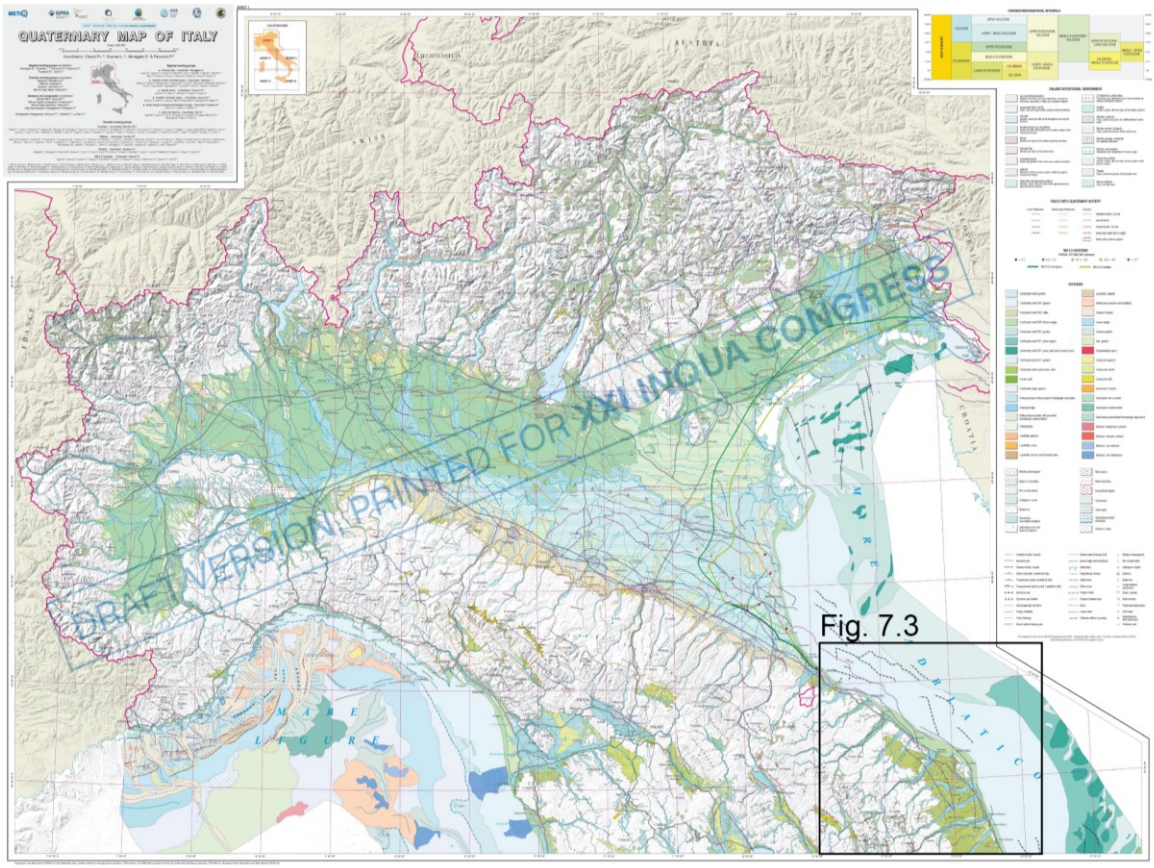

Fig. 7.1. Sheet 1 of the preliminary version of 'Quaternary Map of Italy' at the scale of 1:500.000 (Metiq | Portale del Servizio Geologico d'Italia) was printed for the XXI INQUA Congress, Roma 2023. It displays the Quaternary information of Adriatic regions including faults in the Puglia and Marche-Abruzzo regions.

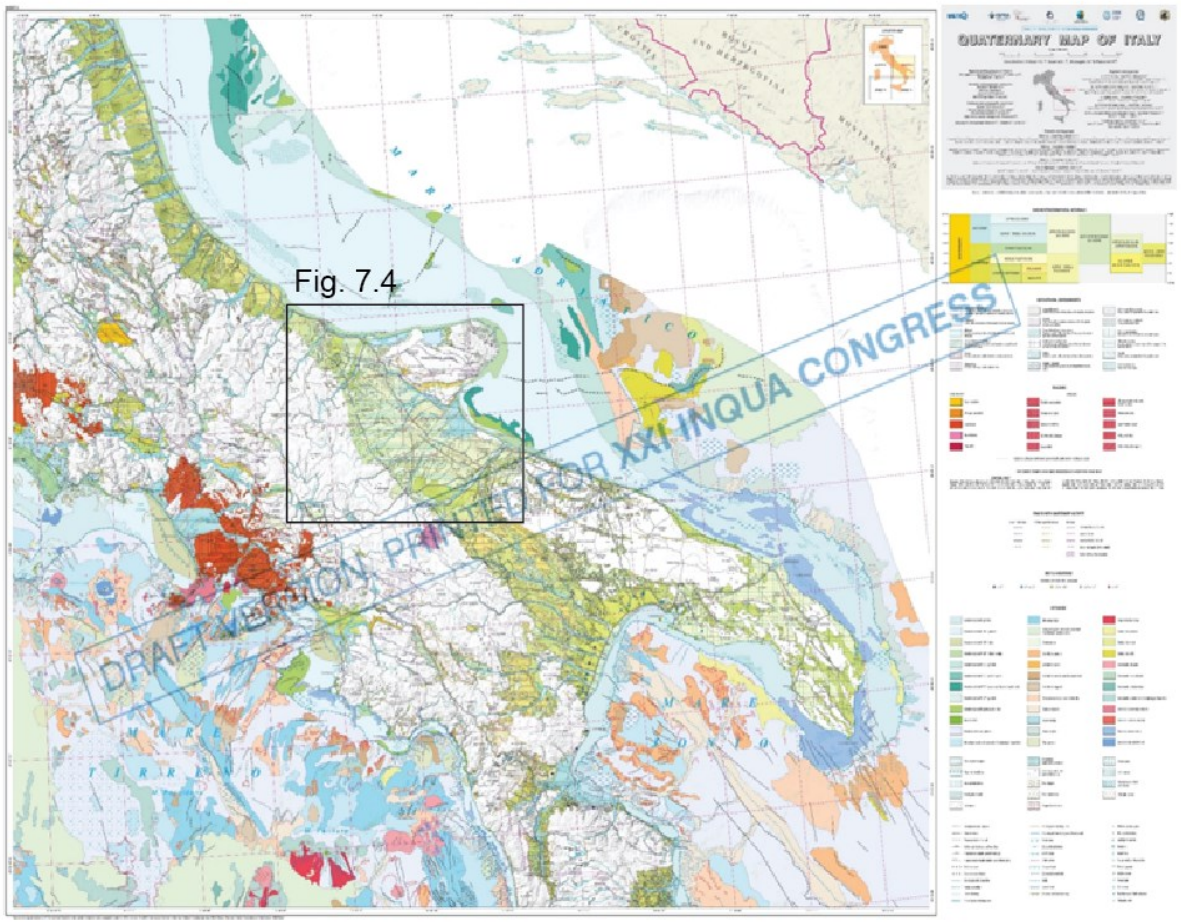

Fig. 7.2. Sheet 3 of the preliminary version of 'Quaternary Map of Italy' at the scale of 1:500.000 (Metiq | Portale del Servizio Geologico d'Italia) was printed for the XXI INQUA Congress, Roma 2023. It displays the Quaternary information of Adriatic regions including faults in the Puglia and Marche-Abruzzo regions.

The Apulian region is characterized by thick crust and autochthonous sedimentary strata which is weakly deformed (Calcagnile and Panza, 1981; Carminati et al., 2010; Petrullo et al., 2017). The region is referred to as the Apulian foreland as it forms the Plio-Pleistocene foreland of the Southern Appenines orogenic wedge (de Alteriis, 1995; Pieri et al., 1997; Fantoni and Franciosi, 2010; De Santis et al., 2023). This foreland is WNW trending antiform obliquely positioned with respect to the Southern Appennines subduction hinge (Biju-Duval et al., 1979; Pieri et al., 1997).

7.3. Quaternary fault systems in the region

The NE-verging fold-and-thrust belt referred as Southern Apennines Frontal Thrust is a part of the central Mediterranean orogenic belt consisting of a pile of thrust-nappes formed by Late Cretaceous-Quaternary convergence between African and Eurasiaan plates (Rosenbaum et al., 2002; Stampfli, 2005; D'Agostino et al., 2008; Turco et al., 2021).

The continuous thrusting and stacking of the thrust sheets over the Apulian Foreland gave birth to the Southern Apennines accretionary wedge (Cello et al., 2000; Mazzoli et al., 2001; Fantoni and Franciosi, 2010; Cicala et al., 2021). The belt consists of tectonic units stacked during Paleogene-Neogene times and overthrust the carbonate platform of the Apulian block. The significant thrust front of the Marche fold and thrust belt runs parallel to the Adriatic coast to the north of Pescara which is tens of km distant from foreland peripheral bulge (Ghisetti and Vezzani, 1998). The Jesi-Nereto-Zaccheo front (JNZ) and Conero-Campomare-Tortoreto front (CT) represent the NNW-SSE trending thrust stacks that extend along the Marche-Abruzzo regions Artoni, 1993; Calamita et al.,1994; Bigi et al., 1999; Artoni and Casero, 1997; Artoni 2007, 2013). These thrust stacks whose tectonic activity stopped in the Middle Pleistocene have formed the imbricate thrust fans of variable sizes and created folds of few hundred meters at the end of major thrust front (Artoni, 2013).

The extensional faults that came into existence by the rollback of the Adria subducting lithosphere influenced the internal portion of the fold-thrust belt. These extensional faults while migrating from the western to the eastern sector of the Orogen dissected the Apennines (Patacca et al. 1990; Amato & Montone 1997). The coastal and intermontane basins came into existence through the interplay of crustal extension connected to the opening of the Tyrrhenian Sea. These basins are controlled by the high and oblique normal faults which show the crosscut relation with the preexisting Appenine frontal thrust (Hippolyte et al. 1994; Ferranti & Oldow 1999).

However, there are also normal faults formed on the foreland ahead of the advancing thrust front. These faults are commonly linked to the pull of the subducting plate or flexure in the foreland due to the load caused by thrust advancement or extension in the hinge zone of the forebulge of the downgoing plate (Royden 1993; Doglioni 1995). These processes may have occurred simultaneously and developed higher amounts of extensional strain (Casciello et al., 2013).

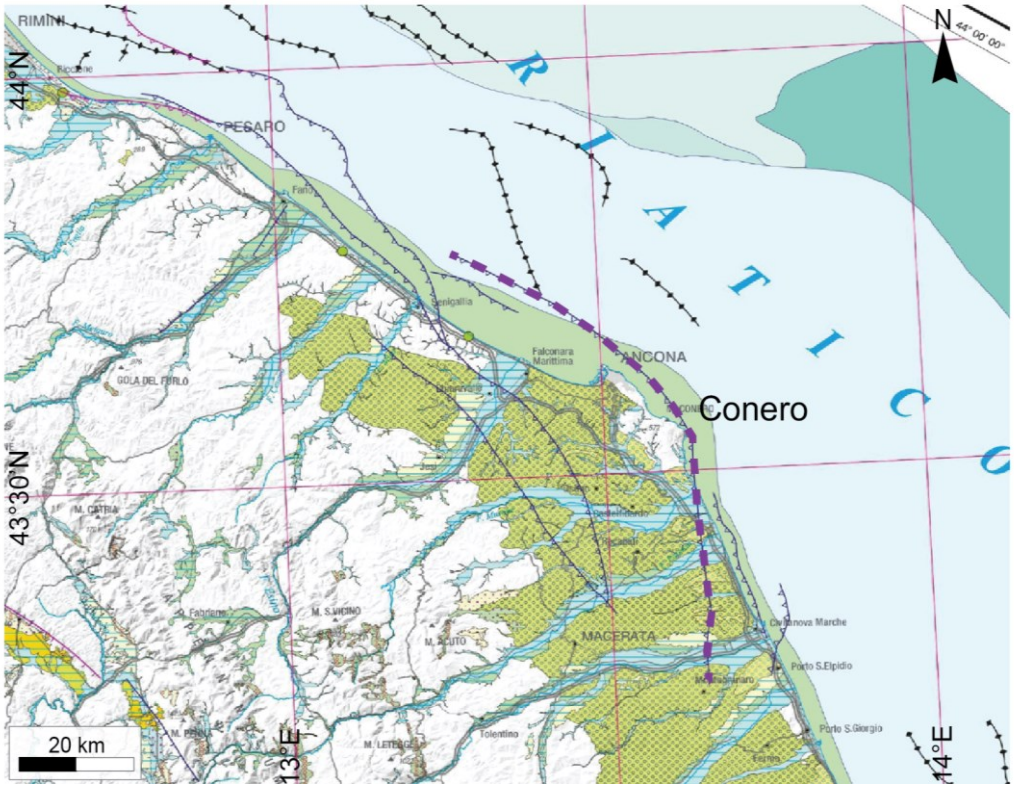

Fig. 7.3. Magnified view of the Abruzzo-Marche regions (from Fig. 7.1) highlighting the Quaternary faults in the area.

Since the Middle Pleistocene, active normal faults have developed in the central belt, including key seismogenic structures. In the Apulian foreland, both the outcropping and submerged Quaternary normal faults have been found in the Ofanto Graben, north of Gargano and in the Apulian Swell both onland and offshore (Basso et al., 2020; Chizzini et al., 2022; Ciaranfi et al., 1983; Cigala et al., 2021; Ridente et al., 2006; Scisciani, 2009; Maesano et al., 2020). The foreland features the faulted blocks to the Bradanic basin in the WSW direction which is

adjacent to the Apennine frontal thrust and towards the Adriatic Sea to ESE (Carissimo et al., 1963; Ricchetti, 1980). Main normal faults are sealed under the thick Plio-Pleistocene sediments in the Ofanto Graben. The evidence of the Plio-Pleistocene activity of the faults have been documented near the Ofanto line which exists near the Murge side of the graben (Figs.7.2, 7.4) (Iannone and Pieri, 1982). The 'Ofanto Line' represents the significant normal fault that is orthogonal to the Appenine frontal thrust. Another prominent normal fault line flanking the Ofanto graben is 'Line of Cervaro' which is also orthogonal to the thrust front and shows the crosscut relation with the front. Middle to Late Pleistocene tectonic activity of the normal faults has been documented in marine terraced deposits of Northern Murge (Figs. 7.2, 7.4) (Iannone and Pieri, 1980; Pieri et al., 1997). In Bradano Basin many normal faults dissect the foreland ramp and are sealed by Quaternary deposits (Pieri et al., 1994, 1996).

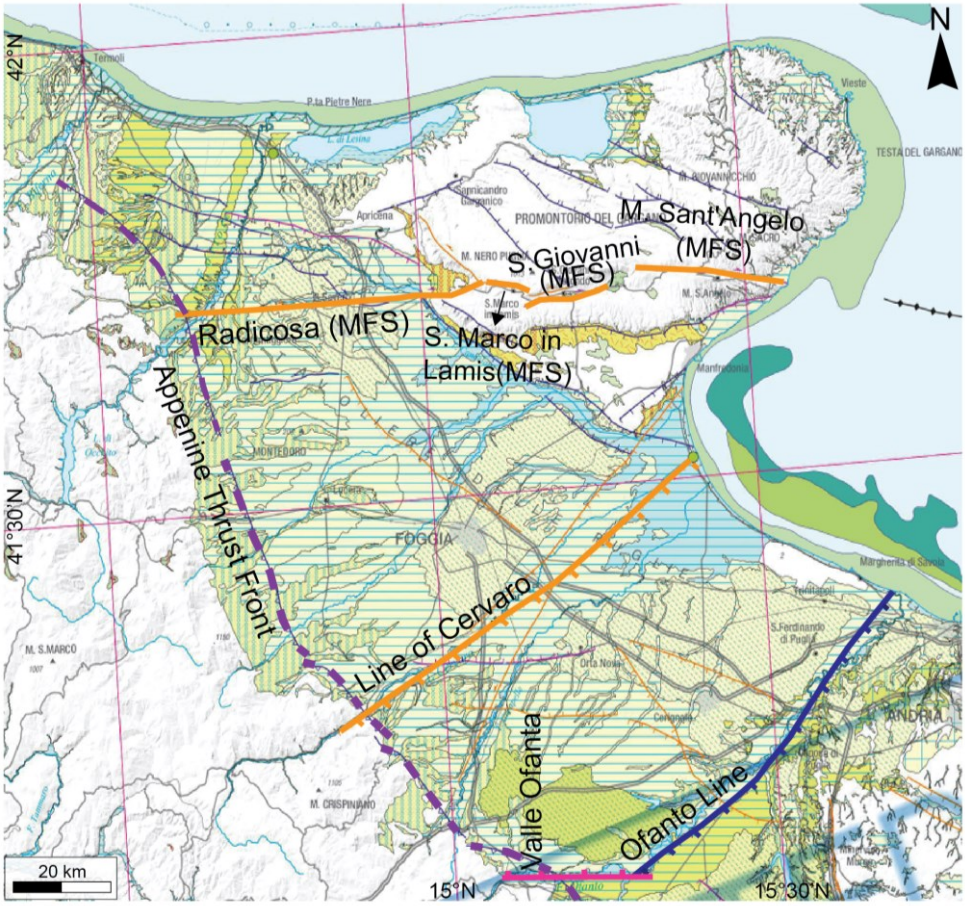

Fig. 7.4. Magnified view of the Apulian foreland (from Fig. 7.2) highlighting the Quaternary faults in the area discussed in this chapter. MFS: Mattinata Fault System.

Cessation of thrusting in the Southern Apennines occurred during the Late Pliocene to Early Pleistocene (Patacca et al. 1990; Piedilato et al., 2005; Mazzoli et al., 2015). Later the strike-slip deformation occurred in the Pleistocene when the architecture of the orogenic wedge started to be modified. The reactivation of existing brittle discontinuities in the Apulian Platform beneath the fold-and-thrust belt likely caused the strike-slip faulting (Bonini and Sani, 2000a).

The Gargano region is a prominent seismic region in the Apulian foreland where the two main E-W trending Quaternary strike-slip fault systems exist; Tremiti Fault System (TFS) and Mattinata Fault Systems (MFS) which are the right lateral strike-slip segments capable of producing earthquakes of high intensity (Postpischl, 1985; Doglioni et al., 1996; Piccardi, 1998).

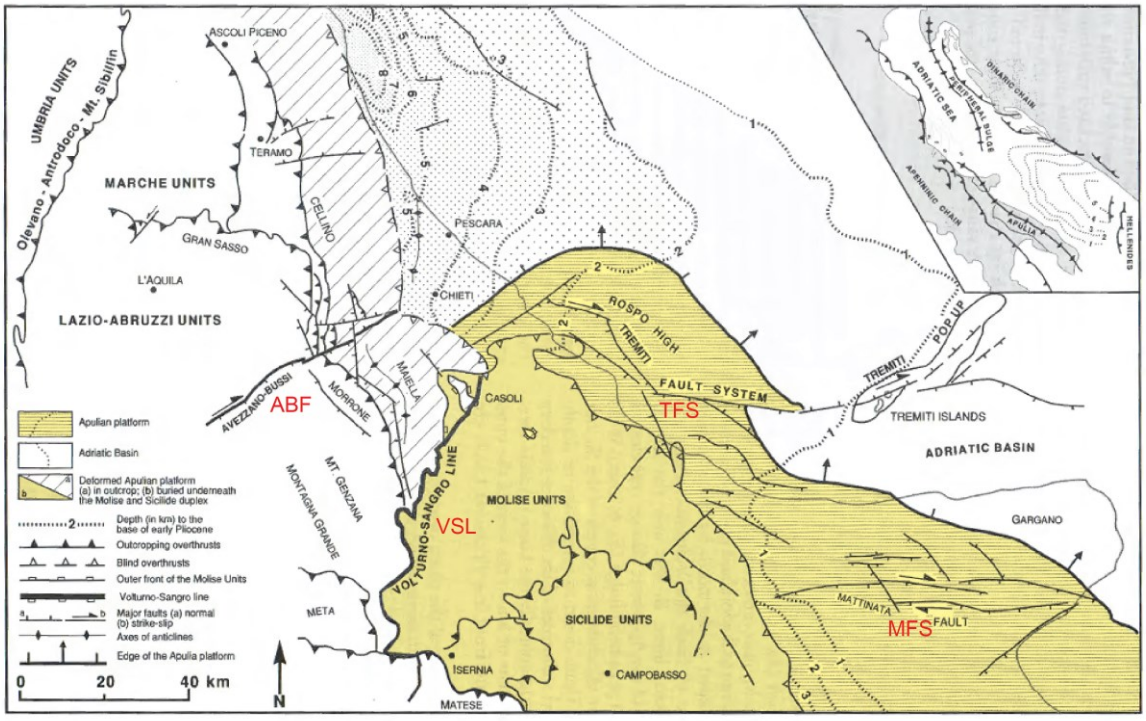

Fig. 7.5. Structural features of Adriatic-Apulia foreland domain (after Ghisetti and Vezzani, 1998). ABF: Avezzano-Bussi Fault; VSL: Volturno-Sangro Line; TFS: Tremiti Fault System; MFS: Mattinata Fault System.

The TFS has accommodated the eastward roll-back of the Apulia-Adriatic plate. The MFS is a spectacular system that stretches 60 km on land and cuts through the Gargano massif. The Radicosa structure of MFS is close to the orogenic wedge and orthogonal to it. (Figs. 7.2, 7.4). The WSW verging Avezzano-Bussi Fault (ABF) and roughly N-S trending Volturno-Sangro Line (VSL) have truncated the Central Apennines (Fig. 7.5). The ABF is a right-lateral strike-slip fault with vertical offsets ~1km. The Lazio-Abruzzi units to the North of AB are linked to the emplacement of the curved Gran Sasso-Mt. Picca thrust front which has folded them (Ghisetti and Vezzani, 1997). This front is crosscut by WNW-ESE to NNW-SSE, trending normal faults that are flanking the Quaternary basins. The VSL is a network of N-S-oriented normal, thrust, and strike-slip faults that mark the boundary between Lazio-Abruzzi and the Maiella units, to the west, from the Sicilide and Molise units, to the east (Fig. 7.5).

7.4. Brief Conclusion and hints for the comparison with the Sicily Channel

Some of the normal faults (Line of Cervaro, Ofanto Line, Valle Ofanto) and Radicosa strike slip fault in the foreland areas are orthogonal to the fronts of the Appenine orogenic system and some them, like the Line of Cervaro, Valle Ofanto and Radicosa crosscuts the orogenic wedge and thus highlight the interaction with Apennine Frontal Thrust.

This scenario is similar to the interaction between the extensional faults of the Sicily Channel foreland area and the associated orogenic wedge. Ahead of this orogenic wedge are found the inversion structures in the sedimentary fill of the Plio-Quaternary basins (Bartole et al., 1991; Boccaletti et al., 1992; McClay and Buchanan, 1992; Gamberi and Argnani 1995; Sulli 2000). The inversion structures have been formed by the compressive forces transmitted by the adjacent thrust structures (Giunta et al., 2000, Nigro and Renda, 2005; Cuffaro et al., 2024). The regions ahead of the Appenine orogenic wedge interacting with the foreland normal faults

may also have developed the inversion structures in the Plio-Quaternary basins as in the Sicilian orogenic wedge and as shown in the offshore Apulian Swell (Chizzini et al., 2022).

The Strike-slip deformation hit the region in the Pleistocene and there exist active strike-slip fault systems in the Apulian foreland. This strike-slip deformation may have inverted the pre-existing normal faults in the region just like in the Sicily Channel where the transpressional tectonics has caused the inversion in the center of the Sicily Channel /Capo Granitola Sciacca fault zone.

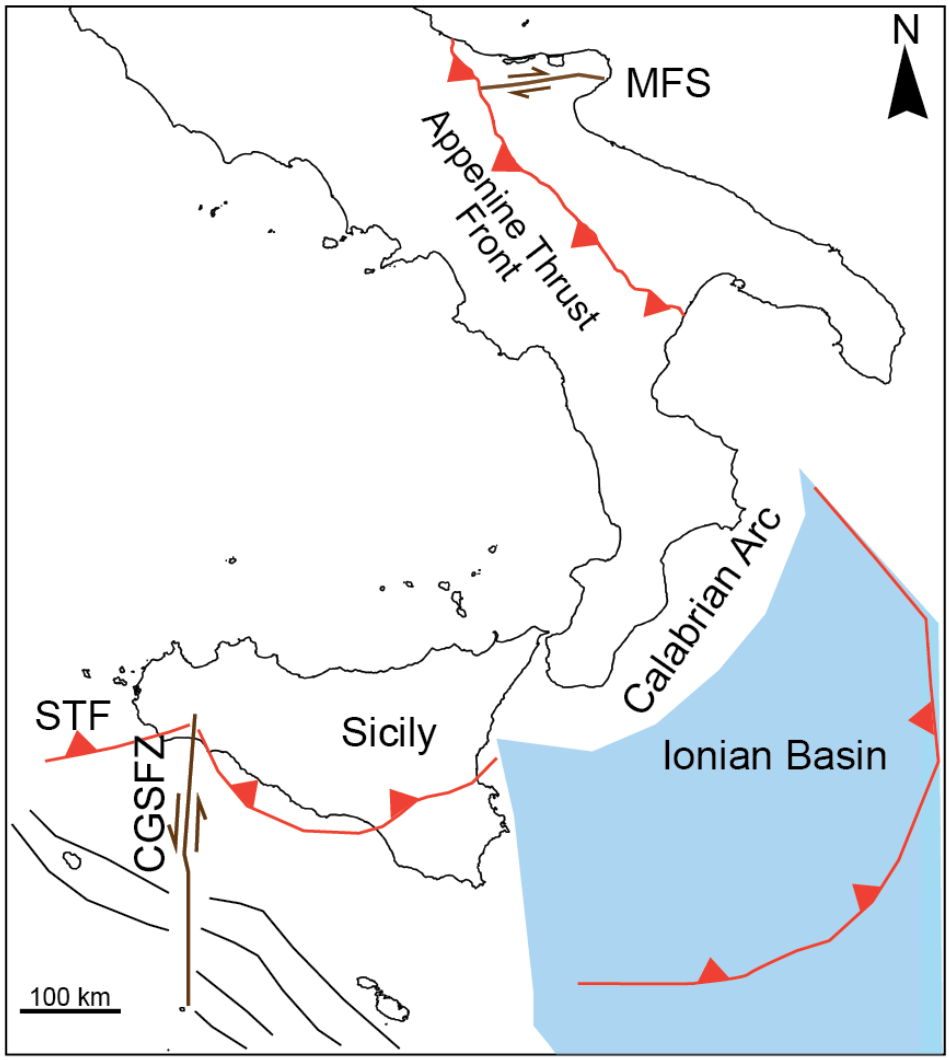

Fig.7.6. Sketch illustrating the similar interaction of Mattinata Fault System (MFS) with the Apennine orogenic wedge in the Apulian foreland and Capo Granitola Sciacca Fault Zone (CGSFZ) with Sicily orogenic wedge in the Sicilian foreland. STF: Sicilian Thrust Front.

The MFS and the CGSFZ (with right lateral and left lateral slips respectively) share several critical similarities that underscore their importance in the Mediterranean geodynamic landscape (Fig. 7.6). The MFS contributes to historical seismic risk assessments and limited current activity in the Apulian foreland, while the CGSFZ shear zone represents the most active tectonic domain showing the dynamic interplay between tectonic activity and volcanic processes, with ongoing deformation in the Sicilian foreland (Postpischl, 1985; Doglioni et al., 1996; Piccardi, 1998; Argnani et al., 2009; Civile et al., 2018; Palano et al., 2020). Both fault zones have preserved the evidence of reactivation under various tectonic regimes with CGSFZ dominated by positive flower structures (Cavallaro et al., 2017; Civile et al., 2021; Maiorana et al., 2023).

Chapter 8

Discussion and Conclusion

The collision between the different plates generate various structural fabrics/features and determines the geodynamic complexity of any region (Roeder, 1979; Royden, 1993; Sokoutis et al., 2005; Niu et al., 2013). Globally the plate interactions at convergent margins featuring a variety of structural and stratigraphic contexts (Roeder, 1979) are well illustrated by Southeast Asia, a region of rapid Neogene transitions in plate interactions and hosts several small oceanic basins and subduction zones (Hamilton, 1979; Lai et al., 2021; Authemayou et al., 2022). For example, the Lower plate in the North Philippines is changing polarity from East to West (Hamilton, 1979; Uyeda and McCabe, 1983). The Australian continental passive margin wedge underthrusts below the Sunda-Banda arc in the Tolo Trough in the Indonesian Archipeleago, showcasing continuous subduction initiation in areas like the Northern Banda Sea and Australia (Hall, 2019; Authemayou et al., 2022; Husson et al., 2022). Another example is of South of Taiwan; the accretionary wedge is documented in Bashi Strait owing to the cause of incipient collision between the Philippine Sea Plate, the Chinese continental margin of the Eurasian Plate (Lee et al., 2006; Eakin et al., 2014).

These complexities are also evidenced in the collision between the African and Eurasiaan plates and some smaller microplates, including the Adria plate, which are involved in the genesis of the Central Mediterranean orogenic belts (Apennines Maghrebides, and the Dinarides–Hellenides) (Gueguen et al., 1998; Carminati and Doglioni, 2005; Mila et al., 2017; Royden and Faccenna, 2018; Maesano et al., 2020; Jolivet et al., 2021). The northwestward-directed Africa/Adria subducting continental lithosphere forming the Apenninic-Maghrebide orogenic wedge is characterized by a widely developed back-arc basin and deep foredeep (Gueguen et al., 1998; Carminati and Doglioni, 2005). The typical thrust belt geometries associated with them and the existence of the extensional basins (Algerian, and Tyrrhenian basins) superimposed on top of these orogens formed during the flexure of the underthrusting lower plate (Channell et al., 1979; Jolivet et al., 1999; Carminati and Doglioni, 2005; Bouyahiaoui et

al., 2015). Carpathian and the Pyrenees orogenic subductions and collions are very similar to Central Mediterranean geodynamics (Carminati and Doglioni, 2005).

In the Western and Central Mediterranean, the southward roll-back of the African/Adriatic lower plate occurred during the collision of Eurasiaan and African plates which was responsible for opening of the Tyrrhenian back-arc basin on the overriding plate (Fabbri et al., 1981; Kastens et al., 1988; Faccenna et al., 2001a, 2001b; Corti et al., 2006) and simultaneously the rifting in the Sicily Channel initiated since Lower Pliocene (Reuther and Eisbacher, 1985; Boccaletti et al., 1987; Cello, 1987; Argnani, 1990). This rifting phase is also linked to the south-westwards migration of Africa in relation to Sicily (Civile et al., 2010, 2021).

The same colliding plates viz Africa, Adria, and Eurasia formed the Sicilian Maghrebian orogen and the Sicily Channel; the latter being the lower plate and foreland of this orogenic system (Argnani, 1990; Dewey et al., 1989; Rosenbaum et al., 2002). During the advancement of the Apennines–Maghrebides orogenic wedge the lithosphere extension was active in this lower plate and thus the two tectonic settings (extensional and compressional) interacted (Finetti, 1984; Corte et al., 2006; Civile et al., 2010; Civile et al., 2021; Sulli et al., 2021; Maiorana et al., 2023): the extensional areas were affected by advancing thrusts thus leading to the inversion where thrusts intersect normal faults and vice versa (Corte et al., 2006).

This thesis describes the behavior of the northern continental margin of the subducting African plate (Sicily Channel) impacted by different deformation phases with some examples from the Adriatic Sea in the Marche, Abruzzo and Puglia regions of Italy. The intricate relation of the two tectonic settings ahead of the Apennines–Maghrebides orogenic system has been documented. The analysis was performed with the aid of subsurface data (seismic reflection

profiles and well logs) and the satellite gravity and heat flow data which was complemented by high-resolution bathymetric data across the focused region.

It has been shown that the deformation intensity and style vary from SE to NW in this part of the lower plate, as it is the home to the Neogene-Quaternary foreland, foredeep, and chain system including, the Pelagian foreland, Gela foredeep basin and Maghrebian chain (Fig. 1.1a). The Pelagian foreland resulted to be fragmented by 1) the NW-oriented SCRZ in its central part, 2) the NNE trending lithospheric separation zone (CGSFZ) making its way from Capo Granitola and Sciacca to Linosa Island (Fedorick et al., 2018; Ferranti et al., 2019; Civile et al., 2021) and 3) the lithospheric-scale discontinuity (SRFS) stretching from southeast mainland Sicily to the SCRZ (Gardiner et al., 1995; Pellegrino et al., 2016). The latter two discontinuities have played a significant role in the kinematic decoupling along the first one (SCRZ) especially along its eastern portions (Civile et al., 2021; Maiorana et al., 2023).

The CGSFZ was affected by transpressional tectonics and is characterized by positive flower and positive inversion structures (Civile et al., 2008; Ghisetti et al., 2009; Civile et al., 2014; Calò and Parisi, 2014; Fedorik et al., 2018) (Fig. 6.12). In this thesis work, it has been shown that the influence of these tectonic features is not limited to the known mapped positions. Inversion structure has reached outside the domain of CGSFZ and affected the southern limit of the Pantelleria Graben by the reactivation of Messinian early Pliocene normal faults since the Pleistocene time.

The SCRZ is the result of the extensional tectonics caused by the extensional stress accumulated at the shallow depth in the hinge zone of the forebulge characterizing the down-bending plate. But at the same time, the mantle convection developed during the slab pull forces and roll-back of the African slab beneath the Tyrrhenian Basin (Argnani, 1990, 2009; Govers and Wortel, 2005; Rosenbaum et al., 2008; Argnani, 2009; Arab et al., 2020; Maiorana et al.,

2023) has promoted extension during Plio-Quaternary which was coupled with volcanic activity. Evidence of volcanic activity are found mainly in the Pantelleria and Linosa islands and the adjacent grabens. The southernmost portion of the Sicily Channel features a pure and continuous extensional regime. The existence of extensive magmatic intrusions is ascribed to a substantial uplift of the Moho depth to shallow levels beneath graben. The existence of several extensive volcanic zones and magmatic intrusion, most of them linked to a Moho rising at relatively shallow depths. The combined behavior of geophysical characters (gravity anomaly) heat flow anomalies and the shallow Moho depths in the Pantelleria Graben are indicative of the volcanism in this graben. The intrusion of magmas and the consequently high heat flow and anomalous behavior of gravimetric data are the factors that can enhance a significant intra-plate deformation in this area.

The extensional stresses nucleated at the forebulge hinge zone have migrated with time towards the NW of the Sicily Channel and crosscut the orogenic wedge which was acting as a load on the bending lower plate during Tortonian-Messinian. The typical compressional tectonics still dominates the NW portion of the Channel, represented by ESE verging ETF which features a clear intersection with the normal fault aligned and likely propagated from the SCRZ. The influence of orogenic wedge deformation on these extensional features has given birth to inversion tectonics (dated Calabrian) that have impacted the sedimentary fill of the syn-rift basins crosscutting the top of the orogenic wedge. The subduction zone highlights successive locking and unlocking between lower and upper plates (Bott et al., 1989). Due to this, the plate interior has experienced significant variations in stress which helps the compressive pulses to impact the areas that have been affected by extension (Gamberi and Argnani, 1995). The recent compressional pulses in the area can be linked to the switch in the regional stress field or the change in the subduction polarity of the African plate as suggested in previous works for the

North of Sicily (Zitellini et al., 2021; Sulli et al.; 2021) and for the SCRZ (Maiorana et al.; 2023). The role of transpression causing the above inversion is still to be defined.

There are other examples in the Central Mediterranean where the foreland areas under extension have experienced compressional/tranpressional pulses. We reviewed the reported literature with a focus on the Quaternary faults of the Puglia-Marche-Abruzzo sector which is a part of the Adriatic foothills, bounded by the Adriatic Sea and the Apennine chain. This sector ahead of the Appenine orogenic wedge features the interaction of normal faults and the strike-slip faults with the orogenic wedge which may also have developed the inversion structures in the Plio-Quaternary basins.

Thus, the coexistence and the complexity of both extensional and compressional/tranpressional tectonic settings is preserved in the areas adjacent to the orogenic wedges as confirmed by the case study of the Sicily Channel Adriatic region (described in chapter 7). The Sicily Channel serves as a natural laboratory, revealing that foreland regions can preserve the record of dynamic processes controlling lithosphere deformation and are drawn to tectonic inversion.

Considering the observations in the Sicily Channel, the major conclusions that come out from this thesis are as follows.

Incipient collisional chains and area close to the outer fronts of the collisional orogenic wedges show complexity in the tectono-stratigraphic framework. The migration of extensional stresses, the location of the hinge zone more towards the orogenic wedge act as a load on the bending lower plate. Due to this migration, the confluence of the opposing extensional and compressional tectonic regimes occurs giving rise to the structural and stratigraphic complexities and multiple phases of inversion mainly positive but locally negative inversion. Thus, compressive deformations extend far beyond the major orogenic fronts and affect the

vast regions of the subducting lower plate which otherwise have been under extension due to its bending. In both foreland area investigated, the role of evolving transcurrent system that might cause inversions is still to be clarified.

The interplay between early structural phase, compressive stress fields and rheological properties of the lower plate plays a crucial role in determining the tectonic architecture of a region. Compressive stresses, determined by the direction and intensity of tectonic forces, control the orientation and magnitude of deformation. During the bending, the slab pull and roll back comes into action which provides a way for the volcanic activity. This thesis confirms the presence of gigantic volcanic bodies and change in of the lithospheric thickness with the migration of extensional stress to the orogenic wedge even crosscutting orthogonally the orogenic wedge.

By the prelimiar comparison of the Sicily Channel Rifting Zone and Adriatic foreland, it appears that the faster retreating Ionian slab in between these two zones might have influenced from far distance the major trascurrent fault systems (MFS and CGFSZ) and inversion structures as well (Fig. 7.6).

This work shows that in collisional orogen, the lower plate and the foreland areas in it does not behave as stable, weakly and passively deformed regions as usually they are categorized. Instead, the lower plate and foreland area are actively deforming, and they alternate phases in which they are part of the orogenic wedge (upper and lower plate coupled/locked) to phases in which they reshape the orogenic wedge (upper and lower plate decoupled/unlocked).

References

- Abbas, A., Zhu, H., Zeng, Z. and Zhou, X., 2018. Sedimentary facies analysis using sequence stratigraphy and seismic sedimentology in the paleogene Pinghu Formation, Xihu depression, east China sea shelf basin. Marine and Petroleum Geology, 93, pp.287-297.
- Adam J, Reuther CD, Grasso M, Torelli L. 2000. Active fault kinematics and crustal stresses along the Ionian margin of southeastern Sicily. Tectonophysics 326(3-4): 217–239.
- Agustina, I., Nasir., F and Setiawan, A., 2017. The Implementation of Image Smoothing To Reduce Noise Using Gaussian Filter. Int. J. of Comput. Appl. 177 (5), 15-19. https://doi.org/10.5120/IJCA2017915755.
- Aksu AE, Hall J, Calon TJ, Barnes MC, Güneş P, Cranshaw JC. 2018. Messinian evaporites across the Anaximander mountains, Sırrı Erinç Plateau and the Rhodes and Finike basins, eastern Mediterranean Sea. Marine Geology 395: 48–64.
- Albinhassan, N., Luo, Y and Al-Faraj, M., 2006. 3D edge-preserving smoothing and applications. Geophys. 71 (4), 5-11. https://doi.org/10.1190/1.2213050.
- Allen PA, Allen JR. 1990. Basin Analysis, Principles & Application. Blackwell Scientific Publication, pp. 115–126.
- Allen PA, Homewood P, eds. 2009. Foreland basins. John Wiley & Sons.
- Allen, P.A. and Allen, J.R., 2013. Basin analysis: Principles and application to petroleum play assessment. John Wiley & Sons.
- Al-Masgari, A.A.S., Elsaadany, M., Latiff, A.A. and Imran, Q.S., 2021. A guideline for seismic sequence stratigraphy interpretation. J Eng Appl Sci, 16, pp.165-183.

- Al-Masgari, A.A.S., Elsaadany, M., Latiff, A.A. and Imran, Q.S., 2021. A guideline for seismic sequence stratigraphy interpretation. J Eng Appl Sci, 16, pp.165-183.

- Amato, A. and Montone, P., 1997. Present-day stress field and active tectonics in southern peninsular Italy. Geophysical Journal International, 130(2), pp.519-534.
- Amilibia Cabeza A, McClay KR, Sābat i Montserrat F, Muṇoz JA, Roca i Abella E. 2005. Analogue modelling of inverted oblique rift systems. Geologica Acta 3(3): 251–271.
- Anderson, H. and Jackson, J., 1987. Active tectonics of the Adriatic region. Geophysical Journal International, 91(3), pp.937-983.

— Anselmetti, F.S. and Eberli, G.P., 1993. Controls on sonic velocity in carbonates. Pure and Applied geophysics, 141, pp.287-323.
— Antonelli C. 1989. A failure-inducement model of research and development expenditure: Italian evidence from the early 1980s. Journal of Economic Behavior & Organization 12(2): 159–180.
— Antonelli M, Franciosi R, Querci A, Ronco G, Vezzanin F. 1988. Paleogeographic evolution and structural setting of the northern side of the Sicily Channel. In: Società Geologica Italiana, 74. Congresso Nazionale, Relazioni, pp. 79–86.
— Arab M, Maherssi C, Granjeon D, Roure F, Dverchere J, Cuilhe L, Hassaim M, Mouchot N, Doublet S, Khomi S. 2020. On the origin and consequences of crustal-scale extension between Africa and Sicily since Late Miocene: insights from the Kaboudia area, western Pelagian Sea. Tectonophysics 795: 228565.
— Argnani A, Bonazzi C. 2005. Malta Escarpment fault zone offshore eastern Sicily: Pliocene-Quaternary tectonic evolution based on new multichannel seismic data. Tectonics 24(4).
— Argnani A, Cornini S, Torelli L, Zitellini N. 1986. Neogene-Quaternary foredeep system in the Strait of Sicily. Mem. Soc. Geol. It. 36: 123–130.
— Argnani A. 1990. The Strait of Sicily rift zone: foreland deformation related to the evolution of a back-arc basin. Journal of Geodynamics 12(2-4): 311–331.
— Argnani A. 1993a. Neogene tectonics of the Strait of Sicily. In: Max MD, Colantoni P, eds. Geological development of the Sicilian-Tunisian Platform. UNESCO Report in Marine Science 58: 55–60.
— Argnani A. 1993b. Neogene basins in the Strait of Sicily (Central Mediterranean): tectonic settings and geodynamic implications. In: Boschi E et al., eds. Recent evolution and seismicity of the Mediterranean region. Kluwer Academic Publication, Dordrecht, pp. 173–187.
— Argnani A. 2018. Subduction evolution of the Dinarides and the Cretaceous orogeny in the Eastern Alps: Hints from a new paleotectonic interpretation. Tectonics 37(2): 621–635.
— Argnani, A., 1990. The Strait of Sicily rift zone: foreland deformation related to the evolution of a back-arc basin. Journal of Geodynamics, 12(2-4), pp.311-331.
— Argnani, A., 2009. Evolution of the southern Tyrrhenian slab tear and active tectonics along the western edge of the Tyrrhenian subducted slab. In: Van Hinsbergen, D.J.J.,

Edwards, M.A., Govers, R. (Eds.), Collision and the Collapse at the Africa-Arabia-Eurasia Subduction Zone. Geological Society London, Special Publication, 311, pp. 193–212.

— Argnani, A., Bortoluzzi, G., Favali, P., Frugoni, F., Gasperini, M., Ligi, M., Marani, M., Mattietti, G. and Mele, G., 1994. Foreland tectonics in the southern Adriatic Sea. Mem. Soc. Geol. It.

— Argnani, A., Cornini, S., Torelli, L. and Zitellini, N., 1987. Diachronous foredeep-system in the Neogene-Quaternary of the Strait of Sicily. Mem. Sot. Geol. Ital., 38: 407-417.

— Argnani, A., Cornini, S., Torelli, L. and Zitellini, N., 1988. Diachronous foredeep-system in the Neogene-Quaternary of the Strait of Sicily. Mem. Sot. Geol. Ital. 38, 407-417.

— Argnani, A., Favalli, P., Frugoni, F., Gasperini, M., Ligi, M., Marani, M., Mattietti, G. and Mele, G., 1993. Foreland deformational pattern in the Southern Adriatic Sea. Annals of Geophysics, 36(2).

— Argnani, A., Torelli, L., 2001. Pelagian Shelf and its graben system (Italy/ Tunisia). Mem. Mus. Natn. Hist. nat. 186, 529-544. https://eurekamag.com/research/020/265/020265291.php.

— Argnani, A.,1990. The strait of sicily rift zone: Foreland deformation related to the evolution of a back-arc basin. J. Geody. 12(2–4), 311–331. https://doi.org/10.1016/0264-3707(90)90028-S.

— Armstrong, P.A. and Chapman, D.S., 1998. Beyond surface heat flow: An example from a tectonically active sedimentary basin. Geology, 26(2), pp.183-186.

— Artoni, A. and Casero, P., 1997. Sequential balancing of growth structures, the late Tertiary example from the central Apennine. BULLETIN-SOCIETE GEOLOGIQUE DE FRANCE, 168, pp.35-50.

— Artoni, A., 1993. Modello sedimentario e di flessurazione di un tratto del margine adriatico in un settore dell'Appennino Centrale. Ph.D. thesis, Universita' di Parma.

— Artoni, A., 2007. Growth Rates and Two-mode Accretion in the Outer Orogenic Wedge-foreland Basin System of Central Apennine (Italy). In: Boll. Soc. Geol. It., vol. 126, pp. 531e556.

— Artoni, A., 2013. The Pliocene-Pleistocene stratigraphic and tectonic evolution of the Central sector of the Western Periadriatic Basin of Italy. Marine and Petroleum Geology, 42, pp.82-106.
— Artoni, A., Casero, P., 1997. Sequential balancing of growth structures, the late Tertiary example from the Central Apennine. Bull. Soc. Geol. France 168, 35e49.
— Ashcroft, W., 2011. A Petroleum Geologist's Guide to Seismic Reflection. Wiley-Blackwell, Oxford, 176 p.
— Ashcroft, W., 2011. A petroleum geologist's guide to seismic reflection. John Wiley & Sons.
— Authemayou, C., Pedoja, K., Chauveau, D., Husson, L., Brocard, G., Delcaillau, B., Perrot, J., Aribowo, S., Yudawati Cahyarini, S., Elliot, M., Hilman Natawidjaja, D., & Scholz, D. (2022). Deformation and uplift at the transition from oceanic to continental subduction, Sumba Island, Indonesia. Journal of Asian Earth Sciences, 236(June), 105316.
— Azubuike, I. M., Akpan, B. N., 2017. Spline Function as an Alternative Method to Seismic Data Analysis. Int. J. Stat. and Appl. 7(1), 36–42.
— Baes, M., Stern, R.J., Whattam, S., Gerya, T.V. and Sobolev, S.V., 2021. Plume-induced subduction initiation: Revisiting models and observations. Frontiers in Earth Science, 9, p.766604.
— Balázs, A., Faccenna, C., Gerya, T., Ueda, K. and Funiciello, F., 2022. The dynamics of forearc–back-arc basin subsidence: Numerical models and observations from Mediterranean subduction zones. Tectonics, 41(5), p.e2021TC007078.
— Balázs, A., Faccenna, C., Ueda, K., Funiciello, F., Boutoux, A., Blanc, E.J.P. and Gerya, T., 2021. Oblique subduction and mantle flow control on upper plate deformation: 3D geodynamic modeling. Earth and Planetary Science Letters, 569, p.117056.
— Balázs, A., Matenco, L., Magyar, I., Horváth, F. and Cloetingh, S.A.P.L., 2016. The link between tectonics and sedimentation in back-arc basins: New genetic constraints from the analysis of the Pannonian Basin. Tectonics, 35(6), pp.1526-1559.
— Bally, AW, 1984. Tectogenesis and seismic reflection. Bulletin of the Geological Society of France, 7 (2), pp.279-285.
— Bartole, R., Torelli, L., Mattei, G., Peis, D. and Brancolini, G., 1991. Stratigraphic-structural setting of the Northern Tyrrhenian Sea: state of the art. STUDI GEOLOGICI CAMERTI. NUOVA SERIE, 1, pp.115-130.

— Bashir, A., Ali, M., Patil, S., Aljawad, M. S., Mahmoud, M., Al-Shehri, D., Hoteit, H., & Kamal, M. S. 2024. Comprehensive review of CO_2 geological storage: Exploring principles, mechanisms, and prospects. Earth-Science Reviews, 249, 104672.
— Bassett, D. and Watts, A.B., 2015. Gravity anomalies, crustal structure, and seismicity at subduction zones: 1. Seafloor roughness and subducting relief. Geochemistry, Geophysics, Geosystems, 16(5), pp.1508-1540.
— Basso J, Artoni A, Torelli L, Polonia A, Carlini M, Gasperini L, Mussoni P. 2021. Oblique plate collision and orogenic translation of the Southern Apennines revealed by post-Messinian interregional unconformities in the Bradano Basin (Ionian Sea - Central Mediterranean). Marine and Petroleum Geology 128: 104999.
— Beccaluva L, Colantoni P, Di Girolamo P, Savelli C. 1981. Upper submarine volcanism in the Strait of Sicily (Banco Senza Nome). Bulletin of Volcanology 44: 573–581.
— Bêche, M., Kirkwood, D., Jardin, A., Desaulniers, E., Saucier, D., Roure, F., 2007. 2D Depth Seismic Imaging in the Gaspé Belt, a Structurally Complex Fold and Thrust Belt in the Northern Appalachians, Québec, Canada, In thrust Belts and Foreland Basins, pp. 75–90.
— Behncke, B., Falsaperla, S. and Pecora, E., 2009. Complex magma dynamics at Mount Etna revealed by seismic, thermal, and volcanological data. Journal of Geophysical Research: Solid Earth, 114(B3).
— Bellino, A., Garibaldi, L. and Godio, A., 2013. An automatic method for data processing of seismic data in tunneling. Journal of Applied Geophysics, 98, pp.243-253.
— Bello, M. and Merlini, S., 2000, October. Structual model of central eastern Sicily. In EAGE Conference on Geology and Petroleum Geology of the Mediterranean and Circum-Mediterranean Basins (pp. cp-109). European Association of Geoscientists & Engineers.
— Bellon H, Letouzey J. 1977. Volcanism related to plate tectonics in the western and eastern Mediterranean. In: Structural History of the Mediterranean Basins. Paris: Technip, pp. 165–184.
— Ben AD, Geletti R, Mocnik ARIANNA. 2010. Relation between recent tectonics and Mesozoic inherited structures of the central-southern Adria plate. Bollettino di Geofisica Teorica e Applicata 51(2-3): 99–115.
— Ben-Avraham, Z., Nur, A. and Giuseppe, C., 1987. Active transcurrent fault system along the north African passive margin. Tectonophysics, 141(1-3), pp.249-260.

— Béranger, K., Mortier, L., Gasparini, G.P., Gervasio, L., Astraldi, M. and Crépon, M., 2004. The dynamics of the Sicily Strait: a comprehensive study from observations and models. Deep Sea Research Part II: Topical Studies in Oceanography, 51(4-5), pp.411-440.
— Bernardelli, P., Cavalli, C., Longoni, R. and Giori, I., 2005. Gravity and magnetic fields of the Central Mediterranean region. CROP Deep Seismic Exploration of the Mediterranean Region, pp.57-67.
— Berra, F., Stucchi, E.M. and Moretti, S., 2019. New information from "old" seismic lines: an updated geological interpretation from the re-processing of the CROP line M-2A/I (Bonifacio Straits) at shallow depths. Italian Journal of Geosciences, 138(1), pp.31-42.
— Bertoni, C., Lofi, J., Micallef, A. and Moe, H., 2020. Seismic reflection methods in offshore groundwater research. Geosciences, 10(8), p.299.
— Bertotti, G., Picotti, V., Chilovi, C., Fantoni, R., Merlini, S. and Mosconi, A., 2001. Neogene to Quaternary sedimentary basins in the south Adriatic (Central Mediterranean): foredeeps and lithospheric buckling. Tectonics, 20(5), pp.771-787.
— Bigi, S., Calamita, F., Cello, G., Centamore, E., Deiana, G., Paltrinieri, W., Pierantoni, P.P., Ridolfi, M., 1999. Tectonics and sedimentation within a Messi nian foredeep in the Central Apennines, Italy. J. Pet. Geol. 22, 5e18.
— Biju-Duval, B., Borsetti, A.M., Colantoni, P., 1985. Geology of the troughs in the Strait of Messina-Tunisia, Pelagian Sea. Geologie des fosses du detroit siculo-tunisien (Mer Pelagienne). Revue - Institut Francais du Petrole. 40, 691-722.
— Biju-Duval, B., Letouzey, J. and Montadert, L., 1979. Variety of Margins and Deep Basins in the Mediterranean: Small Basin Margins.
— Biondi, B.L., 2006. 3D seismic imaging. Society of Exploration Geophysicists.
— Bishop, T.N., Bube, K.P., Cutler, R.T., Langan, R.T., Love, P.L., Resnick, J.R., Shuey, R.T., Spindler, D.A., Wyld, H.W., 1985. Tomographic determination of velocity and depth in laterally varying media. Geophysics 50, 903-923.
— Boccaletti M, Cello G, Tortorici L. 1987. Transtensional tectonics in the Sicily Channel. Journal of Structural Geology 9(7): 869–876.
— Boccaletti, M., Cello, G., Tortorici, L., 1987. Transtensional tectonics in the Sicily Channel. J. Struct. Geol. 9, 869–876. https://doi.org/10.1016/0191-8141(87)90087-3.

— Boccaletti, M., Cerrina Feroni, A., Martinelli, P., Moratti, G., Plesi, G. and Sani, F., 1992. Late Miocene-Quaternary compressive events in the Tyrrhenian side of the Northern Apennines. In Annales Tectonicae (Vol. 6, pp. 214-230).
— Boccaletti, M., Ciaranfi, N., Cosentino, D., Deiana, G., Gelati, R., Lentini, F., Massari, F., Moratti, G., Pescatore, T., Lucchi, F.R. and Tortorici, L., 1990. Palinspastic restoration and paleogeographic reconstruction of the peri-Tyrrhenian area during the Neogene. Palaeogeography, Palaeoclimatology, Palaeoecology, 77(1), pp.41-IN13.
— Boccaletti, M., Nicolich, R. and Tortorici, L., 1984. The Calabrian Arc and the Ionian Sea in the dynamic evolution of the Central Mediterranean. Marine Geology, 55(3-4), pp.219-245.
— Bond, C.E., Lunn, R.J., Shipton, Z.K. and Lunn, A.D., 2012. What makes an expert effective at interpreting seismic images?. Geology, 40(1), pp.75-78. https://doi.org/10.1130/G32375.1.
— Bonini, L., Basili, R., Toscani, G., Burrato, P., Seno, S. and Valensise, G., 2015. The role of pre-existing discontinuities in the development of extensional faults: an analog modeling perspective. Journal of structural geology, 74, pp.145-158.
— Bonini, M. and Sani, F., 2000. Pliocene-Quaternary transpressional evolution of the Anzi-Calvello and Northern S. Arcangelo basins (Basilicata, Southern Apennines, Italy) as a consequence of deep-seated fault reactivation. Marine and Petroleum Geology, 17(8), pp.909-927.
— Bonvalot, S., Balmino, G., Briais, A., M. Kuhn, Peyrefitte, A., Vales N., Biancale, R., Gabalda, G., Reinquin, F., Sarrailh, M., 2012. World Gravity Map. Commission for the Geological Map of the World. Eds. BGI-CGMW-CNES-IRD, Paris. https://doi.org/10.18168/bgi.2
— Bouyahiaoui, B., Sage, F., Abtout, A., Klingelhoefer, F., Yelles-Chaouche, K., Schnürle, P., Marok, A., Déverchère, J., Arab, M., Galve, A. and Collot, J.Y., 2015. Crustal structure of the eastern Algerian continental margin and adjacent deep basin: implications for late Cenozoic geodynamic evolution of the western Mediterranean. Geophysical Journal International, 201(3), pp.1912-1938.
— Brie, A., Endo, T., Hoyle, D., Codazzi, D., Esmersoy, C., Hsu, K., Denoo, S., Mueller, M.C., Plona, T., Shenoy, R. and Sinha, B., 1998. New directions in sonic logging. Oilfield Review, 10(1), pp.40-55.

— Butler RW, Lickorish WH, Grasso M, Pedley HM, Ramberti L. 1995. Tectonics and sequence stratigraphy in Messinian basins, Sicily: constraints on the initiation and termination of the Mediterranean salinity crisis. Geological Society of America Bulletin 107(4): 425–439.
— Butler RW. 2009. Relationships between the Apennine thrust belt, foredeep and foreland revealed by marine seismic data, offshore Calabria. Italian Journal of Geosciences 128(2): 269–278. https://doi.org/10.3301/IJG.2009.128.2.269
— Butler RWH, Grasso M, La Manna F. 1992. Origin and deformation of the Neogene-Recent Maghrebian foredeep at the Gela Nappe, SE Sicily. Journal of the Geological Society 149(4): 547–556. https://doi.org/10.1144/gsjgs.149.4.0547
— Butler, R.W., Maniscalco, R. and R Pinter, P., 2019. Syn-kinematic sedimentary systems as constraints on the structural response of thrust belts: re-examining the structural style of the Maghrebian thrust belt of Eastern Sicily. Italian Journal of Geosciences.
— Buttinelli, M., Maesano, F.E., Sopher, D., Feriozzi, F., Maraio, S., Mazzarini, F., Improta, L., Vallone, R., Villani, F., Basili, R., 2022. Revitalizing vintage seismic reflection profiles by converting into SEG-Y format: case studies from publicly available data on the Italian territory. Ann. Geophys. 65 (5). https://doi.org/10.4401/ag-8883.
— Cabello, F.C., León, J., Iano, Y., & Arthur, R., 2015. Implementation of a fixed-point 2D Gaussian Filter for Image Processing based on FPGA. 2015 Signal Processing: Algorithms, Architectures, Arrangements, and Applications (SPA), pp. 28-33.
— Cai, Y. and Wang, C.Y., 2005. Fast finite-element calculation of gravity anomaly in complex geological regions. Geophysical Journal International, 162(3), pp.696-708.
— Calamita F, Deiana G, Invernizzi MC, Pizzi A. 1991. Tettonica. In: L'AMBIENTE FISICO DELLE MARCHE, pp. 69-80. SELCA.
— Calamita F, Satolli S, Turtu A. 2012. Analysis of thrust shear zones in curve-shaped belts: Deformation mode and timing of the Olevano-Antrodoco-Sibillini thrust (Central/Northern Apennines of Italy). Journal of Structural Geology 44: 179–187.
— Calamita, F., Cello, G., Deiana, G. and Paltrinieri, W., 1994. Structural styles, chronology rates of deformation, and time-space relationships in the Umbria-Marche thrust system (central Apennines, Italy). Tectonics, 13(4), pp.873-881.

— Calanchi N, Colantoni P, Rossi PL, Saitta M, Serri G. 1989. The Strait of Sicily continental rift systems: physiography and petrochemistry of the submarine volcanic centres. Marine Geology 87: 55–83. https://doi.org/10.1016/0025-3227(89)90145-X.
— Calanchi, N., Colantoni, P., Rossi, P.L., Saitta, M., Serri, G., 1989. The Strait of Sicily continental rift system: physiography and petrochemistry of the submarine volcanic centres. Mar. Geol. 87, 55–83. https://doi.org/10.1016/0025-3227(89)90145-X.
— Calò M, Parisi L. 2014. Evidences of a lithospheric fault zone in the Sicily Channel continental rift (southern Italy) from instrumental seismicity data. Geophysical Journal International 199(1): 219–225. https://doi.org/10.1093/gji/ggu249
— Camafort, M., Pérez-Peña, J.V., Booth-Rea, G., Melki, F., Gràcia, E., Azañón, J.M., Galve, J.P., Marzougui, W., Gaidi, S. and Ranero, C.R., 2020. Active tectonics and drainage evolution in the Tunisian Atlas driven by interaction between crustal shortening and mantle dynamics. Geomorphology, 351, p.106954.
— Camerlenghi A, Del Ben A, Hübscher C, Forlin E, Geletti R, Brancatelli G, Micallef A, Saule M, Facchin L. 2020. Seismic markers of the Messinian salinity crisis in the deep Ionian Basin. Basin Research 32(4): 716–738.
— Carapezza M, Nuccio PM, Valenza M. 1981. Genesis and evolution of the fumaroles of Vulcano (Aeolian Islands, Italy): a geochemical model. Bulletin Volcanologique 44: 547–563.
— Carissimo, L., d'Agostino, O., Loddo, C. and Pieri, M., 1963. Petroleum exploration by AGIP Mineraria and new geological information in central and southern Italy, from the Abruzzi to the Taranto gulf. In 6th Petroleum International Congress, Section (Vol. 1, pp. 267-292).
— Carminati E, Doglioni C. 2012. Alps vs. Apennines: The paradigm of a tectonically asymmetric Earth. Earth-Science Reviews 112(1-2): 67–96.
— Carminati E, Lustrino M, Cuffaro M, Doglioni C. 2010. Tectonics, magmatism and geodynamics of Italy: what we know and what we imagine. Journal of the Virtual Explorer 36: 10-3809.
— Carminati, E. and Doglioni, C., 2005. Mediterranean tectonics. Encyclopedia of geology, 2(2005), pp.135-146.
— Carminati, E., Doglioni, C. and Scrocca, D., 2004. Alps vs apennines. Special volume of the Italian Geological Society for the IGC, 32, pp.141-151.

— Carminati, E., Lustrino, M., Cuffaro, M. and Doglioni, C., 2010. Tectonics, magmatism and geodynamics of Italy: what we know and what we imagine. Journal of the Virtual Explorer, 36(8), pp.10-3809.
— Carminati, E., Lustrino, M., Doglioni, C., 2012. Geodynamic evolution of the central and western Mediterranean: Tectonics vs. igneous petrology constraints. Tectonophysics 579, 173–192. https://doi.org/10.1016/j.tecto.2012.01.026.
— Casciello, E., Esestime, P., Cesarano, M., Pappone, G., Snidero, M. and Vergés, J., 2013. Lower plate geometry controlling the development of a thrust-top basin: the tectonosedimentary evolution of the Ofanto basin (Southern Apennines). Journal of the Geological Society, 170(1), pp.147-158.
— Cassano, E., Anelli, L., Cappelli, V. and la Torre, P., 2001. Magnetic and gravity analysis of Italy. In Anatomy of an orogen: The Apennines and adjacent Mediterranean basins (pp. 53-64). Dordrecht: Springer Netherlands.
— Cassinis, R., Scarascia, S., Lozej, A., 2003. The deep crustal structure of Italy and surrounding areas from seismic refraction data; a new synthesis. Boll. Soc. Geol. Ital. 122, 365–376.
— Catalano R, Franchino A, Merlini S, Sulli A. 2000. Central western Sicily structural setting interpreted from seismic reflection profiles. Mem. Soc. Geol. It. 55: 5–16.
— Catalano R, Infuso S, Sulli A. 1995. Tectonic history of the submerged Maghrebian Chain from the Southern Tyrrhenian Sea to the Pelagian Foreland. Terra Nova 7(2): 179–188.
— Catalano R, Valenti V, Albanese C, Accaino F, Sulli A, Tinivella U, Gasparo Morticelli M, Zanolla C, Giustiniani M. 2013. Sicily's fold–thrust belt and slab roll-back: the SI. RI. PRO. seismic crustal transect. J. Geol. Soc. 170(3): 451–464.
— Catalano S, De Guidi G, Lanzafame G, Monaco C, Tortorici L. 2009. Late Quaternary deformation on the island of Pantelleria: new constraints for the recent tectonic evolution of the Sicily Channel Rift (southern Italy). J. Geodyn. 48(2): 75–82.
— Catalano S, De Guidi G, Lanzafame G, Monaco C, Tortorici L. 2009. Late Quaternary deformation on the island of Pantelleria: new constraints for the recent tectonic evolution of the Sicily Channel Rift (southern Italy). Journal of Geodynamics 48(2): 75-82.

— Catalano S, De Guidi G, Monaco C, Tortorici G, Tortorici L. 2008. Active faulting and seismicity along the Siculo–Calabrian Rift Zone (southern Italy). Tectonophysics 453(1-4): 177–192. https://doi.org/10.1016/j.tecto.2007.05.008
— Catalano, R. and Milia, A., 1990. Late Pliocene-Early Pleistocene structural inversion in offshore western Sicily. In The potential of deep seismic profiling for hydrocarbon exploration (pp. 445-449). Technip Paris.
— Catalano, R. and Milia, A., 1990. Late Pliocene-early Pleistocene structural inversion in offshore western Sicily. In: B. Pinet and C. Bois (Editors), The Potential of Deep Seismic Profiling for Hydrocarbon Exploration, Technip, Paris, pp. 445-449.
— Catalano, R., D'Argenio, B., Montanari, L., Morlotti, E., Torelli, L., 1985. Marine geology of the NW Sicily offshore (Sardinia Channel) and its relationships with mainland structures. Boll. Soc. Geol. Ital. 104, 207–215.
— Catalano, R., Di Stefano, P., Sulli, A. and Vitale, F.P., 1996. Paleogeography and structure of the central Mediterranean: Sicily and its offshore area. Tectonophysics, 260(4), pp.291-323.
— Catalano, R., Infuso, S. and Sulli, A., 1995. Tectonic history of the submerged Maghrebian Chain from the Southern Tyrrhenian Sea to the Pelagian Foreland. Terra Nova, 7(2), pp.179-188.
— Catalano, R., Milia, A., 1990. Late Pliocene-lower Pleistocene structural inversion in offshore Western Sicily. In: Pinet, B., Bois, C. (Eds.), Potential of Deep Seismic Profiling for Hydrocarbon Exploration. Edition Technip, Paris, pp. 445–449.
— Catalano, S., Monaco, C., Tortorici, L., 2004. Neogene-Quaternary tectonic evolution of the southern Apennines. Tectonics 23, 1–19. https://doi.org/10.1029/2003TC001512.
— Catalano, S., Pavano, F., Romagnoli, G., Tortorici, G. and Tortorici, L., 2018. Late Tortonian–Quaternary tectonic evolution of central Sicily: the major role of the strike-slip deformation. Geological Magazine, 155(2), pp.536-548.
— Cavallaro D, Brancolini G, Lodolo E, Forlin E, Accaino F, Zecchin M, Brancatelli G. 2021. Morphostructural Setting and Tectonic Evolution of the Central Part of the Sicilian Channel (Central Mediterranean). Lithosphere 2021(1): 1–24. https://doi.org/10.2113/2021/7866771
— Cavallaro D, Monaco C, Polonia A, Sulli A, Di Stefano A. 2017. Evidence of positive tectonic inversion in the north-central sector of the Sicily Channel (Central

Mediterranean). Nat. Hazards 86(Suppl. 2): 233–251. https://doi.org/10.1007/s11069-016-2515-6

— Cavallaro, D., Monaco, C., Polonia, A., Sulli, A. and Di Stefano, A., 2017. Evidence of positive tectonic inversion in the north-central sector of the Sicily Channel (Central Mediterranean). Natural Hazards, 86, pp.233-251.

— Cavazza, W. and Wezel, F.C., 2003. The Mediterranean region—a geological primer. Episodes Journal of International Geoscience, 26(3), pp.160-168.

— Cello G. 1987. Structure and deformation processes in the Strait of Sicily "rift zone." Tectonophysics 141(1-3): 237–247. https://doi.org/10.1016/0040-1951(87)90188-0

— Cello, G., Gambini, R., Mazzoli, S., Read, A., Tondi, E. and Zucconi, V., 2000. Fault zone characteristics and scaling properties of the Val d'Agri Fault System (Southern Apennines, Italy). Journal of Geodynamics, 29(3-5), pp.293-307.

— Centamore, E., Ciccacci, S., Del Monte, M., Fredi, P. and Palmieri, E.L., 1996. Morphological and morphometric approach to the study of the structural arrangement of northeastern Abruzzo (central Italy). Geomorphology, 16(2), pp.127-137.

— Chang, K.T., 2008. Introduction to geographic information systems. Boston: McGraw-Hill, Vol. 4.

— Channell, J.E., d'Argenio, B. and Horvath, F., 1979. Adria, the African promontory, in Mesozoic Mediterranean palaeogeography. Earth-Science Reviews, 15(3), pp.213-292.

— Channell, J.E.T. and Horváth, F., 1976. The African/Adriatic promontory as a palaeogeographical premise for Alpine orogeny and plate movements in the Carpatho-Balkan region. Tectonophysics, 35(1-3), pp.71-101.

— Chapin, D.A., 1996. A deterministic approach toward isostatic gravity residuals—A case study from South America. Geophysics, 61(4), pp.1022-1033.

— Chapman, J.B. and DeCelles, P.G., 2015. Foreland basin stratigraphic control on thrust belt evolution. Geology, 43(7), pp.579-582.

— Chaumillon E, Mascle J. 1997. From foreland to forearc domains: new multichannel seismic reflection survey of the Mediterranean Ridge accretionary complex (Eastern Mediterranean). Marine Geol. 138(3-4): 237–259.

— Chiarabba, C., De Gori, P. and Speranza, F., 2008. The southern Tyrrhenian subduction zone: deep geometry, magmatism and Plio-Pleistocene evolution. Earth and Planetary Science Letters, 268(3-4), pp.408-423.

— Chierici, R., Grassi, S., La Rosa, N., Nannini, R., Squarci, P. and Zurlo, R., 1995, May. Geothermal exploration on Pantelleria Island (Sicily channel): first results. In Proceedings of the world geothermal congress, Florence, Italy, May (pp. 18-31).
— Childs, C., Holdsworth, R.E., Jackson, C.A.L., Manzocchi, T., Walsh, J.J. and Yielding, G., 2017. Introduction to the geometry and growth of normal faults. Geological Society, London, Special Publications, 439(1), pp.1-9.
— Chizzini N, Artoni A, Torelli L, Basso J, Polonia A, Gasperini L. 2022. Tectono-stratigraphic evolution of the offshore Apulian Swell, a continental sliver between two converging orogens (Northern Ionian Sea, Central Mediterranean). Tectonophysics 839: 229544.
— Chizzini N, Artoni A, Torelli L, Maiorana M, Sulli A. 2023. Evidence of new diapiric structures in the southern Adria Plate (Eastern Margin of Tethyan Ocean): Implications for Triassic paleogeography and evaporites remobilization during subduction/collision (Northern Ionian Sea, Central Mediterranean). Marine Geology 465: 107162.
— Christensen, N.I. and Mooney, W.D., 1995. Seismic velocity structure and composition of the continental crust: A global view. Journal of Geophysical Research: Solid Earth, 100(B6), pp.9761-9788. https://doi.org/10.1029/95JB00259
— Cicala, M., Chiarella, D., De Giosa, F. et al. 2022. Conventional data display and implications for the interpretation of seismic profiles: a discussion on the ViDEPI seismic database offshore Apulia (southern Italy). Arab J Geosci 15, 395. https://doi.org/10.1007/s12517-022-09721-z
— Cicala, M., De Giosa, F., Piscitelli, A., Scicchitano, G. and Festa, V., 2024. Conversion of vintage seismic reflection profiles of the ViDEPI dataset crossing the Gondola Line seismogenic fault (offshore Apulia, Adriatic Sea, Southern Italy) to SEG-Y. Data in Brief, p.110705.
— Cicala, M., Festa, V., Sabato, L., Tropeano, M. and Doglioni, C., 2021. Interference between Apennines and Hellenides foreland basins around the Apulian swell (Italy and Greece). Marine and Petroleum Geology, 133, p.105300.
— Civetta L, D'Antonio M, Orsi G, Tilton G.R. 1998. The geochemistry of volcanic rocks from Pantelleria Island, Sicily Channel: petrogenesis and characteristics of the mantle source region. J. Petrology 39(8): 1453–1491. https://doi.org/10.1093/petroj/39.8.1453

— Civetta, K., Cornette, Y., Crisci, G., Gillot, P. Y., Orsi, G. and Requiejo, C. S.. 1984. Geology, geochronology and chemical evolution of the island of Pantelleria. Geol. Mag. 6, 541-562.

— Civile D, Baradello L, Accaino F, Zecchin M, Lodolo E, Ferrante G.M, Markezic N, Volpi V, Burca M. 2023. Fluid-Related Features in the Offshore Sector of the Sciacca Geothermal Field (SW Sicily): The Role of the Lithospheric Sciacca Fault System. Geosciences 13(8): 231. https://doi.org/10.3390/jmse12071142.

— Civile D, Brancolini G, Lodolo E, Forlin E, Accaino F, Zecchin M, Brancatelli G, Billi A. 2021. Morphostructural setting and tectonic evolution of the central part of the Sicilian Channel (Central Mediterranean). Lithosphere.2021(1). https://doi.org/10.2113/2021/7866771.

— Civile D, Lodolo E, Accaino F, Geletti R, Schiattarella M, Giustiniani M, Fedorik J, Zecchin M, Zampa L. 2018. Capo Granitola-Sciacca fault zone (Sicilian Channel, Central Mediterranean): structure vs magmatism. Marine and Petroleum Geol. 96: 627–644. https://doi.org/10.1016/j.marpetgeo.2018.05.016

— Civile D, Lodolo E, Accettella D, Geletti R, Ben-Avraham Z, Deponte M, Facchin L, Ramella R, Romeo R. 2010. The Pantelleria graben (Sicily Channel, Central Mediterranean): an example of intraplate 'passive' rift. Tectonophysics 490(3-4): 173-183.

— Civile D, Lodolo E, Alp H, Ben-Avraham Z, Cova A, Baradello L, Accettella D, Burca M, Centonze J. 2014. Seismic stratigraphy and structural setting of the Adventure Plateau (Sicily Channel). Marine Geophysical Research 35(1): 37–53. https://doi.org/10.1007/s11001-013-9205-5

— Civile D, Lodolo E, Tortorici L, Lanzafame G, Brancolini G. 2008. Relationships between magmatism and tectonics in a continental rift: The Pantelleria Island region (Sicily Channel, Italy). Marine Geol. 251(1–2): 32–46. https://doi.org/10.1016/j.margeo.2008.01.009

— Civile D, Lodolo E, Zecchin M, Ben-Avraham Z, Baradello L, Accettella D, Cova A, Caffau M. 2015. The lost Adventure Archipelago (Sicilian Channel, Mediterranean Sea): Morpho-bathymetry and Late Quaternary palaeogeographic evolution. Global and Planetary Change 125: 36–47.

— Civile, D., Baradello, L., Accaino, F., Zecchin, M., Lodolo, E., Ferrante, G.M., Markezic, N., Volpi, V. and Burca, M., 2023. Fluid-Related Features in the Offshore

Sector of the Sciacca Geothermal Field (SW Sicily): The Role of the Lithospheric Sciacca Fault System. Geosciences, 13(8), p.231.

— Civile, D., Brancolini, G., Lodolo, E., Forlin, E., Accaino, F., Zecchin, M., Brancatelli, G., 2021. Morphostructural Setting and Tectonic Evolution of the Central Part of the Sicilian Channel (Central Mediterranean). Lithosphere 2021(1), 1–24.

— Civile, D., Lodolo, E., Accettella, D., Geletti, R., Ben-Avraham, Z., Deponte, M., Facchin, L., Ramella, R. and Romeo, R., 2010. The Pantelleria graben (Sicily Channel, Central Mediterranean): an example of intraplate 'passive'rift. Tectonophysics, 490(3-4), pp.173-183.

— Civile, D., Lodolo, E., Alp, H., Ben-Avraham, Z., Cova, A., Baradello, L., Accettella, D., Burca, M., Centonze, J., 2014. Seismic stratigraphy and structural setting of the Adventure Plateau (Sicily Channel). Mar. Geophys. Res. 35, 37–53.

— Civile, D., Lodolo, E., Zecchin, M., Ben-Avraham, Z., Baradello, L., Accettella, D., Cova, A., Caffau, M., 2015. The lost adventure archipelago (Sicilian Channel, Mediterranean Sea): morpho-bathymetry.

— Civile, D., Zecchin, M., Forlin, E., Donda, F., Volpi, V., Merson, B. and Persoglia, S., 2013. CO2 geological storage in the Italian carbonate successions. International Journal of Greenhouse Gas Control, 19, pp.101-116. https://doi.org/10.1016/j.ijggc.2013.08.010.

— Cloetingh S, Eldholm O, Larsen B.T., Gabrielsen R.H, Sassi W. 1994. Dynamics of extensional basin formation and inversion: introduction. Tectonophysics 240(1-4): 1–9.

— Cloetingh S, Ziegler P.A., Beekman F, Burov E.B., Garcia-Castellanos D, Matenco L. 2015. Tectonic Models for the Evolution of Sedimentary Basins. In: Treatise on Geophysics: Second Edition, Vol. 6. Elsevier B.V. https://doi.org/10.1016/B978-0-444-53802-4.00117-2

— Cogan J, Rigo L, Grasso M, Lerche I. 1989. Flexural tectonics of southeastern Sicily. J. Geodyn. 11(3): 189–241. https://doi.org/10.1016/0264-3707(89)90007-0

— Cohen, E., Lyche, T., Riesenfeld, R., 1980. Discrete B- splines and subdivision techniques in computer-aided geometric design and computer graphics. Computer Graphics & Image Processing 14(2), 87–111. https://doi.org/10.1016/0146-664X(80)90040-4.

— Colantoni, P., 1975. Note di geologia marina sul Canale di Sicilia. Giorn. Geol. 40, 181-207.
— Colli, L., Ghelichkhan, S. and Bunge, H.P., 2016. On the ratio of dynamic topography and gravity anomalies in a dynamic Earth. Geophysical Research Letters, 43(6), pp.2510-2516.
— Coltelli M, Cavallaro D, D'Anna G, D'Alessandro A, Grassa F, Mangano G, Patanè D, Gresta S. 2016. Exploring the submarine Graham Bank in the Sicily Channel. Ann. Geophys.
— Compagnoni, R., Morlotti, E. and Torelli, L., 1989. Crystalline and sedimentary rocks from the scarps of the Sicily-Sardinia Trough and Cornaglia Terrace (southwestern Tyrrhenian Sea, Italy): paleogeographic and geodynamic implications. Chemical Geology, 77(3-4), pp.375-398.
— Conte A.M, Martorelli E, Calarco M, Sposato A, Perinelli C, Coltelli M, Chiocci F.L. The 1891 submarine eruption offshore Pantelleria Island (Sicily Channel, Italy): Identification of the vent and characterization of products and eruptive style. Geochemistry, Geophysics, Geosystems. 2014 Jun;15(6):2555-74.
— Conti, A., Maffucci, R., Bigi, S., 2022. The use of public vintage seismic reflection profiles: An example of data rescue from the eastern Tyrrhenian margin (Italy), in Interpreting Subsurface Seismic Data, Eds: Rebecca Bell, David Iacopini, Mark Vardy. Elsevier. 127-156. https://doi.org/10.1016/B978-0-12-818562-9.00003-0.
— Cooper, M.A., Williams, G.D., De Graciansky, P.C., Murphy, R.W., Needham, T., De Paor, D., Stoneley, R., Todd, S.P., Turner, J.P. and Ziegler, P.A., 1989. Inversion tectonics—a discussion. Geological Society, London, Special Publications, 44(1), pp.335-347.
— Corradino, J.I., Pullen, A., Leier, A.L., Barbeau Jr, D.L., Scher, H.D., Weislogel, A., Bruner, A., Leckie, D.A. and Currie, L.D., 2022. Ancestral trans–North American Bell River system recorded in late Oligocene to early Miocene sediments in the Labrador Sea and Canadian Great Plains. Bulletin, 134(1-2), pp.130-144.
— Corradino, M., Balázs, A., Faccenna, C. and Pepe, F., 2022. Arc and forearc rifting in the Tyrrhenian subduction system. Scientific Reports, 12(1), p.4728.
— Corti G, Cuffaro M, Doglioni C, Innocenti F, Manetti P. 2006. Coexisting geodynamic processes in the Sicily Channel. Spec. Pap. Geol. Soc. Am. 409(05): 83–96. https://doi.org/10.1130/2006.2409(05).

— Cosentino, D., Cipollari, P., Marsili, P. and Scrocca, D., 2010. Geology of the central Apennines: a regional review. Journal of the virtual explorer, 36(11), pp.1-37.
— Costa, J. C., Schleicher, J., 2011. Double path-integral migration velocity analysis: a real data example. J. Geophy. Eng. 8, 154–16. https://doi.org/10.1088/1742-2132/8/2/003.
— Cox, D.R., Newton, A.M. and Huuse, M., 2020. An introduction to seismic reflection data: Acquisition, processing and interpretation. In Regional geology and tectonics (pp. 571-603). Elsevier.
— Cuevas, E., Luque, A., Escobar, H., 2024. Spline Interpolation. In: Computational Methods with MATLAB®. Synthesis Lectures on Engineering, Science, and Technology. Springer, Cham. https://doi.org/10.1007/978-3-031-40478-8_8.
— Cuffaro, M., Petricca, P., Conti, A., Palano, M., Billi, A. and Bigi, S., 2024. Fault kinematic modeling along a widely deformed plate boundary in southern Italy. Geophysical Research Letters, 51(2), p.e2023GL106854.
— Cuffaro, M., Riguzzi, F., Scrocca, D. and Doglioni, C., 2011. Coexisting tectonic settings: the example of the southern Tyrrhenian Sea. International Journal of Earth Sciences, 100, pp.1915-1924.
— Currado, C. and Fredi, P., 2000. Morphometric parameters of drainage basins and morphotectonic setting of eastern Abruzzo. Memorie della Società Geologica Italiana, pp.411-419.
— D'Agostino, N., Mantenuto, S., D'Anastasio, E., Giuliani, R., Mattone, M., Calcaterra, S., Gambino, P. and Bonci, L., 2011. Evidence for localized active extension in the central Apennines (Italy) from global positioning system observations. Geology, 39(4), pp.291-294.
— Dannowski, A., Kopp, H., Klingelhoefer, F., Klaeschen, D., Gutscher, M. A., Krabbenhoeft, A., Dellong, D., Rovere, M., Graindorge, D., Papenberg, C., & Klaucke, I. (2019). Ionian Abyssal Plain: A window into the Tethys oceanic lithosphere. Solid Earth, 10(2), 447 462. https://doi.org/10.5194/se-10-447-2019
— Dart, C.J., Bosence, W.J., McClay, K.R., 1993. Stratigraphy and structure of the Maltese graben system. J. Geol. Soc. Lond. 150, 1153–1166. https://doi.org/10.1144/gsjgs.150.6.1153.
— Davies, E.R., 2012. Computer and Machine Vision: Theory, Algorithms, Practicalities. 4th ed. Oxford: Elsevier. https://doi.org/10.1016/C2010-0-66926-4.

— Davies, J.H. and Stevenson, D.J., 1992. Physical model of source region of subduction zone volcanics. Journal of Geophysical Research: Solid Earth, 97(B2), pp.2037-2070.
— De Alteriis G. 1995. Different foreland basins in Italy: examples from the central and western Adriatic Sea. Tectonophysics 252: 349–373.
— de Alteriis, G. and Aiello, G., 1993. Stratigraphy and tectonics offshore of Puglia (Italy, southern Adriatic Sea). Marine Geology, 113(3-4), pp.233-253.
— de Alteriis, G., 1995. Different foreland basins in Italy: examples from the central and southern Adriatic Sea. Tectonophysics, 252(1-4), pp.349-373.
— De Santis, V., Scardino, G., Scicchitano, G., Meschis, M., Montagna, P., Pons-Branchu, E., Ortiz, J.E., Sánchez-Palencia, Y. and Caldara, M., 2023. Middle-late Pleistocene chronology of palaeoshorelines and uplift history in the low-rising to stable Apulian foreland: Overprinting and reoccupation. Geomorphology, 421, p.108530.
— DeCelles P.G, Giles K.A. 1996. Foreland basin systems. Basin Research 8(2): 105–123. https://doi.org/10.1046/j.1365-2117.1996.01491.x
— DeCelles PG. 2012. Foreland basin systems revisited: variations in response to tectonic settings. In: Busby C, Pérez A.A. (Eds.), Tectonics of Sedimentary Basins: Recent Advances. Blackwell Publishing Ltd., Chichester, UK, pp. 405–426. https://doi.org/10.1002/9781444347166.ch20
— Del Ben A. 2009. Earthquakes and Shallow Structures in South Adria: Evidence of Recent Inversion Tectonics. Nova Science Publishers, Inc, pp. 147–163 (Chapter 6).
— Del Ben, A. 2010. Direction change of the Calabrian Arc: Causes and effects. Rendiconti Online Societa Geologica Italiana, 11(1), 328–329.
— Del Ben, A., Mocnik, A., Volpi, V. and Karvelis, P., 2015. Old domains in the South Adria plate and their relationship with the West Hellenic front. Journal of Geodynamics, 89, pp.15-28.
— Del Ben, Geletti R, Mocnik AR. 2010. Relation between recent tectonics and Mesozoic inherited structures of the central-southern Adria plate. Bollettino di Geofisica Teorica e Applicata 51(2-3):99-115.
— Delchiaro, M., Iacobucci, G., Della Seta, M., Gribenski, N., Piacentini, D., Ruscitto, V., Zocchi, M. and Troiani, F., 2024. A fluvial record of late Quaternary climate changes and tectonic uplift along the Marche Piedmont Zone of the Apennines: New insights from the Tesino River (Italy). Geomorphology, 445, p.108971.

— Della Seta, M., 2004. Azimuthal transects of stream orientations: An advanced in understanding the regional morphotectonic setting of eastern Abruzzo (Central Italy). Geografia Fisica e Dinamica Quaternaria, 27(1), pp.21-28.
— Della Seta, M., Del Monte, M., Fredi, P., Miccadei, E., Nesci, O., Pambianchi, G., Piacentini, T. and Troiani, F., 2008. Morphotectonic evolution of the Adriatic piedmont of the Apennines: an advancement in the knowledge of the Marche-Abruzzo border area. Geomorphology, 102(1), pp.119-129.
— Dercourt JE, Zonenshain LP, Ricou LE, Kazmin VG, Le Pichon X, Knipper AL, Grandjacquet C, Sbortshikov IM, Geyssant J, Lepvrier C, Pechersky DH. 1986. Geological evolution of the Tethys belt from the Atlantic to the Pamirs since the Lias. Tectonophysics 123(1-4): 241–315.
— Dewey JF, Helman ML, Knott SD, Turco E, Hutton DHW. 1989. Kinematics of the western Mediterranean. Geol Soc Lond Spec Publ 45(1): 265–283.
— Dewey, J.F., Helman, M.L., Turco, E., Hutton, D.H.W., Knott, S.D., 1989. Kinematics of western Mediterranean. Geol. Soc. Special Publ. No. 45, 265–283.
— Di Stefano E, Infuso S, Scarantino S. 1993. Plio-Pleistocene sequence stratigraphy of southwestern offshore Sicily from well logs and seismic sections in a high-resolution calcareous plankton biostratigraphic framework. In: Max MD, Colantoni P, eds. Geological Development of the Sicilian-Tunisian Platform. UNESCO Rep Mar Sci 58: 105–110.
— Dielforder, A., Frasca, G., Brune, S. and Ford, M., 2019. Formation of the Iberian-European convergent plate boundary fault and its effect on intraplate deformation in Central Europe. Geochemistry, Geophysics, Geosystems, 20(5), pp.2395-2417.
— Dilek, Y. and Sandvol, E., 2009. Seismic structure, crustal architecture and tectonic evolution of the Anatolian-African Plate Boundary and the Cenozoic Orogenic Belts in the Eastern Mediterranean Region. Geological Society, London, Special Publications, 327(1), pp.127-160.
— Diviacco, P., Carlino, F.M and Busato., A., 2019. Enhancing the value of public vintage seismic data in the Italian offshore, Geosci. Data J. 6 (1), 6-15.
— Diviacco, P., Wardell, N., Forlin, E., Sauli, C., Burca, M., Busato., Centonze, J., Pelos, C., 2015 Data rescue to extend the value of vintage seismic data: the OGS-SNAP experience. GeoResJ. 6, 44–52. https://doi.org/10.1016/j.grj.2015.01.006.

— Doglioni C, Harabaglia P, Merlini S, Mongelli F, Peccerillo AT, Piromallo C. 1999. Orogens and slabs vs. their direction of subduction. Earth-Science Reviews 45(3-4): 167–208.
— Doglioni, C., 1995. Geological remarks on the relationships between extension and convergent geodynamic settings. Tectonophysics, 252(1-4), pp.253-267.
— Doglioni, C., and Carminati, E., 2002, The effects of four subductions in NE Italy: Transalp Conference, Memorie Scienze Geologiche, v. 54, p. 1–4. Doglioni, C., and Harabaglia, P., 1996, The kinematic paradox of the San Andreas fault: Terra Nova, v. 8, p. 525–531.
— Doglioni, C., Fernandez, M., Gueguen, E., and Sabat, F., 1998, On the inter ference between the early Apennines-Maghrebides backarc extension and the Alps-Betics orogen in the Neogene geodynamics of the Western Mediterranean: Bollettino della Società Geologica Italiana, v. 118, p. 75 89.
— Doglioni, C., Gueguen, E., Harabaglia, P., and Mongelli, F., 1999, On the origin of W-directed subduction zones and applications to the western Mediter ranean: Geological Society Special Publication, v. 156, p. 541–561.
— Dondurur, D., 2018. Acquisition and Processing of Marine Seismic Data. Elsevier, 606 p.
— Elter, P., Grasso, M., Parotto, M. and Vezzani, L., 2003. Structural setting of the Apennine-Maghrebian thrust belt. Episodes Journal of International Geoscience, 26(3), pp.205-211.
— Emery, D. and Myers, K. eds., 2013. Sequence stratigraphy. John Wiley & Sons.
— Etris, E., Crabtree, N.J., Dewar, J., 2001. True depth conversion: More than a pretty picture. CSEG Recorder 26, 11-22.
— European Marine Observation and Data Network (EMODnet)., 2022. 1/16 * 1/16 arc minutes Digital Terrain Model (DTM). http://www.emodnet-bathymetry.eu/.
— Fabbri, A., Gallignani, P. and Zitellini, N., 1981. Geologic evolution of the peri-Tyrrhenian sedimentary basins. In Consiglio nazionale delle ricerche. International conference (pp. 101-126).
— Faccenna C, Funiciello F, Giardini D, Lucente P. 2001a. History of subduction and back-arc extension in the Central Mediterranean. Geophys. J. Int. 145: 809–820.

— Faccenna C, Funiciello F, Giardini D, Lucente P. 2001b. Episodic back-arc extension during restricted mantle convection in the Central Mediterranean. Earth Planet. Sci. Lett. 187: 105–116.
— Faccenna, C. Becker, T.W., Lucente, F. P., Jolivet, L., Rossetti, F., 2001b. History of subduction and back-arc extension in the central Mediterranean. Geophys. J. Int., 145, 809– 820. https://doi.org/10.1046/j.0956-540x.2001.01435.x.
— Faccenna, C., Funiciello, F., Giardini, D. and Lucente, P., 2001. Episodic back-arc extension during restricted mantle convection in the Central Mediterranean. Earth and Planetary Science Letters, 187(1-2), pp.105-116.
— Faccenna, C., Piromallo, C., Crespo-Blanc, A., Jolivet, L. and Rossetti, F., 2004. Lateral slab deformation and the origin of the western Mediterranean arcs. Tectonics, 23(1).
— Fantoni, R. and Franciosi, R., 2010. Tectono-sedimentary setting of the Po Plain and Adriatic foreland. Rendiconti Lincei, 21, pp.197-209.
— Featherstone, W.E. and Dentith, M.C., 1997. A geodetic approach to gravity data reduction for geophysics. Computers & Geosciences, 23(10), pp.1063-1070.
— Fedorik J, Toscani G, Lodolo E, Civile D, Bonini L, Seno S. 2018. Structural analysis and Miocene-to-Present tectonic evolution of a lithospheric-scale, transcurrent lineament: The Sciacca Fault (Sicilian Channel, Central Mediterranean Sea). Tectonophysics 722: 342–355.
— Fer, I., Holbrook, W. S., Steele, J. H., Turekian, K. K., & Thorpe, S. A. 2008. Seismic reflection methods for study of the water column. Elements of Physical Oceanography: A Derivative of the Encyclopedia of Ocean Sciences, 432-441.
— Ferranti L, Pace B, Valentini A, Montagna P, Pons-Branchu E, Tisnérat-Laborde N, Maschio L. 2019. Speleoseismological constraints on ground shaking threshold and seismogenic sources in the Pollino range (Calabria, southern Italy). J. Geophys. Res.: Solid Earth 124(5): 5192–5216.
— Ferranti L, Pepe F, Barreca G, Meccariello M, Monaco C. 2019. Multi-temporal tectonic evolution of Capo Granitola and Sciacca foreland transcurrent faults (Sicily Channel). Tectonophysics 765: 187–204. https://doi.org/10.1016/j.tecto.2019.05.002.
— Ferranti, L. and Oldow, J.S., 1999. History and tectonic implications of low-angle detachment faults and orogen parallel extension, Picentini Mountains, Southern Apennines fold and thrust belt, Italy. Tectonics, 18(3), pp.498-526.

— Finetti I.R, Del Ben A. 2005. Crustal tectono-stratigraphic setting of the Adriatic Sea from new CROP seismic data. CROP project: Deep seismic exploration of the Central Mediterranean and Italy 1: 519–548.
— Finetti I.R. 1984. Geophysical study of the Sicily Channel Rift Zone. Boll. Geofis. Teor. Appl. 26: 3–28.
— Finetti, I.R and Morelli, C., 1972. Regional reflection seismic exploration of the Strait of Sicily. In: Saclant Conference, 7, La Spezia.
— Finetti, I.R., 1984. Geophysical study of the Sicily Channel Rift Zone. Boll. Geofis. Teor. Appl. 26, 3–28. http://hdl.handle.net/11368/1693943.
— Finetti, I.R., Boccaletti, M., Bonini, M., Del Ben, A., Geletti, R., Pipan, M.I.C.H.E.L.E. and Sani, F., 2001. Crustal section based on CROP seismic data across the North Tyrrhenian–Northern Apennines–Adriatic Sea. Tectonophysics, 343(3-4), pp.135-163.
— Finetti, I.R., Del Ben, A., 2005. Crustal tectono-stratigraphic setting of the Pelagian foreland from new CROP seismic data. In: Finetti, I.R. (Ed.), CROP PROJECT: Deep Seismic Exploration of the Central Mediterranean and Italy. Elsevier B.V., pp. 581–595.
— Flis, M.F., Butt, A.L. and Hawke, P.J., 1998. Mapping the range front with gravity-are the corrections up to it?. Exploration Geophysics, 29(4), pp.378-383.
— Fosdick, J.C., Romans, B.W., Fildani, A., Bernhardt, A., Calderón, M. and Graham, S.A., 2011. Kinematic evolution of the Patagonian retroarc fold-and-thrust belt and Magallanes foreland basin, Chile and Argentina, 51 30′ S. Bulletin, 123(9-10), pp.1679-1698.
— Fossen, H., Cavalcante, C., Konopásek, J., Meira, V.T., de Almeida, R.P., Hollanda, M.H.B. and Trompette, R., 2020. A critical discussion of the subduction-collision model for the Neoproterozoic Araçuaí-West Congo orogen. Precambrian Research, 343, p.105715.
— Franke, R. 1982. Smooth Interpolation of Scattered Data by Local Thin Plate Splines. Computer and Mathematics with Applications 8 (4), 273–281.
— Gallais, F., Gutscher, M. A., Graindorge, D., Chamot-Rooke, N., & Klaeschen, D. 2011. A Miocene tectonic inversion in the Ionian Sea (central Mediterranean): Evidence from multichannel seismic data. Journal of Geophysical Research: Solid Earth, 116(12). https://doi.org/10.1029/2011JB008505

— Gallais, F., Gutscher, M.-A., Klaeschen, D., Graindorge, D. 2012. Two-stage growth of the Calabrian accretionary wedge in the Ionian Sea (Central Mediterranean): constraints from depht-migrated multichannel seismic data. Mar. Geol. 326-328, 28–45. https://doi.org/10.1016/j.margeo.2012.08.006

— Gamberi F, Argnani A. Basin formation and inversion tectonics on top of the Egadi foreland thrust belt (NW Strait of Sicily). Tectonophysics. 1995 Dec 30;252(1-4):285-94.

— Gamberi, F. and Argnani, A., 1993. Seismostratigraphic analysis of the Neogene basins superposed on the Maghrebian orogen west of the Egadi Islands: preliminary results. In Geological Development of the Sicilian-Tunisian Platform (Vol. 58, pp. 61-64). Unesco Paris.

— Gamberi, F. and Argnani, A., 1995. Basin formation and inversion tectonics on top of the Egadi foreland thrust belt (NW Strait of Sicily). Tectonophysics, 252(1-4), pp.285-294.

— Gambino S, Barreca G, Gross F, Monaco C, Krastel S, Gutscher M.A. 2021. Deformation pattern of the northern sector of the Malta escarpment (Offshore SE Sicily, Italy): fault dimension, slip prediction, and seismotectonic implications. Front. Earth Sci. 8: 594176.

— Gardiner W, Grasso M, Sedgeley D. 1995. Plio-Pleistocene fault movement as evidence for mega-block kinematics within the Hyblean—Malta Plateau, Central Mediterranean. J. Geodyn. 19(1): 35–51.

— Gasparo Morticelli M, Valenti V, Catalano R, Sulli A, Agate M, Avellone G, Albanese C, Basilone L, Gugliotta C. 2015. Deep controls on foreland basin system evolution along the Sicilian fold and thrust belt. Bull. Soc. Géol. Fr. 186(4-5): 273–290.

— Gawthorpe, R.L. and Leeder, M.R., 2000. Tectono-sedimentary evolution of active extensional basins. Basin Research, 12(3-4), pp.195-218.

— Gerya, T., 2022. Numerical modeling of subduction: State of the art and future directions. Geosphere, 18(2), pp.503-561.

— Ghielmi M, Amore M.R., Bolla E.M., Carubelli P, Knezaurek G, Serraino C. 2012. The Pliocene to Pleistocene succession of the Hyblean foredeep (Sicily, Italy). In: AAPG Internat. Conf. Exhib. Milan, Italy, October (Vol. 23, p. 26).

— Ghisetti, F. and Vezzani, L., 1997. Interfering paths of deformation and development of arcs in the fold-and-thrust belt of the central Apennines (Italy). Tectonics, 16(3), pp.523-536.
— Ghisetti, F.C., Gorman, A.R., Grasso, M., Vezzani, L., 2009. Imprint of foreland structure on the deformation of a thrust sheet: the Plio-Pleistocene Gela Nappe (southern Sicily, Italy). Tectonics 28, TC4015. https://doi.org/10.1029/2008TC002385.
— Gibson, R.I. and Millegan, P.S. eds., 1998. Geologic applications of gravity and magnetics: Case histories. Society of Exploration Geophysicists and American Association of Petroleum Geologists.
— Giunta, G., Nigro, F. and Renda, P., 2000. Extensional tectonics during Maghrebides chain building since late Miocene: examples from Northern Sicily. In Annales Societatis Geologorum Poloniae (Vol. 70, No. 1, pp. 81-98). Polskie Towarzystwo Geologiczne.
— Giunta, G., Nigro, F., Renda, P., and Goirgianni, A., 2000, The Sicilian Magrebides Tyrrhenian Margin: A neotectonic evolutionary model: Bol lettino della Società Geologica Italiana, v. 119, p. 553–565.
— Giustiniani, M., Tinivella, U. and Nicolich, R., 2015. Reflection seismic sections across the Geothermal Province of Tuscany from reprocessing CROP profiles. Geothermics, 53, pp.498-507.
— Govers R, Wortel M.J.R. 2005. Lithosphere tearing at STEP faults: Response to edges of subduction zones. Earth Planet. Sci. Lett. 236(1-2): 505–523.
— Grasso M, Pedley MH, Reuther CD. 1985. The geology of the Pelagian Islands and their structural setting related to the Pantelleria rift (central Mediterranean Sea). CENTRO 1(2): 1-19.
— Grasso M, Reuther CD. 1988. The western margin of the Hyblean Plateau a neotectonic transform system on the SE Sicilian foreland. Ann. Tect. 2: 107–120.
— Grasso M, Torelli L, Mazzoldi G. 1999. Cretaceous–Palaeogene sedimentation patterns and structural evolution of the Tunisian shelf, offshore the Pelagian islands (central Mediterranean). Tectonophysics 315(1-4): 235-250.
— Grasso M., Lanzafame G., Rossi P.L., Schmincke H.U., Tranne C.A., Lajoie J. and Lanti E., 1991b Volcanic evolution of the island of Linosa, Strait of Sicily, Mem. Soc. geol. ital. 47, 509-525.

— Grasso M., Pezzino A., Reuther C.D., Lanza R. and Miletto M., 1991a. Late Cretaceous and Recent tectonic stress orientations recorded by basalt dykes at Capo Passer (south-eastern Sicily). Tectonophysics 185, 247-259.
— Grasso M., Torelli L., 1999. Cretaceous-Paleogene sedimentation patterns and structural 688 evolution of the Tunisian shelf, offshore the Pelagian Islands (Central Mediterranean). Tectonophysics 315 (1999) 235-250. http://dx.doi.org/10.1016/S0040-1951(99)00285-1.
— Grasso, M., 2001. The Apenninic—Maghrebian orogen in southern Italy, Sicily and adjacent areas. In Anatomy of an orogen: the Apennines and adjacent Mediterranean basins (pp. 255-286). Dordrecht: Springer Netherlands.
— Gries, D., Schneider, F.B., 1993. Boolean Expressions. In: A Logical Approach to Discrete Math. Texts and Monographs in Computer Science. Springer, New York, NY. https://doi.org/10.1007/978-1-4757-3837-7_3.
— Guarnieri, P., 2006. Plio-Quaternary segmentation of the south Tyrrhenian forearc basin. International Journal of Earth Sciences, 95, pp.107-118.
— Gueguen, E., Doglioni, C., Fernandez, M., 1998. On the post-25 Ma geodynamic evolution of the western Mediterranean. Tectonophysics 298, 259–269. https://doi.org/10.1016/S0040-1951(98)00189-9.
— Gueguen, E., Doglioni, C., Fernandez, M., 1998. On the post-25 Ma geodynamic evolution of the western Mediterranean. Tectonophysics 298(1–3), 259–269.
— Guerrera, F. and Martín-Martín, M., 2014. Geodynamic events reconstructed in the Betic, Maghrebian, and Apennine chains (central-western Tethys). Bulletin de la Société géologique de France, 185(5), pp.329-341.
— Güneş P, Aksu AE, Hall J. 2018. Tectonic and sedimentary conditions necessary for the deposition of the Messinian evaporite successions in the eastern Mediterranean: A simple 2D model. Marine and Petroleum Geology 96: 51-70.
— Güneş, P., Aksu, A.E. and Hall, J., 2018. Tectonic and sedimentary conditions necessary for the deposition of the Messinian evaporite successions in the eastern Mediterranean: A simple 2D model. Marine and Petroleum Geology, 96, pp.51-70.
— Hackney, R., 2020. Gravity, data to anomalies. Encyclopedia of Solid Earth Geophysics, pp.1-10.
— Hall, R. 2019. The subduction initiation stage of the Wilson cycle, Geological Society, London, Special Publications, 470(1), 415-437. https://doi.org/10.1144/SP470.3

— Hamilton, W.B., 1994. Subduction systems and magmatism. Geological Society, London, Special Publications, 81(1), pp.3-28.
— Haq B, Gorini C, Baur J, Moneron J, Rubino JL. 2020. Deep Mediterranean's Messinian evaporite giant: How much salt? Global and Planetary Change 184: 103052.
— Harangi, S., Downes, H. and Seghedi, I., 2006. Tertiary-Quaternary subduction processes and related magmatism in the Alpine-Mediterranean region. Geological Society, London, Memoirs, 32(1), pp.167-190.
— Hart, B. S. 1999. Definition of subsurface stratigraphy, structure and rock properties from 3-D seismic data. Earth-science reviews, 47(3-4), 189-218.
— Hatton, L., Worthington, M.H. and Makin, J., 1986. Seismic data processing: theory and practice. Merlin Profiles Ltd.
— Hieke, W., Hirschleber, H.B. and Dehghani, G.A., 2003. The Ionian Abyssal Plain (central Mediterranean Sea): Morphology, subbottom structures and geodynamic history–an inventory. *Marine Geophysical Researches*, *24*, pp.279-310.
— Hill, S.J. and Rüger, A., 2019. Illustrated Seismic Processing: Volume 1: Imaging. Society of Exploration Geophysicists.
— Hippolyte, J.C., Angelier, J. and Roure, F.B., 1994. A major geodynamic change revealed by Quaternary stress patterns in the Southern Apennines (Italy). Tectonophysics, 230(3-4), pp.199-210.
— Holland CW, Etiope G, Milkov AV, Michelozzi E, Favali P. 2003. Mud volcanoes discovered offshore Sicily. Marine Geology 199(1-2): 1-6.
— Hou, T., Liu, H., Zhu, J., Liu, T., Liu, L., Li, Y., Qian, C. and Xin, Y., 2020. Piezoelectric geophone: a review from principle to performance. Ferroelectrics, 558(1), pp.27-35.
— Husson, L., Riel, N., Aribowo, S., Authemayou, C., de Gelder, G., Kaus, B. J. P, Mallard, C., Natawidjaja, D. H., Pedoja, K., Sarr, A. C. (2022). Slow Geodynamics and Fast Morphotectonics in the far East Tethys. Geochemistry, Geophysics, Geosystems, 23, e2021GC010167.
— Iannone, A. and Pieri, P., 1982. Caratteri neotettonici delle Murge. Geologia Applicata e idrogeologia, 17, pp.147-160.
— Illies, J.H., 1981. Graben formation—the Maltese Islands—a case history. In Developments in Geotectonics (Vol. 17, pp. 151-168). Elsevier.
— Imbò G. 1965. Catalogue of the active volcanoes of the world, Italy (Vol. 18). Rome: IAVCEI.

— Innangi S, Tonielli R, Romagnoli C, Budillon F, Di Martino G, Innangi M, Laterza R, Le Bas T, Lo Iacono C. 2019. Seabed mapping in the Pelagie Islands marine protected area (Sicily Channel, southern Mediterranean) using remote sensing object based image analysis (RSOBIA). Marine Geophysical Research 40: 333-355.
— ISIDe Working Group. 2007. Italian Seismological Instrumental and Parametric Database (ISIDe) (Version 1). National Institute of Geophysics and Volcanology (INGV). https://doi.org/10.13127/ISIDE
— Jammes, S., Huismans, R.S. and Muñoz, J.A., 2014. Lateral variation in structural style of mountain building: controls of rheological and rift inheritance. Terra Nova, 26(3), pp.201-207.
— Jeng, Y., Li, Y. W., Chen, C. S., Chien, H. Y., 2009. Adaptive filtering of random noise in near-surface seismic and ground-penetrating radar data. J. Appl. Geophys. 68(1), 36–46. https://doi.org/10.1016/j.jappgeo.2008.08.013.
— Jiang, J., Ren, H. and Zhang, M., 2021. A convolutional autoencoder method for simultaneous seismic data reconstruction and denoising. IEEE geoscience and remote sensing letters, 19, pp.1-5.
— Jiang, X. J., Scott, P. J., 2020. Free-form surface filtering using wavelets and multiscale decomposition, in, Advanced Metrology 2, 195–246. https://doi.org/10.1016/b978-0-12-821815-0.00009-5.
— Jolivet L, Baudin T, Calassou S, Chevrot S, Ford M, Issautier B, Lasseur E, Masini E, Manatschal G, Mouthereau F, Thinon I. 2021. Geodynamic evolution of a wide plate boundary in the Western Mediterranean, near-field versus far-field interactions. BSGF-Earth Sciences Bulletin 192(1): 48.
— Jolivet, L., Frizon de Lamotte, D., Mascle, A. and Séranne, M., 1999. The Mediterranean basins: Tertiary extension within the Alpine orogen—An introduction. Geological Society, London, Special Publications, 156(1), pp.1-14.
— Jolivet, L., Menant, A., Roche, V., Le Pourhiet, L., Maillard, A., Augier, R., Do, Couto D., Gorini, C., Thinon, I., Canva, A., 2021. Transfer zones in Mediterranean back-arc regions and tear faults. Bull. Soc. Geol. France 192 (1), 11. https://doi.org/10.1051/bsgf/2021006.
— Jones, P.C., Johnson, A.C., von Frese, R.R. and Corr, H., 2002. Detecting rift basins in the Evans Ice Stream region of West Antarctica using airborne gravity data. Tectonophysics, 347(1-3), pp.25-41.

— Jongsma, D., Van Hinte, J.E., Woodside, J.M., 1985. Geologic structure and neotectonics of the North African continental margin south of Sicily. Mar. Petrol. Geol. 2, 156–179.
— Jordan, N.J., White, J.C., Macdonald, R. and Rotolo, S.G., 2021. Evolution of the magma system of Pantelleria (Italy) from 190 ka to present. Comptes Rendus. Géoscience, 353(S2), pp.133-149.
— Jourdon, A., Le Pourhiet, L., Mouthereau, F. and Masini, E., 2019. Role of rift maturity on the architecture and shortening distribution in mountain belts. Earth and Planetary Science Letters, 512, pp.89-99.
— Kastens, K., Mascle, J., Auroux, C., Bonatti, E., Broglia, C., Channell, J., Curzi, P., Emeis, K.C., Glaçon, G., Hasegawa, S. and Hieke, W., 1988. ODP Leg 107 in the Tyrrhenian Sea: Insights into passive margin and back-arc basin evolution. Geological Society of America Bulletin, 100(7), pp.1140-1156.
— Kearey, P., Klepeis, K.A. and Vine, F.J., 2009. Global tectonics. John Wiley & Sons.
— Khomsi S, Jemia MGB, de Lamotte DF, Maherssi C, Echihi O, Mezni R. 2009. An overview of the Late Cretaceous–Eocene positive inversions and Oligo-Miocene subsidence events in the foreland of the Tunisian Atlas: Structural style and implications for the tectonic agenda of the Maghrebian Atlas system. Tectonophysics 475(1): 38-58.
— Krijgsman W, Hilgen FJ, Raffi I, Sierro FJ, Wilson DS. 1999. Chronology, causes and progression of the Messinian salinity crisis. Nature 400(6745): 652-655.
— Kuhlmann J, Asioli A, Trincardi F, Klügel A, Huhn K. 2017. Landslide frequency and failure mechanisms at NE Gela Basin (Strait of Sicily). Journal of Geophysical Research: Earth Surface 122(11): 2223-2243.
— Lai, C.-K., Xia, X.-P., Hall, R., Meffre, S., Tsikouras, B., Rosana BalangueTarriela, M. I., et al. (2021). Cenozoic evolution of the Sulu Sea arc-basin system: An overview. Tectonics, 40, e2020TC006630. https://doi.org/10.1029/2020TC006630
— Lamb, S. and Watts, A., 2010. The origin of mountains–implications for the behaviour of Earth's lithosphere. Current Science, pp.1699-1718.
— Lanari, R., Boutoux, A., Faccenna, C., Herman, F., Willett, S. D., & Ballato, P. (2023). Cenozoic exhumation in the Mediterranean and the Middle East. Earth-Science Reviews, 237, 104328. https://doi.org/10.1016/j.earscirev.2023.104.

— Lanzafame AC. 1994. SiII resonance multiplets in the Sun. Astronomy and Astrophysics 287: 972-981.
— Le Breton E, Handy MR, Molli G, Ustaszewski K. 2017. Post-20 Ma motion of the Adriatic Plate: New constraints from surrounding orogens and implications for crust-mantle decoupling. Tectonics 36(12): 3135-3154. https://doi.org/10.1002/2016TC004443
— Lecomte, I., Lavadera, P. L., Anell, I., Buckley, S. J., Schmid, D. W., & Heeremans, M. 2015. Ray-based seismic modeling of geologic models: Understanding and analyzing seismic images efficiently. Interpretation, 3(4), SAC71-SAC89.
— Lee, D.H. and Acharya, T.D., 2017. Comparison of complete bouguer anomalies from satellite marine gravity models with shipborne gravity data in East Sea, Korea. Journal of Marine Science and Technology, 25(6), p.1.
— Lentini F, Carbone S, Catalano S, Monaco C. 1990. Tettonica a thrust neogenica nella Catena Appenninico-Maghrebide: esempi dalla Lucania e dalla Sicilia. Studi Geol. Camerti Vol. speciale: 19–26.
— Lentini F, Carbone S, Catalano S. 1994. Main structural domains of the central Mediterranean region and their Neogene tectonic evolution. Boll. Geof. Teor. Appl. 36: 103–125.
— Lentini F, Catalano S, Carbone S. 1996. The external thrust system in southern Italy; a target for petroleum exploration. Petroleum Geoscience 2(4): 333–342. doi:10.1144/petgeo.2.4.333
— Lentini, F., Carbone, S. and Guarnieri, P., 2006. Collisional and postcollisional tectonics of the Apenninic-Maghrebian orogen (southern Italy).
— Lentini, F., Carbone, S., & Guarnieri, P., 2006. Collisional and postcollisional tectonics of the Apenninic-Maghrebian orogen (southern Italy). Postcollisional Tectonics and Magmatism in the Mediterranean Region and Asia, Yildirim Dilek, Spyros Pavlides. doi.org/10.1130/2006.2409(04
— Lickorish WH, Grasso M, Butler RW, Argnani A, Maniscalco R. 1999. Structural styles and regional tectonic setting of the “Gela Nappe” and frontal part of the Maghrebian thrust belt in Sicily. Tectonics 18(4): 655-668.
— Lodolo E, Civile D, Zanolla C, Geletti R. 2012. Magnetic signature of the Sicily Channel volcanism. Marine Geophysical Research 33: 33-44.

— Lodolo E, Civile D, Zecchin M, Zampa LS, Accaino F. 2019. A series of volcanic edifices discovered a few kilometers off the coast of SW Sicily. Marine Geology 416: 105999. https://doi.org/10.1016/j.margeo.2019.105999.
— Lodolo E, Loreto MF, Melini D, Spada G, Civile D. 2022. Palaeo-shoreline configuration of the Adventure Plateau (Sicilian channel) at the last glacial maximum. Geosciences 12(3): 125.
— Lofi J, Sage F, Déverchère J, Loncke L, Maillard A, Gaullier V, Thinon I, Gillet H, Guennoc P, Gorini C. 2011. Refining our knowledge of the Messinian salinity crisis records in the offshore domain through multi-site seismic analysis. Bulletin de la Société géologique de France 182(2): 163-180.
— Loreto, M.F., Palmiotto, C., Muccini, F., Ferrante, V. and Zitellini, N., 2021. Inverted Basins by Africa–Eurasia Convergence at the Southern Back-Arc Tyrrhenian Basin. Geosciences, 11(3), p.117.
— Maesano, F.E., Tiberti, M.M. and Basili, R., 2020. Deformation and fault propagation at the lateral termination of a subduction zone: The Alfeo fault system in the Calabrian Arc, Southern Italy. Frontiers in Earth Science, 8, p.107.
— Maesano, F.E., Volpi, V., Civile, D., Basili, R., Conti, A., Tiberti, M.M., Accettella, D., Conte, R., Zgur, F. and Rossi, G., 2020. Active extension in a foreland trapped between two contractional chains: the South Apulia fault system (SAFS). Tectonics, 39(7), p.e2020TC006116.
— Maffucci, R., Petracchini, L., Livani, M., Billi, A., Carminati, E., Cuffaro, M., Petricca, P., Doglioni, C., 2020. Seismic Reflection Profile Dataset in a 3D Environment of the Northern Adriatic Area (Italy). GFZ Data Services. https://doi.org/10.5880/fidgeo.2020.027.
— Mahood G, Hildreth W. 1983. Large partition coefficients for trace elements in high-silica rhyolites. Geochimica et Cosmochimica Acta 47(1): 11-30. https://doi.org/10.1016/0016-7037(83)90087-X.
— Maiorana M, Artoni A, Le Breton E, Sulli A, Chizzini N, Torelli L. 2023. Is the Sicily Channel a simple Rifting Zone? New evidence from seismic analysis with geodynamic implications. Tectonophysics 864: 230019.
— Maiorana M, Spatola D, Todaro S, Caldareri F, Parente F, Severini A, Sulli A. 2024. Seismo-stratigraphic and morpho-bathymetric analysis revealing recent fluid-rising

phenomena on the Adventure Plateau (northwestern Sicily Channel). Marine Geophysical Research 45(3): 15.

— Maiorana, M., Artoni., Le Breton, E., Sulli., Chizzini., N., Torelli, L., 2023. Is the Sicily Channel a simple Rifting Zone? New evidence from seismic analysis with geodynamic implications. Tectonophysics 864, 230019. https://doi.org/10.1016/j.tecto.2023.230019.

— Mantovani, E., Viti, M., Babbucci, D., Tamburelli, C. and Cenni, N., 2020. Geodynamics of the central-western Mediterranean region: plausible and non-plausible driving forces. Marine and Petroleum Geology, 113, p.104121.

— Mantovani, E., Viti, M., Babbucci, D., Tamburelli, C. and Cenni, N., 2019. How and why the present tectonic setting in the Apennine belt has developed. Journal of the Geological Society, 176(6), pp.1291-1302.

— Manzi V, Argnani A, Corcagnani A, Lugli S, Roveri M. 2020. The Messinian salinity crisis in the Adriatic foredeep: evolution of the largest evaporitic marginal basin in the Mediterranean. Marine and Petroleum Geology 115: 104288.

— Manzi V, Roveri M, Argnani A, Cowan D, Lugli S. 2021. Large-scale mass-transport deposits recording the collapse of an evaporitic platform during the Messinian salinity crisis (Caltanissetta basin, Sicily). Sedimentary Geology 424: 106003.

— Martorelli, E., Petroni, G., Chiocci, F.L. and Pantelleria Scientific Party, 2011. Contourites offshore Pantelleria Island (Sicily Channel, Mediterranean Sea): depositional, erosional and biogenic elements. Geo-Marine Letters, 31, pp.481-493.

— Mascle, A. and Puigdefàbregas, C., 1998. Tectonics and sedimentation in foreland basins: results from the Integrated Basin Studies project. Geological Society, London, Special Publications, 134(1), pp.1-28.

— Masrouhi A, Ghanmi M, Slama MMB, Youssef MB, Vila JM, Zargouni F. 2008. New tectono-sedimentary evidence constraining the timing of the positive tectonic inversion and the Eocene Atlasic phase in northern Tunisia: implication for the North African paleo-margin evolution. Reports. Geoscience 340(11): 771-778.

— Mazzoli, S., Ascione, A., Buscher, J.T., Pignalosa, A., Valente, E. and Zattin, M., 2014. Low-angle normal faulting and focused exhumation associated with late Pliocene change in tectonic style in the southern Apennines (Italy). Tectonics, 33(9), pp.1802-1818.

— Mazzoli, S., Barkham, S., Cello, G., Gambini, R., Mattioni, L., Shiner, P. and Tondi, E., 2001. Reconstruction of continental margin architecture deformed by the contraction of the Lagonegro Basin, southern Apennines, Italy. Journal of the Geological Society, 158(2), pp.309-319.
— McClay, K.R. and Buchanan, P.G., 1992. Thrust faults in inverted extensional basins. In: K.R. McCIay (Editor), Thrust Tecton- ics. Chapman and Hall, London, pp. 93- 104.
— McClay, K.R., Dooley, T., Whitehouse, P. and Mills, M., 2002. 4-D evolution of rift systems: Insights from scaled physical models. AAPG bulletin, 86(6), pp.935-960.
— McDermott, C., Collier, J.S., Lonergan, L., Fruehn, J., Bellingham, P., 2019. Seismic velocity structure of seaward-dipping refectors on the South American continental margin. Earth Planet Sci. Lett. 521, 14–24. https://doi.org/10.1016/j.epsl.2019.05.049.
— McKenzie, D.P., 1967. Some remarks on heat flow and gravity anomalies. Journal of Geophysical Research, 72(24), pp.6261-6273.
— Meccariello M, Ferranti L, Barreca G, Palano M. 2017. New insights on the tectonics of the Lampedusa Plateau from the integration of offshore, onland and space geodetic data. Ital. J. Geosci. 136: 1–42. https://doi.org/10.3301/IJG.2017.02.
— Meccariello, M., 2017. Tectonic evolution and current deformation of the NW Sicily Channel and the Lampedusa Plateau based on multi-resolution seismic profiles analysis (Doctoral dissertation, Univeristy of Naples Federico II).
— Micallef A, Camerlenghi A, Garcia-Castellanos D, Cunarro Otero D, Gutscher MA, Barreca G, Spatola D, Facchin L, Geletti R, Krastel S, Gross F. 2018. Evidence of the Zanclean megaflood in the eastern Mediterranean Basin. Scientific Reports 8(1): 1-8.
— Micallef A, Geldmacher J, Watt SF, Ferrante GM, Ford J, Lodolo E, Civile D, Hodgetts AG, Felgendreher M, Licari JG, Hauff F. 2024. Submarine volcanism in the Sicilian Channel revisited. Marine Geology: 107342. https://doi.org/10.1016/j.margeo.2024.107342
— Micallef, A., Geldmacher, J., Watt, S.F., Ferrante, G.M., Ford, J., Lodolo, E., Civile, D., Hodgetts, A.G., Felgendreher, M., Licari, J.G. and Hauff, F., 2024. Submarine volcanism in the Sicilian Channel revisited. Marine Geology, p.107342.
— Micallef, A., Georgiopoulou, A., Mountjoy, J., Huvenne, V.A., Iacono, C.L., Le Bas, T., Del Carlo, P. and Otero, D.C., 2016. Outer shelf seafloor geomorphology along a carbonate escarpment: The eastern Malta Plateau, Mediterranean Sea. Continental Shelf Research, 131, pp.12-27.

— Miccadei, E., Piacentini, T., Pozzo, A.D., Corte, M.L. and Sciarra, M., 2013. Morphotectonic map of the Aventino-Lower Sangro valley (Abruzzo, Italy), scale 1: 50,000. Journal of Maps, 9(3), pp.390-409.
— Mila, A., Torrente, M.M., Iannace, P., 2017. Pliocene-Quaternary orogenic systemb in central Mediterranean,: the apulia-southern Apennines-Tyrrhenian Sea example. Tectonics 1–19. https://doi.org/10.1002/2017tc004571.
— Miles, P. R., Schaming, M and Lovera, R., 2007. Resurrecting vintage paper seismic records, Marine Geophys. Res. 28 (4), 319-329.
— Milia A, Iannace P, Torrente MM. 2021. The meeting place of backarc and foreland rifting: The example of the offshore western Sicily (Central Mediterranean). Global and Planetary Change 198: 103408.
— Milia, A., Iannace, P., Tesauro, M., Torrente, M.M., 2018. Marsili and Cefalù basins: the evolution of a rift system in the southern Tyrrhenian Sea (Central Mediterranean). Glob. Planet. Change 171, 225–237. https://doi.org/10.1016/j. gloplacha.2017.12.003.
— Milia, A., Torrente, M.M., 2014. Early-stage rifting of the Southern Tyrrhenian region: the Calabria-Sardinia breakup. J. Geodyn. 81, 17–29. https://doi.org/10.1016/j. jog.2014.06.001.
— Milia, A., Torrente, M.M., Massa, B., Iannace, P., 2013. Progressive changes in rifting directions in the Campania margin (Italy): new constrains for the Tyrrhenian Sea opening. Glob. Planet. Chang. 109, 3–17. https://doi.org/10.1016/j. gloplacha.2013.07.003.
— Milia, A., Torrente, M.M., Tesauro, M., 2017a. From stretching to mantle exhumation in a triangular backarc basin (Vavilov basin, Tyrrhenian Sea, western Mediterranean). Tectonophysics 710–711, 108–126. https://doi.org/10.1016/j.tecto.2016.10.017.
— Minissale, A., Donato, A., Procesi, M., Pizzino, L. and Giammanco, S., 2019. Systematic review of geochemical data from thermal springs, gas vents and fumaroles of Southern Italy for geothermal favourability mapping. Earth-Science Reviews, 188, pp.514-535.
— Mitchum Jr, R.M., Vail, P.R. and Sangree, J.B., 1977. Seismic stratigraphy and global changes of sea level: Part 6. Stratigraphic interpretation of seismic reflection patterns in depositional sequences: Section 2. Application of seismic reflection configuration to stratigraphic interpretation... https://doi.org/10.1306/M26490C8.

— Molli, G., Carlini, M., Vescovi, P., Artoni, A., Balsamo, F., Camurri, F., Clemenzi, L., Storti, F. and Torelli, L.O.R.E.N.Z.O., 2018. Neogene 3-D structural architecture of the north-west Apennines: The role of the low-angle normal faults and basement thrusts. Tectonics, 37(7), pp.2165-2196.
— Monaco, C., Catalano, S., Cocina, O., De Guidi, G., Ferlito, C., Gresta, S., Musumeci, C. and Tortorici, L., 2005. Tectonic control on the eruptive dynamics at Mt. Etna Volcano (Sicily) during the 2001 and 2002–2003 eruptions. Journal of Volcanology and Geothermal Research, 144(1-4), pp.211-233.
— Monaco, C., Tortorici, L. and Paltrinieri, W., 1998. Structural evolution of the Lucanian Apennines, southern Italy. Journal of Structural Geology, 20(5), pp.617-638.
— Montazeri, M., Uldall, A., Moreau, J., Nielsen, L., 2018. Pitfalls in velocity analysis for strongly contrasting, layered media—example from the Chalk Group, North Sea. J Appl. Geophys. 149, 52–62. https://doi.org/10.1016/j.jappgeo.2017.12.003.
— Montone, P., Amato, A. and Pondrelli, S., 1999. Active stress map of Italy. Journal of Geophysical Research: Solid Earth, 104(B11), pp.25595-25610.
— Morelli, C., 1990. The regional meaning of the Bouguer gravity anomalies in the Mediterranean. Journal of geodynamics, 12(2-4), pp.123-136.
— Morelli, C., Gantar, C., Pisani, M., 1975. Bathymetry, gravity and magnetism in the Straits of Sicily and Ionian Sea. Boll. Geofis. Teor. Appl. 17, 39–58
— Morley, C.K., 2002. A tectonic model for the Tertiary evolution of strike–slip faults and rift basins in SE Asia. Tectonophysics, 347(4), pp.189-215.
— Mosegaard, K., Tarantola, A., 1995. Monte Carlo sampling of solutions to inverse problems. J. Geophys. Res.: Solid Earth 100(B7). 12431-12447.
— Mueller C, Micallef A, Spatola D, Wang X. 2020. The tsunami inundation hazard of the Maltese Islands (central Mediterranean Sea): A submarine landslide and earthquake tsunami scenario study. Pure and Applied Geophysics 177: 1617-1638.
— Nalpas T, Le Douaran S, Brun JP, Unternehr P, Richert JP. 1995. Inversion of the Broad Fourteens Basin (offshore Netherlands), a small-scale model investigation. Sedimentary Geology 95(3-4): 237-250.
— Nicolosi, I., Speranza, F. and Chiappini, M., 2006. Ultrafast oceanic spreading of the Marsili Basin, southern Tyrrhenian Sea: Evidence from magnetic anomaly analysis. Geology, 34(9), pp.717-720.

— Nigro, F.A.B.R.I.Z.I.O. and Renda, P.I.E.T.R.O., 2005. Transtensional/extensional fault activity from the Mesozoic rifting to Tertiary chain building in Northern Sicily (Central Mediterranean). Geologica Carpathica, 56(3), p.255.
— Niu, Y., Zhao, Z., Zhu, D.C. and Mo, X., 2013. Continental collision zones are primary sites for net continental crust growth—A testable hypothesis. *Earth-Science Reviews*, *127*, pp.96-110.
— Nowell, D.A.G., 1999. Gravity terrain corrections—an overview. Journal of Applied Geophysics, 42(2), pp.117-134.
— Orsi, G., Gallo, G. and Zanchi, A., 1991. Simple-shearing block resurgence in caldera depressions. A model from Pantelleria and Ischia. Journal of Volcanology and Geothermal Research, 47(1-2), pp.1-11.
— Pace P, Scisciani V, Calamita F, Butler RW, Iacopini D, Esestime P, Hodgson N. 2015. Inversion structures in a foreland domain: seismic examples from the Italian Adriatic Sea. Interpretation. 3(4):SAA161-76.
— Pace, P. and Calamita, F., 2014. Push-up inversion structures v. fault-bend reactivation anticlines along oblique thrust ramps: examples from the Apennines fold-and-thrust belt (Italy). Journal of the Geological Society, 171(2), pp.227-238.
— Pace, P., Scisciani, V., Calamita, F., Butler, R.W., Iacopini, D., Esestime, P. and Hodgson, N., 2015. Inversion structures in a foreland domain: seismic examples from the Italian Adriatic Sea. Interpretation, 3(4), pp.SAA161-SAA176.
— Palano M, Ferranti L, Monaco C, Mattia M, Aloisi M, Bruno V, Cannavò F, Siligato G. 2012. GPS velocity and strain fields in Sicily and southern Calabria, Italy: Updated geodetic constraints on tectonic block interaction in the central Mediterranean. Journal of Geophysical Research: Solid Earth 117(B7). https://doi.org/10.1029/2012JB009254
— Palano M, Ursino A, Spampinato S, Sparacino F, Polonia A, Gasperini L. 2020. Crustal deformation, active tectonics and seismic potential in the Sicily Channel (Central Mediterranean), along the Nubia–Eurasia plate boundary. Scientific Reports 10(1): 21238.
— Panzera F, Lombardo G, Sicali S, D'Amico S. 2017. Surface geology and morphologic effects on seismic site response: The study case of Lampedusa, Italy. Physics and Chemistry of the Earth, Parts A/B/C 98: 62-72.
— Parotto, M. and Praturlon, A., 2004. The southern Apennine arc. Geology of Italy. Special Volume of the Italian Geological Society for the IGC , 32 , pp.33-58.

— Patacca, E. and Scandone, P., 1989. Post-Tortonian mountain building in the Apennines. The role of the passive sinking of a relic lithospheric slab. Atti dei Convegni Lincei, 80, pp.157-176.
— Patacca, E., Sartori, R. and Scandone, P., 1990. Tyrrhenian basin and Apenninic arcs: kinematic relations since late Tortonian times. Memorie della Società Geologica Italiana , 45 , pp.425-451.
— Peccerillo A. 2005. Plio-quaternary volcanism in Italy (Vol. 365). New York: Springer-Verlag Berlin Heidelberg.
— Pellegrino AG, Maniscalco R, Speranza F, Hernandez-Moreno C, Sturiale G. 2016. Paleomagnetism of the Hyblean Plateau, Sicily: a review of the existing data set and new evidence for lack of block rotation from the Scicli-Ragusa Fault System. Italian Journal of Geosciences 135(2): 300-307.
— Pellen R, Aslanian D, Rabineau M, Suc JP, Cavazza W, Popescu SM, Rubino JL. 2022. Structural and sedimentary origin of the Gargano-Pelagosa gateway and impact on sedimentary evolution during the Messinian Salinity Crisis. Earth-Science Reviews 232: 104114. https://doi.org/10.1016/j.earscirev.2022.104114
— Pepe, F., Bertotti, G., Cella, F. and Marsella, E., 2000. Rifted margin formation in the south Tyrrhenian Sea: A high-resolution seismic profile across the north Sicily passive continental margin. Tectonics, 19(2), pp.241-257.
— Pepe, F., Bertotti, G., Cloetingh, S., 2004. Tectono-stratigraphic modelling of the north Sicily continental margin (southern Tyrrhenian Sea). Tectonophysics 384 (1–4), 257–273.
— Pepe, S., 2005. Effect of dietary polyunsaturated fatty acids on age-related changes in cardiac mitochondrial membranes. Experimental gerontology, 40(5), pp.369-376.
— Pérez-Gussinyé M, Collier JS, Armitage JJ, Hopper JR, Sun Z, Ranero CR. 2023. Towards a process-based understanding of rifted continental margins. Nature Reviews Earth & Environment 4(3): 166-184.
— Petrullo, A.V., Agosta, F., Prosser, G. and Rizzo, E., 2017. Cenozoic tectonic evolution of the northern Apulian carbonate platform (southern Italy). Italian Journal of Geosciences, 136(2), pp.296-311.
— Piccardi, L., 1998. Actual kinematics, seismic behaviour and historical seismology of the Monte Sant'Angelo fault (Gargano, Italy): the possible surface rupture of the

"legendary" earthquake of the 493 AD. Geografia Fisica e Dinamica Quaternaria , 21 (1), pp.155-166.

— Piccardi, L., Sani, F., Moratti, G., Cunningham, D. and Vittori, E., 2011. Present-day geodynamics of the circum-Adriatic region: An overview. Journal of geodynamics, 51(2-3), pp.81-89.

— Piedilato, S. and Prosser, G., 2005. Thrust sequences and evolution of the external sector of a fold and thrust belt: an example from the Southern Apennines (Italy). Journal of Geodynamics, 39(4), pp.386-402.

— Pieri, P., Festa, V., Moretti, M. and Tropeano, M., 1997. Quaternary tectonic activity of the Murge area (Apulian foreland-Southern Italy).

— Plan, M.A., 2015. Sicily Channel/Tunisian Plateau: Topography, circulation and their effects on biological component.

— Platt, J.P., Behrmann, J.H., Cunningham, P.C., Dewey, J.F., Helman, M., Parish, M., Shepley, M.G., Wallis, S. and Western, P.J., 1989. Kinematics of the Alpine arc and the motion history of Adria. Nature, 337(6203), pp.158-161.

— Plint, A.G. and Nummedal, D., 2000. The falling stage systems tract: recognition and importance in sequence stratigraphic analysis. Geological Society, London, Special Publications, 172(1), pp.1-17.

— Polonia A, Torelli L, Mussoni P, Gasperini L, Artoni A, Klaeschen D. 2011. The Calabrian Arc subduction complex in the Ionian Sea: Regional architecture, active deformation, and seismic hazard. Tectonics 30(5).

— Polonia, A., Torelli, L., Artoni, A., Carlini, M., Faccenna, C., Ferranti, C., Gasperini, L., Govers, R., Klaeschen, D., Monaco, C., Neri, G., Nijholt, N., Orecchio, B., Wortel, R. (2016). The Ionian and Alfeo-Etna fault zones: new segments of an evolving plate boundary i n the central Mediterranean sea? Tectonophysics 675, 69–90. https://doi. org/10.1016/j.tecto.2016.03.016

— Polonia, A., Torelli, L., Artoni, A., Carlini, M., Faccenna, C., Ferranti, C., Gasperini, L., Govers, R., Klaeschen, D., Monaco, C., Neri, G., Nijholt, N., Orecchio, B., Wortel, R. (2016). The Ionian and Alfeo-Etna fault zones: new segments of an evolving plate boundary i n the central Mediterranean sea? Tectonophysics 675, 69–90.

— Polonia, A., Torelli, L., Gasperini, L., Mussoni, P., 2012. Active faults and historical earthquakes in the Messinian strait area (Ionian Sea). Nat. Hazards Earth Syst. Sci. 12, 2311–2328. https://doi.org/10.5194/nhess-12-2311-2012.

— Polonia, A., Torelli, L., Mussoni, P., Gasperini, L., Artoni, A. and Klaeschen, D., 2011. The Calabrian Arc subduction complex in the Ionian Sea: Regional architecture, active deformation, and seismic hazard. Tectonics, 30(5).
— Pon, S., Lines, L.R., 2005. Sensitivity analysis of seismic depth migrations. *Geophysics 70.* https://doi.org/10.1190/1.1897036.
— Posamentier, H.W., Paumard, V. and Lang, S.C., 2022. Principles of seismic stratigraphy and seismic geomorphology I: Extracting geologic insights from seismic data. Earth-Science Reviews, 228, p.103963.
— Postpischl, D., 1985. Catalogo dei terremoti italiani dall\'anno 1000 al 1980. Quaderni de «La Ricerca Scientifica».
— Proietti, G., Cvetkovi´c, M., Safti´c, B., Conti, A., Romano, V., Bigi, S., 2022. 3D modelling and capacity estimation of potential targets for CO2 storage in the Adriatic Sea, Italy. Petrol. Geosci. 28 (1). https://doi.org/10.1144/petgeo2020-117.
— Ragg S, Grasso M, Müller B. 1999. Patterns of tectonic stress in Sicily from borehole breakout observations and finite element modeling. Tectonics 18(4): 669-685.
— Raimondo, T., Hand, M. and Collins, W.J., 2014. Compressional intracontinental orogens: Ancient and modern perspectives. Earth-Science Reviews, 130, pp.128-153.
— Reuther, C.D., Eisbacher, G.H., 1985. Pantelleria rift-crustal extension in a convergent intraplate setting. Geol. Rundsch. 74, 585–597. http://dx.doi.org/10.1007/BF01821214.
— Richardson RM. 1992. Ridge forces, absolute plate motions, and the intraplate stress field. Journal of Geophysical Research: Solid Earth 97(B8): 11739-11748.
— Ridente, D. and Trincardi, F., 2006. Active foreland deformation evidenced by shallow folds and faults affecting late Quaternary shelf–slope deposits (Adriatic Sea, Italy). Basin Research, 18(2), pp.171-188.
— Rigane A, Gourmelen C. 2011. Inverted intracontinental basin and vertical tectonics: The Saharan Atlas in Tunisia. Journal of African Earth Sciences 61(2): 109-128.
— Robinson, A.H., 1995. Elements of cartography. Wiley Co. NY, USA.
— Roeder, D., 1979. Continental collisions. Reviews of Geophysics, 17(6), pp.1098-1109.
— Rointan, A., Soleimani, M.M., Aghajani, H., 2021. Improvement of seismic velocity model by selective removal of irrelevant velocity variations. Acta. Geod. Geophys. 56, 145–176. https://doi.org/10.1007/s40328-020-00329-x.\

— Roksandić, M.M., 1978. Seismic facies analysis concepts. Geophysical prospecting, 26(2), pp.383-398.
— Romagnoli C, Belvisi V, Innangi S, Di Martino G, Tonielli R. 2020. New insights on the evolution of the Linosa volcano (Sicily Channel) from the study of its submarine portions. Marine Geology 419: 106060.
— Rooney TO. 2017. The Cenozoic magmatism of East-Africa: Part I—Flood basalts and pulsed magmatism. Lithos 286: 264-301.
— Rosenbaum G, Weinberg RF, Regenauer-Lieb K. 2008. The geodynamics of lithospheric extension. Tectonophysics 458(1-4): 1-8.
— Rosenbaum, G. and Lister, G.S., 2004. Neogene and Quaternary rollback evolution of the Tyrrhenian Sea, the Apennines, and the Sicilian Maghrebides. Tectonics, 23(1).
— Rosenbaum, G., Lister, G., Duboz, C., 2002. Reconstruction of the tectonic evolution of the Western Mediterranean since the Oligocene. J. Virtual Explor. 8, 107–130.
— Rosenbaum, G., Lister, G.S. and Duboz, C., 2002. Relative motions of Africa, Iberia and Europe during Alpine orogeny. Tectonophysics, 359(1-2), pp.117-129.
— Rosie, A.M., 1966. Information And Communication Theory. Blackie, London. Rosin, P., 2000. Fitting superellipses. IEEE Trans. Pattern Anal. Machine Intell. 22 (7).
— Rossi, P. L., Tranne, C. A., Calanchi, N., & Lanti, E., 1996. Geology, stratigraphy and volcanological evolution of the island of Linosa (Sicily Channel). Acta Vulcanologica. 8, 73–90
— Rotolo SG, Castorina F, Cellura D, Pompilio M. 2006. Petrology and geochemistry of submarine volcanism in the Sicily Channel Rift. The Journal of Geology 114(3): 355-365.
— Roure, F., 2008. Foreland and Hinterland basins: what controls their evolution?. Swiss Journal of Geosciences, 101, pp.5-29.
— Roure, F., Casero, P. and Vially, R., 1991. Growth processes and melange formation in the southern Apennines accretionary wedge. Earth and Planetary Science Letters, 102(3-4), pp.395-412.
— Roure, F., Casero, P., Addoum, B., 2012. Alpine inversion of the North African margin and delamination of its continental lithosphere. Tectonics 31, TC3006. https://doi. org/10.1029/2011TC002989.
— Roure, F., Howell, D.G., Müller, C. and Moretti, I., 1990. Late Cenozoic subduction complex of Sicily. Journal of Structural Geology, 12(2), pp.259-266.

— Roveri M, Flecker R, Krijgsman W, Lofi J, Lugli S, Manzi V, Sierro FJ, Bertini A, Camerlenghi A, De Lange G, Govers R. 2014. The Messinian Salinity Crisis: Past and future of a great challenge for marine sciences. Marine Geology 352: 25-58.
— Royden L, Faccenna C. 2018. Subduction Orogeny and the Late Cenozoic Evolution of the Mediterranean Arcs. Annual Review of Earth and Planetary Sciences 46: 261–289. https://doi.org/10.1146/annurev-earth-060115-012419.
— Royden, L., Faccenna, C., 2018. Subduction Orogeny and the Late Cenozoic evolution of the Mediterranean Arcs. Annu. Rev. Earth Planet. Sci. 46, 216–289. https://doi.org/10.1146/annurev-earth-060115-012419.
— Royden, L.H., 1993. Evolution of retreating subduction boundaries formed during continental collision. Tectonics, 12(3), pp.629-638.
— Santos, H. B., Schleicher, J., & Novais, A., 2013. Initial-model construction for MVA techniques. 75th European Association of Geoscientists and Engineers Conference and Exhibition 2013 Incorporating SPE EUROPEC 2013: Changing Frontiers 2149–2153. https://doi.org/10.3997/2214-4609.20130939.
— Sartori, R., 2003. The Tyrrhenian back-arc basin and subduction of the Ionian lithosphere. Episodes Journal of International Geoscience, 26(3), pp.217-221.
— Satolli, S., Pace, P., Viandante, M.G. and Calamita, F., 2014. Lateral variations in tectonic style across cross-strike discontinuities: an example from the Central Apennines belt (Italy). International Journal of Earth Sciences, 103, pp.2301-2313.
— Scalera, G., Calcagnile, G. and Panza, G.F., 1981. On the "400-kilometers" discontinuity in the Mediterranean area. The solution of the inverse problem in geophysical interpretation, pp.335-339.
— Scarascia, S., LOZEJ, A.T. and Cassinis, R., 1994. Crustal structures of the Ligurian, Tyrrhenian and Ionian seas and adjacent onshore areas interpreted from wide-angle seismic profiles. Bollettino di Geofisica Teorica ed Applicata, 36(141-44), pp.5-19.
— Scarfì, L., Messina, A. and Cassisi, C., 2013. Sicily and Southern Calabria focal mechanism database: a valuable tool for local and regional stress field determination. Annals of Geophysics.
— Scisciani V. 2009. Styles of positive inversion tectonics in the Central Apennines and in the Adriatic foreland: Implications for the evolution of the Apennine chain (Italy). Journal of Structural Geology 31(11): 1276-1294.

— Scisciani, V., Patruno, S., Tavarnelli, E., Calamita, F., Pace, P. and Iacopini, D., 2019. Multi-phase reactivations and inversions of Paleozoic–Mesozoic extensional basins during the Wilson cycle: case studies from the North Sea (UK) and the Northern Apennines (Italy). Geological Society, London, Special Publications, 470(1), pp.205-243.
— Scisciani, V., Tavarnelli, E. and Calamita, F., 2002. The interaction of extensional and contractional deformations in the outer zones of the Central Apennines, Italy. Journal of Structural Geology, 24(10), pp.1647-1658.
— Scrocca, D., Carminati, E. and Doglioni, C., 2005. Deep structure of the southern Apennines, Italy: Thin-skinned or thick-skinned?. Tectonics, 24(3).
— Sdrolias, M. and Müller, R.D., 2006. Controls on back-arc basin formation. Geochemistry, Geophysics, Geosystems, 7(4).
— Seismic data Network Access Point (SNAP). https://snap.ogs.trieste.it
— Shekar, B and Sethi, H., 2018. Full Waveform Inversion for microseismic events using sparsity constraints. Geophysics 84, 1-83. https://doi.org/10.1190/geo2017-0822.1.
— Sheriff, R.E., Geldart, L.P., 1995. Exploration Seismology, 2nd edn. Cambridge University Press. Cambridge. https://doi.org/10.1017/CBO9781139168359.
— Shillington K. Charles Warren: Royal Engineer in the Age of Empire. 2021. eBook Partnership.
— Sibson RH. 1995. Selective fault reactivation during basin inversion: potential for fluid redistribution through fault-valve action. Geological Society, London, Special Publications 88(1): 3-19.
— Sokoutis, D., Burg, J.P., Bonini, M., Corti, G. and Cloetingh, S., 2005. Lithospheric-scale structures from the perspective of analogue continental collision. *Tectonophysics*, *406*(1-2), pp.1-15.
— Sopher, D., 2018. Converting scanned images of seismic reflection data into SEG-Y format. Earth Science Informatics 11, 241. https://doi.org/10.1007/s12145-017-0329-z.
— Soubaras, R., 1996. Ocean bottom hydrophone and geophone processing. In SEG Technical Program Expanded Abstracts 1996 (pp. 24-27). Society of Exploration Geophysicists.
— Soubaras, R., 1996. Ocean bottom hydrophone and geophone processing. In SEG Technical Program Expanded Abstracts 1996 (pp. 24-27). Society of Exploration Geophysicists.

— Spatola D, Micallef A, Sulli A, Basilone L, Ferreri R, Basilone G, Bonanno A, Pulizzi M, Mangano S. 2018. The Graham Bank (Sicily Channel, central Mediterranean Sea): seafloor signatures of volcanic and tectonic controls. Geomorphology 318: 375-389. https://doi.org/10.1016/j.geomorph.2018.07.006.
— Spatola D, Sulli A, Casalbore D, Chiocci FL. 2021. First evidence of contourite drifts in the North-Western Sicilian active continental margin (Southern Tyrrhenian Sea). Journal of Marine Science and Engineering 9(10): 1043.
— Speranza, F., Villa, I.M., Sagnotti, L., Florindo, F., Cosentino, D., Cipollari, P. and Mattei, M., 2002. Age of the Corsica–Sardinia rotation and Liguro–Provençal Basin spreading: new paleomagnetic and Ar/Ar evidence. Tectonophysics, 347(4), pp.231-251.
— Stampfli GM, Borel GD. 2004. The TRANSMED transects in space and time: constraints on the paleotectonic evolution of the Mediterranean domain. In: The TRANSMED Atlas. The Mediterranean region from crust to mantle: Geological and geophysical framework of the Mediterranean and the surrounding areas. Berlin, Heidelberg: Springer Berlin Heidelberg, 53-80.
— Stampfli, G.M., 2005. Plate tectonics of the Apulia-Adria microcontinents. CROP Project-Deep Seismic explorations of the Central Mediterranean and Italy, Section, 11, pp.747-766.
— Stern, R.J. and Gerya, T., 2018. Subduction initiation in nature and models: A review. Tectonophysics, 746, pp.173-198.
— Stern, R.J., 2002. Subduction zones. Reviews of geophysics, 40(4), pp.3-1.
— Stripling, A.A., 1958. Velocity Log Characteristics. Transactions of the AIME, 213(01), pp.207-212.
— Sulli A, Morticelli MG, Agate M, Zizzo E. 2021. Active north-vergent thrusting in the northern Sicily continental margin in the frame of the quaternary evolution of the Sicilian collisional system. Tectonophysics 802: 228717.
— Sulli A. 2000. Structural framework and crustal characteristics of the Sardinia Channel Alpine transect in the central Mediterranean. Tectonophysics 324(4): 321–336.
— Sulli, A., Morticelli, M.G., Agate, M. and Zizzo, E., 2021. Active north-vergent thrusting in the northern Sicily continental margin in the frame of the quaternary evolution of the Sicilian collisional system. Tectonophysics, 802, p.228717.

— Sulli, A., Morticelli, M.G., Agate, M., Zizzo, E., 2021. Active north-vergent thrusting in the northern Sicily continental margin in the frame of the quaternary evolution of the Sicilian collisional system. Tectonophysics 802, 228717. ISSN 0040-1951. https://doi.org/10.1016/j.tecto.2021.228717.

— Tanimoto, T., Yano, T. and Hakamata, T., 2013. An approach to improve Rayleigh-wave ellipticity estimates from seismic noise: application to the Los Angeles Basin. Geophysical Journal International, 193(1), pp.407-420.

— Tavani, S., Smeraglia, L., Fabbi, S., Aldega, L., Sabbatino, M., Cardello, G.L., Maresca, A., Schirripa Spagnolo, G., Kylander-Clark, A., Billi, A. and Bernasconi, S.M., 2023. Timing, thrusting mode, and negative inversion along the Circeo thrust, Apennines, Italy: How the accretion-to-extension transition operated during slab rollback. Tectonics, 42(6), p.e2022TC007679.

— Tavarnelli, E., Butler, R.W.H., Decandia, F.A., Calamita, F., Grasso, M., Alvarez, W., Renda, P., Crescenti, U. and D'offizi, S., 2004. Implications of fault reactivation and structural inheritance in the Cenozoic tectonic evolution of Italy. The geology of Italy, special, 1, pp.209-222.

— Tavarnelli, E., Renda, P., Pasqui, V. and Tramutoli, M., 2003. Composite structures resulting from negative inversion: an example from the Isle of Favignana (Egadi Islands). BOLLETTINO-SOCIETA GEOLOGICA ITALIANA, 122(2), pp.319-326.

— Tectono-stratigraphic. Tectonophysics, 839 (August). https://doi.org/10.1016/j.tecto.2022.229544

— Tesauro, M., Kaban, M.K., Cloetingh, S.A.P.L., 2008. EuCRUST-07: a new reference model for the European crust. Geophys. Res. Lett. 35, L05313. https://doi.org/10.1029/2007GL032244.

— Thore, P., Shtuka, A., Lecour, M., Ait-Ettajer, T., Cognot, R., 2002. Structural uncertainties: Determination, management, and applications. *Geophysics* 67, 840–852. https://doi.org/10.1190/1.1484528.

— Tonielli R, Innangi S, Di Martino G, Romagnoli C. 2019. New bathymetry of the Linosa volcanic complex from multibeam systems (Sicily Channel, Mediterranean Sea). Journal of Maps 15(2): 611-618. https://doi.org/10.1080/17445647.2019.1642807.

— Torelli L, Grasso M, Mazzoldi G, Peis D, Gori D. 1995. Cretaceous to Neogene structural evolution of the Lampedusa shelf (Pelagian Sea, Central Mediterranean). Terra Nova 7(2):200-12.

— Torelli L, Grasso M, Mazzoldi G, Peis D. 1998. Plio–Quaternary tectonic evolution and structure of the Catania foredeep, the northern Hyblean Plateau and the Ionian shelf (SE Sicily). Tectonophysics 298(1-3): 209-221. https://doi.org/10.1016/S0040-1951(98)00185-1.
— Torelli L, Zitellini N, Argnani A, Brancolini G, De Cillia C, Peis D, Tricart P. 1993. Sezione geologica crostale dall'avampaese Pelagiano al bacino di retroarco Tirrenico (Mediterraneo Cent rale). Mem Soc Geol It 47:385–399.
— Torelli, L., Grasso, M., Mazzoldi, G., Peis, D., Gori, D., 1995. Cretaceous to Neogene structural evolution of the Lampedusa Shelf (Pelagian Sea, Central Mediterranean). Terra Nova 7(2), 200–212. https://doi.org/10.1111/j.1365-3121.1995.tb00689.x.
— Torelli, L., Zitellini, N., Argnani, A., Brancolini, G., Cillia, C., Peis, D.,Tricart, P., 1991. Sezione geologica crostale dall'avampaese pelagiano al bacino di retroarco tirrenico (Mediterraneo centrale). Mem. Soc. Geol. Ital. 4, 385-399.
— Torelli, L., Zitellini, N., Argnani, A., Brancolini, G., Cillia, C., Peis, D.,Tricart, P., 1991. Sezione geologica crostale dall'avampaese pelagiano al bacino di retroarco tirrenico (Mediterraneo centrale). Mem. Soc. Geol. Ital. 4, 385-399.
— Trincardi, F. and Zitellini, N., 1987. The rifting of the Tyrrhenian Basin. Geo-marine letters, 7(1), pp.1-6.
— Turco, E., Macchiavelli, C., Penza, G., Schettino, A. and Pierantoni, P.P., 2021. Kinematics of deformable blocks: application to the opening of the tyrrhenian basin and the formation of the apennine Chain. Geosciences, 11(4), p.177.
— Underhill JR, Paterson S. 1998. Genesis of tectonic inversion structures: seismic evidence for the development of key structures along the Purbeck–Isle of Wight Disturbance. Journal of the Geological Society 155(6): 975-992.
— Unser, M., 1999, Splines. A perfect fit for signal and image processing: IEEE Signal Processing Magazine 16(6) 22-38. https://doi.org/10.1109/79.799930.
— Usman, M., Siddiqui, N.A., Garzanti, E., Jamil, M., Imran, Q.S. and Ahmed, L., 2021a. 3-D seismic interpretation of stratigraphic and structural features in the Upper Jurassic to Lower Cretaceous sequence of the Gullfaks Field, Norwegian North Sea: A case study of reservoir development. Energy Geoscience, 2(4), pp.287-297.
— Usman, M., Siddiqui, N.A., Zhang, S.Q., Mathew, M.J., Zhang, Y.X., Jamil, M., Liu, X.L. and Ahmed, N., 2021b. 3D geo-cellular static virtual outcrop model and its

implications for reservoir petro-physical characteristics and heterogeneities. Petroleum Science, 18(5), pp.1357-1369.

— Uyeda, S., 1982. Subduction zones: An introduction to comparative subductology. Tectonophysics 81, 3–4. https://doi.org/10.1016/0040-1951(82)90126-3.

— Vail, P.R., Mitchum Jr, R.M. and Thompson III, S., 1977. Seismic stratigraphy and global changes of sea level: Part 3. Relative changes of sea level from Coastal Onlap: section 2. Application of seismic reflection Configuration to Stratigrapic Interpretation.

— Van Dijk G, Maars J, Andreetto F, Hernández-Molina FJ, Rodríguez-Tovar FJ, Krijgsman W. 2023. A terminal Messinian flooding of the Mediterranean evidenced by contouritic deposits on Sicily. Sedimentology 70: 1195–1223. https://doi.org/10.1111/sed.13074.

— Van Hinsbergen, D.J.J., Wissers, R.L.M., Spakman, W., 2014. Origin and consequences of western Mediterranean subduction, rollback and slab segmentation. Tectonics 33(4), 347-595. https://doi.org/10.1002/2013TC003349

— Van Wagoner, J.C., Mitchum, R.M., Campion, K.M. and Rahmanian, V.D., 1990. Siliciclastic sequence stratigraphy in well logs, cores, and outcrops: concepts for high-resolution correlation of time and facies.

— Vidal, N., Alvarez-Marrón, J. and Klaeschen, D., 2000. The structure of the Africa-Anatolia plate boundary in the eastern Mediterranean. Tectonics, 19(4), pp.723-739.

— Viger A, Dominguez S, Mazzotti S, Peyret M, Henriquet M, Barreca G, Monaco C, Damon A. 2024. Interseismic and long-term deformation of southeastern Sicily driven by the Ionian slab roll-back. EGUsphere 2024: 1-44.

— Vine, F.J. and Matthews, D.H., 1963. Magnetic anomalies over oceanic ridges. Nature Publishing.

— Visibility of petroleum exploration data in Italy (ViDEPI). https://www.videpi.com

— Volpi V, Civile D, Lodolo E, Romeo R, Accettella D, Accaino F, Ferrante GM. 2022. Seabed and shallow morphological setting of the western Sicilian Channel. Bulletin of Geophysics and Oceanography 63(3): 357-376. https://hdl.handle.net/20.500.14083/14502.

— Volpi, V., Forlin, F., Donda, F., Civile, D., Facchin, L., Sauli, S., Merson, B., Sinza-Mendieta, K., & Shams, A. 2015. Southern adriatic sea as a potential area for CO2 geological storage. Oil and Gas Science and Technology, 70(4), 713–728. https://doi.org/10.2516/ogst/2014039.

— Wang Z, Liu L, Fu Y, Zhao L, Lin J, Jin Z, Zheng B. 2023. Multistage plate subduction controls intraplate volcanism and cratonic lithospheric thinning in Northeast Asia. Earth-Science Reviews: 104590.
— Washington HS. 1909. ART. VIII.--The Submarine Eruptions of 1831 and 1891 near Pantelleria. American Journal of Science (1880-1910) 27(158): 131.
— White, J.C., Neave, D.A., Rotolo, S.G. and Parker, D.F., 2020. Geochemical constraints on basalt petrogenesis in the Strait of Sicily Rift Zone (Italy): Insights into the importance of short lengthscale mantle heterogeneity. Chemical Geology, 545, p.119650.
— Williams G.D, Powell C.M, Cooper M.A. 1989. Geometry and kinematics of inversion tectonics. Geological Society, London, Special Publications 44(1): 3-15.
— Winnock, E., 1981. Structure du bloc pélagien. In Consiglio nazionale delle ricerche. International conference (pp. 445-464).
— Winnock, E., 1981. Structure du Bloc Pelagien. In: Wezel, I.F.C. (Ed.), Sedimentary Basins of Mediterranean Margins. Tecnoprint, Bologna, pp. 445–464.
— Wolf, S.G., Huismans, R.S., Muñoz, J.A., Curry, M.E. and van der Beek, P., 2021. Growth of collisional orogens from small and cold to large and hot—Inferences from geodynamic models. Journal of Geophysical Research: Solid Earth, 126(2), p.e2020JB021168.
— Wong, J., Han, L., Stewart, R.R., Bentley, L.R. and Bancroft, J.C., 2009. Geophysical well logs from a shallow test well and automatic determination of formation velocities from full-waveform sonic logs. CSEG Rec, 34, pp.21-30.
— Würtz, M. and Rovere, M., 2015. Atlas of the Mediterranean seamounts and seamount-like structures Gland, Switzerland: IUCN. p. 276.
— Yilmaz, Ö., 2001. Seismic Data Analysis. Society of Exploration Geophysicists, pp. 2065. https://doi.org/10.1190/1.9781560801580.
— Zarudzki, E.F.K., 1972. The Strait of Sicily. A Geophysical Study. Rev. Geograph, Phys. et Geo. Dynam. 14, 11-28.
— Zheng, Y.F. and Zhao, Z.F., 2017. Introduction to the structures and processes of subduction zones. Journal of Asian Earth Sciences, 145, pp.1-15.
— Ziegler PA, Cloetingh S, van Wees JD. 1995. Dynamics of intra-plate compressional deformation: the Alpine foreland and other examples. Tectonophysics 252(1-4): 7-59.

— Ziegler PA, Cloetingh S. 1994. Dynamic Processes Governing Development of Rifted Basins. Paris: Technip. https://doi.org/10.1016/S0012-8252(03)00041-2.
— Ziegler PA, Dèzes P. 2006. Crustal evolution of western and central Europe. Geological Society, London, Memoirs 32(1): 43-56.
— Ziegler, P.A., Bertotti, G. and Cloetingh, S.A.P.L., 2002. Dynamic processes controlling foreland development: the role of mechanical (de) coupling of orogenic wedges and forelands. EGS Spec. Publ, 1, pp.29-91.
— Zitellini N, Ranero CR, Loreto MF, Ligi M, Pastore M, D'Oriano F, Sallares V, Grevemeyer I, Moeller S, Prada M. 2020. Recent inversion of the Tyrrhenian Basin. Geology 48(2): 123-127. https://doi.org/10.1130/G46774.1.
— Zoback ML, Zoback M, Watts A, Schubert G. 2007. Lithosphere stress and deformation. Treatise on Geophysics: 253-273.

Acknowledgment

I express my deepest gratitude to **Allah ﷻ Almighty**, who is the eternal source of wisdom, and to the **Holy Prophet Muhammad** ﷺ, an inspiration and complete suite of life for humanity. They provided me with the courage and determination to embark on and successfully complete this Ph.D. research journey.

I am sincerely indebted to the University of Parma (Unipr), Italy, for awarding me a fully funded Ph.D. scholarship, enabling me to pursue and accomplish my ambitious research goals. My heartfelt appreciation extends to my esteemed supervisor, **Professor Andrea Artoni**, for his invaluable support and guidance throughout the course of my degree and research, which significantly enhanced my research skills and contributed to the preparation for publication of my work in international journals. I extend my gratitude to **Professor Torelli** for providing me with the opportunity to be in discussion with his critical and very valuable reviews.

I wish to express special thanks to **Dr. Nicolo Chizzni** for his constructive scientific discussions for my studies and software training crucial to my research, I also appreciate the contributions of **Prof. Attilio Sulli, Prof. Eline Le Breton, and Dr. Mariagiada Maiorana** for their valuable comments and discussions during the different stages of my research. I am thankful to **Dr. Tamara Yegorova and Dr. Anna Murovskaya** for their valuable discussions to enhance my skills.

My heartfelt appreciation goes to my beloved parents, **Mr. Ghulam Qadir Sheikh and Mrs. Ayesha**, my siblings, for their support. Despite the geographical distance, their continuous remembrance during special occasions and celebrations has been a source of strength. I am sincerely thankful for their sincere and warm camaraderie, which made it possible for me to navigate life in a foreign country while completing my research. From the depths of my heart, I express gratitude to my friend **Dr. Muhammad Usman** for his unwavering support, help and insightful discussions throughout my PhD venture and I also thank all my friends for the laughter and joyous moments we shared together.

AASIYA QADIR

Supplementary Material

For this PhD thesis, a substantial volume of datasets has been used and generated, each comprising a considerable amount of data. To facilitate accessibility, all datasets are stored in a dedicated Google Drive folder, along with the corresponding png and Excel files for the tables and the:

https://drive.google.com/drive/folders/1BJiqC9NefuxzLoZvN9ObMyXiq1BABdME?usp=sharing.

List of files in the folder:

Chapter 5: Data sets used for the building of velocity models and the time-to-depth conversions of the seismic interpretation (Supp. Mat. 5.1, 5.2, 5.3), the details of the interpolation tests (Appendix A) and the interpretation of volcanic bodies in depth using MOVE suite (Appendix B) (for detail refer to the respective file in the folder).

Chapter 6: Seismic interpretation of CS89-01 multichannel seismic reflection profile (Fig. 6.5).